1979

THE VIBRATIONAL ANALYSIS OF HALOGEN DERIVATIVES OF METHYLSILANES, AND DIMETHYLARSINE AND DIMETHYLPHOSPHINE.

ALLAN JORGEN FREDERIK. CLARK
University of Windsor

NOTICE

AVIS

The quality of this microfiche is heavily dependent upon the quality of the original thesis submitted for microfilming. Every effort has been made to ensure the highest quality of reproduction possible.

If pages are missing, contact the university which granted the degree.

Some pages may have indistinct print especially if the original pages were typed with a poor typewriter ribbon or if the university sent us a poor photocopy.

Previously copyrighted materials (journal articles, published tests, etc.) are not filmed.

Reproduction in full or in part of this film is governed by the Canadian Copyright Act, R.S.C. 1970, c. C-30. Please read the authorization forms which accompany this thesis.

La qualité de cette microfiche dépend grandement de la qualité de la thèse soumise au microfilmage. Nous avons tout fait pour assurer une qualité supérieure de reproduction.

S'il manque des pages, veuillez communiquer avec l'université qui a conféré le grade.

La qualité d'impression de certaines pages peut laisser à désirer, surtout si les pages originales ont été dactylographiées à l'aide d'un ruban usé ou si l'université nous a fait parvenir une photocopie de mauvaise qualité.

Les documents qui font déjà l'objet d'un droit d'auteur (articles de revue, examens publiés, etc.) ne sont pas microfilmés.

La reproduction, même partielle, de ce microfilm est soumise à la Loi canadienne sur le droit d'auteur, SRC 1970, c. C-30. Veuillez prendre connaissance des formules d'autorisation qui accompagnent cette thèse.

THIS DISSERTATION HAS BEEN MICROFILMED EXACTLY AS RECEIVED

LA THÈSE A ÉTÉ MICROFILMÉE TELLE QUE NOUS L'AVONS REÇUE

THE VIBRATIONAL ANALYSIS OF HALOGEN

DERIVATIVES OF METHYLSILANES, AND

DIMETHYLARSINE AND DIMETHYLPHOSPHINE

by

Allan Jörgen Frederik Clark

A Dissertation
submitted to the Faculty of Graduate Studies
through the Department of Chemistry in Partial Fulfillment
of the requirements for the Degree
of Doctor of Philosophy at
The University of Windsor

Windsor, Ontario, Canada
1979

720775

ABSTRACT

THE VIBRATIONAL ANALYSIS OF HALOGEN
DERIVATIVES OF METHYLSILANES, AND
DIMETHYLARSINE AND DIMETHYLPHOSPHINE

by

Allan Jörgen Frederik Clark

The Raman and vibrational spectra of fifteen partially substituted methyl and halogen derivatives of silane are examined, along with those of dimethylarsine and -phosphine. Fundamental modes are determined and assigned. The assignment is in most cases aided by a normal coordinate analysis and other calculations using data from specifically deuterated homologues. For the CH_3SiH_2X (X= halogen) series, these are the d_3- and d_2- compounds; for CH_3SiHX_2 the d_3- and d_7- compounds and for $(CH_3)_2SiHX$ the d_1- homologue. The fully substituted trifluoro- and triiodomethylsilanes are also studied as is methylsilane, for which both d_3- homologues and the d_6- compound are reported. Details of the preparative routes to these partially and fully deuterated methylsilanes, and the subsequent halogenation reactions are given. The compounds are characterised, and their deuterium content measured by nuclear magnetic resonance spectroscopy. For dimethylarsine and -phosphine as for the silane derivatives, difficulties in assigning the vibrations involving the hydrogen atom(s) bonded to the central atom are approached by an examination of the d_1- compounds which provide sufficient evidence to assign the vibrational spectra. The assignments of all compounds are discussed in relation to previous reports, where these exist.

iii

To my family;

past and present, here and gone.

TABLE OF CONTENTS

LIST OF TABLES

LIST OF FIGURES

xvi

LIST OF ABBREVIATIONS.

ca.	-	about
approx.	-	approximate(ly)
Me	-	methyl
n.m.r.	-	nuclear magnetic resonance
TMS	-	tetramethylsilane
ppm	-	parts per million
Hz	-	Hertz (sec^{-1})
dep., dp-	depolarised
pol., p -	polarised
Ra.	-	Raman
i.r.	-	infrared
str.	-	stretch
def.	-	deformation
(a)	-	antisymmetric
(s)	-	symmetric
sc	-	scissors
sh	-	shoulder
NCA	-	Normal Coordinate Analysis
p.e.d.	-	potential energy distribution
f, f.c.	-	force constant
GHFF	-	General harmonic force field
VFF	-	Valence force field
cm^{-1}	-	wavenumber
mm	-	millimeter (10^{-3} meters)
pm	-	picometer (10^{-12} meters)
aJ	-	attojoules (10^{-18} joules)
eV	-	electron-volts
o.d.	-	outside diameter
R.T.	-	room temperature

CHAPTER 1.1

INTRODUCTION

The work covered by this dissertation is presented in three parts. The first part contains a general description of the procedures and methods, both theoretical and practical, that are used throughout the experimental part. This includes a chapter on nuclear magnetic resonance spectroscopy which was the principal tool for purity determination. The theoretical descriptions are not intended to be all-encompassing or in all cases completely general; emphasis is placed on the application of the particular procedure to this work.

Part I contains the bulk of the preparative and spectroscopic work and discussions of the vibrational analyses of fifteen derivatives of methyl- and dimethylsilane. While the fully substituted methyl and/or halogen derivatives of silane have been extensively studied, the three series of partially substituted compounds (i.e. CH_3SiH_2X, CH_3SiHX_2 and $(CH_3)_2SiHX$; X = halogen) have received scant, if any, attention. Reference is made to any existing work in the discussion of the assignment of each series. The assignment process is presented in many cases in the same way as it was originally elucidated, without the benefit of hindsight.

Part II contains a vibrational study of two alkyl Group V hydrides, which had been either unreported or erroneously assigned. This work derives from earlier directions in the research group.

Routine experimental details not pertaining directly to the work are collected in the Appendix. The dissertations

of previous students were often consulted during the course
of this research for the many practical details necessary to
carry out the work. Thus many techniques which are now con-
sidered second nature have been included for this reason.

References have been collected at the end of each part
as there was found to be little duplication between the parts.

One final comment will be made about the literature, and
that is the recognition of one invaluable aid in the study of
vibrational spectroscopy. I refer of course to Gerhard
Herzberg's book on "The Infrared and Raman Spectra of Poly-
atomic Molecules"[1] which will probably be found to be just
as useful in another thirty-four years. As a synthetic
chemist in this area, much use was made of the chapter on
silicon in Wiberg and Amberger's book on the "Hydrides of the
Elements of Main Groups I-IV"[2] which was valuable both for
the direct information it contained and its extensive
bibliography.

CHAPTER 1.2

NUCLEAR MAGNETIC RESONANCE SPECTRA
OF METHYLSILANE DERIVATIVES

Nuclear magnetic resonance (n.m.r.) spectroscopy proved to be the most convenient and informative technique for both qualitative and quantitative determination of reaction products. This was equally true for the examination of results of trap-to-trap distillations and the estimation of sample purity, both before and after recording the vibrational spectra. For routine measurements, ^{1}H n.m.r. spectra could be rapidly and accurately recorded, while ^{19}F n.m.r. took more time but was nevertheless a useful tool. Despite the fact that, apart from the rare measurement of an unrecorded chemical shift, no internal standard was used, and thus no absolute chemical shifts evaluated, much information was still available from these spectra. This information was derived firstly from measurements of the difference in chemical shifts, either from two kinds of the same type of nucleus in the same molecule or from signals from two different compounds in the same sample, and secondly from the observation of spin-spin coupling with other magnetic nuclei.

Spin-spin coupling transforms a single signal into a series of lines with equal spacing called the coupling constant, J, due to modification of the magnetic field in the vicinity of the nucleus under observation by neighbouring nuclei with nuclear spins. These can be aligned either with or against the applied magnetic field, H_0', either enhancing or reducing the local effective magnetic field. For example, in all the $CH_3SiH_nX_{3-n}$ (n=1-3) compounds in this work, the

Si<u>H</u> signals appear as quartets from coupling with the spins of the three hydrogens in the methyl group. If these spins are aligned with H_O, the magnetic field experienced by the Si<u>H</u> proton(s) is enhanced and the signal appears to slightly lower field than it otherwise would (for a local field of strength H_O) and is correspondingly found slightly upfield when the methyl protons are aligned against H_O. In other words, with neighbouring spins augmenting the local field, a smaller H_O is needed for a transition of the spin state to occur, and vice-versa.

Simple statistics show, however, that these arrangements, all with or all against H_O, are not the most common, as the spins have a three times greater probability of being either two with and one against or one with and two against, as shown below:

$$H_O \uparrow$$

$$\downarrow\downarrow\downarrow$$
$$\downarrow\downarrow\uparrow \quad \downarrow\uparrow\downarrow \quad \uparrow\downarrow\downarrow$$
$$\uparrow\uparrow\downarrow \quad \uparrow\downarrow\uparrow \quad \downarrow\uparrow\uparrow$$
$$\uparrow\uparrow\uparrow$$
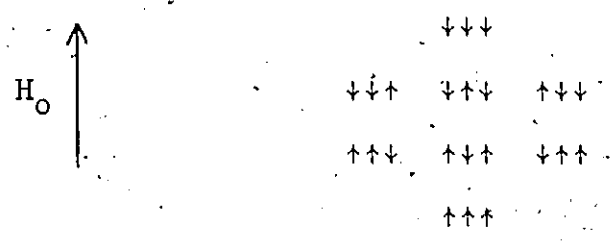
Thus the Si<u>H</u>$_n$ signal appears as a quartet with intensities 1:3:3:1. This simple interpretation of the splitting patterns however, is applicable only to so-called first-order spectra where $\Delta\delta_{AB} \gg J_{AB}$, i.e. when the difference in the chemical shifts (δ) for two nuclei is large compared to the coupling constant (J) from spin-spin interaction between them. This is the case for all the silane derivatives studied in this work, for which δ and J values have been well documented in

the literature[3-5]. The number of lines present can be deter--
mined by the expression $2nI + 1$, where n is the number of
magnetically equivalent nuclei of spin I. For ^1H, ^{19}F, ^{13}C
and ^{29}Si nuclei with $I = \frac{1}{2}$, this simplifies, as in the example
above, to $n + 1$, with intensities calculable from Pascal's
triangle. The magnitude of the separation, J, is invariant
(unlike the value for δ, which is proportional to H_o).
Thus, for example, a value for J_{HF}, (the coupling constant
for interacting hydrogen and fluorine nuclei, expressed in
Hz) in a particular compound will be the same measured at
different instrument operating frequencies, or indeed even in
separate ^1H and ^{19}F n.m.r. experiments.

When coupling is with a nucleus in 100% abundance, e.g.,
with ^{19}F or ^2H (for all practical purposes, in the deuterated
compounds), then the entire signal will be split and the
chemical shift is taken as the centre of gravity of the split
signals. When the interacting nucleus is less abundant, e.g.
^{13}C (1.1% abundant) or ^{29}Si (4.7%), the coupling will appear
as satellites, split either side of the main signal by $J/2$.
The main signal is not split because there is no interaction
with the non-magnetic nuclei, in this case ^{12}C and ^{28}Si or
^{30}Si. These satellite spectra are very useful, firstly in
the determination of the identity of a compound, since each
J value will be a characteristic of that particular compound
(although its value may not necessarily be unique) and second-
ly as an approximation of the proportion of small amounts of
impurities present. The latter is carried out by a compari-

son of the peak area of an impurity with that of a satellite which for ^{13}C and ^{29}Si will be approximately 0.6% and 2.5% of the total signal respectively. For coupling with ^2H nuclei (I = 1) the splitting patterns are a 1:1:1 triplet for coupling with one deuteron, a 1:2:3:2:1 quintet for coupling with two, and a 1:3:6:7:6:3:1 septet for coupling with three deuterons. The coupling constants involving coupling with ^2H (or D as it will be written for convenience), J_{DX}, where X is any magnetic nucleus, are related to the J_{HX} values in the corresponding isotopic molecules by the ratio of the gyromagnetic ratios γ_D/γ_H which is 0.1535. Thus under normal resolution, J_{HX} would have to be ≥ 6 Hz in order for J_{DX} to be observed. Since J_{HH} in the silane derivatives discussed in this work are ~ 4 Hz or less, splitting of J_{HD} is not normally observed.

1.2.1 ^1H n.m.r. of the Methylsilanes

For CH_3SiH_3 two signals are expected, for the methyl and silyl hydrogens each split into quartets by each other. The difference in chemical shifts of the two signals is 3.43 ppm (205.8 Hz at 60 MHz) and the coupling constant J_{HH} is 4.68 Hz[3]. Deuterating at either carbon or silicon not only effectively removes one resonance but causes the splitting to collapse (see above). The spectra of the three hydrogen containing methylsilanes are shown in Figure 1.1 where the satellites due to J_{CH}, the high field signal, and to J_{SiH} are clearly observable. The extent of deuteration in CH_3SiD_3 and CD_3SiH_3 can be measured by integrating the

CH$_3$SiH$_3$

CH$_3$SiD$_3$
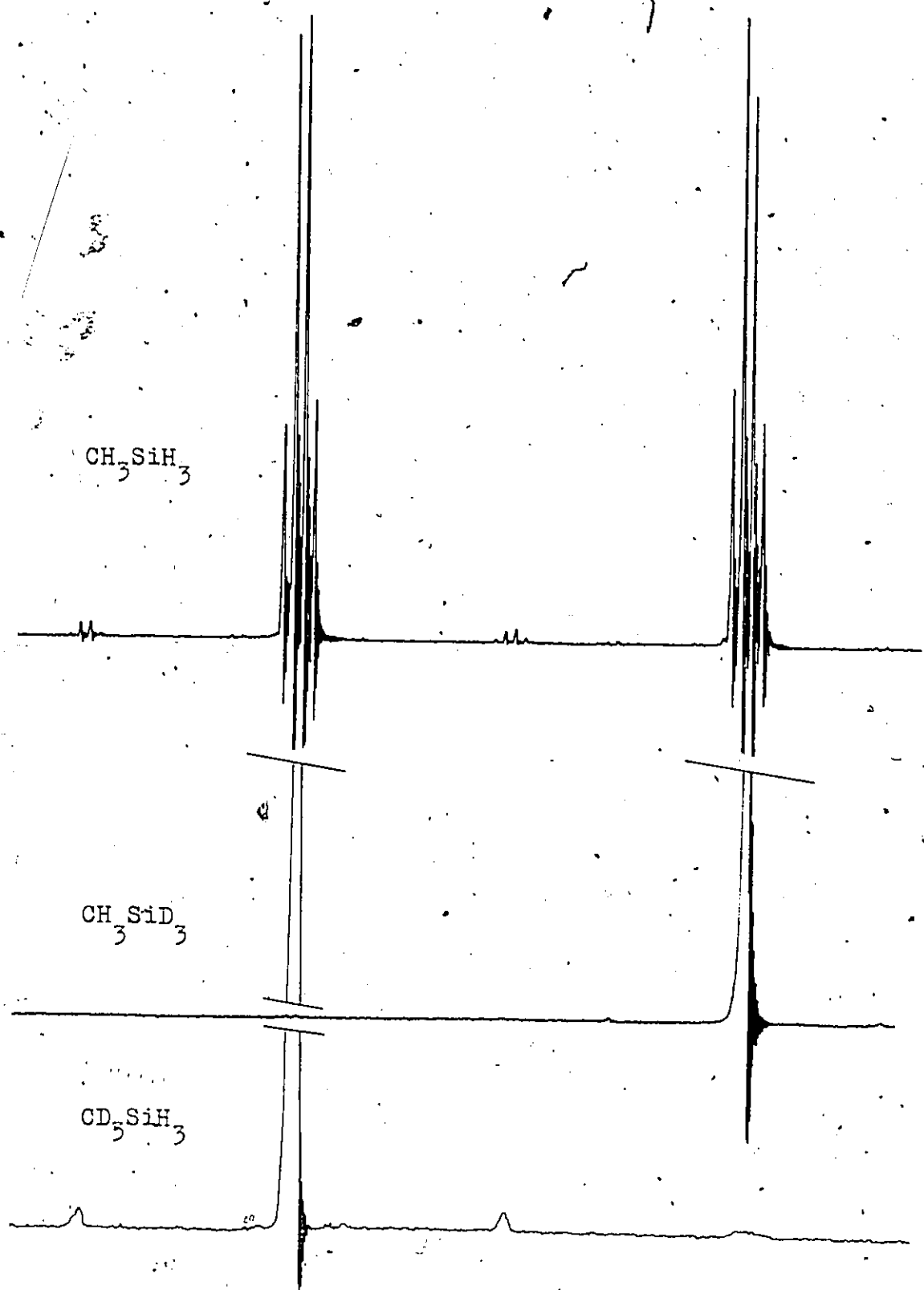
CD$_3$SiH$_3$

Figure 1.1 ^{1}H n.m.r. spectra of the methylsilanes

peaks due to residual hydrogen nuclei, or estimated by comparison with satellites. In the spectrum of CD_3SiH_3 the signal due to unreacted SiH_4 from the reaction mixture was distinguished principally by the distinctive values for J_{SiH} and also by the chemical shift differences for CD_3SiH_3 with residual methyl protons.

1.2.2 ^{1}H n.m.r. of Chloro-, Bromo- and Iodo-methylsilanes

For the normal compounds $CH_3SiH_nX_{3-n}$ ($n = 1,2$; $X = Cl, Br, I$) the extent of halogenation of CH_3SiH_3 can be determined by the relative intensities of the CH_3- signals, which appear as 1:2:1 triplets for mono-substitution and doublets for di-substitution, the latter resonances also appearing to lower field. Previously determined values for the chemical shifts and their differences and coupling constants are listed in Tables 1.1 and 1.2. Both SiH_n resonances ($n = 1,2$) appear as quartets to lower field, but the relative intensities are not proportional to the amounts present, being the signals due to different numbers of protons. These patterns and chemical shift differences are illustrated in Figure 1.2, where a product mixture from a reaction between CH_3SiH_3 and BBr_3 (mainly CH_3SiH_2Br) has in time undergone disproportionation to give the di-, mono- and un-substituted methylsilane derivatives. The inserts are the satellites due to coupling of the silylene protons with ^{29}Si in CH_3SiH_2Br.

Where the halogen is not the same, as in a partial exchange reaction for instance, the compounds involved can

Table 1.1

^1H n.m.r. parameters of selected silanes

	δCH_3	δSiH	$\tilde{\Delta\delta}^a$	J_{SiH}	J_{CH}	J_{HH}
SiH_4	-	3.20[1]	-	202.5[2]	-	-
CH_3SiH_3	0.10	3.53	3.43	194.2	122.1	4.68
CH_3SiH_2F	0.37	4.77	4.40	222.3	120.7	3.27
CH_3SiH_2Cl	0.54	4.73	4.19	229.0	122.8	3.61
CH_3SiH_2Br	0.72	4.51	3.79	231.1	123.7	3.71
CH_3SiH_2I	0.99	4.14	3.15	231.0	124.4	3.86
$(CH_3SiH_2)_2O$	0.26	4.66	4.40	(212.3)	(120.0)	3.30
CH_3SiHF_2	0.28	4.77	4.49	273.1	121.3	1.22
CH_3SiHCl_2	0.80	5.59	4.79	280.8	124.2	2.29
CH_3SiHBr_2	1.12	5.69	4.57	280.8	125.1	2.52
CH_3SiHI_2	1.71	5.20	3.49	271.6	126.4	2.94
$(CH_3)_2SiH_2$	0.09	3.79	3.70	188.6	120.7	4.17
$(CH_3)_2SiHF$	0.26	4.81	4.55	215.8	120.0	2.69
$(CH_3)_2SiHCl$	0.47	4.87	4.40	222.8	121.8	3.09
$(CH_3)_2SiHBr$	0.66	4.84	4.18	225.0	122.4	3.20
$(CH_3)_2SiHI$	0.92	4.80	3.88	224.8	123.1	3.41
$[(CH_3)_2SiH]_2O$	0.15	4.73	4.58	(205.2)	(118.8)	2.80
CH_3SiF_3	0.53[3]	-	-	-	-	-
CH_3SiCl_3	1.14[3,4]	-	-	-	127.2[5]	-
CH_3SiBr_3	~1.56[5]	-	-	-	-	-
CH_3SiI_3	2.40[6]	-	-	-	128.7[6]	-
$(CH_3)_2SiF_2$	0.32[3]	-	-	-	-	-
$(CH_3)_2SiCl_2$	0.80[3,4] 0.76[7]	-	-	-	123.2[5]	-
$(CH_3)_2SiBr_2$	1.18[5] 1.07[7]	-	-	-	124.5[5]	-
$(CH_3)_2SiI_2$	1.60[5]	-	-	-	125.8[5]	-

a) $\Delta\delta = \delta SiH - \delta CH_3$

1)ref.8; 2)ref.9; 3)ref.10; 4)ref.11; 5)this work; unpublished data; 6)ref.12; 7)ref.13.

Table 1.2

Differences in δCH_3 and δSiH resonances for halogenated methylsilanes.

X =	Cl		Br		I	
	$\Delta\delta CH_3$	$\Delta\delta SiH$	$\Delta\delta CH_3$	$\Delta\delta SiH$	$\Delta\delta CH_3$	$\Delta\delta SiH$
CH_3SiH_3						
	0.44	1.20	0.62	0.98	0.89	0.61
CH_3SiH_2X						
	0.26	0.86	0.40	1.18	0.72	1.06
CH_3SiHX_2						
$(CH_3)_2SiH_2$						
	0.38	1.08	0.57	1.05	0.83	1.01
$(CH_3)_2SiHX$						
	0.31	-	0.46	-	0.68	-
$(CH_3)_2SiX_2$						

Table 1.3 ^1H n.m.r. data for fluoromethylsilanes

	δCH_3	δSiH	$\Delta\delta^a$	SGF†		this work	
				J^{vic}_{HF}	$J^{gem}_{H'F}$	J^{vic}_{HF}	$J^{gem}_{H'F}$
$CH_3SiH'_2F$		4.77		8.3	48.8		
CH_3SiD_2F	0.37	-	4.40	8.3	7.47^b	8.34	7.48
$CD_3SiH'_2F$	-	4.77		-	48.8		
$(CH_3SiH_2)_2O$	0.26	4.66	4.40	-	-	-	-
$CH_3SiH'F_2$		4.77		6.63	67.5		
CH_3SiDF_2	0.28	-	4.49	6.63	10.36^b	6.79	10.49
$CD_3SiH'F_2$	-	4.77		-	67.5		68.3
$(CH_3SiHF)_2O$	0.27	4.74	4.47	6.61	68.2		68.5
$(CH_3)_2SiHF$	0.26	4.81	4.55	7.63	52.1		
$[(CH_3)_2SiH]_2O$	0.15	4.73	4.58	-	-	-	-

a) $\Delta\delta = \delta SiH - \delta CH_3$ †) ref. 5

b) J^{gem}_{DF} calculated as $0.1535 \cdot J^{gem}_{HF}$
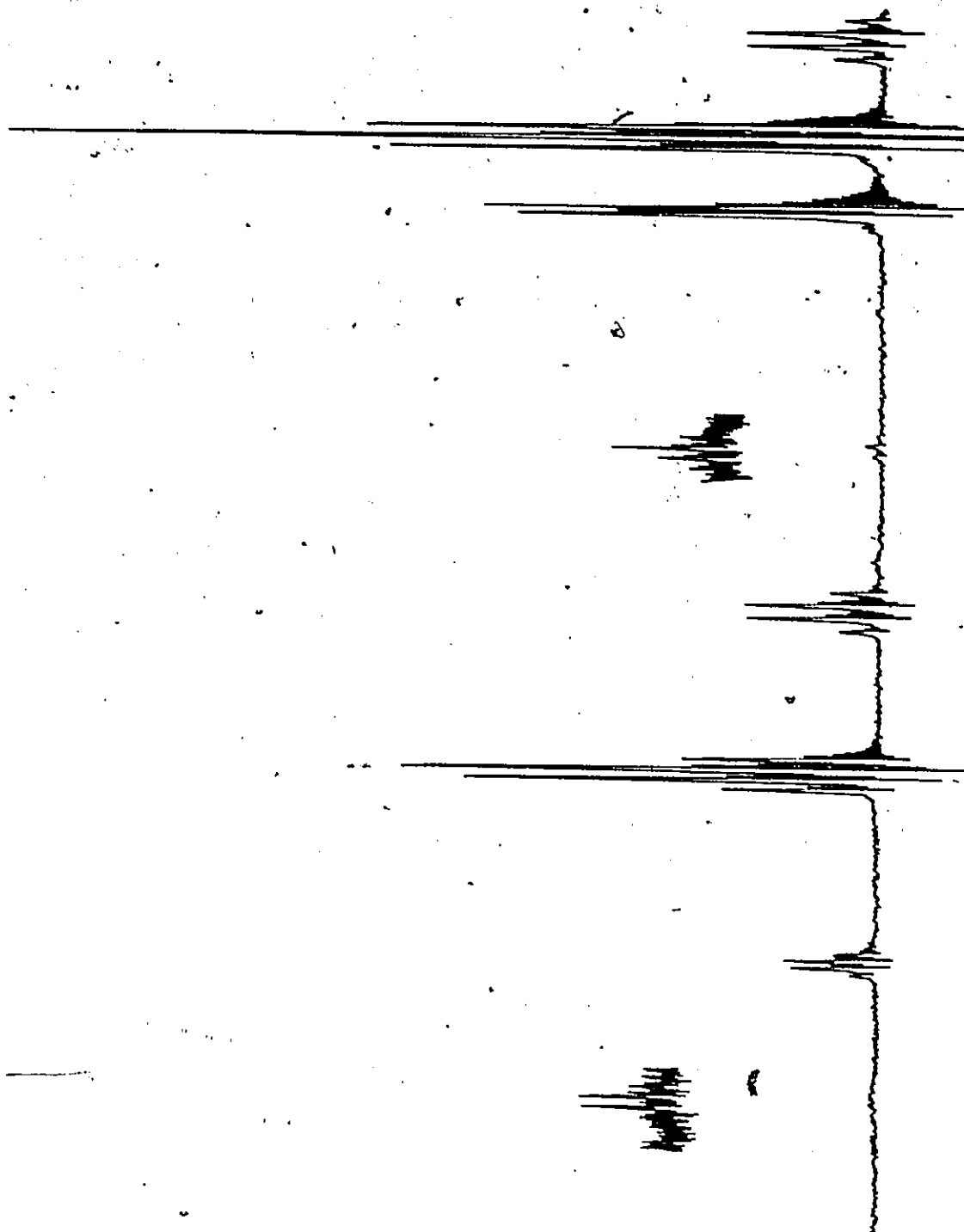
Figure 1.2 Disproportion products of bromomethylsilane, showing peaks due to CH_3SiHBr_2, CH_3SiH_2Br and CH_3SiH_3

be determined by differences in chemical shift, either between CH_3- and SiH_n- resonances in the same molecule, or between the $\delta\ CH_3$ or $\delta\ SiH_n$ positions in the two different molecules. The latter difference is also the most useful way of distinguishing between two compounds when either the methyl or silyl groups are deuterated. In contrast to chemical shift differences, the J_{HH} values are of little diagnostic value, being small and fairly similar.

Deuteration at either carbon or silicon removes one resonance and splitting patterns as for the methylsilanes, producing a single resonance. In most cases, however, chemical shift differences can still be measured as there are usually a sufficient number of residual protons to produce an observable signal, either as CHD_2 or $SiH(D)$. Use is also made of J_{CH} and J_{SiH} (for directly bonded protons) although J_{CH} is not as definitive as J_{SiH} due to the lower intensity and narrower, overlapping ranges of values. For mono-[3] and di-substituted[4] derivatives respectively these are 120.7-124.4 and 121.3-126.4 Hz for J_{CH} (122.1 Hz for CH_3SiH_3, in both ranges) but fall into two separate regions for J_{SiH}, 222.3-231.1 and 271.6-280.8 Hz respectively (194.2 Hz for CH_3SiH_3). There is also coupling between methyl protons and ^{29}Si (J_{HCSi}) to the extent of ~ 8 Hz; but these are of little value since the satellites are too close to the methyl resonance and insensitive to changes in halogen. Typical spectra obtained for mono- and di-substituted derivatives, respectively the monobromides and diiodides are shown in

CH_3SiH_2Br

CD_3SiH_2Br

CH_3SiD_2Br
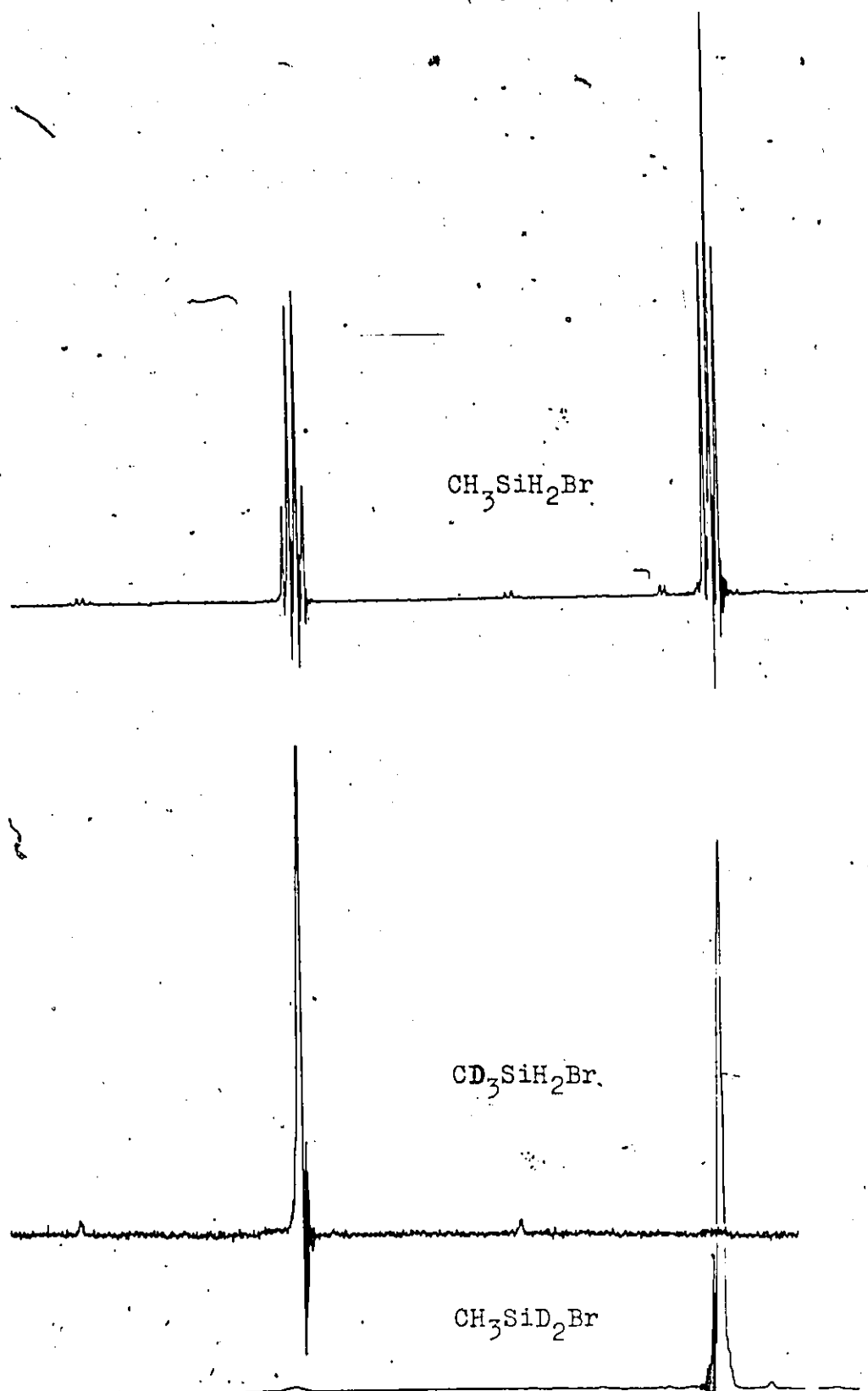
Figure 1.3 ^{1}H n.m.r. spectra of bromomethylsilanes

CH$_3$SiHI$_2$

CD$_3$SiHI$_2$

CH$_3$SiDI$_2$.
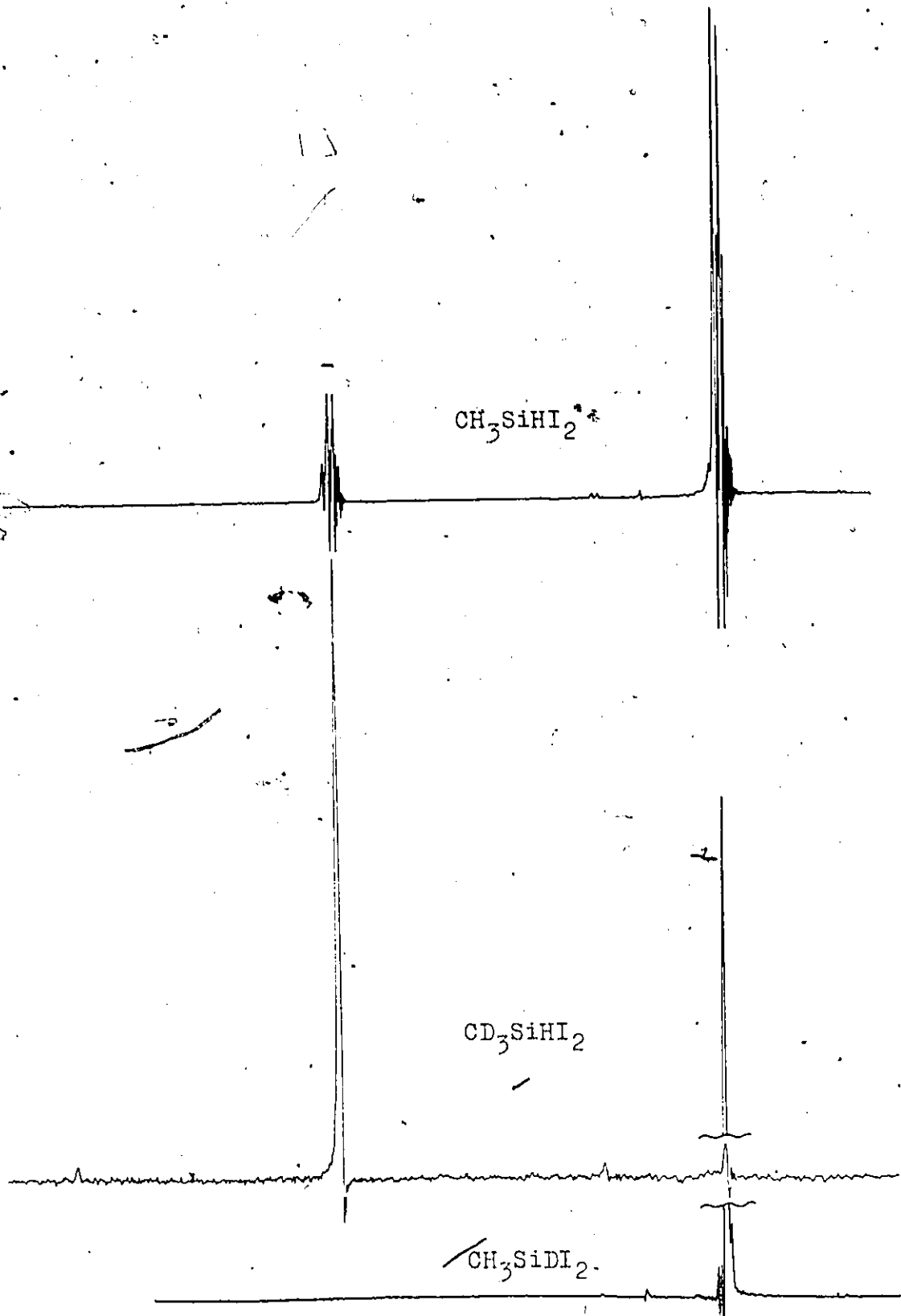
Figure 1.4 ^{1}H n.m.r. spectra of diiodomethylsilanes

Figures 1.3 and 1.4.

1.2.3 ^{1}H n.m.r. of Chloro-, Bromo- and Iodo-dimethylsilanes

The ^{1}H n.m.r. spectra of the $(CH_3)_2SiHX$ compounds
(X = Cl, Br, I) exhibit the expected seven line Si$\underline{H}$ signal and
doublet C$\underline{H}_3$ resonance and are shown in Figure 1.5, where the
spectra have been offset relative to their chemical shifts.
The inserts are the ^{13}C satellites and the high-field satel-
lite from ^{29}Si coupling. Deuteration at silicon again pro-
duces a singlet due to δ C$\underline{H}_3$, as J_{HD} is again too small to
be observed other than as line-broadening. The spectra of
these $(CH_3)_2SiDX$ compounds are shown in Figure 1.6, which
shows the SiH region as well as the C$\underline{H}_3$ resonances which in
this case are not offset corresponding to their relative
chemical shifts.

Values of chemical shifts are found to vary by
~0.1 ppm depending on the concentration of compound in the
sample, so some slight differences in the figures in Tables
1.1 and 1.2 were observed. The values for J however are
essentially constant for varying concentrations[4].

1.2.4 ^{1}H and ^{19}F n.m.r. for Fluorine Containing Compounds

Few of the methods described above were necessary
for the fluoro- derivatives due to the large splitting of ^{1}H
resonances by ^{19}F nuclei, which was observed even for vicinal
protons ($\underline{H}$CSi$\underline{F}$) where J_{HF}^{vic} is 6-8 Hz. In fluoro-methylsilane
and -dimethylsilane ^{1}H signals are split into doublets, and
in difluoromethylsilane into triplets. The spectra are shown
in Figures 1.7, 1.8 and 1.9.
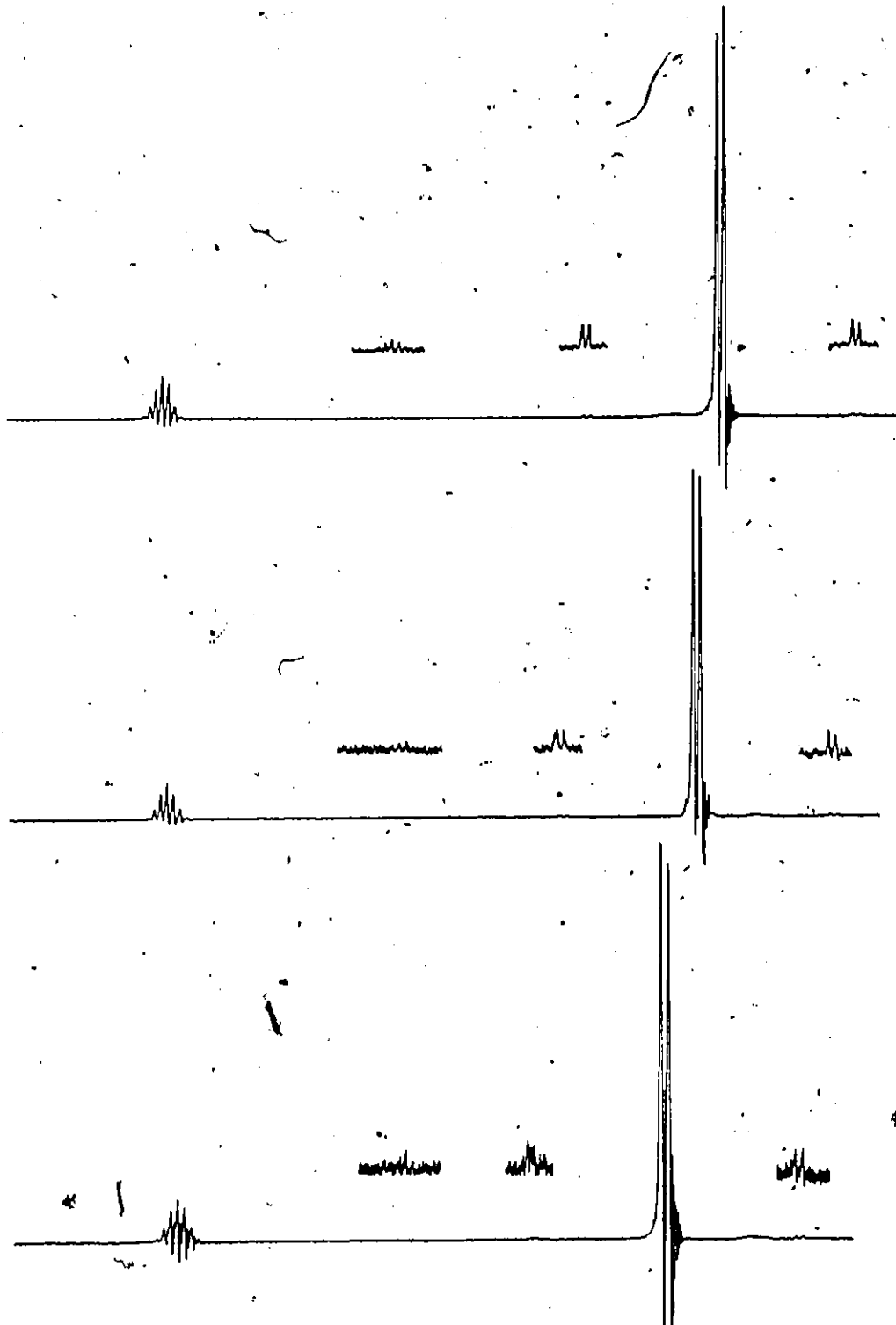
Figure 1.5 ^{1}H n.m.r. spectra of (top to bottom)
$(CH_3)_2SiHCl$, $(CH_3)_2SiHBr$ and $(CH_3)_2SiHI$
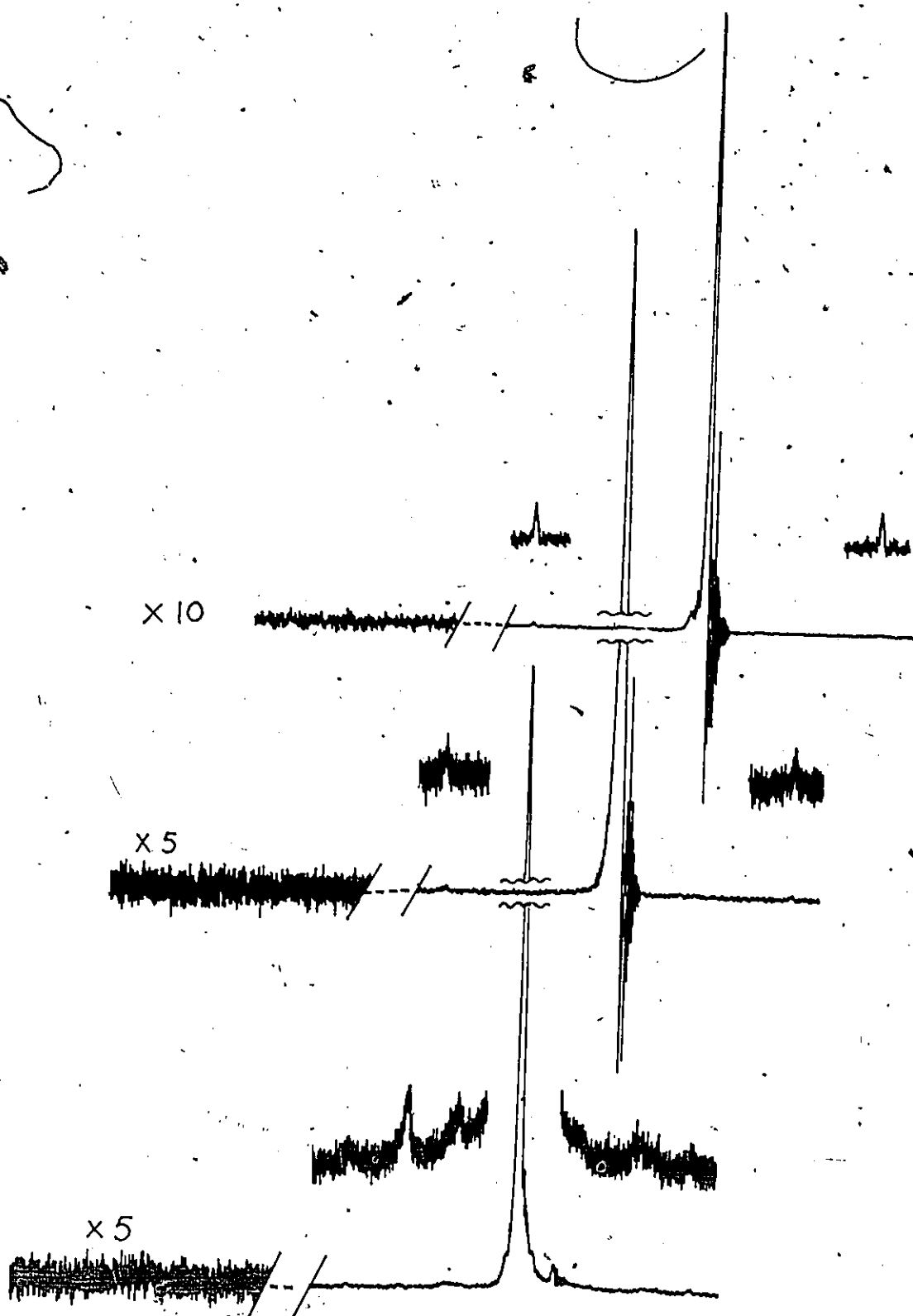
Figure 1.6   Partial ^{1}H n.m.r. spectra of (top to bottom)
$(CH_3)_2SiDCl$, $(CH_3)_2SiDBr$ and $(CH_3)_2SiDI$

CH_3SiH_2F

CD_3SiH_2F
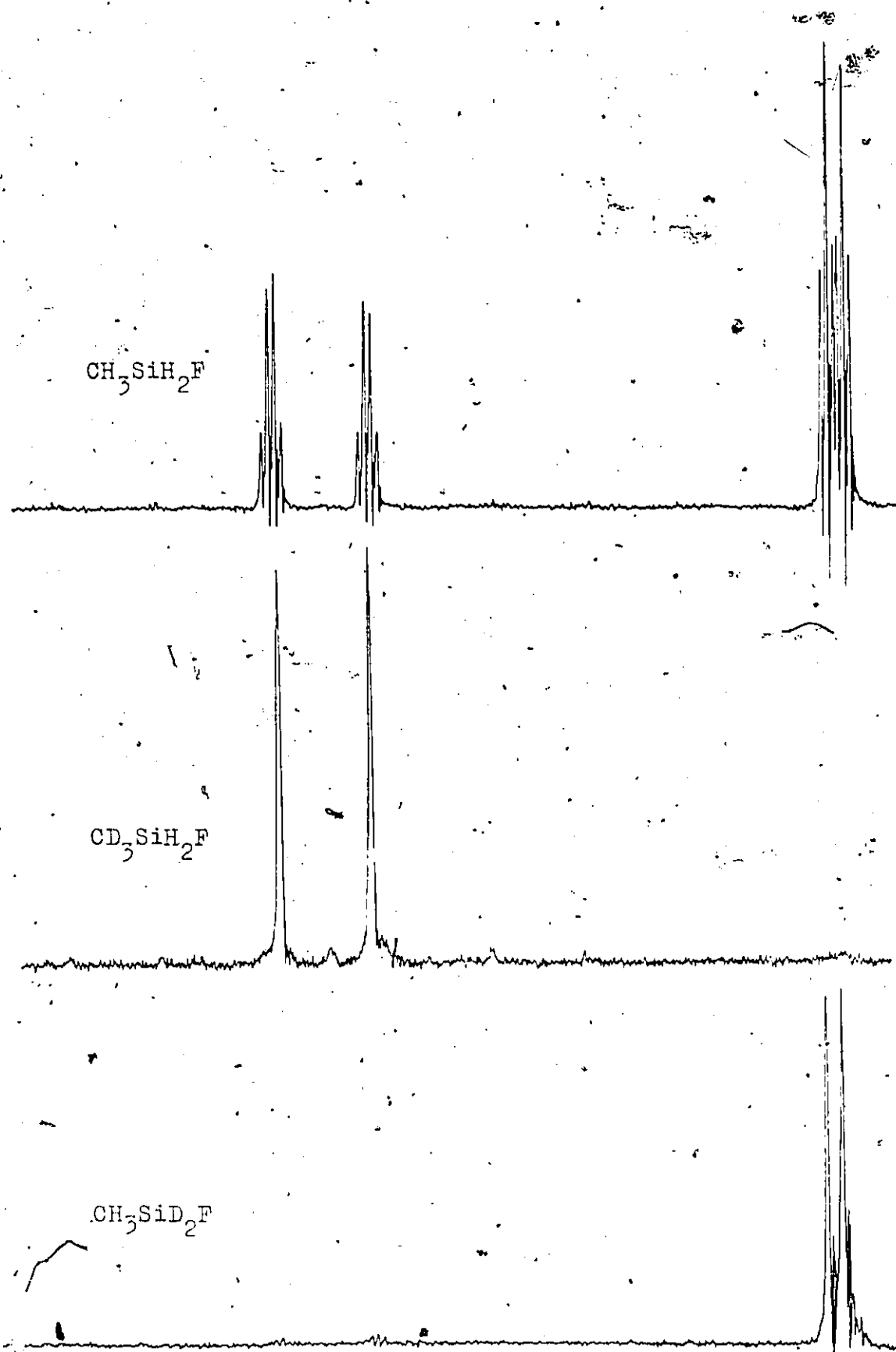
CH_3SiD_2F

Figure 1.7 ^1H n.m.r. spectra of fluoromethylsilanes

CH₃SiHF₂

CD₃SiHF₂

CH₃SiDF₂

×10
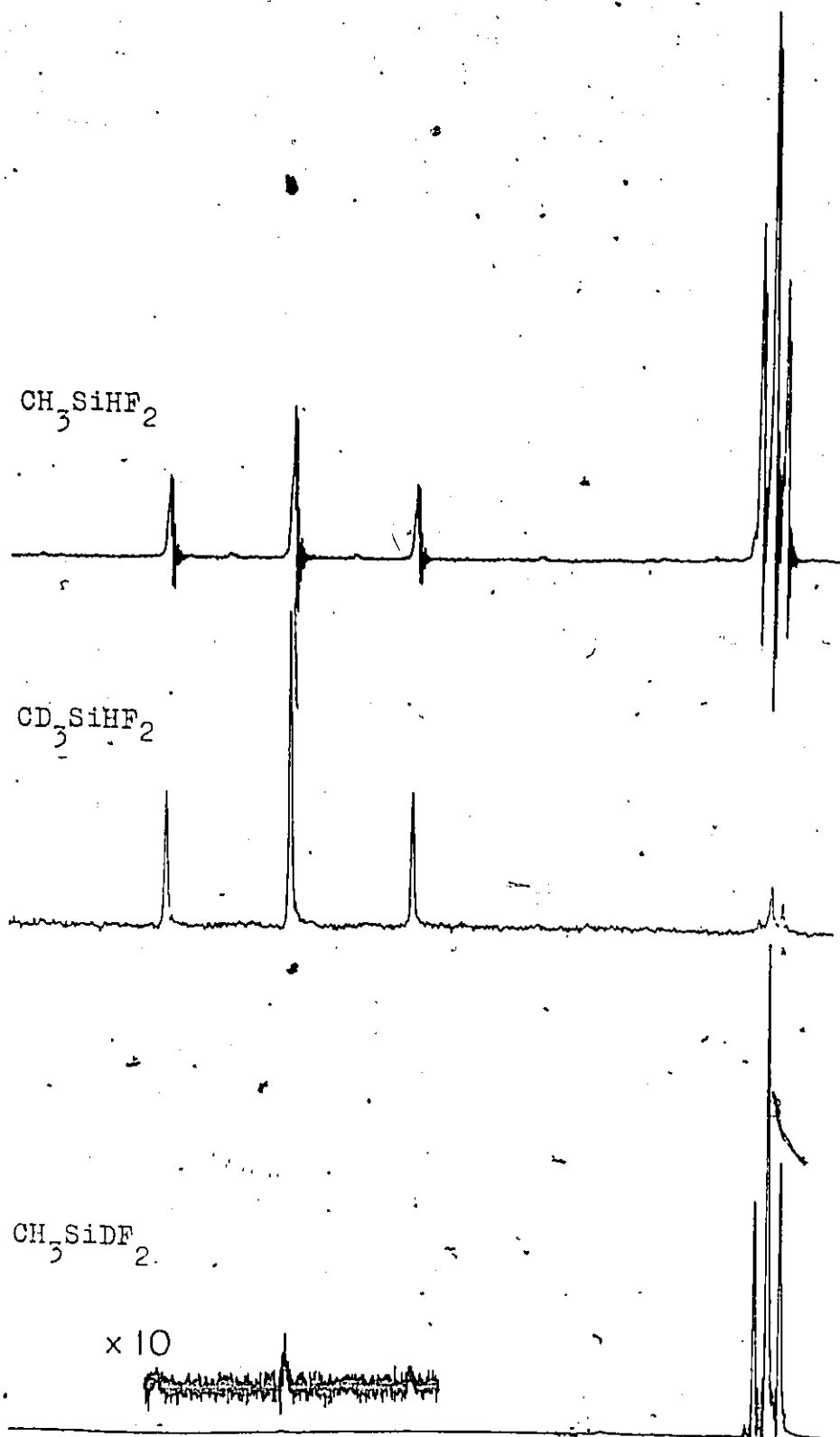
Figure 1.8 ¹H n.m.r. spectra of difluoro-methylsilanes
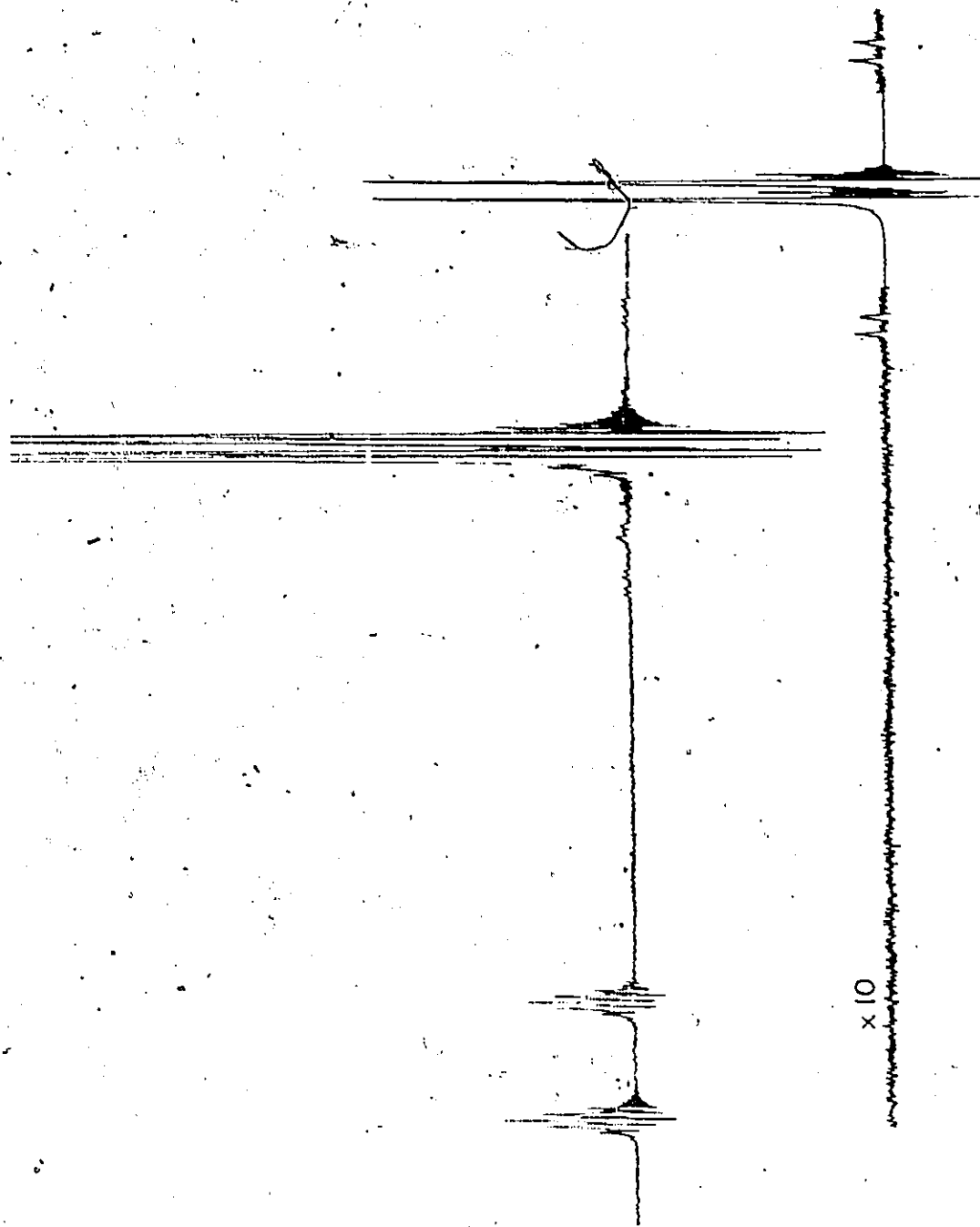
Figure 1.9 ^{1}H n.m.r. spectra of (top) $(CH_3)_2SiHF$ and $(CH_3)_2SiDF$

In the infrared spectrum of CH_3SiDF_2, the SiD stretching region was found to contain two almost equally intense, sharp lines separated by $\sim 30\ cm^{-1}$, even though the ^1H n.m.r. spectrum indicated no apparent (hydrogen-containing) impurity. No other known SiD stretching frequency fitted the "extra" frequency, so a ^{19}F n.m.r. investigation was undertaken to see if an impurity containing fluorine but not hydrogen was present. As the values for the coupling constant J_{HF}^{gem} {H-Si-F} are large[4], it was expected that coupling involving deuterium (J_{DF}^{gem}) would be observed which would serve as an added means of identification. While the instrument was in the ^{19}F mode, the opportunity to record the spectrum of CH_3SiD_2F also arose, and this will be dealt with first.

The ^{19}F n.m.r spectrum of CH_3SiD_2F should consist of a 1:2:3:2:1 quintet of 1:3:3:1 quartets from coupling with two deuterium and three hydrogen nuclei respectively, producing a twenty line spectrum. Preliminary observations however, indicated a spectrum of only eight lines, although each line had some fine structure (Figure 1.10b). Such a spectrum would only be possible if both J_{HF}^{vic} and J_{DF}^{gem} were the same, i.e. if the quartets (or quintets) are overlapped with each other just one value of J apart. This eight line spectrum would then have a theoretical intensity of 1:5:12:18:18:12: 5:1. The observed intensity for each "packet" of lines (since the fine structure splitting was too small to generate separate integration signals) was found to be

$$1.0\ :\ 5.2\ :\ 11.9\ :\ 18.2\ :\ 17.8\ :\ 12.1\ :\ 5.0\ :\ 0.7$$

(A)
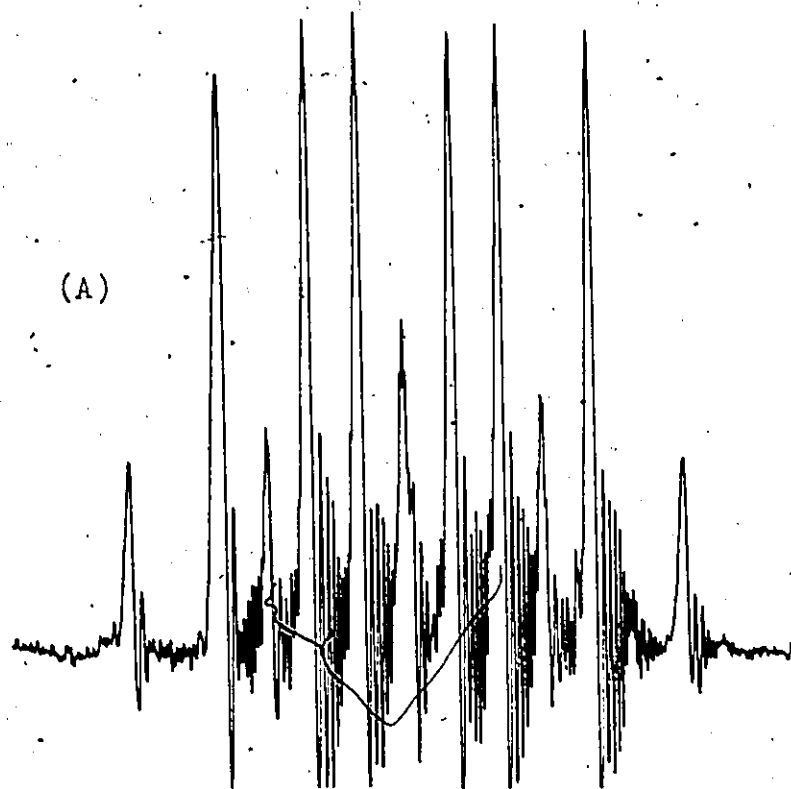
Figure 1.10 ^{19}F n.m.r. spectra of (A) CH_3SiDF_2
and (B) CH_3SiD_2F

(B)
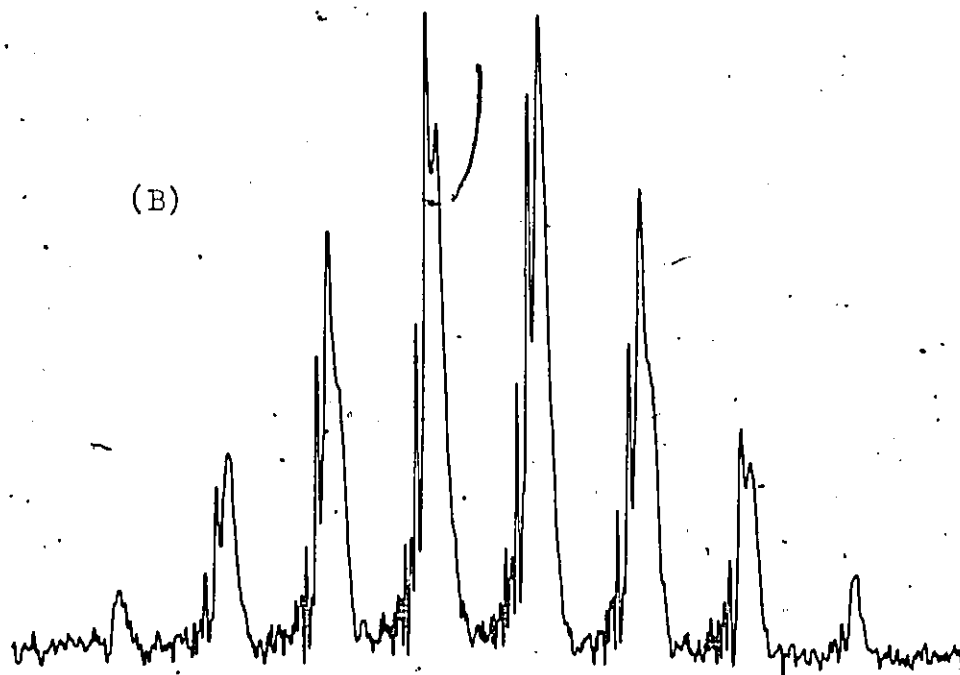
where the central peaks have been normalised to 18 intensity units. The patterns in the fine structure could be duplicated as shown in Figure 1.11 using values of $J_{HF}^{vic} = 8.34$ Hz and $J_{DF}^{gem} = 7.48$ Hz, (both ± 0.06 Hz). This latter value corresponds at a J_{HF}^{gem} for CH_3SiH_2F of 48.7±0.4 Hz compared to the literature value of 48.8±0.2 Hz[3].

The spectrum of CH_3SiDF_2 (Figures 1.10a and 1.12) was found to contain an impurity to slightly lower field, which was assumed to be $(CH_3SiDF)_2O$, formed presumably from Sb_2O_3 formed in SbF_3 from moisture prior to packing the exchange column, as the column was heated and pumped overnight prior to exchange. Although reported as having the same chemical shift as CH_3SiDF_2[5] it was found to be 0.75±0.03 ppm downfield. (The Si-D stretching frequency expected from this molecule by comparison with $(CH_3SiHF)_2O$[12] is not expected to produce the "extra" band in the vibrational spectrum CH_3SiDF_2 in either position or intensity, and the observed doublet was subsequently explained by Fermi resonance). The expected ^{19}F n.m.r. spectrum is a 1:1:1 triplet of 1:3:3:1 quartets. An eleven line spectrum is observed in which the highest field resonance of the low field quartet overlaps with the lowest field signal of the high field quartet. For this coincidence to be exact the coupling constants would have to be in a 2:3 ratio. The results, listed in Table 1.3, along with other fluoro- derivative published data, show $J_{HF}^{vic} = 6.79\pm0.06$ Hz and $J_{DF}^{gem} = 10.49\pm0.08$ Hz, a ratio of 2: 3.08. The splitting patterns of both compounds are shown in
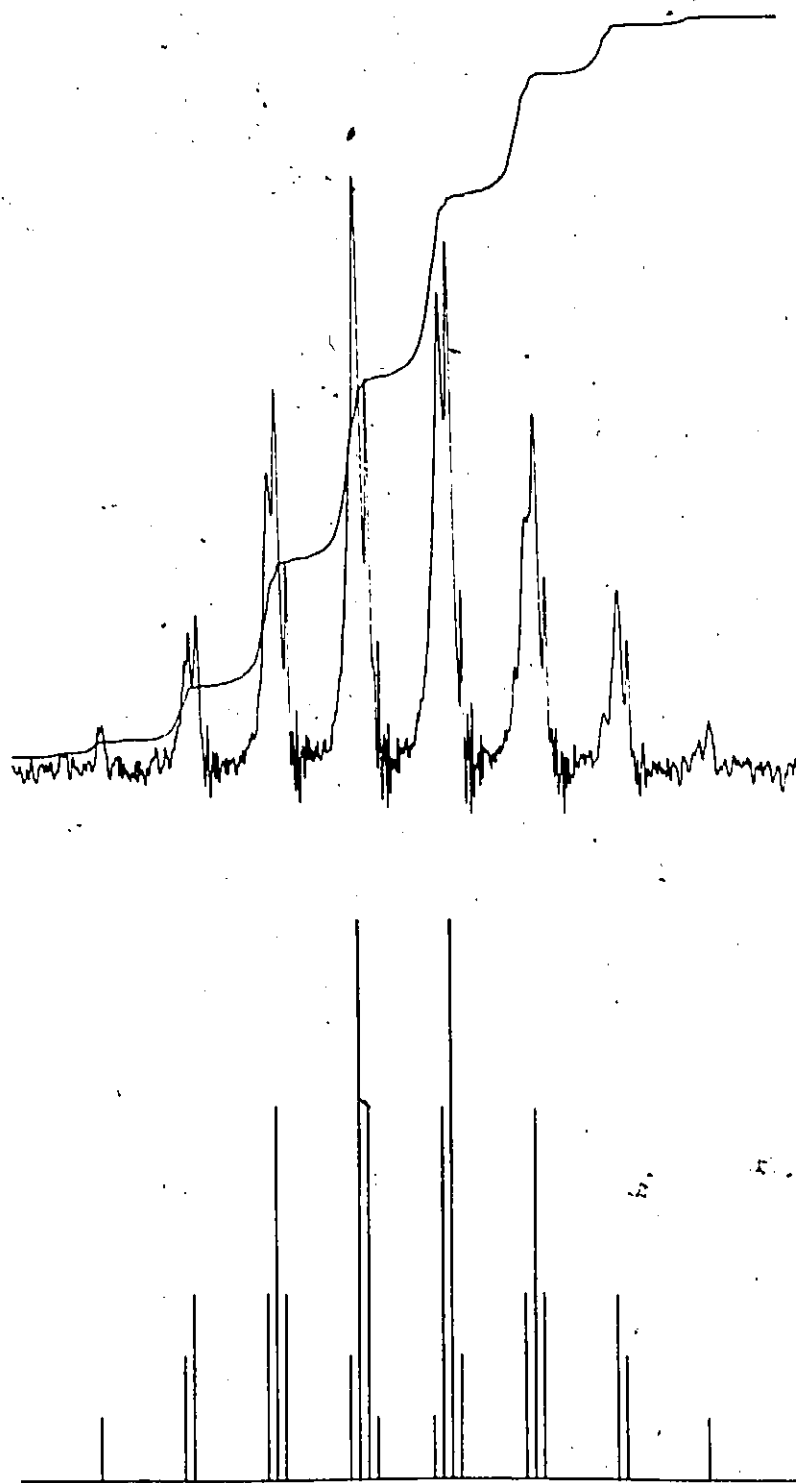
Figure 1.11   Observed and calculated ^{19}F n.m.r. spectrum of CH_3SiD_2F
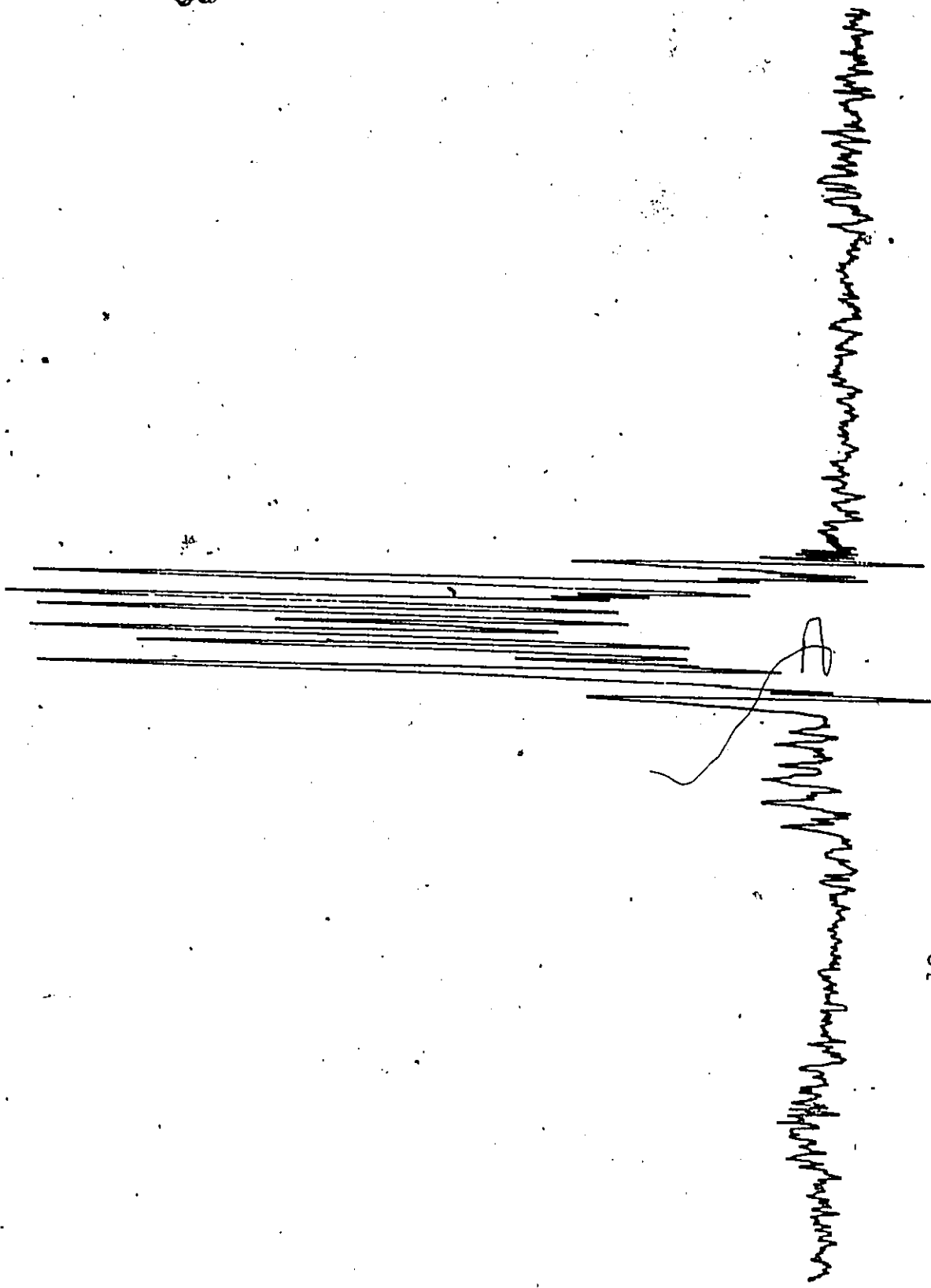
Figure 1.12 ^{19}F n.m.r. spectrum of CH_3SiDF_2

Figure 1.13. The extreme peaks in Figure 1.12, most notice-
able to low field, are the satellites due to coupling with
the ^{29}Si nucleus, with an observed J_{SiF} of 291.4 ± 3.0 Hz,
compared with a literature value of 291 ± 3 Hz[5]. No signal
integration was recorded, but the $(CH_3SiDF)_2O$ impurity can
be seen to be ca. 5% by comparison with the ^{29}Si satellites,
as described above. Reinvestigating the ^1H n.m.r. spectrum
(Figure 1.8), the triplet due to the $C\underline{H}_3$ protons is seen to
be unsymmetrical. Since J_{HF}^{vic} for both CH_3SiDF_2, and
$(CH_3SiDF)_2O$ are virtually the same (6.63 and 6.61 Hz respec-
tively[4,5]) and the methyl resonance of the siloxane is expect-
ed to higher field (see Table 1.1), it is probable that the
expected doublet from $(CH_3SiDF)_2O$ is exactly underneath
the two high field signals of the $C\underline{H}_3SiDF_2$ triplet. (J_{HD} is
~ 0.2 Hz in both cases and so unobservable). This would
indicate a difference in chemical shift of $J_{HF}^{vic}/2$ or 0.055
ppm for the two compounds under these conditions.

The formation of the fluorosiloxane by oxide impurity
in SbF_3 also occurred in the preparation of CD_3SiHF_2, but
before the ^{19}F.m.r. investigation described above was
carried out and so at first not immediately suspected. The
^1H n.m.r. spectrum of the exchange products produced what
appeared to be a 1:1:2:1:1 quintet with equidistant spacing
(Figure 1.14a), but which obviously could not be caused by a
single compound. This can also be inferred from the observa-
tion that the equal peak heights in Figure 1.14b are not
consistent with the signal integration. The possibility of
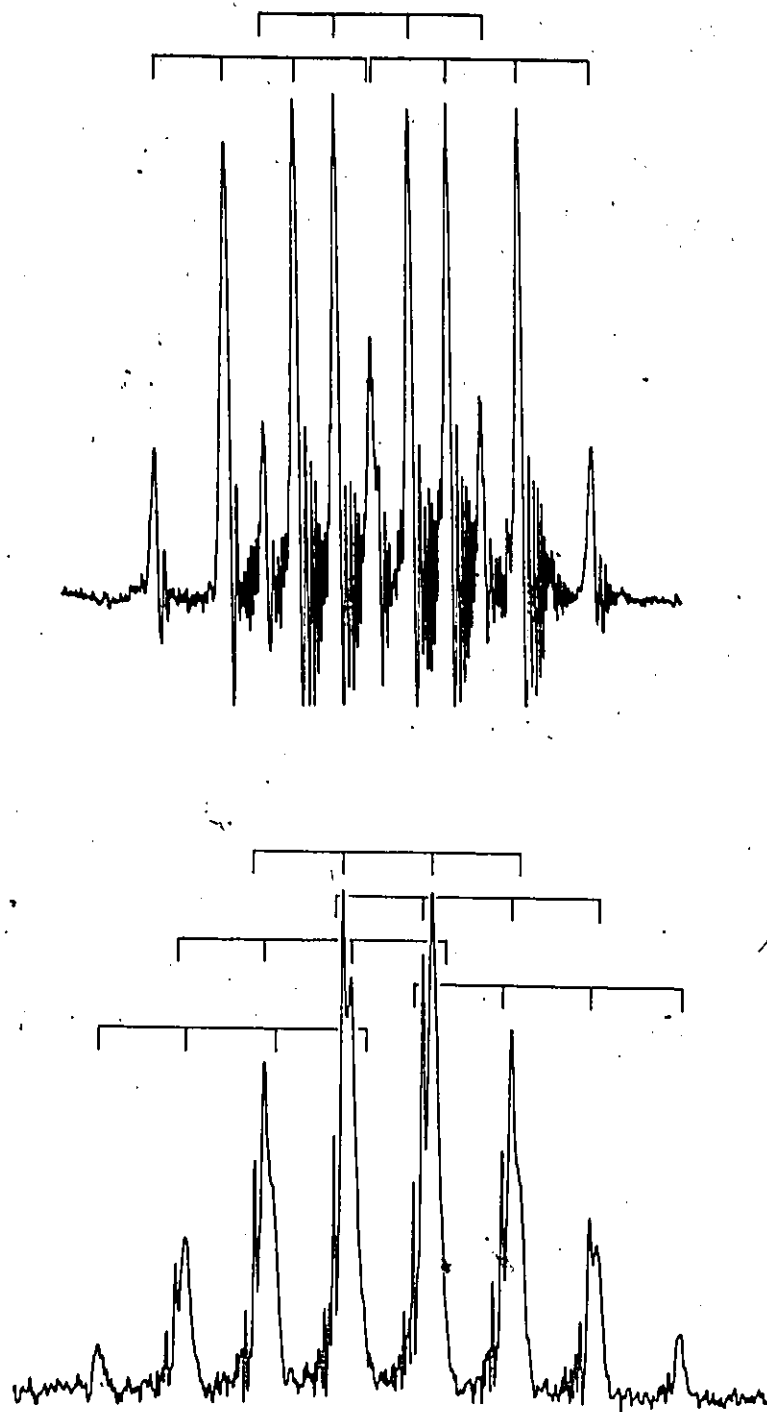
Figure 1.13   Coupling patterns in ^{19}F n.m.r. spectra
of (top) CH_3SiDF_2 and CH_3SiD_2F
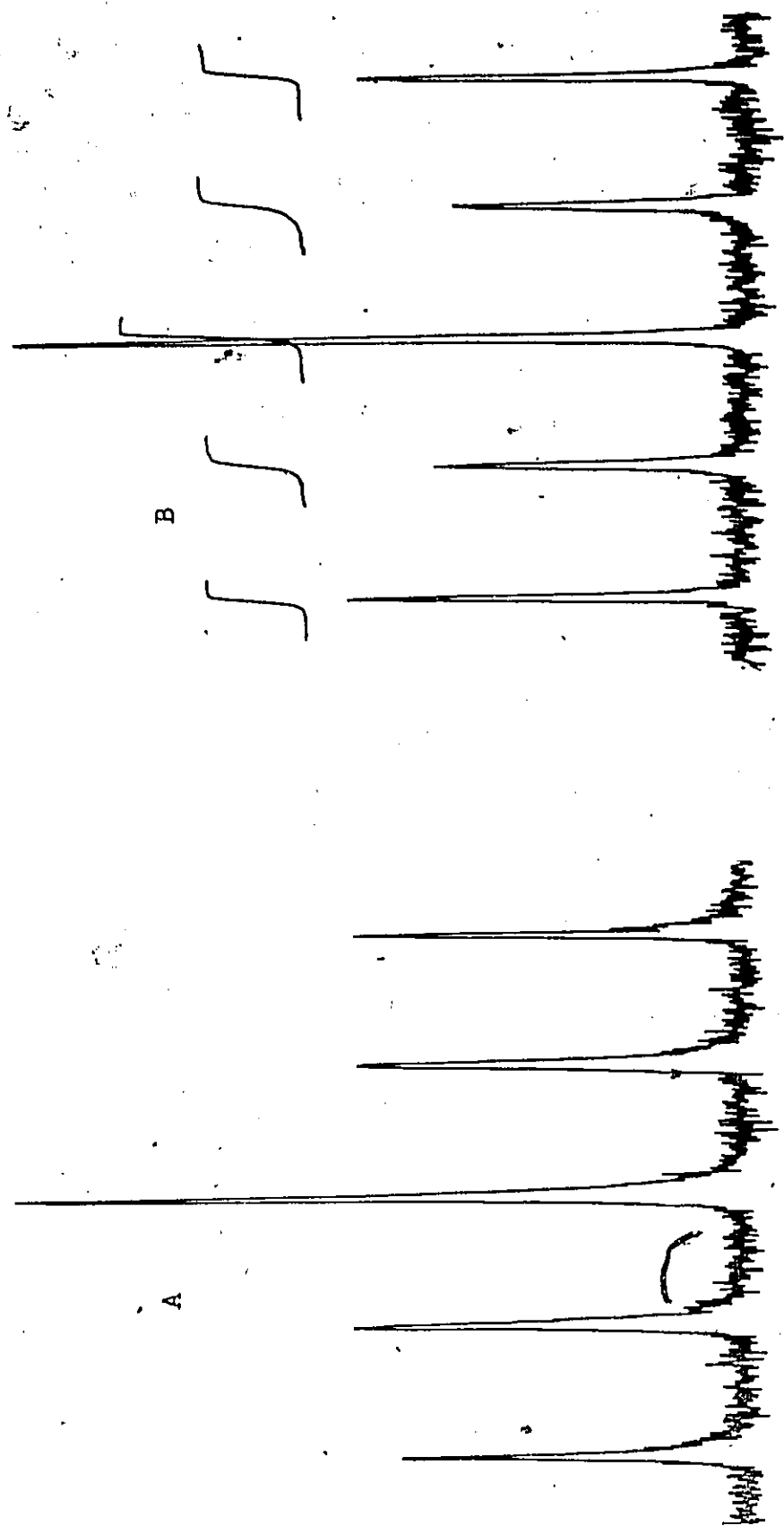
Figure 1.14 ^{1}H n.m.r. spectra of SiH region of "CD$_3$SiHBr$_2$ - SbF$_3$" sample

disproportion to CD_3SiF_3, which would not give a signal, and $\cdot CD_3SiH_2F$, which has virtually the same chemical shift and would be present as a doublet, was ruled out by the coupling constant J_{HF}^{gem}, which, as mentioned above, is ~ 48 Hz for CD_3SiH_2F, but which measured at ~ 68 Hz. Reaction of the mixture with BF_3, to restore the fluoro- compound at the expense of the siloxane[13], reduced the inner doublet (and produced the spectrum in Figure 1.14b) which led to the result that the impurity was $(CD_3SiHF)_2O$. In the concentrations in which each was present in the mixture, the chemical shifts were the same within measurable limits and the J_{HF}^{gem} were observed to be 68.3 ± 0.6 Hz for CD_3SiHF_2 and 68.5 ± 0.6 Hz for $(CD_3SiHF)_2O$, which together account for the "uniqueness" of the original spectrum. Passage of the mixture through a trap at $-112^\circ C$ completely separated the two compounds as can be seen from Figure 1.15. The small triplet to high field in the spectrum of CD_3SiHF_2 is due to the resonance of residual methyl protons, presumably in the form CHD_2SiHF_2, showing a J_{HF}^{vic} of ~ 6.3 Hz, but not the coupling due to J_{HH} (~ 1.2 Hz) which at this intensity is observable only as line-broadening.

1.2.5 Stability of Halogenomethylsilanes

The compounds studied in this work were kept in sealed capillary tubes at room temperature after their spectra had been recorded. No special precautions were taken to protect them from light. ^1H n.m.r. spectra were recorded from time to time, but except for small peaks due to hydrolysis in
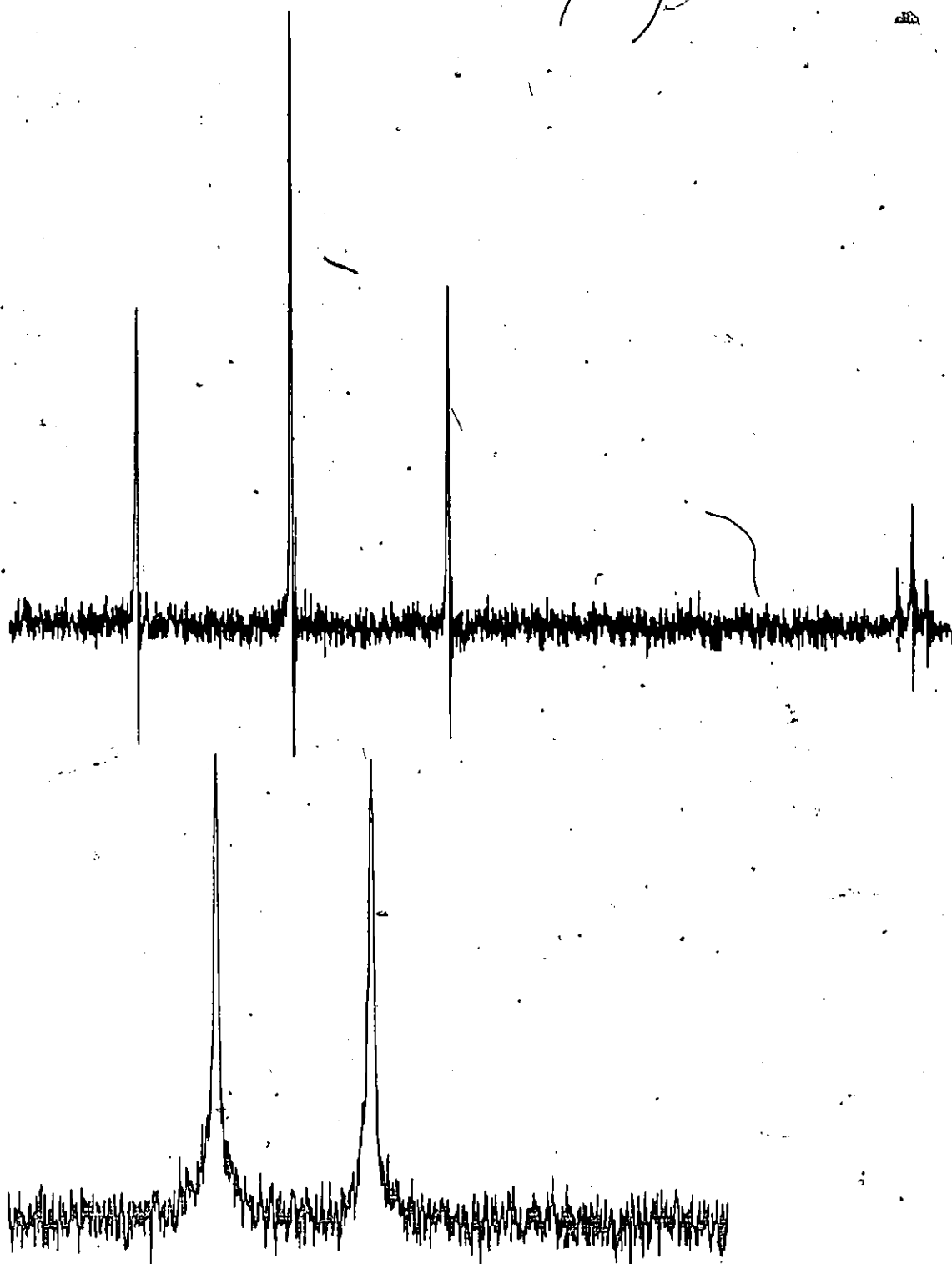
<u>Figure 1.15</u> ^1H n.m.r. spectra of components of CD_3SiHF_2
and $(CD_3SiHF)_2O$ mixture

samples used for recording infrared spectra, most were identical with the original spectra. Exceptions were some samples containing an impurity which disproportionated (as did the sample giving the spectrum in Figure 1.2), although purer samples of the same compounds generally did not. Disproportionation in pure samples was observed however in the case of the monofluoromethylsilanes, which,after a period of over a year or more at room temperature were found to have completely disproportionated to the difluoro- derivative and methylsilane. Figure 1.2.16 shows the ^{1}H n.m.r. spectra of the resulting disproportionation of (A) CD_3SiH_2F and (B) CH_3SiD_2F.

1.2.6 ^{13}C n.m.r. Spectra of the Methyl-d$_3$-silanes

Although the ^{13}C n.m.r. spectra were recorded for most of the compounds prepared in this work as part of a more comprehensive n.m.r. study [14], only the spectra of the CD_3-methylsilanes will be discussed here. These were recorded as a purity check, especially for CD_3SiD_3 which previously had only been checked by mass spectrometry. The spectrum of CD_3SiD_3 is shown in Figure 1.2.17 where only the expected 1:3:6:7:6:3:1 septet resonances (or the more intense components) are observed, at δ -15.86 ppm (δ -15.59 ppm for CD_3SiD_3), i.e. upfield from TMS. This "deuterium shift", or difference in chemical shifts where the carbon nucleus becomes more shielded, has been observed for the $Me_2SiH'X$ (H' = H,D) series [14] and other species [15], and can be explained

34
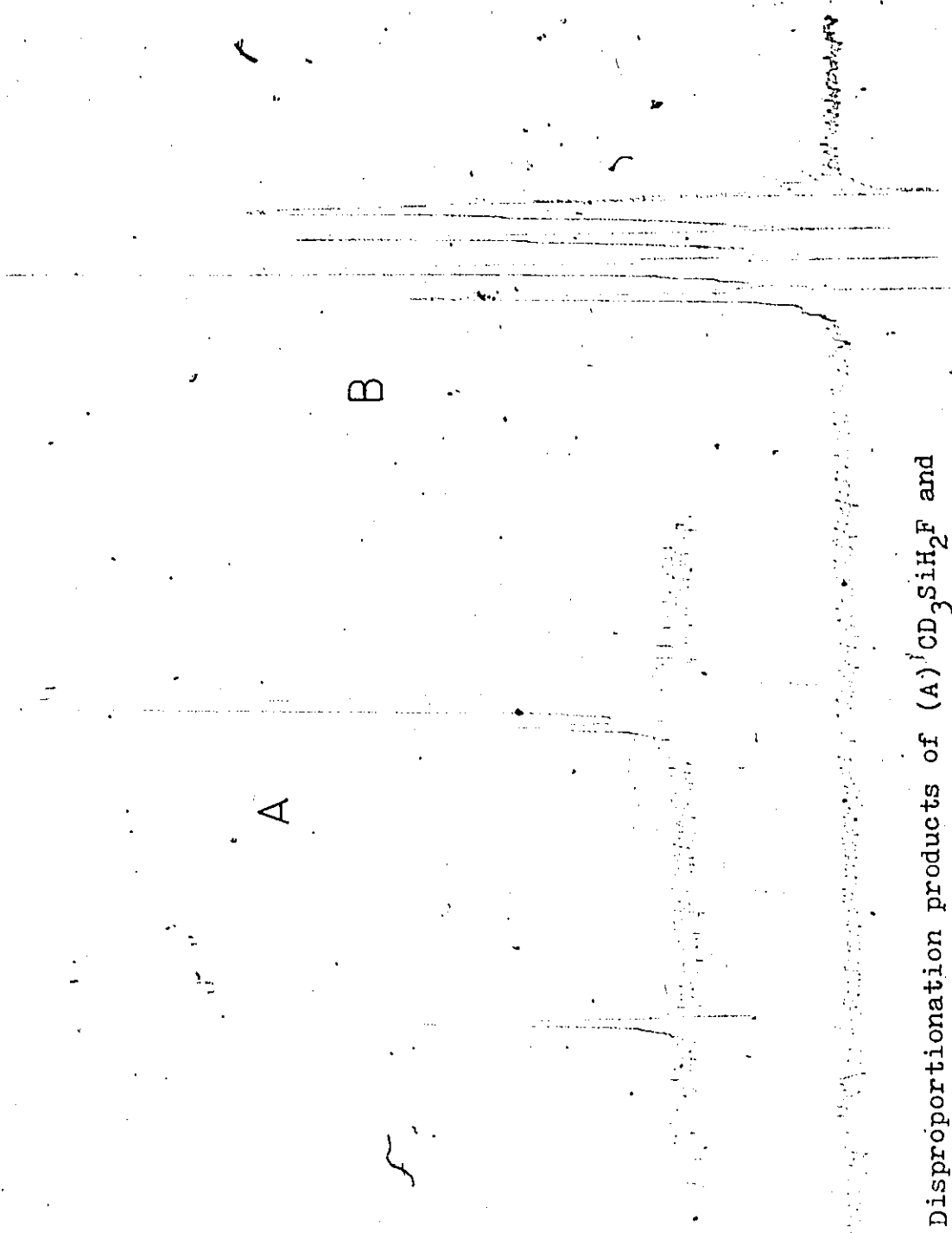
Figure 1.16   Disproportionation products of (A) CD$_3$SiH$_2$F and (B) CH$_3$SiD$_2$F

CDCl$_3$
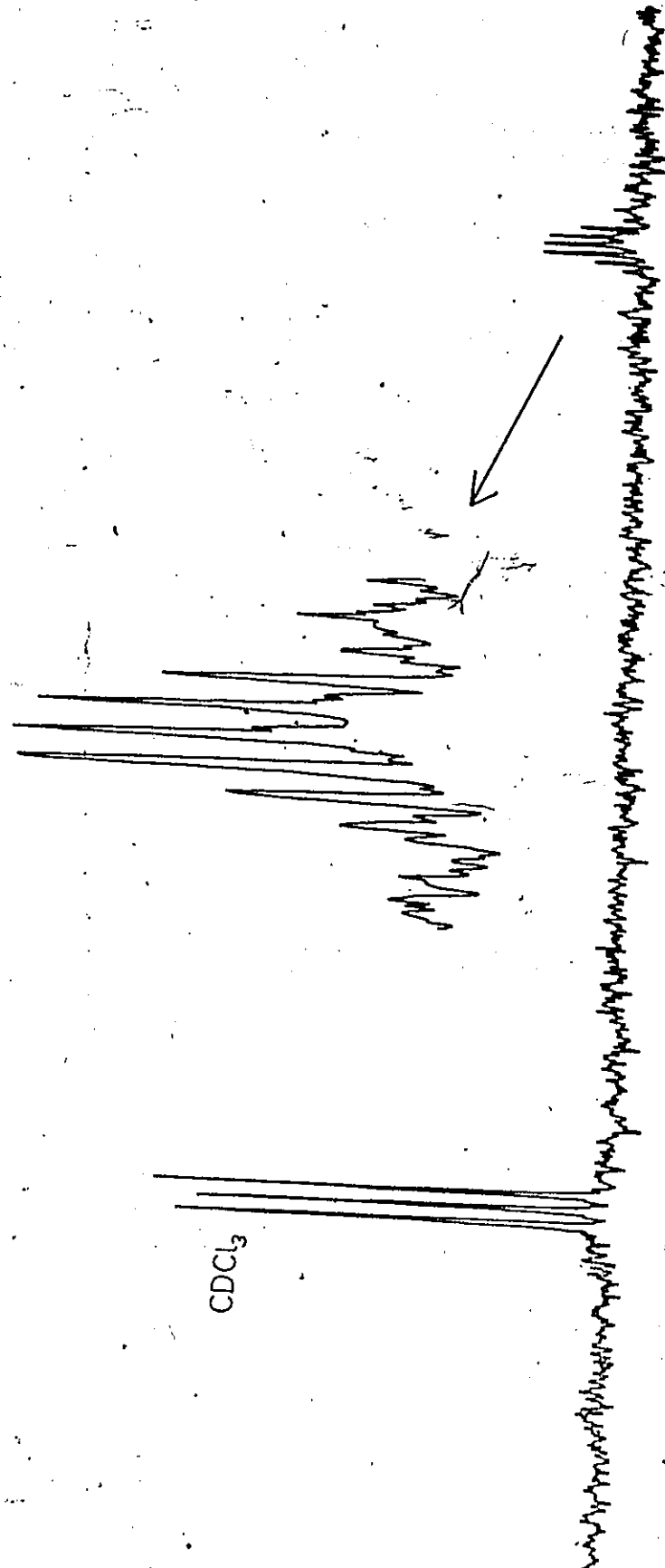
Figure 1.12 ^{13}C n.m.r. spectrum of CD$_3$SiD$_3$

in terms of different vibrational effects of the two iso-
topes[16]. The coupling constant, J_{CD}, with a value of 18.91
Hz, was found to be the same for both molecules. This again
is in keeping with the existing data[15], and corresponds to
a J_{CH} value in the corresponding CH_3- compounds of 123.2 Hz,
compared to a literature value for CH_3SiH_3 of 122.1 Hz[3].

CHAPTER 1.3

VIBRATIONAL SPECTROSCOPY

Infrared and Raman spectroscopy have been used as the standard methods for the study of molecular vibrations for quite some time. Even though the Raman effect was first demonstrated experimentally in 1928[17] (having been theoretically predicted by Smekal in 1923[18]) it has only been comparatively recently, with the advent of the laser to overcome problems of intensity, that it has been regarded as a routine laboratory technique. Infrared spectroscopy, on the other hand, has its origins in the last century and has long been established as a standard analytical tool[19], especially since the Second World War. The difference in the cause of the two effects (a change of polarisability as against a change in the dipole moment, respectively, caused by the vibration) leads to differing activities and relative intensities, and the combined use of these two techniques in solving vibrational and structural problems has long been acknowledged. Suffice it to mention here the landmark works of Herzberg[1] and Wilson, Decius and Cross [20] which together cover the vibrational and group theoretical aspects, as well as some very readable accounts by Woodward[21,22]. For the experimental details pertaining to this work, the reader is referred to Appendix III.

It is probably useful at this point to discuss some of the common terminology used in this thesis (and in other sources). As in most branches of science, the spoken or colloquial terminology frequently differs from the technically

more correct forms because it is usually more concise. Such is the case in vibrational spectroscopy, where the most common misnomer involves the word "frequency" (units: sec^{-1}), which is still used to refer to the position or energy of a spectral feature, which was previously measured as its wavelength, and more recently in wavenumbers (cm^{-1}), which are proportional to energy. In Raman spectroscopy, two spectra are recorded to determine polarisation ratios to aid in distinquishing the totally symmetric modes. The bands which are significantly reduced in intensity (by more than 6/7) are called polarised bands, and the spectrum also a "polarised" or "perpendicular" ($\perp$) scan, the latter term describing the alignment of the polariser-analyser in front of the collimator. The other spectrum is often called the "parallel" or "normal" spectrum. Following conventional practice, this is shown above the perpendicular spectrum throughout this thesis. The terms "fundamental modes", "fundamentals", "normal modes" and "modes" will be often found freely interchanged throughout the text.

The molecules investigated in this thesis fall into two point groups; the CH_3SiX_3 compounds (X = H, F, Cl, Br, I)[*] belonging to the C_{3v} point group and the other halogenated methylsilanes to the C_s group. This latter produces a' and a" vibrational modes, depending on whether the vibrations are symmetric or asymmetric with respect to the lone symmetry

---

[*] Throughout the rest of the text, X will denote the halogens F, Cl, Br and I unless otherwise stated.

plane in the molecule. All of the vibrations are infrared and Raman active. The C_{3v}' group gives rise to a_1, a_2 and e modes of which both a_1 and e are active in both effects with a single a_2 mode, the torsional fundamental, inactive. The totally symmetric species of each group, a' and a_1, produce polarised bands in the Raman spectra. It is also possible to draw some conclusions as to the species of the modes from the gas phase infrared bands where these can be resolved. Except for CH_3SiX_3, the molecules are asymmetric tops, and as such will exhibit A, B or C-type bands when the change in dipole moment for the vibration is parallel to the least, intermediate or largest moment of inertia[23], although one should be wary about drawing far-reaching conclusions from them[24].

The fact that all vibrational modes are allowed means that all the expected 3N-6 fundamentals (N = number of atoms) should be present, although the torsional mode is not observed. (These modes have been observed or calculated to be less than 200 cm^{-1} for similar methysilicon compounds, and while they may be expected to interact to a certain extent with low frequency skeletal modes, their exclusion from the analysis is not expected to significantly affect the analysis). The species and activities of these modes can be determined from tables[25]. The first problem is to pick out these fundamentals from the spectra, since in practice the number of observed bands is usually different from the number of expected frequencies, taking into account degeneracies arising from

local symmetry considerations (as in the methyl group). Even if the numbers are the same, this is no guarantee that each band is a fundamental.

The observation of too many bands is in fact quite common, even when the sample is pure and no decomposition is occurring. These may arise from overtones, combination or difference bands and Fermi resonance. The first three involve the simultaneous excitation of more than one vibrational level, either for the same mode (overtones) or different ones (combination or difference bands). These are denoted as $2\nu_j$, $\nu_j + \nu_k$ or $\nu_j - \nu_k$, respectively[*]. Higher forms and combinations of them can also exist e.g. $3\nu_j$, $2\nu_j + \nu_k$, $2\nu_j + \nu_k - \nu_1$ or $\nu_j + \nu_k - \nu_k$ (hot bands), although under the experimental conditions used here these latter, or even difference bands, which are less intense than the corresponding combinations, are not expected to be observed. The binary combinations, however, are quite often observed with low intensity, particularly in the infrared spectra. This intensity can be —and often is — increased through interaction with a fundamental which has almost exactly the same frequency as the sum, if the fundamental and overtone or combination have a common species (which for the molecules in this study is often the case). The resulting perturbation of the two energy levels causes the higher level to be dis-

---

[*] Because of anharmonicity effects, the observed frequency for overtones and combinations is slightly less than $2\nu_k$ or $\nu_j + \nu_k$; in contrast the value of $\nu_j - \nu_k$ will be exactly the difference between the two observed frequencies[26].

placed upwards and the lower down, and is called Fermi resonance[27]. The two states are said to "repel" each other to produce an observed splitting in the frequencies greater than otherwise expected. The overtone or combination band will also "borrow" intensity from the fundamental, so that the two bands approach each other in intensity. The closer the two unperturbed energy levels, the greater is the repulsion and the more similar the intensities. Common examples exist in CO_2 and CCl_4 (the first from an overtone[28], the second from a combination band[29] where the difference band has also been observed[30]). The appearance of forbidden bands can sometimes occur in liquid or solid spectra, where the intermolecular forces may result in sufficient distortion to lower the symmetry of the molecule, and hence allow the vibration, but this is not relevant to these molecules.

The appearance of fewer bands than anticipated can result from the non-appearance of allowed bands, because of low intensity. This problem is usually overcome by a combination of infrared and Raman techniques since it is unlikely that the vibration would have very low intensity in both effects. As a general rule-of-thumb, asymmetric vibrations tend to be stronger in the infrared whereas symmetric bands are more intense in the Raman. (This contrast in intensities is also noted for the total spectrum, Raman spectra becoming more intense as the halogen mass becomes larger, with the opposite effect in the infrared). The other main cause is accidental degeneracy, or the overlapping of two or more bands. If the

bands are of different species it may be possible to detect from a comparison of the normal and polarised Raman spectra although assigning frequencies to the two modes may be difficult.

Some or all of the above effects can combine to produce misleading information particularly if one compound is studied in isolation. Many ambiguities can be resolved, however, if a series of related compounds are studied, especially for detecting overlapping bands. The normally observed gradual shift of some frequencies accompanying a change of one substituent will often reveal when two bands in a spectrum are superimposed. Specific deuteration will produce different overtone and combination bands, and often remove one component from Fermi resonance. A combination of these two practices is usually sufficient to overcome most of these problems. There are examples of just about all of the above in individual moecules discussed in this thesis and these will be presented as they occur.

CHAPTER 1.4

NORMAL COORDINATE ANALYSIS

AND THE CALCULATION OF

FORCE CONSTANTS

1.4.1 Normal Co-ordinate Analysis

Normal Co-ordinate Analysis (NCA) is a method for describing the vibrations of a molecule in terms of the individual motions of each atom, which can be expressed in convenient mathematical terms. The resulting derivatives are well developed and full descriptions can be found in the classic texts by Wilson, Decius and Cross[20] and others[1,21], and will not be repeated here.

A molecule may be represented as a collection of balls connected by springs, and the simplest case, that of a diatomic molecule will be briefly presented. By Hooke's Law, the potential energy of the molecule is given by

$$V = \tfrac{1}{2}kx^2 \qquad\qquad (4.1)$$

where k is the force constant of the spring and x the displacement of the balls from the equilibrium position. Once set in motion, the frequency of oscillation is given by

$$\nu = \frac{1}{2\pi}\sqrt{\frac{k}{\mu}} \qquad\qquad (4.2)$$

where μ is the reduced mass of the balls. Equation 4.1 can be recognised as that for a parabola, but this model does not hold for a real molecule. For the model, the potential energy increases symmetrically for increasing displacements in both directions, whereas for a molecule the energy reaches a constant value for large separations (the dissociation energy) and rapidly rises to infinity as the nuclei approach each other. This real potential function

(or potential energy curve) is well represented by a polynomial expansion (a Taylor series)

$$V(r) = V(r_e) + \left(\frac{\partial V}{\partial r}\right)(r-r_e) + \frac{1}{2!}\left(\frac{\partial^2 V}{\partial r^2}\right)(r-r_e)^2 +$$

$$\frac{1}{3!}\left(\frac{\partial^3 V}{\partial r^3}\right)(r-r_e)^3 + \cdots \qquad (4.3)$$

where r and r_e are the internuclear and equilibrium separations respectively, and the differentials are evaluated at $r=r_e$. The choice of a reference potential energy of zero at $V(r_e)$ and a minimum in the curve at r_e eliminates the first two terms. The approximation is now made that at small amplitudes the motion is harmonic, so cubic and higher terms are neglected, and Equation 4.3 simplifies to

$$V(r) = \frac{1}{2}\left(\frac{\partial^2 V}{\partial r^2}\right)(r-r_e) \qquad (4.4)$$

Comparison with Equation 1.1 shows that

$$k = \left(\frac{\partial^2 V}{\partial r^2}\right)_{r=r_e} \qquad (4.5)$$

Thus the force constant is a measure of the change of the slope of the potential function about the equilibrium position. In the calculation, the vibrations of the molecule are described by a superposition of the simultaneous simple harmonic motions of each atom, which are in turn described by the force constants and the structural parameters. These are known as the F and G matrices respectively when the simultaneous equations thus set up are expressed in matrix form. The size of the F matrix

depends on which internal coordinate system is used to define the nuclear motions and their interactions with each other. In general, for n internal coordinates, the F matrix will be a symmetric n x n matrix which defines $n(n + 1)/2$ force constants. A knowledge of their values allows for an equation of the form

$$| F - \lambda G^{-1}| = 0 \qquad\qquad (4.6)$$

to be solved for the frequencies, λ, of the "normal vibrations" of the molecule. A knowledge of all the force constants means that the "general harmonic" force field (GHFF) is well defined.

However, in practice it is normally the force constants that we wish to determine in order to test predicted assignments of the experimentally measured vibrational frequencies. The problem lies in the fact that the $n(n + 1)/2$ force constants are always larger than the $3n - 6$ vibrational frequencies, and so a determination of the GHFF is impossible with this information. The solution is to either increase the amount of information from other sources, or to reduce the number of force constants, or possibly both.

One of the most common ways of increasing the number of observables is by isotopic substitution. Because the bonding characteristics are due to electronic factors only, this change of mass leaves the force field essentially unchanged while producing a new set of frequencies (see

Equation 4.2).* Other additional information can be
obtained from Coriolis zeta constants, centrifugal
distortion constants and mean amplitudes of vibration. The
first two are calculated[1,31] from rotational structure in
vibrational bands, and give information about off-diagonal
force constants in the former case and both diagonal and
interaction terms in the latter. The extent to which these
data are useful is obviously restricted by the ability to
measure the effect of rotational interactions, which in
general becomes smaller as the molecule becomes heavier.
Mean amplitudes of vibration are measured from electron
diffraction experiments[32], and are straightforwardly
connected with force constants; a large amplitude means
that the potential function has a broad minimum and hence a
small force constant. When the measured amplitude is between
two non-bonded atoms (connected to a common atom),
information about the stretch-bend interaction can be
obtained. Once again, this approach is limited by the
availability of such data.

Even with these extra data it is the rule rather than
the exception that the GHFF cannot be uniquely determined
except for the simpler molecules; for example for XH_3 and
XH_4 (X = N,P,As;C,Si,Ge)[33], but not for CH_3X and CD_3X[34].
Thus a reduction in the number of force constants is

---

* This will not double the number of _independent_ observables,
since there exist certain relationships between the two
frequency sets dependent on structural data only and not on
the force field. These give rise to the isotope rules and
are discussed later.

necessitated. This can be accomplished in several ways, one
of which is to ignore the interaction terms completely, i.e.
set all off-diagonal terms in the F matrix to zero. This
results in a simple valence force field (SVFF), which
although it can be uniquely determined (since the number of
force constants is at most equal to the number of frequencies)
does not in general produce a good agreement. Another way is
to define the internal coordinates in such a way as to
reduce the number of interaction terms present. This is an
important advantage of using the Urey-Bradley model [35]
(UBFF) in which the interactions are assumed to be caused
by repulsions between non-bonded atoms. There are several
other fields that have been used; the orbital valency force
field[36] (OVFF) and hybrid orbital force field[37] (HOFF) being
two of the better known. Each model has its relative merits
and disadvantages, and correspondingly its supporters and
detractors. Much depends on the molecules studied and
personal preferences as to which is considered closest to
reality.

1.4.2 Calculation of Force Constants

The problems encountered in the execution and
application of a NCA fall into two categories; those
inherent in the method itself, and those involving its
application. The most obvious of the former difficulties,
that of calculating a large number of force constants from
a smaller number of observed frequencies, has just been
discussed. Probably the most common way of decreasing this

disparity, by isotopic substitution, specifically of deuterium for selected hydrogen atoms, introduces the other inherent shortcoming, in that throughout the derivation of the method a quadratic field has been assumed, i.e. the vibrations are all simple harmonic. Departure from this assumption will be most evident for large amplitude vibrations, which are precisely those expected for vibrations involving light nuclei, such as H and D. These modes will thus be less accurately calculated, to an extent of about 5% for the stretching modes, compared to about 2% for other vibrations.

In practice, the calculation of the force field starts with a set of estimated values for the force constants. The frequencies thus calculated are compared with those observed, and force constant values changed in order to achieve a better agreement. The closeness of the agreement is determined by a least-squares "best fit" criterion and a number of successive adjustments are made, hopefully improving the fit each time. If this occurs the solution is said to converge. However, convergence and a good fit are only mathematical standards imposed upon the calculation and are not necessarily indicative of a favourable solution by physical standards. In general a whole family of solutions, based on which interaction terms were used, the order of varying force constants and even on initial values for the SVFF, can be obtained which produce a good fit. This is shown in the next chapter, where a variety of solutions was

obtained for MeGeCl$_3$, all of which reproduced the observed frequencies perfectly but with different descriptions of the normal modes for some of those frequencies.

These descriptions are obtained from the calculation of the potential energy distribution (p.e.d) among the force constants, or the potential energy matrix. The elements of this matrix are calculated from

$$\left[V_\phi^\lambda \right] = \left[J_\phi^\lambda \right]\left[\Lambda \right]^{-1} \left[\phi^* \right] \qquad (4.7) \text{ (ref.38)}$$

and describes the contributions of each force constant ϕ to the potential energy V^λ associated with each vibrational frequency λ, and hence the nuclear motions primarily responsible for each frequency are obtained. $\left[J_\phi^\lambda \right]$ is a matrix of derivatives of the form $\frac{\partial \lambda}{\partial \phi}$, reflecting the effect each force constant has on the resulting frequency; $\left[\Lambda \right]^{-1}$ is a diagonal matrix whose elements are the inverse of the frequencies, and $\left[\phi^* \right]$ is a diagonal matrix whose elements are $\left[\phi \right]$.

The force field used in this study was a compromise between the SVFF and GHFF, where some interaction terms were used, the rest being set to zero. This is called a modified valence force field (MVFF), but deciding which interactions are to be included regrettably introduces a degree of arbitrariness into the problem which often prevents a useful comparison with other MVFF calculations which often use different terms.

The force constants for the initial SVFF are usually

taken from values calculated for similar molecules, or if these are not available, simply guessed. After these have been refined by the least-squares program, interaction terms are introduced and the calculation is repeated, usually many times, each time allowing different force constants to vary and possibly introducing new interaction terms until a final best fit is obtained. (As mentioned above, this is not necessarily indicative of a "best" solution; for a number of the calculations, convergence produced poorer results as far as the p.e.d's were concerned). A test of the final force field is whether the force constants can be transferred to a similar molecule or atomic group and reproduce the frequencies for that molecule or group. Examples of this are when the molecule can be split into units whose vibrations do not overlap. Such a case is methylstannane[39], CH_3SnH_3, where the force constants from CH_4 and SnH_4 were used to reproduce the frequencies due to the CH_3- and $-SnH_3$ groups, the calculation thus only being required to evaluate $\underline{f}$ (SnC). This concept of "group force constants" has been used extensively for the methyl group[40-42] and carried to its ultimate conclusion in two monumental papers by Schachtschneider and Snyder, who using no more than 36 force constants, reproduced all the observed frequencies (and calculated the forbidden ones) for straight-chain alkanes from C_2 to C_{14}[43], and a variety of branched alkanes[44] to better than 1%. This is really not so unexpected when one thinks of the success that the "group frequency" concept has

had in organic chemistry. However, these examples work only because in the case of CH_3SnH_3 the frequencies of the two groups are well separated, and for the alkanes because there are only C-H and C-C bonds present, and the molecular environment is fairly similar for each group. The approach was tried for this work, by calculating force constant values for SiH_3X, SiH_2X_2 and $SiHX_3$ compounds, but a useful comparison was precluded for the methylated derivatives by considerable mixing of the methyl group vibrations with Si-H bending motions. Usually these motions, which showed large contributions from more than one diagonal force constant, were prone to poor agreement or to being incorrectly ordered. They were also particularly dependent on the effect of interaction terms. This latter property could be used as a method of choosing relevant interaction terms. There are several other methods for deciding which interactions to use and which to keep at zero; for example, terms uniquely determined for simpler, related molecules can be introduced but held fixed at their characteristic value, or interactions involving vibrations whose frequencies are well separated can be kept at zero. The major criterion used in the calculations presented later is that terms not including a common bond were set to zero and of the remainder, only those included which had a significant and beneficial effect on both the frequency fit and the p.e.d. Only when agreement was still poor, or if the p.e.d. indicated that the calculations were in the wrong

order were terms not involving a common bond introduced, and even then a common atom was required.

From the foregoing discussion it would appear that NCA is a numbers game with limited practical use, except for those few molecules whose GHFF can be determined. However, for the majority of the users of this method this is not the ultimate aim. What is sought is some insight into the nature of the vibrations so that assignment of the observed bands will be more plausible in cases where there is some doubt. Thus calculations for a single molecule are not very informative, or even necessarily a support of the assignment, unless calculated from simpler molecules, or for such cases as CH_3SnH_3 mentioned above, where the group frequencies are well separated. (CH_3SiI_3 [10] fits this condition even better). So one is generally more interested in the observation of trends, both in force constants and p.e.d.'s, obtained from an internally consistent set of calculations applied to a chemically (and better still, structurally) related series of compounds. Then some useful information may be extracted without having to discuss absolute values, although these should be in reasonable agreement with other published values.

A short example illustrates these points. In the published assignments for the SiH_3X series, the a_1 and e SiH_3 deformation frequencies in SiH_3F [45] are in reverse order compared to the rest of the series. The corresponding SiD_3 vibrations offered no help because, except in SiD_3Br,

the e mode was not observed. A NCA was carried out, and upheld this ordering, with the force constants and p.e.d.'s showing no irregularities. The relevant data are gathered in Table 1.4.1. The frequencies from the two deformations and the e SiH_3 rock essentially fixed the $\underline{f}$ HSiH and $\underline{f}$ HSiX values, enabling the unobserved band to be calculated. The value of $\underline{f}$ HSiX is seen to increase fairly regularly with lighter halogen , while $\underline{f}$ HSiH remains relatively constant, which is reasonable since there is no X atom involved. (The slight increase in $\underline{f}$ HSiH for SiH_3Br arises from the inclusion of the e deformation frequency for SiD_3Br in the refinement procedure. In attempting to replicate this observed frequency, $\underline{f}$ HSiH has to increase slightly; notice here the calculated frequency is lower, but higher for the H compound). The contributions from the force constants in the p.e.d. also change in a regular manner, suggesting an internal consistency in the calculations.

1.4.3 Force Constants and Bond Strength

Since the force constant only provides information in the region about the minimum in the potential curve, any discussion about bond strength (which is concerned with the depth of the well) cannot proceed without knowledge of the rest of the potential function for the bonds involved. However, quite often the assumption is made for a given series of related compounds that these potential functions are similar in form, or change only slightly and then in a

Table 1.4.1　Observed and calculated frequencies (cm^{-1}), and p.e.d. and force constants (Nm^{-1}) for SiH$_3$ vibrations in SiH$_3$X compounds

Mode	obs.	calc.	p.e.d.	obs.	calc.	p.e.d.	(1)f_{HSiH}	(2)f_{HSiX}
	SiH$_3$F[a]			SiD$_3$F[b]				
e def.	943	943.7	80(1)+25(2)	n.o.	671.2	78(1)+27(2)	43.9	69.3
a$_1$ def.	990	990.5	58(2)+37(1)	704	703.7	53(2)+34(1)		
e rock	728	721.9	74(2)+27(1)	549	553.6	72(2)+29(1)		
	SiH$_3$Cl[a]			SiD$_3$Cl[b]				
e def.	954	954.3	88(1)+14(2)	n.o.	679.0	90(1)+12(2)	43.4	61.8
a$_1$ def.	949	950.3	57(2)+40(1)	702	701.1	57(2)+40(1)		
e rock	664	658.3	88(2)+15(1)	488	491.9	90(2)+12(1)		
	SiH$_3$Br[c]			SiD$_3$Br[c]				
e def.	946	950.1	91(1)+12(2)	686	676.7	95(1)+9(2)	44.3	56.7
a$_1$ def.	930	932.1	55(2)+43(1)	684	684.4	55(2)+43(1)		
e rock	633	630.4	90(2)+12(1)	464	466.8	92(2)+10(1)		
	SiH$_3$I[d]			SiD$_3$I[e]				
e def.	941	941.0	93(1)+9(2)	n.o.	671.8	94(1)+7(2)	42.7	51.6
a$_1$ def.	903	904.7	53(2)+44(1)	664	662.7	54(2)+44(1)		
e rock	592	591.5	96(2)+9(1)	435	435.4	98(2)+7(1)		

a) ref.45　b) ref.46　c) ref.47　d) ref.48　e) ref.49

regular manner which allows for some comparison between force constants and bond strengths.

The series Me_nGeF_{4-n} (n = 1-3) was prepared and the vibrational spectra recorded in this laboratory[50]. Force constant calculations were performed for the series (n = 0-4), and the results show that all the stretching force constants increase as fluorine is substituted for methyl groups. Thus on the above assumptions, stronger bonds might be expected for the compounds with more fluorine atoms.

One directly measurable consequence of an increase in bond strength is a corresponding shortening of the bond in question. Data are available for the fluoromethylgermanes[51,52] from electron diffraction studies which confirm this decrease in bond length. These data are collected in Table 1.4.2. This correlation is not too surprising since both measurements involve conditions about the equilibrium distance. It was also suggested that there is an increase in the polarity of the bond as it becomes shorter[51]. This is supported by the calculation of the formal charges on the methyl group(s) and germanium and fluorine atoms. These charges are calculated by Huheey's method[55] and are based on a relationship between the orbital electronegativity for the element M and the charge δ_M on that element, involving valence shell ionisation potentials and electron affinities[56-58]. The calculated charges are listed in the first three columns of Table 1.4.3. It is noticeable that the methyl group is always positive and the fluorine atoms

Table 1.4.2 Selected physical data for the methylgermanium fluorides

		GeF_4	$MeGeF_3$	Me_2GeF_2	Me_3GeF	Me_4Ge
Force constants ($N.m^{-1}$)	$\underline{f}$ CH	-	494	488	480	477
	$\underline{f}$ GeC	-	337	325	298	268
	$\underline{f}$ GeF	545	475	417	382	-
Electron diffraction [a] (pm)	r (GeC)	-	190.4	192.8	193.2	194.5 [b]
	r (GeF)	167 [c]	171.4	173.9	174.2	-
	$\angle$ CGeF	-	113.2°	107.3°	105.1° [d]	-
	$\angle$ CGeC	-	-	121.0°	113.5° [d]	-
	$\angle$ FGeF	109.5°	105.5°	105.4°	-	-

a) ref. 51   b) ref. 53   c) ref. 54   d) ref. 52

Table 1.4.3 Correlation of bond angles with calculated partial charges

| | (1) δGe | (2) δMe | (3) δF | no. of ε in Ge orbitals | | |
				(4) GeC	(5) GeF	(6)Total
Me$_4$Ge	-0.092	+0.023	-	1.023	-	4.092
Me$_3$GeF	-0.053	+0.103	-0.258	1.103	0.742	4.051
Me$_2$GeF$_2$	+0.008	+0.230	-0.234	1.230	0.766	3.992
MeGeF$_3$	+0.117	+0.455	-0.191	1.455	0.809	3.882
GeF$_4$	+0.368	-	-0.092	-	0.908	3.632

| | (7) CGeC | (8) | (9) CGeF | (10) | (11) FGeF | (12) |
	Σε(Ge)*	angle	Σε(Ge)*	angle	Σε(Ge)*	angle
Me$_4$Ge	2.046	109.5	-	-	-	-
Me$_3$GeF	2.203	113.5(7)	1.845	105.1(4)	-	-
Me$_2$GeF$_2$	2.460	121.0(35)	1.996	107.3(7)	1.532	105.4(20)
MeGeF$_3$	-	-	2.264	113.2(6)	1.618	105.5(9)
GeF$_4$	-	-	-	-	1.816	109.5

* total no. of electrons in Ge orbitals contained in bond angles

always negative, with respect to germanium. Assuming one electron in each Ge sp^3 orbital, the numbers of electrons occupying these orbitals in bonding to the methyl group and fluorine atoms will be greater to, and less than one respectively, and these numbers are in columns 4 and 5. Adding up the total number of electrons in the Ge orbitals, according to the number of Ge-C and Ge-F bonds present, produces column 6, which not surprisingly reproduces column 1 in a different form. Correlation of $|\delta_{Ge} - \delta_{Me}|$ and $|\delta_{Ge} - \delta_F|$, the separation of charge in the bonds, or bond polarity, with the Ge-C and Ge-F bond lengths produces a straight line[51], as does a plot of columns 4 and 5 against the bond lengths, within the estimated error limits. Turning attention to the bond angles, columns 7, 9 and 11 list the number of electrons in the two Ge orbitals defined by the bond angle, i.e. twice the number in a Ge-C bond for a CGeC angle, one Ge-C plus one Ge-F bond for a CGeF angle and so on, and are followed in columns 8, 10 and 12 by the experimentally determined values of these angles. Correlation between numbers of electrons at Ge and bond angles is also linear within the quoted uncertainties. The main observation from these calculations is that the largest angles (CGeC) contain most electrons in their component bonds at Ge, and the smallest angles (FGeF) involve the fewest. Also, all the CGeC angles are greater than tetrahedral, and the FGeF angles less than tetrahedral in the mixed compounds.

Having arrived at values of relative charges on each

type of nucleus, and quantitatively correlated these with force constants, it is possible to speculate on the effect that the change in nuclear charge has on the immediately surrounding electrons. The technique known as ESCA (Electron Spectroscopy for Chemical Analysis) measures the energy of core electrons for an atom under investigation, and this binding energy is obviously dependent on the atomic environment. The fluoromethylgermanes have been the subject of one such study[59] where the binding energies of the electrons in the germanium 3d, and the carbon and fluorine 1s orbitals were measured. The results, shown in Table 1.4.4 along with the relevant force constant and structural data from Table 1.4.2, show that all three binding energies increased as fluorine was substituted for methyl groups, reflecting the increasingly positive (or for fluorine the decreasingly negative) charges on each nucleus. If it is assumed that the increased binding in the core levels must be reflected in increased binding in the valence levels, then VSEPR theory would require an increased repulsion between adjacent bonds, and a consequent opening of angles between these bonds. A look at Table 1.4.4 confirms that the argument has come full circle.

Table 1.4.4 Selected physical data for the methylgermanium fluorides

		GeF_4	$MeGeF_3$	Me_2GeF_2	Me_3GeF	Me_4Ge
Force constants ($N.m^{-1}$)	f CH	-	494	488	480	477
	f GeC	-	337	325	298	268
	f GeF	545	475	417	382	-
Electron diffraction [a] (pm)	r (GeC)	-	190.4	192.8	193.2	194.5 [b]
	r (GeF)	167 [c]	171.4	173.9	174.2	-
	∠ CGeF	-	113.2°	107.3°	105.1° [d]	-
	∠ CGeC	-	-	121.0°	113.5° [d]	109.5°
	∠ FGeF	109.5°	105.5°	105.4°	-	-
Binding energy [e] (aJ)	Ge (3d) [f]	6.707	6.292	6.394	5.984	5.786
	C (1s) [g]	-	46.640	46.616	46.491	46.435
	F (1s) [g]	118.08	110.86	111.80	110.63	-

a) ref. 51 b) ref. 53 c) ref. 54 d) ref. 52 e) ref. 59

f) relative to $Ar(2p_{\frac{1}{2}}) = 39.835$ aJ

g) relative to $Ne(2s^2) = 7.766$ aJ

CHAPTER 1.5

THE ASSIGNMENT OF

VIBRATIONAL SPECTRA

The assignment of the observed bands to specific fundamentals, which can only begin after the identites and purities of the compounds have been confirmed, is accomplished in several steps, the first of which is "by inspection". The spectra are divided into regions in which specific vibrations are known to occur. These bands are eliminated from the list of expected fundamentals, thus narrowing the choice for the modes which are less certain.

1.5.1 · Preliminary Assignment by Inspection.

The first region usually examined is in the range 3000-1000 cm^{-1}, where the vibrations due to C-H, C-D, Si-H and Si-D stretching appear at ca. 2900, 2200, 2100 and 1600 cm^{-1} respectively. Fundamentals due to symmetric and asymmetric stretching motions are most readily distinguished in the Raman spectra. The methyl group deformations occur from about 1450 cm^{-1} (for CH_3) to about 1000 cm^{-1} (for CD_3), and are usually seen more clearly in the infrared spectra, where band contours can often be used as an aid to assignment. The next is the skeletal deformation region, below 350 cm^{-1}, where the identification is dependent mainly on the Raman spectra. For the compounds studied here, these deformations are those bending vibrations not involving hydrogen or deuterium. This leaves the region from 1000-350 cm^{-1}, in which, for the halogenated species studied here, the symmetric Si-X stretch (X = Cl, Br, I) is clearly observed as a strong, polarised band in the Raman spectra at about 500, 400 and 350 cm^{-1} respectively. (Silicon-fluorine stretches are very weak in

the Raman effect and are usually found at about 900 cm^{-1} in the vicinity of the methyl rocks).This leaves motions due to Si-C stretching, Si-H(D) bending and methyl rocking to be assigned, and herein lie most of the problems. Some general methods used to help assign the bands in this region are;

a) Comparison with other molecules

The unassigned fundamentals are compared with vibrational modes which have been confidently assigned in a structurally related, usually simpler molecule. The most common pitfall is the choice of a molecule which, although apparently suitable, is not sufficiently similar to offer a meaningful comparison. Further problems arise if two frequences are compared which result from motions involving dissimilar atoms. Examples of these are described in detail in Chapter II.3.

b) Isotopic substitution

In this study deuteration was carried out at selected hydrogen sites. The large shift of frequency due to doubling the mass of one atom (see equation 4.2) in a vibration immediately distinguishes motions involving this atom. Sometimes a slight shift in the frequencies of motions not involving that atom can occur, and where extensive coupling of vibrations has occurred, the removal of a component of that coupling through deuteration can change the resulting frequency of a vibration by a considerable degree.

1.5.2 Supporting Calculations

i) The Product Rule

The concept of isotopic substitution is based on the assumption that the substitution does not change the potential function of the molecule. If the force constants are the same, then the change in the frequencies of the vibrations involving motion of the substituted atom(s) should involve only structural factors. This has developed into the so-called Teller- Redlich product rule [60,61] whereby the ratios of the products of the frequencies for each symmetry species can be calculated according to the general equation

$$\frac{\Pi\omega'}{\Pi\omega} = k \qquad\qquad (5.1)$$

where ω' and ω are the zero-order vibrational frequencies for the isotopically substituted and normal compound respectively and k is a term involving only ratios of masses and some-times moments of inertia (depending on the symmetry species) for the two molecules. This calculation can be performed fairly easily for small molecules (triatomics, for instance), but for larger molecules becomes very tedious. In practice the calculated ratio can be obtained from the products of the two sets of frequencies for the two molecules calculated using the same force constant set. These force constants need not necessarily be representative of the "real" force field as long as the same values are used. The symmetry species of each frequency is determined from the atomic displacement matrix and the ratios calculated. Thus for the

compounds of C_s symmetry discussed in this thesis there are different ratios for a' and a" modes. The ratios are calculated on the assumption of quadratic forces, and as such the frequencies involved are the zero-order or harmonic frequencies ω, rather than the observed anharmonic frequencies λ, with which they are compared. If the isotopically substituted molecule is the heavier of the two (as is the case with deuteration) then the anharmonicity constants $\omega_i' - \nu_i'$ are smaller than $\omega_i - \nu_i$ and so the observed ratio should be slightly larger than the calculated ratio.

ii) <u>Use of Force Constants</u>

Although force constant values can be an invaluable tool in the assignment of vibrational spectra, erroneous conclusions are often drawn as a result of carelessness or inexperience. Such was the case for the fluoromethylgermanes already mentioned, and this example will be followed through step by step from the original, incorrect assignment to what is now considered the correct one.

The descriptions of the fundamentals and the observed frequencies are given in Tables A2-A7. The modes involving the methyl group(s) and the Ge-C and Ge-F stretches were straightforwardly assigned leaving only the skeletal bending region. The assignment of these frequencies was first attempted by comparison with related compounds. The vibrational spectrum of Me_3GeF had previously been published [62] and comparison with other trimethylgermyl compounds, notably the chloro- derivative[63], confirmed the assignment. The three

skeletal modes in MeGeF$_3$ (ν_5, ν_{11} and ν_{12}) were all apparently depolarised which necessitated the use of other methods. They were eventually assigned on the basis of the energy associated with the predominant angle change producing the motion. Thus the mode depending on the CGeF angle deformation (ν_{11}, the GeF$_3$ rock) was compared to the single skeletal mode in CH$_3$GeH$_2$F[64] at 215 cm^{-1}, and the fundamental dependent on a change in the FGeF angle (ν_{12}, the GeF$_3$ asymmetric deformation) to the lowest wavenumber vibration in H$_2$GeF$_2$[65], and to the highest skeletal mode in MeGeHF$_2$[66], both at 280 cm^{-1}. (The other two modes in the latter compound, dependent on the CGeF angle deformation, occurred at 215 cm^{-1}). The remaining skeletal fundamental, ν_5, the GeF$_3$ symmetric deformation, involves changes in both CGeF and FGeF angles and so was assigned to the intermediate frequency, just as the symmetric methyl deformation (ca. 1250 cm^{-1}) occurs between the asymmetric deformation (ca. 1400 cm^{-1}) and the methyl rock (ca. 800 cm^{-1}) in the analogous methyl group vibrations.

For the Me$_2$GeF$_2$ compound, five skeletal modes were expected, but only two envelopes were observed in the Raman spectrum of this region. The higher at 259 cm^{-1} was polarised and assigned as ν_9, the GeF$_2$ scissors mode, again by comparison with H$_2$GeF$_2$[65] and MeGeHF$_2$[66]. The remaining four fundamentals had to be assigned tentatively to the other envelope which showed two maxima separated by only 15 cm^{-1}. Thus the normal coordinate analysis was performed on the

three compounds.

In the course of this analysis, only corresponding force constants were allowed to vary in each step of the calculation and interaction terms were introduced and varied at the same stage of the calculation. A scheme showing the force constants used and the order of refinement is shown in Figure 1.5.1. Thus in step 1, only force constants involving the methyl and GeF "ends" were allowed to change, whereas in step 2, those involving the GeC bond(s) were unconstrained, and so on.

Because the ordering of the skeletal fundamentals of Me_2GeF_2 was not known (i.e. it was not known which frequencies to attempt to match) the calculations of the monofluoro- and trifluoro- compounds were completed first. The value for f CGeF in Me_2GeF_2 was then fixed at the average value from $MeGeF_3$ and Me_3GeF and the calculation for Me_2GeF_2 resumed. When f CGeF was finally allowed to vary in stages 4 and 6, the four frequencies picked out from the Raman spectrum were well reproduced and the values of the force constants involved, f CGeC, f CGeF and f FGeF appeared to be in line with expected values, i.e. f CGeC not significantly different, f CGeF in between the values for the other two compounds and f FGeF a little lower than its value in $MeGeF_3$. The values are listed in Table 1.5.1 and the p.e.d.'s among them in Tables A3, A6 and A7.

For a better overall comparison the calculations were extended to include GeF_4 and Me_4Ge using published spectroscopic data[67,68]. While the resultant stretching force

CH_3GeF_3	$(CH_3)_2GeF_2$	$(CH_3)_3GeF$

Stage 1

f CH	f CH	f CH
f CH/CH	f CH/CH	f CH/CH
f HCH	f HCH	f HCH
f HCH/HCH	f HCH/HCH	f HCH/HCH
f GeF	f GeF	f GeF
f GeF/GeF	f GeF/GeF	
f FGeF	f FGeF	
f FGeF/FGeF		

Stage 2

f HCGe	f HCGe$^{\parallel,\perp}$	f HGGe$^{\parallel,\perp}$
f HCGe/HCGe	f HCGe$^{\parallel,\perp}$/HCGe$^{\perp,\perp}$	f HCGe$^{\parallel,\perp}$/HCGe$^{\perp,\perp}$
f CGeF	f CGeF	f CGeF
	f CGeC	f CGeC

Stage 3

f GeC	f GeC	f GeC
	f GeC/GeC	f GeC/GeC
f GeF	f GeF	f GeF
f GeC/GeF	f GeC/GeF	f GeC/GeF

Stage 4

All main (diagonal) force constants

Stage 5

All interaction (off-diagonal) force constants

Stage 6

All chosen force constants

Figure 1.5.1

Table 1.5.1 Force Constant values for the fluoromethyl-germanes

Force constant	No.	Values* in:				
		GeF$_4$	MeGeF$_3$	Me$_2$GeF$_2$	Me$_3$GeF	Me$_4$Ge
f CH	1	-	494	488	480	477
f GeC	2	-	337	325	298	268
f GeF	3	545	475	417	382	-
f HCH	4	-	49	49	49	48
f HCGe$^\perp$	5	-	46	42	43	46
f HCGe$^\parallel$	6	-		45	42	
f CGeC	7	-	-	68	68	51
f CGeF	8	-	46	44	39	-
f FGeF	9	71	92	77	-	-
f CH/CH	10	-	4	4	5	5
f GeC/GeC	11	-	-	-1	4	10
f GeF/GeF	12	22	18	7	-	-
f HCH/HCH	13	-	-2	-3	-2	-4
f HCGe$^\perp$/HCGe$^\perp$	14	-	-2	2	4	-1
f HCGe$^\perp$/HCGe$^\parallel$	15	-		-2	-3	
f GeC/GeF	16	-	-2	3	6	-
f XGeX/XGeX#		13				6

*) units: Nm^{-1} for stretching; Nm.rad^{-2} for bending force constants

#) X = F or C; see text

constants fitted nicely into expected trends, the bending force constants, f FGeF and f CGeC respectively, were found not to fit at all well (Table 1.5.1). In retrospect this is not surprising because the force constants f FGeF/FGeF and f CGeC/CGeC were not used since only interaction terms common to all three molecules were utilised. (This also helped to minimise the number of force constants). In the tetrasubstituted compounds, however, their inclusion is essential for the solution of the problem, whereas they are not needed in the other three because the interaction they describe is "absorbed" by a change in the CGeF angle, which is reflected in the value of f CGeF, rather than a f FGeF/FGeF term. This motion is depicted in Figure 1.5.2:

GeF$_4$ MeGeF$_3$
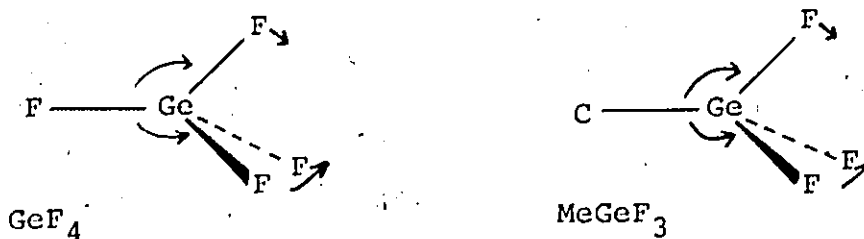
Figure 1.5.2

A comparison with the spectrum of MeSiF$_3$, however, suggests that the assignment of MeGeF$_3$ as outlined above is error, if the two are comparable. NCA calculations on all MeSiX$_3$ molecules (see Chapter I.2) point to an assignment which places ν_5, the symmetric deformation, at the highest skeletal frequency (which band also appears the most polarised of the three bands in that region if the Raman spectrum) followed by ν_{12}, the asymmetric deformation and finally ν_{11}, the SiF$_3$ rock at the lowest frequency. A similar ordering

for MeGeF$_3$ cannot be reproduced under the conditions out-
lined above, but is possible when the interaction terms
$\underline{f}$ CGeF/CGeF or $\underline{f}$ FGeF/FGeF or both are included in the calc-
ulation. Furthermore, the values of $\underline{f}$ CGeF and $\underline{f}$ FGeF vary
widely depending on which of the interactions are used. When
both are used, a variety of results are obtained depending
on which other interactions are used and initial starting
values, since four variables are being used to calculate only
three frequencies. (However, when the calculation was attempt-
ed with $\underline{f}$ CGeF/FGeF as the only interaction term for the
entire MeGeX$_3$ series, the solution would not converge,
although it did for the MeSiX$_3$ series). Some representative
values for the different conditions are shown in Table 1.5.2.
Thus the inclusion of only one extra interaction term can
calculate a different assignment based on the same observed
spectra. Indeed, choosing the values from the first column
in Table 1.5.2 would indicate a smooth, consistent trend for
both $\underline{f}$ CGeF and especially $\underline{f}$ FGeF if they were used in
Table 1.5.1. Thus for a series such as the fluoromethyl-
germanes, where the molecules are not similar in structure

Table 1.5.2 Force constant values (Nm.rad^{-2}) for bending
force constants in MeGeF$_3$

	3 f.c.	3 f.c.	4 f.c.		
·$\underline{f}$ CGeF	61.7	45.3	50.3	52.6	59.5
$\underline{f}$ FGeF	76.1	89.1	85.1	83.3	80.0
$\underline{f}$ CGeF/CGeF	16.4	0[*]	5.0	7.3	14.4
$\underline{f}$ FGeF/FGeF	0[*]	12.9	8.9	7.2	9.1

[*]fixed

(in terms of symmetry and number of like atoms) the use of normal coordinate analysis to compare bending modes is tenuous, although, as has already been discussed above, the comparison of stretching force constants can have some physical meaning.

The ability to reproduce just about any assignment removes some of the credibility from NCA in a case such as the one above, but it can also prove very useful in others. This is illustrated by the assignment of the fundamentals of $MeSiF_3$, as is discussed in Chapter I.2, and the reassignment of $MeGeF_3$ and subsequently of $MeGeCl_3$, as presented here.

In the series $MeGeX_3$, there is little doubt regarding the assignments of $MeGeI_3$ [69] and $MeGeBr_3$ [70], but there have been three different assignments for the skeletal modes of $MeGeCl_3$ [63,71,72]. Assuming that nature requires a smooth trend of force constants on passing from iodide to fluoride, then each different assignment can be calculated, and those versions discarded which give force constant values that do not fit acceptable trends. In this case, the force constants, including the interaction terms, are describing the same motion in each molecule, since they each have the same geometry (and hence symmetry) and so whether one particular interaction term is used or not should have little effect on the final result, as long as each molecule is treated similarly. The skeletal deformation frequencies and possible assignments are shown in Table 1.5.3. Assignments (a) and (b) are the two possible assignments assuming that ν_5 is the

Table 1.5.3 Observed deformation frequencies (cm^{-1}) and possible assignments for MeGeX$_3$

X =	F (a)	(b)	(c)	Cl (d)	(e)	(f)	Br	I
ν_{11} GeX$_3$ rock	194	254	194	180	144	143	162	156
ν_5 GeX$_3$ def.(s)	292	292	254	180	179	136	125	98
ν_{12} GeX$_3$ def.(a)	254	194	292	141	179	177	94	72

assignment (c) ref.50 (d) ref. 63 (e) ref. 72 (f) ref. 73

highest of the three bands as is probably the case in MeSiF$_3$ (if the polarisation data is correct), and (c) is the assignment already published[50]. For MeGeCl$_3$, columns (d), (e) and (f) are the three published assignments. Force constant calculations were performed for all the assignments in Table 1.5.3 using LARMOL (see Appendix 4) and the values of those force constants responsible for the skeletal deformations are listed in Table 1.5.4 (abstracted from Table A8). Looking first at MeGeI$_3$ and MeGeBr$_3$, since these assignments are not in doubt, it is seen that as X becomes lighter, the values for f XGeX and fCGeX decrease slightly, while the interaction terms are small, positive and increase. For MeGeCl$_3$, assignments (e) and (f) produce a large increase in f XGeX and a

Table 1.5.4 Bending force constants (Nm.rad^{-2}) for MeGeX$_3$

X →	F (a)	(b)	(c)	Cl (d)	(e)	(f)	Br	I
f CGeX	59.5	95.8	45.2	60.7	36.0	34.0	60.6	64.8
f XGeX	79.9	45.8	94.2	71.7	106.5	85.2	68.2	75.6
fCGeX/CGeX	14.4	17.9	0*	6.2	0.7	-1.3	3.8	0.9
fXGeX/XGeX	9.1	4.5	0*	8.9	9.4	-12.0	4.4	3.6

*fixed; initial values <0.1

large decrease in $\underline{f}$ CGeX, while (f) also gives negative interaction terms. By contrast, the values which reproduce assignment (d) are fairly consistent with those from $MeGeI_3$ and $MeGeBr_3$ and on this account would seem the most probable. The near coincidence of ν_5 and ν_{11} is also observed in the silicon analogue. If (d) is then the favoured assignment for $MeGeCl_3$, and the trend of approximately constant (possibly slightly increasing) $\underline{f}$ XGeX and $\underline{f}$ CGeX values and positive, increasing interaction terms is to be maintained, then assignment (a) is the 'logical choice for $MeGeF_3$, and in fact this does parallel the most favoured assignment for $MeSiF_3$.

   iii) Other Calculations

        Unfortunately, the NCA was not so definitive for the assignment of $MeSiF_3$, so alternative methods were sought that might elucidate the problem. One that was used for the silane series, using a different type of force field, is repeated here as a confirmation of the assignment for the methylgermane analogues. In the chapter on "Vibrations" in Herzberg's book[1], the author developes expressions for the potential energy of a molecule in terms of a "central force field", first described by Dennison[74]. This assumes that the force acting on a given atom is the resultant of the attractions (and repulsions) of all the other atoms, bonded and non-bonded, and as such these forces lie along the interatomic axes. The result is an expression relating normal vibrations, the force constants and the geometry of the molecule as variables, along with the masses of the atoms. Thus for a

pyramidal XY_3 molecule (such as NH_3) the potential energy is expressed in the form of two force constants (one reflecting the force between X and Y, the other between Y and Y) and the changes in the distances between them. These changes are then expressed, in turn, in terms of the displacement coordinates for each atom and the angle ß, the angle between the three-fold symmetry axis and each X-Y bond, and the symmetry coordinates. The result of these manipulations in this case is a situation where the force constants cancel out of the resultant expression, which then consists of one geometric parameter (ß) and the four fundamental frequencies as the only variables. This expression (ref. 1, p. 163) is given as:

$$\cos^2 \beta = \left(\frac{4\nu_3^2 \nu_4^2}{\nu_1^2 \nu_2^2} + \frac{3m_y - 3m_x}{3m_y + 3m_x} \right)^{-1} \tag{5.2}$$

where the ν_i are the observed fundamental frequencies and m_x and m_y are the masses of X and Y. The beauty of this method is that being independent of the force constant values, the calculation avoids many of the uncertainties and assumptions inherent in NCA. When this method is applied to the second and third row trihalides, however, it becomes clear that the calculated value of ß is about $10°$ less than the experimentally determined value (Table 1.5.5).

In testing the simple applicability of this approach to the $MeMX_3$ series (M=Si,Ge) it has to be assumed that the methyl group has little influence on the skeletal vibrations of these molecules, either by ignoring it altogether or by

1

Table 1.5.5   Comparison of β values for selected XY_3 molecules

	β_{obs}	β_{calc}	$\beta_{obs} - \beta_{calc}$
PF_3	62°	56°	6°
PCl_3	$.64^o$	51°	13°
PBr_3	65°	55°	10°
AsF_3	60°	45°	15°
$AsCl_3$	59°	50°	9°

adding its mass to the M atom creating a "MeM" atom of mass 43 and 94 (for silicon and germanium respectively) at the apex of the pyramid. As a result of this simplification, one of the three skeletal modes present in $MeMX_3$ "disappears". In an XY_3 molecule there are only two deformations, analogous to the symmetric and asymmetric MX_3 deformations, ν_5 and ν_{12} in $MeMX_3$. The MX_3 rock, ν_{11}, involves the deformation of the CMX angle and has the MX_3 unit rocking virtually unchanged. In terms of the XY_3 molecule, this simply corresponds to a rotation, and thus does not appear in the calculation. This turns out to be extremely useful, since now the one a_1 mode and two e modes for $MeMX_3$ become one a_1 and one e for the XY_3 analogue. Thus if the a_1 mode can be determined un-ambiguously from the polarised Raman spectrum, which is usually the case as most of the compounds are liquids at room temperature, then only two assignments are possible, and this method will, if the assumptions are valid, disting-uish between them. The values used in calculating β for the various $MeGeX_3$ molecules, and the approximate description of the fundamentals used appear in Table 1.5.6. In accordance

Table 1.5.6 Frequencies and descriptions of fundamental vibrations used in β calculations for MeGeX$_3$

MeMX$_3$ XY$_3$		F (a)* (b) (c)			Cl (d) (e) (f)			Br	I
XY sym.str.	$\nu_4 \equiv \nu_1$	730	730	730	398	398	398	264	195
XY$_3$ sym.def.	$\nu_5 \equiv \nu_2$	292	292	254	180	179	136	125	92
XY asym.str.	$\nu_{10} \equiv \nu_3$	742	742	742	424	424	424	312	251
XY$_3$ asym.def.	$\nu_{12} \equiv \nu_4$	254	194	292	141	179	177	94	67

*for assignments and references, see Table 1.5.3.

with the evidence from Table 1.5.5, the calculation of α, the XGeX angle (related to β by $\sin \alpha/2 = \sqrt{3}/2 \sin \beta$) was performed with β and $(\beta+10)$. The results are displayed in Table 1.5.7 where i) and ii) refer to the two approximations as to the mass of M described above (i.e. Ge and "MeGe"). Two calculations were performed for MeGeI$_3$ using frequencies from the liquid (+50°C) spectra[69] used in Table 1.5.6, and

Table 1.5.7 Calculated values for β and α for MeGeX$_3$

			β	α	$\beta+10$	α
MeGeF$_3$	(a)	i)	54.8	90.1	64.8	103.2
		ii)	54.2	89.2	64.2	102.4
	(b)	i)	39.0	66.1	49.0	81.6
		ii)	38.1	64.5	48.1	80.2
	(c)	i)	64.4	102.7	74.4	113.0
		ii)	64.1	102.4	74.1	112.8
MeGeCl$_3$	(d)	i)	54.6	89.8	64.6	102.9
		ii)	53.9	88.8	63.9	102.1
	(e)	i)	62.6	100.5	72.6	111.5
		ii)	62.3	100.2	72.3	111.2
	(f)	i)	69.1	108.0	79.1	116.5
		ii)	69.0	107.9	79.0	116.4
MeGeBr$_3$			58.7	95.4	79.1	107.5
MeGeI$_3$			59.9	97.6	69.9	108.9

also from the solid, where ν_1 to ν_4 are 196; 91, 242 and 67,
cm^{-1} respectively. These latter values give rise to angles of
$\alpha=98.6°$ and $\alpha'=110.0°$, not appreciably different from the
results in the Table. Also for X=Br and I, the mass of the
methyl group was ignored, due to the decreasing difference
in the two approximations as X becomes heavier.

Any discussion involving a comparison of α' with
experimentally determined values of XGeX must be approached.
with caution because of the many assumptions made in the
method. Such a comparison, if one is to be attempted, should
start with the tribromide, since it is the only molecule
which is unambiguously assigned that has had its structure
determined[75]. The agreement (Table 1.5.8) is almost
embarrassingly close, but it is not suggested that this is

Table 1.5.8 Calculated α' values and observed XGeX angles
for MeGeX$_3$ molecules

		α'	XGeX	difference
MeGeF$_3$	(a)	102.8		2.7
	(b)	80.9	105.5[a]*	24.6
	(c)	112.9		7.4
MeGeCl$_3$	(d)	102.5		3.9
	(e)	111.35	106.4[b]	4.95
	(f)	116.45		10.05
MeGeBr$_3$		107.5	107.1[c]	0.4
MeGeI$_3$		108.9	–	–

a) ref. 51 b) ref. 76 c) ref. 75
*) Durig et al. (ref. 73) obtained ClGeCl 112.9°, but used
an incorrect assumed GeC bond length

a vindication of the method and its applicability. However, from the force constant arguments already presented, the preferred assignment at this point is (d), which is the closest, albeit marginally, to the experimental result. For MeGeF$_3$ the favoured assignment (a) is again the closest. However, more important is the trend in angles, getting wider as the halogen becomes larger, as observed experimentally. It is this observation which is considered the crux of the argument.

Despite some of the foregoing discussion on the validity of using frequencies alone, considering the change in frequencies in a series can be informative if used with care. A survey of the percentage increases in frequency on going to a lighter halogen is presented in Table 1.5.9. This reveals that the assignments proposed above for MeGeF$_3$ and MeGeCl$_3$

Table 1.5.9   Change in wavenumber for skeletal bending modes in MeGeX$_3$ molecules (%)

	F(a)	Cl(d)	Br	I
ν_{11} GeX$_3$ rock	194 ←8—	180 ←11—	162 ←4—	156
ν_5 GeX$_3$ def.(s)	292 ←62—	180 ←44—	125 ←28—	98
ν_{12} GeX$_3$ def.(a)	254 ←80—	141 ←50—	94 ←31—	72

	F {from Cl(d)}		Cl {from Br}	
	(b)	(c)	(e)	(f)
GeX$_3$ rock	254 ←41	194 ←8	144 ←12	143 ←12
GeX$_3$ def.(s)	292 ←62	254 ←41	179 ←43	136 ←9
GeX$_3$ def.(a)	194 ←38	292 ←107	179 ←90	177 ←88

are the only ones which produce a consistently increasing proportional change in wavenumber, except for the GeX_3 rock, where the actual increase is small, and thus the proportional increases more prone to error. If in fact it is the mass of halogen which is the major factor in determining the energies of the skeletal vibrations, then one would expect the changes to be as shown using the (a) and (d) assignments for $MeGeF_3$ and $MeGeCl_3$, with ν_{12} increasing more rapidly than ν_{11}, as it is more sensitive to a change in halogen (since it depends on XGeX, as opposed to CGeX). Reflecting a change in both XGeX and CGeX, ν_5 increases at a rate intermediate between the other two. Note that once again, assignments (e) and (f) for $MeGeCl_3$ could be rejected on this count, as both of these versions call for a lowering of the wavenumber for the GeX_3 rock compared to the bromine derivative and indeed even below the value in $MeGeI_3$.

This new assignment for $MeGeF_3$ is not totally inconsistent with the frequency comparisons presented at the beginning of this chapter for the original assignment. The skeletal deformation mode in MeGeF [64] at 215 cm^{-1} arising from the CGeF angle change, was used to assign the GeF_3 rocking mode in $MeGeF_3$ to the lowest frequency at 194 cm^{-1}, which is 10% lower. The highest frequency in $MeGeF_3$ at 292 cm^{-1} was originally assigned as the asymmetric GeF_3 deformation by comparison with the FGeF deformations in H_2GeF_2 [65] and $MeGeHF_2$ [66], both at 280 cm^{-1}. It is probably most fortuitous, but nevertheless interesting to note that 280 cm^{-1} less 10%

is 252 cm^{-1}. It may be more reassuring to observe the symmetric deformation between the asymmetric deformation and the rock, seeing as it is the result of a combination of the angle changes causing the other two vibrations but this is not a concrete argument against its occurrence at the highest frequency. Indeed, it is found between the other two modes when the halogen is much heavier than silicon in the MeSiX$_3$ analogues, and it is approximately coincident with the higher of the other two in MeSiCl$_3$. However, as is mentioned in Chapter I.2 the chloride seems to be the crossover point. The Raman spectrum of that region recorded in this laboratory (see Figure I.2.7) indicates that the symmetric deformation is if anything probably the higher of the two "coincident" frequencies, and that the crossover has already taken place.

The foregoing discussion has attempted to point out some of the dangers in drawing conclusions solely from either frequencies or force constants alone. This is especially true for bending modes, where for approximately tetrahedral groups there are several ways to define the interaction terms especially where the atoms or groups bonded to the central atom are dissimilar. Stretching force constants, on the other hand, are usually fairly well defined and therefore their values are more reliable. Also, because of the rule of thumb relationship with bond strengths within a related series, the direction of the trend can often be predicted. Unless the problem is well defined, therefore, additional data and calculations should be used in conjunction with a NCA.

REFERENCES

1. G. Herzberg, "Molecular Spectra and Molecular Structure II. Infrared and Raman Spectra of Polyatomic Molecules," Van Nostrand, Princeton, N.J., 1945.

2. E. Wiberg and E. Amberger, "Hydrides of the Elements of Main Groups I-IV," Elsevier, Amsterdam, 1971.

3. E.A.V. Ebsworth and S.G. Frankiss, Trans. Faraday Soc. 59, 1518 (1963).

4. E.A.V. Ebsworth and S.G. Frankiss, Trans. Faraday Soc. 63, 1574 (1967).

5. S.G. Frankiss, J. Phys. Chem. 71, 3418 (1967)

6. E.A.V. Ebsworth and J.J. Turner, J. Phys. Chem. 67, 805 (1963)

7. E.A.V. Ebsworth and J.J. Turner, J. Chem. Phys. 36, 2628 (1962)

8. H. Vahrenkamp and H. Nöth, J. Organomet. Chem. 12, 281 (1968)

9. M.P. Brown and D.E. Webster, J. Phys. Chem. 64, 698 (1960)

10. A.J.F. Clark and J.E. Drake, Spectrochim. Acta 32A, 1419 (1976)

11. K. Moedritzer and J.E. Van Wazer, Inorg. Chem. 6, 93 (1967)

12. E.W. Kifer and C.H. Van Dyke, Inorg. Chem. 11, 404 (1972)

13. H.J. Emeléus and M. Onyszchuk, J. Chem. Soc. 1958, 604.

14. A.J.F. Clark, J.E. Drake and R.E. Humphries, to be published.

15. C.R. Lassigne and E.J. Wells, J. Mag. Res. 31, 195 (1978)

16. C.J. Jameson, J. Chem. Phys. 66, 4977; 4983 (1977)

17. C.V. Raman, Ind. J. Phys. 2, 387 (1928); C.V. Raman and K.S. Krishnan, Ind. J. Phys. 2, 399 (1928): Nature 121, 501 (1928): Proc. Roy. Soc. London 122A, 23 (1928)

18. A. Smekal, Naturwiss. 11, 873 (1923)

19. W.W. Coblentz, "Investigation of Infra-red Spectra," Carnegie Inst. Pub., Washington, 1908.

20. E.B. Wilson, J.C. Decius and P.C. Cross, "Molecular Vibrations," McGraw-Hill, New York, N.Y., 1955.

21. L.A. Woodward, "Introduction to the theory of molecular vibrations and vibrational spectroscopy," Clarendon Press, Oxford, 1972.

22. L.A. Woodward, in "Raman Spectroscopy; Theory and Practice," Vol. 1, ed. H.A. Szymanski, Plenum Press, New York, N.Y., 1970.

23. reference 1, p.469 et seq.

24. reference 1, p.484

25. reference 1, p. 136-139; reference 5, p.232 et seq.

26. reference 1, p.269.

27. E. Fermi, Z. Physik 71,250 (1931)

28. A. Adel and D.M. Dennison, Phys. Rev. 43,716 (1933)

29. A. Langseth, Z. Physik 72,350 (1931)

30. R. Ananthakrishnan, Proc. Ind. Acad. Sci. 2A,452 (1935)

31. e,g. I.M. Mills, J. Mol. Spectry. 5,334 (1960).

32. e.g. S.J. Cyvin, "Molecular Vibrations and Mean Square Amplitudes," Elsevier, Amsterdam, 1968.

33. J.L. Duncan and I.M. Mills, Spectrochim. Acta 20,523 (1964)

34. J. Aldous and I.M. Mills, Spectrochim. Acta 19,1567 (1963)

35. H.C. Urey and C.A. Bradley, Phys. Rev. 38,1969 (1931)

36. D.F. Heath and J.W. Linnett, Trans. Faraday Soc. 54,264 (1949); J.W. Linnett and P.J. Wheatley, ibid. 54,39 (1949), and references therein.

37. I.M. Mills, Spectrochim. Acta 19,1585 (1963)

38. J.L. Hencher, Ph.D. thesis, McMaster University, 1964.

39. H. Kimmel and C.R. Dillard, Spectrochim. Acta 24A,909 (1968)

40. B.L. Crawford, Jr. and S.R. Brinkley, _J. Chem. Phys._ **9**, 69 (1941).

41. J.L. Duncan, _Spectrochim. Acta_ **20**, 1197; 1807 (1964).

42. T. Shimanouchi, I. Nakagawa, J. Hiraishi and M. Iishi, _J. Mol. Spectry._ **19**, 78 (1966)

43. J.H. Schachtschneider and R.G. Snyder, _Spectrochim. Acta_ **19**, 117 (1963)

44. R.G. Snyder and J.H. Schachtschneider, _Spectrochim. Acta_ **21**, 169 (1965)

45. C. Newman, J.K. O'Loane, S.R. Polo and M.K. Wilson, _J. Chem. Phys._ **25**, 855 (1956)

46. C. Newman, S.R. Polo and M.K. Wilson, _Spectrochim. Acta_ **10**, 793 (1959)

47. H. Bürger, J. Cichon and A. Ruoff, _Spectrochim. Acta_ **30A**, 223 (1974)

48. R.N. Dixon and N. Sheppard, _Trans. Faraday Soc._ **53**, 282 (1957)

49. H.R. Linton and E.R. Nixon, _Spectrochim. Acta_ **12**, 41 (1958)

50. J.W. Anderson, G.K. Barker, A.J.F. Clark, J.E. Drake and R.T. Hemmings, _Spectrochim. Acta_ **30A**, 1081 (1974)

51. J.E. Drake, R.T. Hemmings, J.L. Hencher, F.M. Mustoe and Q. Shen, _J. Chem. Soc. Dalton_ **1976**, 394

52. J.L. Hencher, unpublished observations.

53. J.L. Hencher and F.M. Mustoe, _Can. J. Chem._ **53**, 3542 (1975)

54. A.D. Caunt, H. Mackle and L.E. Sutton, _Trans. Faraday Soc._ **47**, 943 (1951)

55. J.E. Huheey, _J. Phys. Chem._ **69**, 3284 (1965)

56. J. Hinze and H.H. Jaffé, _J. Amer. Chem. Soc._ **84**, 540 (1962)

57. J. Hinze, M.A. Whitehead and H.H. Jaffé, _J. Amer. Chem. Soc._ **85**, 148 (1963)

58. J. Hinze and H.H. Jaffé, _J. Phys. Chem._ **67**, 1501 (1963)

59. J.E. Drake, C. Riddle and L. Coatsworth, _Can. J. Chem._ **53**, 3602 (1975)

60. E. Teller, quoted in W.R. Angus et al., J. Chem. Soc. 1936,971

61. O. Redlich, Z. physik. Chem. B28,371 (1935)

62. K. Licht and P. Köhler, Z. anorg. allgem. Chem. 383,174 (1971)

63. D.F. Van de Vondel and G.P. Van der Kelen, Bull. Soc. Chim. Belges 74,453 (1965)

64. G.K. Barker, J.E. Drake, R.T. Hemmings and B. Rapp, Spectrochim. Acta 28A,1113 (1972)

65. T.N. Srivastava, J.E. Griffiths and M. Onyszchuk, Can. J. Chem. 41,2101 (1963)

66. G.K. Barker, J.E. Drake, R.T. Hemmings and B. Rapp, J. Chem. Soc. A1971,3291

67. E.R. Lippincott and M.C. Tobin, J. Amer. Chem. Soc. 75, 4141 (1953)

68. A.D. Caunt, L.N. Short and L.A. Woodward, Trans. Faraday Soc. 48,873 (1952)

69. J.R. Durig, C.F. Jumper and J.N. Willis Jr., J. Mol. Spectry. 37,260 (1971)

70. J.W. Anderson, G.K. Barker, J.E. Drake and R.T. Hemmings, Can. J. Chem. 49,2931 (1971)

71. D.F. Van de Vondel, G.P. Van der Kelen and G. Van Hooydonk, J. Organomet. Chem. 23,431 (1970)

72. J.R. Aronson and J.R. Durig, Spectrochim. Acta 20,219 (1964)

73. J.R. Durig, P.J. Cooper and Y.S. Li, J. Mol. Spectry. 57,169 (1975).

74. D.M. Dennison, Phil. Mag. 1,195 (1926)

75. J.E. Drake, R.T. Hemmings, J.L. Hencher, F.M. Mustoe and Q. Shen, J. Chem. Soc., Dalton 1976,811

76. J.E. Drake, J.L. Hencher and Q. Shen, Can. J. Chem. 55, 1104 (1977)

PART I

CHAPTER I.1

VIBRATIONAL SPECTRA OF
THE METHYLSILANES

I.1.1   Introduction

The vibrational spectrum of methylsilane was first published in an infrared study about 25 years ago[1] in an organic chemistry journal. This gives a hint as to the impetus behind advances in organosilicon chemistry, as a comparison with organic chemistry. Subsequently, others have recorded the infrared spectra of CH_3SiH_3[2], along with CH_3SiD_3[3] and Raman and infrared spectra of CH_3SiH_3, CH_3SiHD_2 and CH_3SiD_3[4]. Several normal co-ordinate analyses of varying sophistication have been performed, on CH_3SiH_3 alone[2,5-7] and with CH_3SiD_3[8,9]. Two of the more interesting analyses used a force field calculated from data on CH_3SiH_3 and CH_3SiD_3 to predict the fundamentals for the perdeuteromethyl derivatives; CD_3SiH_3 only in one[10], and both in the other[11]. It was realized early in this work that the methyl-d_3 derivatives of the mono- and dihalogenomethylsilanes would be needed to assist in the vibrational assignments, and although only the $CD_3SiH_nX_{3-n}$ (n = 1,2) were eventually used, CD_3SiD_3 was also prepared to test the accuracy of Clark and Weber's[11] predictions. A force field was calculated using the data from the four isotopic variations, but comparison of force constants other than those for stretching is not really useful, due to the differing variety of interaction terms used in the two studies.

I.1.2 Preparation

i) CH_3SiH_3 and CH_3SiD_3

These compounds were prepared by the reduction by excess $LiAlH_4$ and $LiAlD_4$ of CH_3SiHCl_2 and CH_3SiCl_3 respectively[12,13]. A three-necked, round-bottomed flask containing a Teflon coated magnetic stirring bar was fitted with a right-angled tipping tube, and connected to the vacuum line manifold by a condenser (Figure A.1K) designed to contain a dry ice/methanol slush bath. The tipping was filled with the lithium salt (1 - 5 g), and the apparatus was evacuated. Dry dibutyl ether, followed by the chloromethylsilane, was distilled into the flask and the condenser then filled with the dry ice slush. The whole apparatus was closed to the manifold and some of the lithium salt (approx. 1/5) was tipped into the stirred liquids. After approximately 20-30 seconds the apparatus was opened to allow any gases to expand into the manifold which was then closed to the apparatus, and these gases passed into a train of U-traps containing liquid nitrogen. The condenser effectively prevented the ether or unreacted chlorosilane from leaving the reaction vessel. This procedure was repeated until all of the lithium salt was used, or until there was no further evolution of gases from the reaction mixture. The products from the U-traps were collected and passed through traps held at $-78^{\circ}C$ which trapped any ether which escaped the condenser, $-160^{\circ}C$, which held the methylsilane, and $-196^{\circ}C$. The purity of the products was checked principally by ^1H n.m.r. and vapour pressure measurements.

ii) CD_3SiH_3 and CD_3SiD_3

The silanes SiH_4 and SiD_4 were required as starting materials for the preparation of these compounds. Silane was obtained commercially, and silane-d_4 was prepared by the $LiAlD_4$ reduction of $SiCl_4$ in a manner analogous to the preparations above, except that the products were passed through a trap at $-160^{\circ}C$ prior to collection in a trap at $-196^{\circ}C$. Purity was checked by ^1H n.m.r. for SiH_4 and by Raman spectroscopy for SiD_4, to detect any unreduced Si-Cl bonds.

Dry hexamethylphosphoramide (HMPA; approx. 50 ml) was poured under positive dry nitrogen pressure (applied through the manifold) into a three-necked flask (150 ml) containing a Teflon coated stirring bar, and fitted with a tipping tube so that the stem of the tube hung vertically. The solvent (vapour pressure at $22^{\circ}C$ 0.2 mm Hg) was pumped on for about 5-10 minutes. Again under a positive pressure of dry nitrogen, small pieces of potassium (approx. 0.2 g), which had been rinsed in low boiling point petroleum ether, were placed in the neck of the reaction vessel and held there until the nitrogen flow had evaporated the ether. The potassium was then added to the solution which turned a dark blue colour as the potassium dissolved. The stopper to the neck of the reaction vessel was replaced and the solution pumped on for approx. 0.5 h until the vapour pressure of the neat solvent had been attained. The tipping tube was then immersed in liquid nitrogen and an excess (with respect to potassium) of the silane was condensed into it. The stopcock

to the manifold was closed and the silane allowed to warm

up. At first, bubbles on the surface of the solution took

on a yellow sheen. As the silane became absorbed into the

solution and reaction (equation 1) took place, the solution

$$2SiH_4 + 2K \xrightarrow{\text{HMPA}} 2SiH_3^-K^+ + H_2 \qquad (1)$$
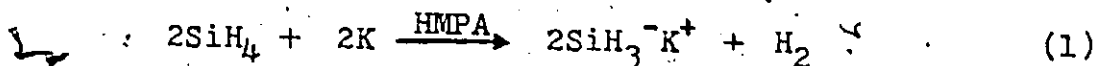
became clear and turned to a bright, yellow colour. The

reaction vessel was opened to the pump through a train of

U-traps at $-196^\circ C$, to retain excess silane, until the vapour

pressure returned again to approximately that of the neat

solvent. The tipping tube was again immersed in liquid

nitrogen and CD_3I condensed into it. The CD_3I was allowed

to warm and as reaction (equation 2) took place so the solu-

tion became cloudy and turned white in colour. (Care had to

$$SiH_3K + CD_3I \longrightarrow CD_3SiH_3 + KI \qquad (2)$$
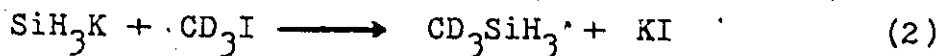
be taken at this point to keep the reaction vessel from

becoming too warm, by occasional immersion in an ice bath,

otherwise the solution took on a reddish tint and the yield

became low to non-existent). The resulting gases were passed

through a trap at $-78^\circ C$ to retain iodomethane, $-160^\circ C$ to

retain the methylsilane and $-196^\circ C$ to retain any excess silane.

A possible contaminant, dimethylsilane, which arises from the

removal of two hydrogens from silane in the first stage

(cf. equation (1)) is almost impossible to separate complete-

ly from methylsilane (the melting points differ by $6^\circ C$[15]).

Purity was checked by Raman spectroscopy, which

would detect CD_3I from the strong C-I stretch at 501 cm^{-1} [16],

by ^{1}H n.m.r. spectroscopy for CD_3SiH_3, which indicated greater than 97.5 mol % D for the CD_3 group, and ^{13}C n.m.r. spectroscopy, which showed only the expected septet resonances for both compounds.

The mass spectrum of both CD_3SiD_3 and CD_3SiH_3 was also recorded, with that of CD_3SiD_3 indicating less than 1.5% of dimethylated species, by comparison of base peak intensities for CH_3SiH_3 and $(CH_3)_2SiH_2$[17]. The molecular ion and CSi^+ intensities were both very low, less than 0.5% of the base peak, which corresponded to $(M-2D)^+$. The $CSiD_n$ pattern was almost identical to that for $CSiH_n$ observed for CH_3SiH_3, with decreasing intensities from the base peak to CSi^+. The products of Si-C fission, predominantly SiD_2^+ and Si^+, were also similar. This previous work[17] suggested, albeit on little evidence, that the hydrogens, which are of course indistinguishable, were stripped from silicon first and then carbon, presumably due to the lower bond energy (by ca. 10 kcal.mol^{-1}) for Si-H[18] than for C-H[19]. However, the mass spectrum for CD_3SiH_3 and later CH_3SiD_3 could not be as straightforward as this, due to the different masses of the hydrogens on carbon and silicon, and the small but definite difference in bond energies between H and D bound to the same atom (cf. D(H-H) = 104.21, D(H-D) = 105.03 and D(D-D) = 106.01 kcal. mol^{-1} [20]). Computer reduction of the data to give monoisotopic abundancies revealed that for CX_3SiX_3 (X = H or D) the intensity of the CX_2SiX^+ peak should be at least as great as, and probably greater than that of

CX_3Si^+. The stability of this former ion could be accounted for by a double-bonded resonance structure $CX_2 = SiX$, or by the ability of silicon to form quasistable divalent compounds (e.g. SiF_2[21], $SiCl_2$, SiH_2, $HSiCl$, $HSiF$[22]). However, without a metastable study the origin of these ions is speculation. Two previous studies observed metastable transitions involving loss of D_2 from $CH_3SiD_3^+$ [23] and H_2 from $CH_3SiH_2^+$ [17,23], but there was no transition observed that involved loss of a hydrogen molecule other than from silicon. If this observation is assumed to hold rigourously then formation of CX_2SiX^+ from the energetically unfavourable* ion $CX_2SiX_3^+$ is unlikely and it can be postulated that loss of X from carbon in CX_3SiX^+ is an important process.

I.1.3 Calculations

The molecular geometry was taken from microwave data[27], which gave the following parameters; C-H 110, Si-C 186.7 and Si-H 148.4 pm, $\angle$ HCH 107.7°, and $\angle$ HSiH 108.3°. The calculated frequencies were fitted to the liquid Raman data. Despite incorporating any effects arising from intermolecular attraction, this allows for much better distinction than do the gaseous infrared spectra between nearly degenerate modes and in the overlapping CD_3 and SiH_3 (and residual SiH) stretching regions. The Raman spectra of CH_3SiH_3 and

---

* Although thermochemically unfavourable from data on neutral species, the sign of the dipole moment of methylsilane indicates that silicon is the more negative site (ref. 24), contrary to simple electronegativity ideas (ref. 25) and bond moment calculations (ref. 26), and thus favours fission of the Si-H bond relative to C-H after the removal of an electron.

CH_3SiD_3 were also recorded in this work, mainly because the
only previously recorded spectra were obtained using photo-
graphic plates[4], and also to provide some internal consistency.
Thus at high laser power (ca. 1.5 W) and narrow slitwidths
(2 cm^{-1}), the symmetric and asymmetric SiH_3 deformations
which had been assigned to an envelope centred at 947 cm^{-1}
have been resolved into maxima at 962 and 944 cm^{-1}. Other
slight differences have also been taken into account.

I.1.4   Vibrational Spectra

The molecules have C_{3v} symmetry[7,27], and as such all
fundamentals except the a_2 torsional mode should be observed.
As well as being polarised in the Raman effect, the a_1 modes
are expected to exhibit A-type bands in the infrared spectra.
The numbering, activity and approximate description of the
modes is set out in Table I.1.1.

The spectra for CH_3SiH_3 and CH_3SiD_3 do not differ mark-
edly from those already published[1-4] except, as noted above,
for some increased resolution in parts of the Raman spectra,
and so are not shown. The infrared spectra of CD_3SiH_3 and
CD_3SiD_3 are shown in Figures I.1.1 and I.1.2 and the Raman
spectra in Figures I.1.3-I.1.5. The observed frequencies
for these two molecules are listed in Tables I.1.2 and I.1.3.

As might be expected, interpretation of the spectra for
these molecules is more complicated than that of the CH_3-
derivatives because of the "piling-up" of fundamentals as
they decrease in wavenumber on deuteration, and because of
interference from vibrations due to residual hydrogen atoms,

Figure I.1.1 Infrared spectrum of gaseous CD_3SiH_3 (pressure 11 mm Hg)
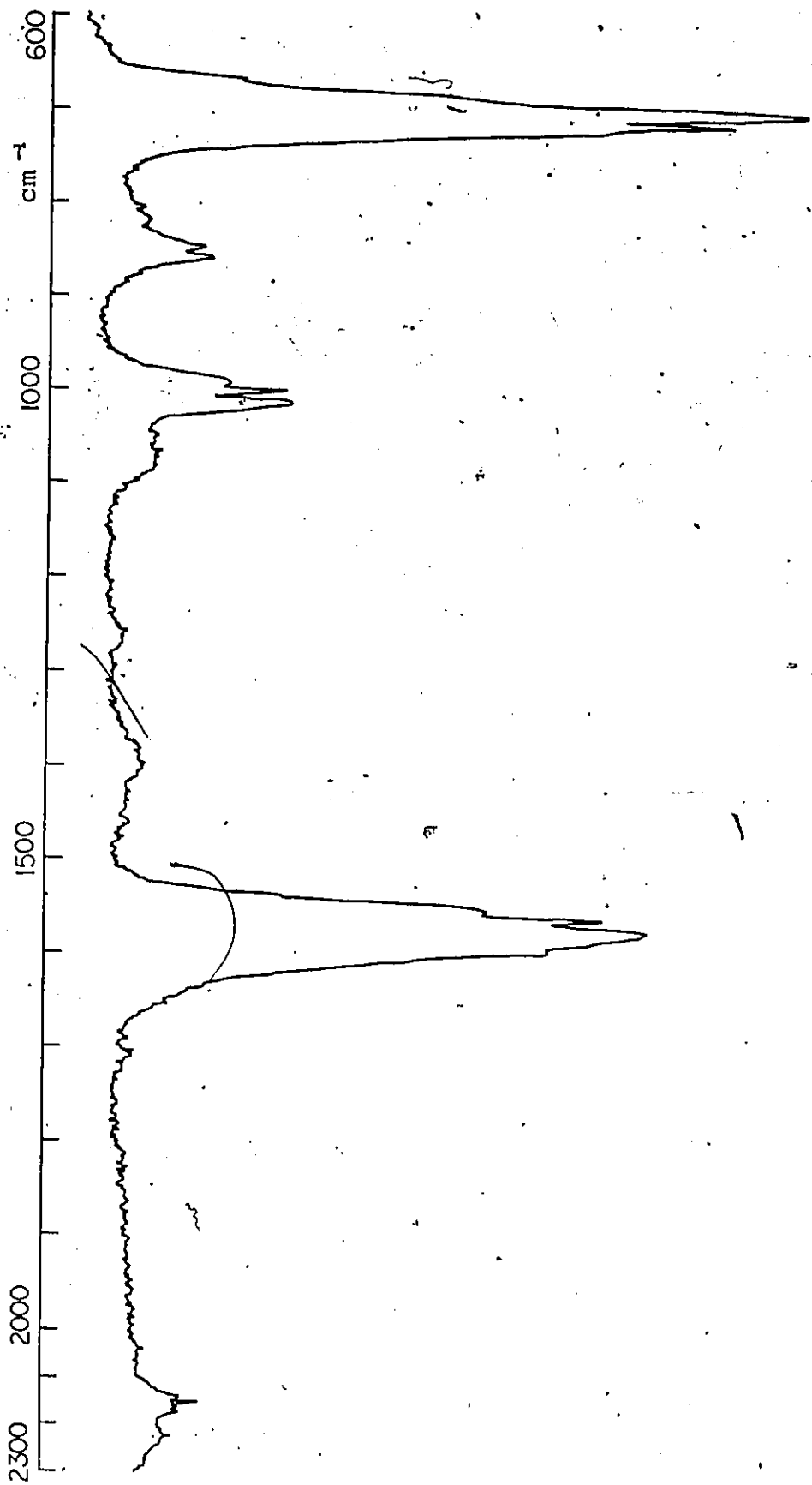
Figure I.1.2 Infrared spectrum of gaseous CD_3SiD_3 (pressure 8.5 mm Hg)
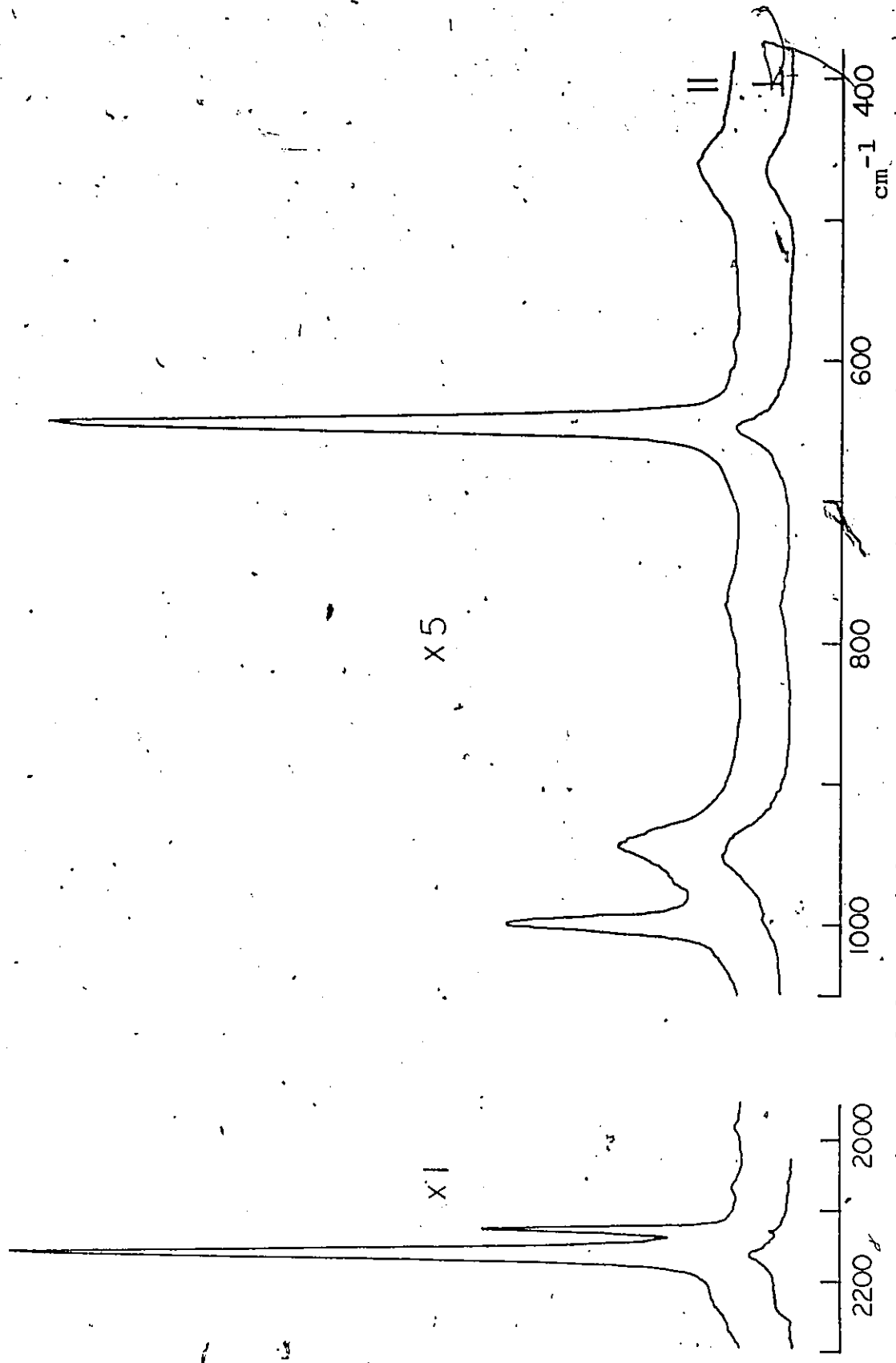
Figure I.1.3 Partial Raman spectrum of liquid CD_3SiH_3
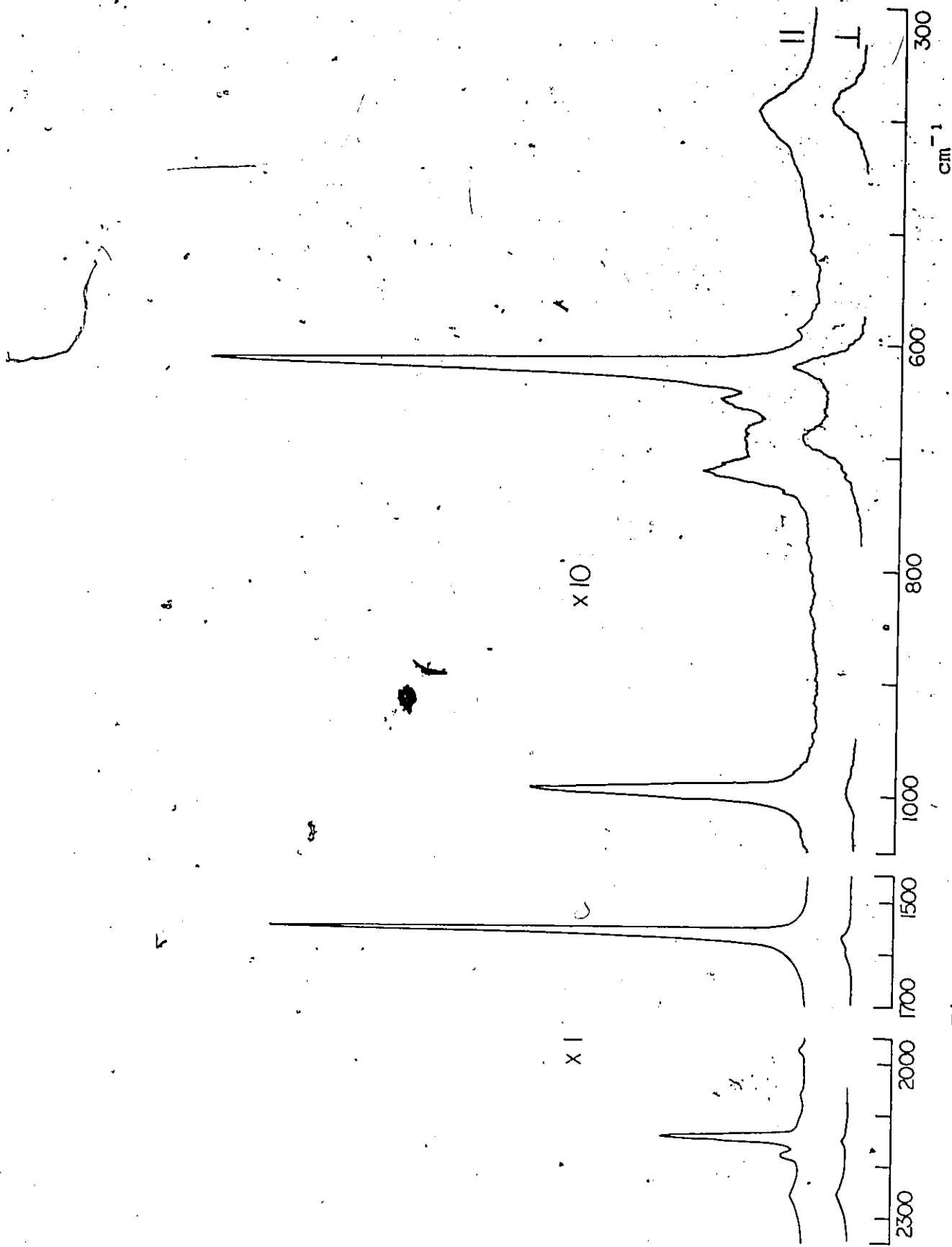
Figure I.1.4 Partial Raman spectrum of liquid CD_3SiD_3

CD₃SiH₃

CD₃SiD₃
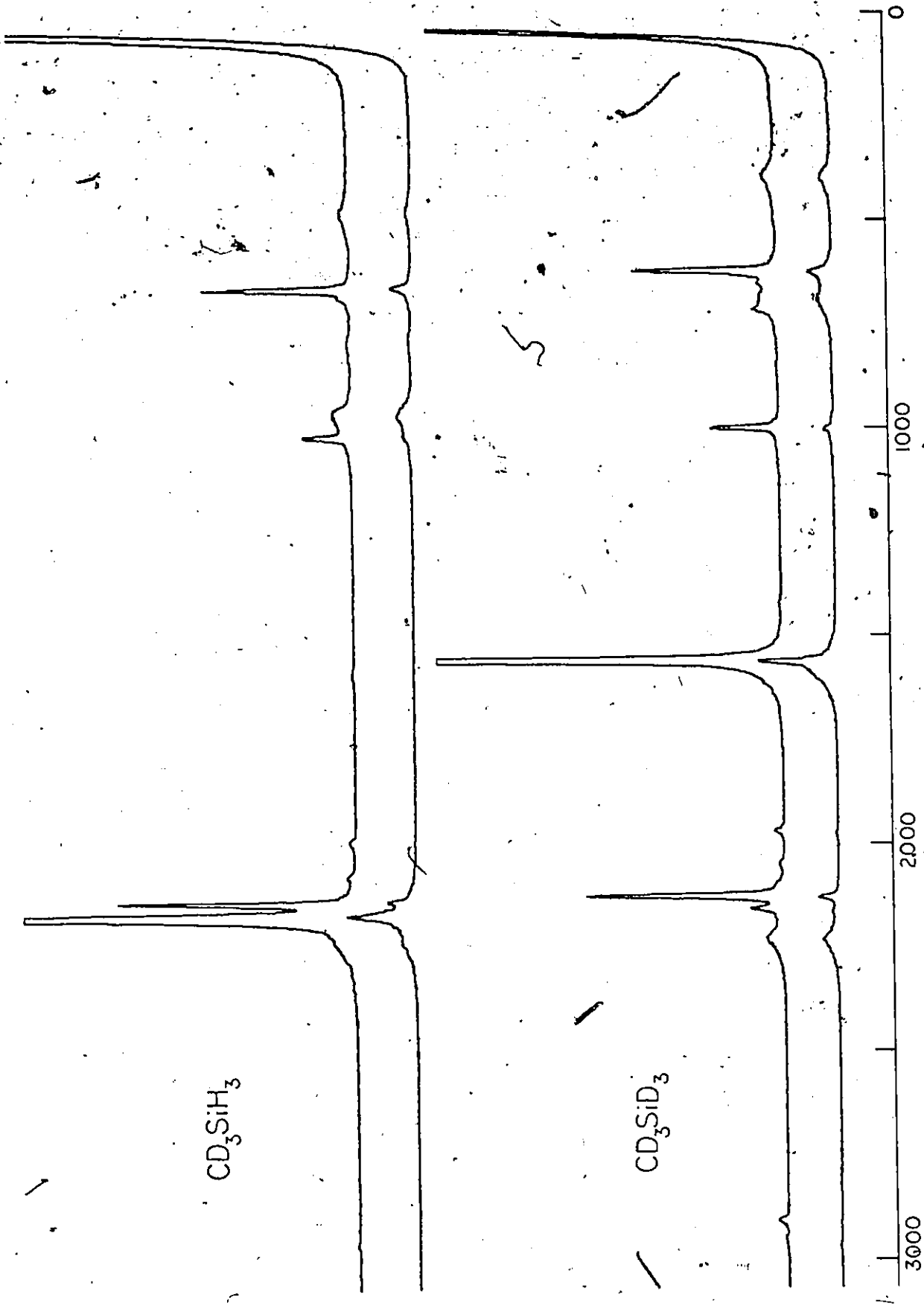
Figure 11.5 Raman spectra (cm⁻¹) of the Methylsilanes

3000   2000   1000   0

Table I.1.1 Numbering, approximate description, and activity of the vibrational modes of CH_3'SiH_3' (H' = H,D)

Approximate Description	Class of vibration		
	a_1	a_2	e
CH_3 stretch	ν_1		ν_7
SiH_3 stretch	ν_2		ν_8
CH_3 def.	ν_3		ν_9
SiH_3 def.	ν_4		ν_{10}
CSi stretch	ν_5		
CH_3 rock			ν_{11}
SiH_3 rock			ν_{12}
torsion		ν_6	
Activity:	i.r.,R(pol.)	inactive	i.r.,R(dep.)

Table I.1.2 Vibrational spectra (cm^{-1}) of CD_3SiH_3 and CD_3SiD_3

CD₃SiH₃		CD₃SiD₃		Assignment
IR (gas)	Raman (liq)	IR (gas)	Raman (liq)	
~2235 sh	2231 wsh, dp	2234 wbr	2230 mw, dp	ν_7
R 2181 }		1577 }	1580 w, dp	ν_2
Q 2170 } vs	2164 vs, p	Q 1562 } vs	1559 vs, p	ν_8
P 2157 }		P 1550		
	2129 s, p	~ 2133 vwsh	2131 s, p	ν_1
	2068 vw		2052 vw	$2\nu_9$
	1982 vw		1972 vw	$2\nu_3$
	1044 vw, dp		1036*	~ν
R 1015 }		R 1013 }		
Q 1004 } s	1000 m, p	Q 1001 } m	998 m, p	ν_3
P 998 }		P 990 }		
R 950 }	~ 957 wsh, dp	693 B, vs	682 w, dp	ν_{10}
Q 941 } vs	945 m, p	717 vs	710 w, p	ν_4
P 930 }				
773 m	774 wbr, dp		389 w, dp	ν_{12}
R 657 }		R 633 }		
Q 642 } mw	645 ms, p	Q 617 } vvw	619 ms, p	ν_5
P 631 }		P 604 }		
	457 w, dp	668 vw	646 w, p	ν_{11}

Abbreviations are s - strong, m - medium, w - weak, br - broad, sh - shoulder, v - very, p - polarised, dp - depolarised. The numbering of modes is kept constant for a particular mode regardless of a change of order to facilitate comparisons. * See text.

Table I.1.3

Observed and Calculated Frequencies, and Potential Energy Distribution of the Methylsilanes

Mode	Description	CH₃SiH₃ Obs.	CH₃SiH₃ Calc.	CH₃SiD₃ Obs.	CH₃SiD₃ Calc.	CD₃SiH₃ Obs.	CD₃SiH₃ Calc.	CD₃SiD₃ Obs.	CD₃SiD₃ Calc.
ν_1	CH₃ str. (a₁)	2920; 96(1)	2938.8	2917; 96(1)	2938.8	2129; 95(1)	2114.1	2131; 96(1)	2114.2
ν_2	SiH₃ str. (a₁)	2161; 97(2)	2173.4	1556; 97(2)	1548.3	2164; 97(2)	2173.1	1559; 92(2)	1548.3
ν_3	CH₃ def. (a₁)	1257; 64(4) +48(5) −36(14) +14(12) +12(10)	1261.7	1257; 65(4) +48(5) −36(14) +14(12) +12(10)	1261.0	1000; 50(4) +37(5) −28(14) +23(3) −14(18) +11(12)	997.3	996; 57(4) +42(5) −32(14) +23(3) −15(18) +12(12) +11(10)	992.1
ν_4	SiH₃ def. (a₁)	948; 55(7) +46(6) −15(15)	946.1	652; 39(3) +27(7) +23(6) +11(19)	655.7	945; 49(7) +41(6) −14(15)	940.4	710; 45(7) +38(6) +20(3) −12(15) −10(19)	711.2
ν_5	CSi str. (a₁)	700; 97(3)	701.9	733; 59(3) +28(7) +24(6) −13(19)	734.9	645; 80(3) +10(18)	641.6	619; 60(3) +10(7)	617.3
ν_7	CH₃ str. (e)	2976; 101(1)	2981.8	2975; 101(1)	2981.7	2231; 100(1)	2224.9	2230; 100(1)	2224.7
ν_8	SiH₃ str. (e)	2162; 101(2)	2169.7	1578; 101(2)	1571.9	2164; 101(2)	2169.6	1580; 101(2)	1571.7
ν_9	CH₃ def. (e)	1422; 113(4) −11(10)	1420.4	1422; 113(4) −11(10)	1420.4	1043; 108(4) −10(10)	1040.1	1036; 109(4) −10(10)	1039.2
ν_{10}	SiH₃ def. (e)	960; 91(6) +14(7)	962.3	685; 110(6) −10(13)	678.6	957; 104(6) −10(13)	954.6	682; 71(6) +19(7) +15(5)	688.6
ν_{11}	CH₃ rock (e)	870; 56(5) +19(6) +16(7) +14(16)	863.3	821; 85(5) +14(16) −12(12) +11(7)	825.3	457; 109(5) +61(7) −39(16) −16(12) −10(17)	451.0	646; 43(5) +40(6) +11(7) +10(16)	661.1
ν_{12}	SiH₃ rock (e)	532; 91(7) +74(5) −39(16) −11(12) −10(17)	536.0	426; 107(7) +48(5) −34(16)	428.1	774; 50(7) +26(5) +17(16)	758.3	389; 89(7) +78(5) −39(16) −11(12) −10(17)	383.9

*Only contributions of 10% or more of the force constants (in parentheses) are included.

such as the SiH stretch, or CH bends in the infrared, that are usually fairly intense. This interference is especially noticeable in the former case where the SiH stretch and CD_3 stretches are in the same region. Because of this near coincidence and the weakness of CH bends in the Raman effect, more reliance is placed on the Raman data than on the infra-red. The Raman effect also produces significantly narrower bandwidths, which reduces the chances of overlap, as is exemplified by the full width at half maximum of ca. 15 cm^{-1} for the SiH_3 stretches compared to ca. 90 cm^{-1} in the infra-red. This is best seen in the 2200 cm^{-1} region of CD_3SiH_3 where the infrared spectrum shows an apparently symmetrical A-type band at 2170 cm^{-1}, with slight broadening to high wavenumber at the base. This actually consists of four fundamentals; ν_1 and ν_7, the CD_3 stretches and ν_2 and ν_8, the SiH_3 stretches. In the Raman spectrum there are three distinct bands, two sharp, polarised bands at 2129 (ν_1) and 2164 cm^{-1} (ν_2) and in the polarised scan, a broad band at 2231 cm^{-1} (ν_7). The asymmetric SiH_3 stretch, ν_8, is assigned at the same wavenumber as the symmetric stretch, as is the case in CH_3SiH_3. In the infrared spectrum of this same region in CD_3SiD_3, the residual SiH stretch overlaps with the weak CD_3 stretches, but in the Raman spectrum these stretches are clearly seen at 2230 (dep., ν_7) and 2131 cm^{-1} (pol., ν_1). The peak arising from SiH present is small and is seen at 2164 cm^{-1}.

The symmetric CD_3 deformations, ν_3, appear as medium

to strong A-type bands and medium, polarised-bands at ~ 1000 cm^{-1}, but there is less confidence about the asymmetric deformations, ν_9 which are overlapped by ν_3 in the infrared, and virtually absent in the Raman spectra. However, the fact that two bands are observed in the deformation overtone region (cf. the ~ 2800 cm^{-1} region in CH_3^- compounds) of the Raman spectra at 1982 and 2068 cm^{-1} for CD_3SiH_3 and 1972 and 2052 cm^{-1} in CD_3SiD_3 allows for an indirect estimate of the frequency. It is most probable that the more intense low wavenumber band is the overtone of ν_3 (2x1000 for CD_3SiH_3 and 2x996 cm^{-1} for CD_3SiD_3), and if the assumption is made that the high wavenumber band is $2\nu_9$ rather than $\nu_3 + \nu_9$ (i.e. has the representation $a_1 + e$ rather than e and hence is probably more intense), this puts a lower limit on ν_9 of 1034 and 1026 cm^{-1} for CD_3SiH_3 and CD_3SiD_3 respectively. Assuming that the effects of anharmonicity and Fermi resonance with ν_3^{28} are similar to those for $2\nu_3$, this places ν_9 at 1043±10 and 1036±10 cm^{-1} respectively. Comparison with similar modes in CD_3GeH_3[29] indicates that these numbers are not unreasonable (ν_3 is at 977.5 and ν_9 at 1032 cm^{-1}).

The SiH_3 deformations, ν_4 and ν_{10}, appear in the same envelope in the infrared spectrum of CD_3SiH_3 and produce a peak with a maximum at 945 cm^{-1} in the Raman spectrum which shifts slightly in the perpendicular scan, indicating different frequencies for ν_4 and ν_{10}. These are estimated at ca. 957 (ν_{10}) and 945 cm^{-1} (ν_4). The SiC stretch, ν_5, is then assigned to the remaining strong polarised feature in

the Raman and medium weak A-type band in the infrared spectrum, ca. 644 cm^{-1}. The remaining two e fundamentals at 773 and 460 cm^{-1} are designated the SiH_3 rock and CD_3 rock respectively from the potential energy distribution of the normal co-ordinate analysis. However, due to extensive mixing, this conventional description is only approximate, and will be more fully discussed in the following section.

Apart from the SiD_3 rock, ν_{12} at 390 cm^{-1} (and again the p.e.d. shows this mode to be heavily mixed with the methyl rock), the remaining four fundamentals of CD_3SiD_3 are found between 720 and 600 cm^{-1}. The infrared spectrum of this region (Figure I.1.6) shows one intense envelope with two maxima at 717 and 704 cm^{-1}. The SiC stretch, ν_5, is only observed at high pressures (160 mm Hg) using the absorption expansion facility as an A-type feature in the low wavenumber tail of this envelope. The weakness of this band was also noted in the infrared spectrum of $(CH_3)_2SiD_2$[30], where in fact it was unobserved in the gas phase and was only weakly present in the solid state spectrum. The Raman spectrum shows three distinct bands (Figure I.1.7); the strong, polarised peak at 619 cm^{-1}, presumably ν_5, the SiC stretch, the others being at 646 and 710 cm^{-1}. With the polarizer perpendicular, however, only two bands are seen; the polarised portion of the 619 cm^{-1} band and a new maximum at 682 cm^{-1}, which is thus assigned as an e mode. It is difficult to determine the depolarisation ratio of the band at 646 cm^{-1} as it is overlapped by both the 619 and 682 cm^{-1} bands, but

Figure I.1.6 Infrared spectrum (750–650 cm $^{-1}$) of CD_3SiD_3
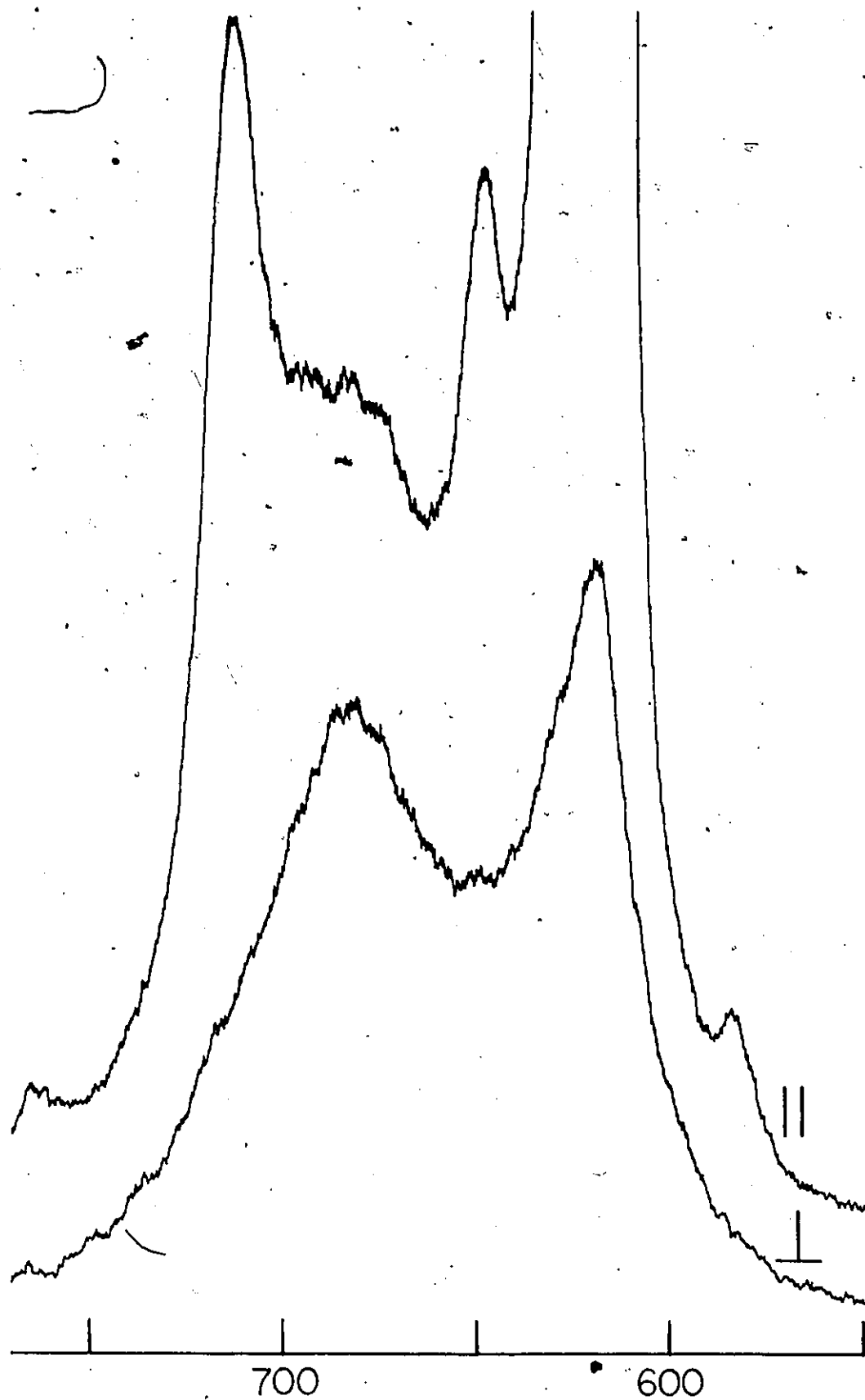
Figure I.1.7 Raman spectrum (770–550 cm⁻¹) of liquid CD_3SiD_3

the peak at 710 cm^{-1} completely disappears into the tail of
the 682 cm^{-1} band and is therefore assigned as the a$_1$ mode.
This arrangement appears to be borne out by the NCA. The two
weak bands at 763 and 583 cm^{-1} in Figure I.1.7 (both polarised)
are most probably 2 ν_{12} (2x389 cm^{-1}) and the usually intense
symmetric Si-O stretch; the latter arising from the slight
hydrolysis that is inevitable when making repeated manipula-
tions on the vacuum line. There was no evidence of the hydro-
lysis product in the ^{1}H n.m.r. spectrum of the original
sample.

I.1.5   Calculations and Discussion

Despite the large number of force constant calculations
for methylsilane referred to in the Introduction, only the
results of Lannon et al[10] and Clark and Weber[11] will be
discussed in relation to the findings for this work as they
were the only ones to calculate values for the as then
unreported deuteromethyl compounds.

In the calculation of the force field the usual dilemma
concerning the number of interaction force constants to use
was encountered. In this case the course of including those
interactions which can reasonably be expected to occur was
followed rather than one which would be more mathematically
elegant. The final choice consisted of 19 force constants
(seven diagonal and 12 interactions) compared to Clark and
Weber's 15 and the 14 of Lannon et al. Inclusion of most of
those extra terms was necessary to account for differences
introduced by the CD$_3$ group relative to the CH$_3$ group.

Using more interaction terms should mean a more accurate reproduction of the observed frequencies, and this is indeed the case. The other studies, having only the CH_3- compounds as their data base, should be expected to show a relatively large error in their predictions for the CD_3 derivatives, while using frequencies from all four molecules the results of this work should be more of a compromise, showing a relatively larger error in the CH_3- compounds. However this expected increase in error in the CH_3- derivatives is more than made up for by the extra interaction force constants, as Table I.1.4 shows. The force constants values used in this work are listed in Table I.1.5 and the diagonal terms compared with other values in Table I.1.6. Some differences will be accounted for by the different interaction terms used, as in the case of my values for $\underline{f}$ HCH. The values of Duncan[8] are also included, as an inspection of his a' values (he used symmetry co-ordinate force constants i.e. separate force constants for symmetric and asymmetric modes) shows the set to have greater internal consistency than that of Lannon et al.who used the same method. (It should also be noted, especially with respect to Table I.1.4 that Lannon et al used one more significant figure in the force constants for calculation of the frequencies).

Although the force constants used in this study reproduce the frequencies to 6.5 cm^{-1}, or less than 6%, anharmonicity corrections are probably of this order, again reflecting the approximate nature of the force field. The most noticeable

Table I.1.4 Average frequency error for force constant calculations

	Lannon[a] et al	Clark and[b] Weber	this work
CH_3SiH_3	6.7	12.0	6.3
CH_3SiD_3	7.3	15.0	6.0
CD_3SiH_3	22.6	24.3	6.7
CD_3SiD_3	--	27.0	7.0
no. of force constants used	14	15	19

a) ref. 10;   b) ref. 11

Table I.1.5 Force constant values for the methylsilanes

No.	Description	Value*
1	f CH	481.
2	f SiH	270.
3	f CSi	295.5
4	f HCH	61.
5	f HCSi	45.
6	f HSiH	50.
7	f CSiH	59.
8	f CH/CH	8.4
9	f SiH/SiH	3.5
10	f HCH/HCH	5.7
11	f HCH/HCSi	8.5
12	f HCSi/HCSi	6.4
13	f HSiH/HSiH	4.7
14	f HSiH/CSiH	4.1
15	f CSiH/CSiH	3.5
16	f t-HCSi/CSiH	12.2
17	f c-HCSi/CSiH	-3.2
18	f CSi/HCSi	16.0
19	f CSi/CSiH	12.3

* Units are $N.m^{-1}$ for stretching and $N.m\ rad^{-2}$ for bending force constants.

Table I.1.6 Comparison of diagonal force constant values

	L,W & N[a]	Duncan[b]	C & W[c]	this work
f CH	483.6	489.5	477.	481.
f SiH	271.7	273.5	271.	270.
f SiC	319.4	297.0	322.	295.5
f HCH	51.9	51.1	53.	61.
f HCSi	41.9	40.9	58.7	45.
f HSiH	44.4	46.2	41.2	50.
f CSiH	49.8	55.8	53.4	59.

a) ref. 10; b) ref. 8; c) ref. 11
stretching constants $N.m^{-1}$; bending $N.m\ rad^{-2}$

features of Table I.1.5 are the relatively large values for
interaction terms involving the C-Si bond. Force constants
16 and 17 affect the e modes, and 18 and 19 the a_1 modes.
Force constant 18 is necessary to keep the CD_3 deformations
ν_3 and ν_9 in the correct order, a problem which the other
workers did not have to resolve. Force constant 16, which
descibes the "whiplash" motion of hydrogen atoms trans to
each other, is especially prominent in ν_{11} and ν_{12}, the CH_3
and SiH_3 rocks. As mentioned above, the 774 and 457 cm^{-1}
bands in CD_3SiH_3 were assigned as the SiH_3 and CD_3 rocks
respectively based on the major contributor to the p.e.d.;
in this case f CSiH and f HCSi respectively, although this
is possibly contrary to intuition. However, if only the
contributions from force constant 16 are considered, it
would appear that these assignments should be reversed,
because in the other three molecules force constant 16

contributes an average of $-37(\pm 3)\%$ for the silyl rock and $+13(\pm 3)\%$ for the methyl rock, whereas it is the opposite in CD_3SiH_3 (+17% for silyl and -39% for methyl rock). A lesser but similar effect is also noticed for force constant 17. The ordering of ν_{11} and ν_{12} in CD_3SiH_3 based on contributions of the diagonal force constants appeared surprising at the outset, but is the assignment proposed by Clark and Weber, although not by Bannon et al. It would have been interesting to see their p.e.d.'s which unfortunately did not appear in either paper. Based on related molecules [31], the frequencies 774 and 457 cm^{-1} appear both too high and too low for either mode, although it should be expected that the CD_3 rock would be the higher of the two (cf. SiH_3 rock vs. CD_3 rock in SiH_3X and CD_3X [30]). It is interesting however, to note the trends in the analogous CD_3CH_3 and SiD_3SiH_3 molecules compared to MH_3MH_3 and MD_3MD_3 ($M = C^{31};Si^{13}$). In these cases the MH_3 and MD_3 rocks in the mixed compound are higher and lower respectively than in the symmetric compounds (when the symmetric (e_g) and asymmetric (e_u) rocks in the latter have been averaged). This is most dramatically seen in SiD_3SiH_3 where the SiH_3 rock increases from 502 to 936 cm^{-1} (over 85%), while the SiD_3 rock falls from 376 to 311 cm^{-1}. The assignment proposed by the force constant calculation in this work follows this same trend, as can be seen in Table I.1.3. (These trends are not followed in the heavier analogues CH_3GeH_3 [29] and SiH_3GeH_3 [10], however).

Apart from this point, the only other deviations are

Table I.1.7 Comparison of calculated and observed frequencies for CD_3SiH_3 and CD_3SiD_3

	CD_3SiH_3				CD_3SiD_3		
	calc[a]	obs[a]	calc[b]	calc[c]	calc[a]	obs[a]	calc[b]
ν_1	2114.1	2129	2155.5	2113.0	2114.2	2131	2153.3
ν_2	2173.1	2164	2148.8	2172.2	1548.3	1559	1533.6
ν_3	997.3	1000	1038.0	1045.8	992.1	996	1022.0
ν_4	940.4	945	921.0	931.5	711.2	710	723.3
ν_5	641.6	645	617.1	607.3	617.3	619	577.0
ν_7	2224.9	2231	2191.7	2213.1	2224.7	2230	2179.7
ν_8	2169.6	2164	2170.7	2171.0	1571.7	1580	1574.8
ν_9	1040.1	1043	1029.9	1013.9	1039.2	1036	1029.0
ν_{10}	954.6	957	955.8	956.4	688.6	682	647.3
ν_{11}	451.0	457	487.9	720.8	661.6	646	705.8
ν_{12}	758.3	774	729.8	477.2	383.9	389	400.1

a) this work; b) ref. 11; c) ref. 10

relatively minor, as can be seen from Table I.1.7. Both the other calculations have the CD_3 deformations, ν_3 and ν_9 reversed in CD_3SiH_3 (but not in CD_3SiD_3 by Clark and Weber); the latter also get the SiH_3 and CD_3 stretches mixed up, (and the SiH_3 stretches in the reverse order) and more understandably, in the "congested" region of CD_3SiD_3 where the assignments of the 682 and 646 cm^{-1} bands are reversed.

CHAPTER I.2

TRIFLUOROMETHYLSILANE

AND

TRIIODOMETHYLSILANE

I.2.1 Introduction

Reports of the vibrational spectra of CH_3SiX_3 compounds started to appear in the literature around 1950. (X = F[32], Cl[33-35], Br[36]), in contrast to the corresponding germanium compounds CH_3GeX_3, which were first reported in the mid-1960's (X = Cl[37,38]). The report of the spectra of CH_3GeF_3 described in Chapter 1.5 completed the germanium series (X = Br[39], I[40,41], F[42]), whereas at that time the only mention of CH_3SiI_3 had been in a boiling point determination in 1951[43], and then later in an n.m.r. study in 1973[44]. The value of the chemical shift from the latter report is in disagreement with those recorded in this study, however. The methylsilane derivatives were useful to the work presented in the following chapters as a guide to the frequencies that might be expected to appear in the skeletal deformation region, and so CH_3SiI_3 was prepared and the vibrational spectra recorded[45]. Initial NCA calculations on various silane and methylsilane derivatives produced a range of values that might reasonably be expected for any particular force constant. The report on CH_3SiF_3[32], which distinguished the modes only as far as a' or e without specifically assigning them, also included an NCA, the force constant values from which (there was no p.e.d. reported) were grossly different from those encountered here. It was also obvious from the observation of infrared bands at 1032 cm^{-1} (weak) and 1148 cm^{-1} (strong) that the sample, for which no information as to its purification

was given, contained some SiF$_4$ (ν_3 at 1031.8 cm^{-1} [46]) and a significant amount of a siloxane, respectively (cf. asymmetric Si-O-Si stretch in (SiH$_2$F)$_2$O at 1134 cm^{-1} and in (CH$_3$SiHF)$_2$O at 1115 cm^{-1} [47]). It is to be expected from the similarity of SiF$_3$ stretching and CH$_3$ rocking frequencies, and the probability of mechanical coupling between the former and the SiC stretching mode that considerable mixing might be present. To partially reduce this, the CD$_3$SiF$_3$ derivative was prepared and its vibrational spectrum and that of CH$_3$SiF$_3$ recorded in this laboratory using the laser Raman instrument, rather than rely on the incomplete spectrum from the original photographically produced spectrum[32]. At the time of writing, the purity of the CD$_3$SiF$_3$ samples was not known; however, the frequencies in its spectra could be deduced from bands common to both samples, which were prepared by different methods. An NCA was then performed for CH$_3$SiF$_3$, along with the other CH$_3$SiX$_3$ compounds, and in conjunction with the estimated frequencies of CD$_3$SiF$_3$, with the aim of correctly describing the vibrational modes.

I.2.2 Preparation

i) CH$_3$SiF$_3$ and CD$_3$SiF$_3$

Trifluoromethylsilane was prepared by the trans-halogenation of CH$_3$SiCl$_3$, by passage through a column (Figure A3.C) packed with antimony trifluoride and glass wool[48]. Exchange tended to be minimal unless the chloride was exposed to the column under forcing conditions. This was

accomplished either by rapid warming of the frozen chloride in the bulb of the column with a hot water bath, or by allowing the CH_3SiCl_3 to expand into the column from the bulb for 4-5 minutes at room temperature. ^1H n.m.r. showed complete reaction after 4-6 passes, the Raman spectrum showed no bands corresponding to the usually strong Si-Cl stretching modes, and the infrared spectrum only a trace of SiF_4, from the appearance of a band at 1032 cm^{-1}. The presence of a small amount of SiF_4 seemed to be unavoidable, as it was present in each of the several times the preparation was attempted. The similar volatilities of CH_3SiF_3 and SiF_4 ruled out any complete separation by simple fractionation.

Samples of CD_3SiF_3 were prepared (i) from CD_3SiBr_3, formed by the reaction of CD_3SiH_3 with BBr_3 at room temperature, and (ii) from the products of a reaction between CD_3SiH_3 and ICl[49]. Both these products were fluorinated by SbF_3 as for CH_3SiF_3. The latter reaction produced iodine and no hydrogen and a sharp singlet in the ^1H n.m.r. spectrum at about δ 2.95 ppm, along with signals due to partially fluorinated products. The sharpness of the singlet suggested that it was not due to SiH bonded to a CD_3 group (it is also too far upfield) and is thought to be due to HCl (cf. chemical shifts (δ) of neat HI and HBr at ca. -11 ppm and -4 ppm respectively[50]), formed presumably according to the equations

$$\overset{\delta+\,\delta-}{CD_3SiH_3} + \overset{\delta+\,\delta-}{I\text{-}Cl} \longrightarrow CD_3SiH_2Cl + HI$$

$$HI + ICl \longrightarrow I_2 + HCl \quad etc.$$
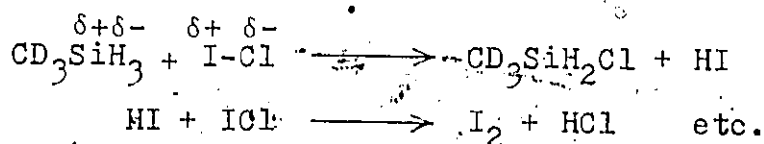
for an overall reaction for complete halogenation

$$CD_3SiH_3 + 6ICl \longrightarrow CD_3SiCl_3 + 3HCl + 3I_2$$
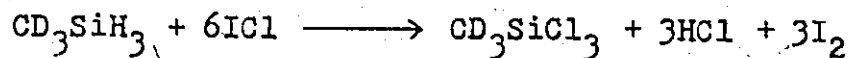
Neither sample was considered to be satisfactorily pure, however. The reaction in (i) produced what was thought to be small amounts of $(CD_3)_2SiBr_2$, and while the ^1H n.m.r. from reaction (ii) showed only the sharp singlet described above, there was at the time no other means of testing its purity. By comparing the spectra of the two samples, however, it was possible to obtain a good approximation as to the appearance of the spectrum of the pure compound. Results of the NCA calculations for the two trifluorides indicate that the proposed vibrational frequencies from the above method were reasonable.

ii) $\underline{CH_3SiI_3}$

Triiodomethylsilane was prepared from CH_3SiH_3 by the action of excess HI in the presence of AlI_3[51] in a type E reaction vessel. Even after reaction at room temperature for several hours, however, there remained traces of CH_3SiHI_2, which was collected in a trap at $-45^\circ C$ along with CH_3SiI_3 when the reaction products were fractionated. Excess HI and hydrogen were pumped off through a trap at $-196^\circ C$ which retained the HI. The two iodo- compounds were separated by raising the trap temperature to $0^\circ C$ and pumping off the CH_3SiHI_2. As expected, CH_3SiI_3 had low volatility (melting point was determined as $9.8 \pm 0.2^\circ C$; b. pt. $229 \pm 1^\circ C$[43]) and was almost impossible to move around the vacuum line. So a U-trap was specially made (Appendix AI.F) so that the tri-iodide could be condensed into a capillary tube and sealed

with a minimum of manipulation. The ^{1}H n.m.r. spectrum showed only a singlet, with a chemical shift of δ 2.40 ± 0.02 ppm for the "neat" liquid (containing 5% internal TMS) and δ 2.32(5) ± 0.02 ppm for a dilute sample (8% in cyclohexane), producing a chemical shift at infinite dilution of δ 2.32 ± 0.03 ppm. This large dilution shift of -0.08 ppm is typical of other iodomethylsilanes, viz. -0.06 for CH_3SiH_2I[52], -0.08 for CH_3SiHI_2 and -0.09 ppm for $(CH_3)_2SiHI$[53]. Coupling constants had the values J_{CH} 128.7 ± 0.2 Hz and J_{SiH}^{gem} 8.1 ± 0.2 Hz. These values continue a trend of an almost monotonic linear increase in shift and J_{CH} as iodine atoms are substituted for hydrogen in the iodomethylsilanes, as shown in Table I.2.1. This value for CH_3SiI_3 differs from that of another study[44] which produced chemical shift values for Me_3SiI, Me_2SiI_2 and $MeSiI_3$ of 0.53, 1.09 and 0.91 ppm respectively. Note that this requires a <u>decrease</u> in δ (i.e. an increase in shielding) on going from Me_2SiI_2 to $MeSiI_3$, in contrast to the approximately additive properties noted for halogen

<u>Table I.2.1</u> ^{1}H n.m.r. data for iodomethylsilanes

	CH_3SiH_3	CH_3SiH_2I[a]	CH_3SiHI_2[b]	CH_3SiI_3
(CH_3)[c]	0.10	0.99	1.71	2.40
J_{CH} (Hz)	122.1	124.4	126.4	128.7

a) ref. 52 b) ref. 53 c) neat liquid

substitution [52,53]. Indeed, values for this latter series, taken from the literature and this work produce an almost exactly additive trend, with observed shifts for Me_4Si, Me_3SiI[52], Me_2SiI_2 and $MeSiI_3$ of 0.00, 0.81, 1.60 and 2.40 ppm respectively. Similar trends are also noted for the analogous germanes, where the values corresponding to Table I.2.1 are 0.35 (CH_3GeH_3)[54], 1.11[55], 1.87[55] and 2.61 ppm (CH_3GeI_3)[56] and to the fully substituted series above 0.13 (Me_4Ge)[54], 0.98[57], 1.91[55], and 2.61 ppm (CH_3GeI_3).

I.2.3. Vibrational Spectra

i) CH_3SiF_3

The CH_3SiX_3 molecules belong to the C_{3v} point group, and as such give rise to twelve normal modes, $5a_1 + a_2 + 6e$. The a_1 and e modes are active in both the Raman and infrared effects, with the a_1 modes being polarised in the Raman spectra, and showing A-type contours in the infrared effect. The a_2 mode, the torsion, is inactive. The numbering of the modes and their approximate description is shown in Table I.2.2.

The infrared spectrum is similar to that reported previously [32], except for the absence of absorptions in the 1200-1050 cm^{-1} region. Small bands at 1032 and 389 cm^{-1} indicated the presence of small amounts of SiF_4, although this latter band is in the position as the highest skeletal deformation. Apart from the intense SiF_3 stretching modes, and the medium A-type band of the symmetric methyl deformation, ν_2, the other bands are noticeably weak, particularly

Table I.2.2 Numbering, approximate description and activity of fundamental modes for CH_3SiX_3

Description	a_1	a_2	e
CH_3 asym. stretch			ν_7
CH_3 sym. stretch	ν_1		
CH_3 asym. def.			ν_8
CH_3 sym. def.	ν_2		
CH_3 rock			ν_9
SiC stretch	ν_3		
SiX_3 asym. stretch			ν_{10}
SiX_3 sym. stretch	ν_4		
SiX_3 rock			ν_{11}
SiX_3 sym. def.	ν_5		
SiX_3 asym. def.			ν_{12}
torsion		ν_6	
Activity :	i.r., Ra(pol)	inactive	i.r.,Ra(dep)

the CH_3 stretching modes.

The Raman spectrum, the major portion of which is shown in Figure I.2.1, is also very simple, the bands other than that at 704 cm^{-1}, assumed to be ν_3, the SiC stretch, and the almost equally intense symmetric CH_3 stretching band being very weak. In the asymmetric CH_3 stretching region, two features are observed; the usual depolarised band expected for ν_7, and a weaker, polarised band 20 cm^{-1} to lower wavenumber, at which position it is unlikely to be an impurity. A lowering of the symmetry by association in the liquid phase could result in a removal of the degeneracy of ν_7, but the splitting is larger than might be expected
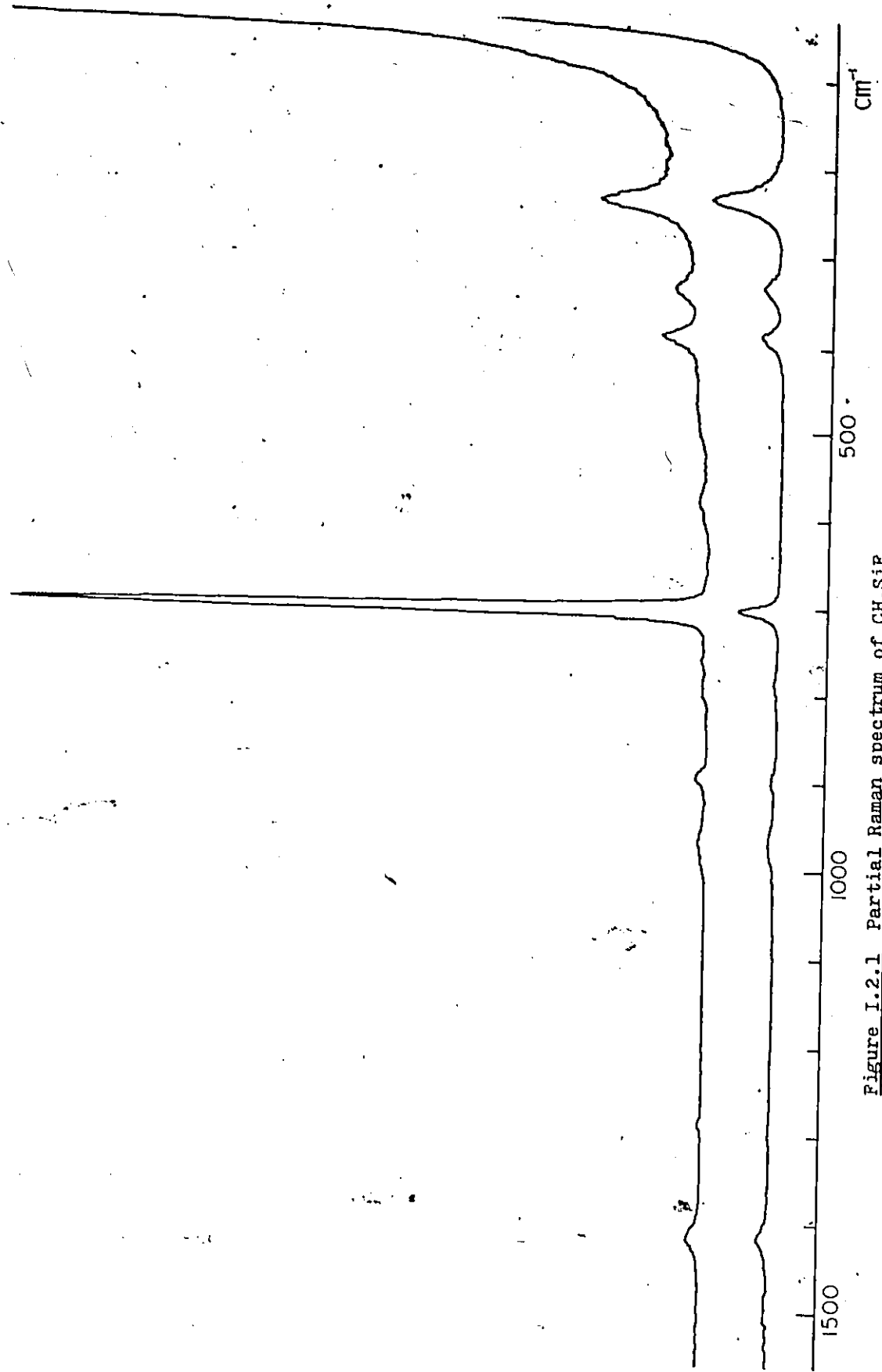
Figure I.2.1 Partial Raman spectrum of CH_3SiP_3

for such an effect. Although fluorine bridging is present in CH_3SnF_3[58], and is thought to occur in CH_3GeF_3[55], this is only a solid state effect and is not considered to be a factor in CH_3SiF_3. Apart from the methyl deformation modes, the only other regions that contain any fundamentals are 1000-700 cm^{-1} and below 400 cm^{-1}. The first of these regions is shown in Figure I.2.2, where the two highest bands at 972 (dep.) and 893 cm^{-1} (pol.) are assigned as the SiF_3 stretching modes, ν_{10} and ν_4 respectively. The remaining fundamental expected in this region is ν_9, the methyl rock, which should be depolarised, and thus is assigned to the weak band at 786 cm^{-1}. The weak, polarised band at 801 cm^{-1}, marked by an asterisk, is due to SiF_4. The three expected fundamentals in the skeletal deformation region are shown in Figure I.2.3, where, in contrast to the spectrum of CH_3GeF_3[42], the perpendicular scan identifies the single a_1 mode. The ordering of the other two modes was only determined after calculations similar to those performed for CH_3GeF_3 (chapter 1.5), and will be presented later.

ii) $\underline{CD_3SiF_3}$

The spectra attributable to CD_3SiF_3 were deduced from comparison of the spectra from the two samples of unknown purity. Since they were prepared by different procedures, it is hoped that the impurities present will not be the same. If this is the case, then bands present in the spectrum of only one of the samples can be neglected, and those that appear with the same relative intensity in both
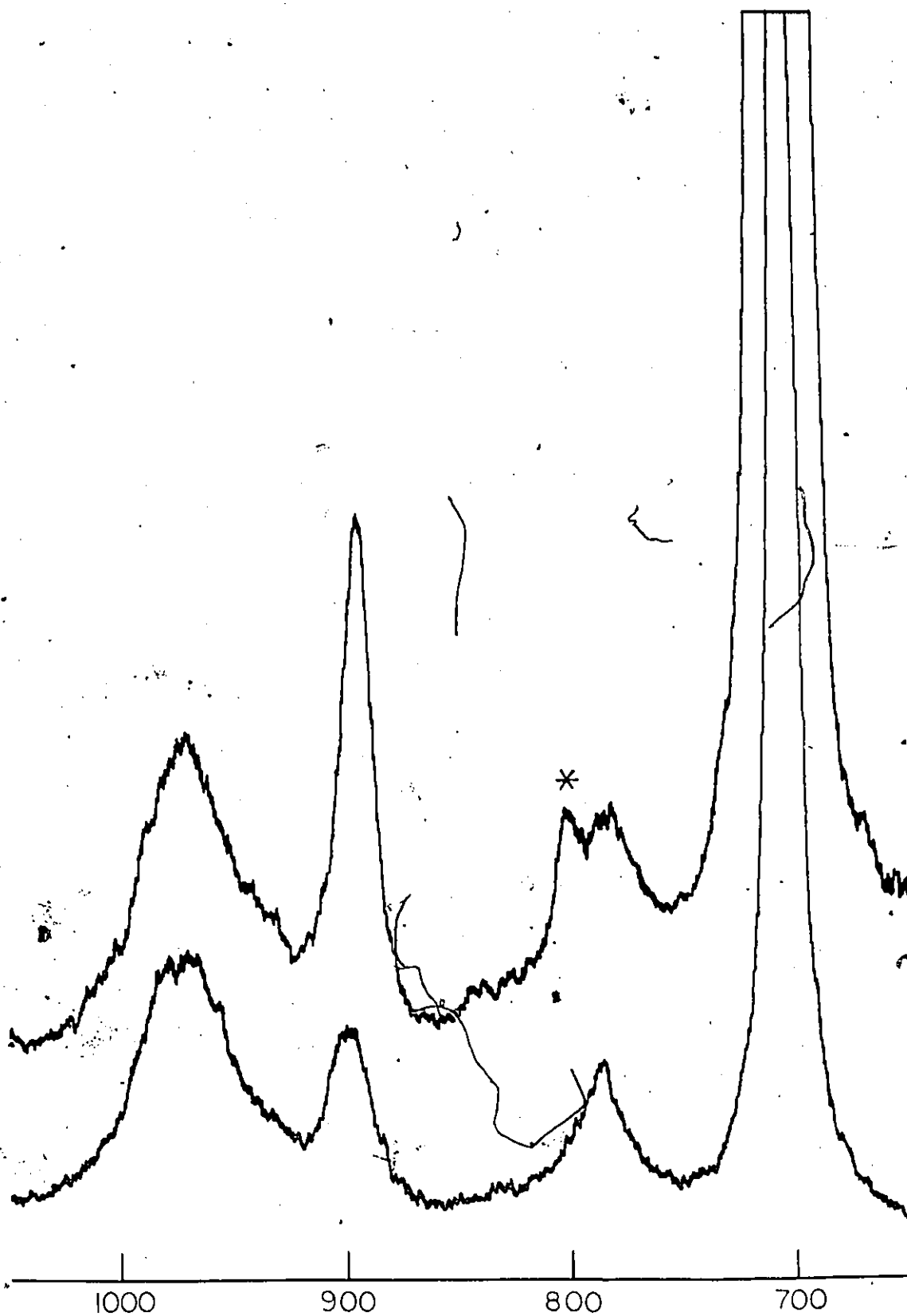
Figure I.2.2   Raman spectrum (650-1050 cm^{-1}) of CH$_3$SiF$_3$
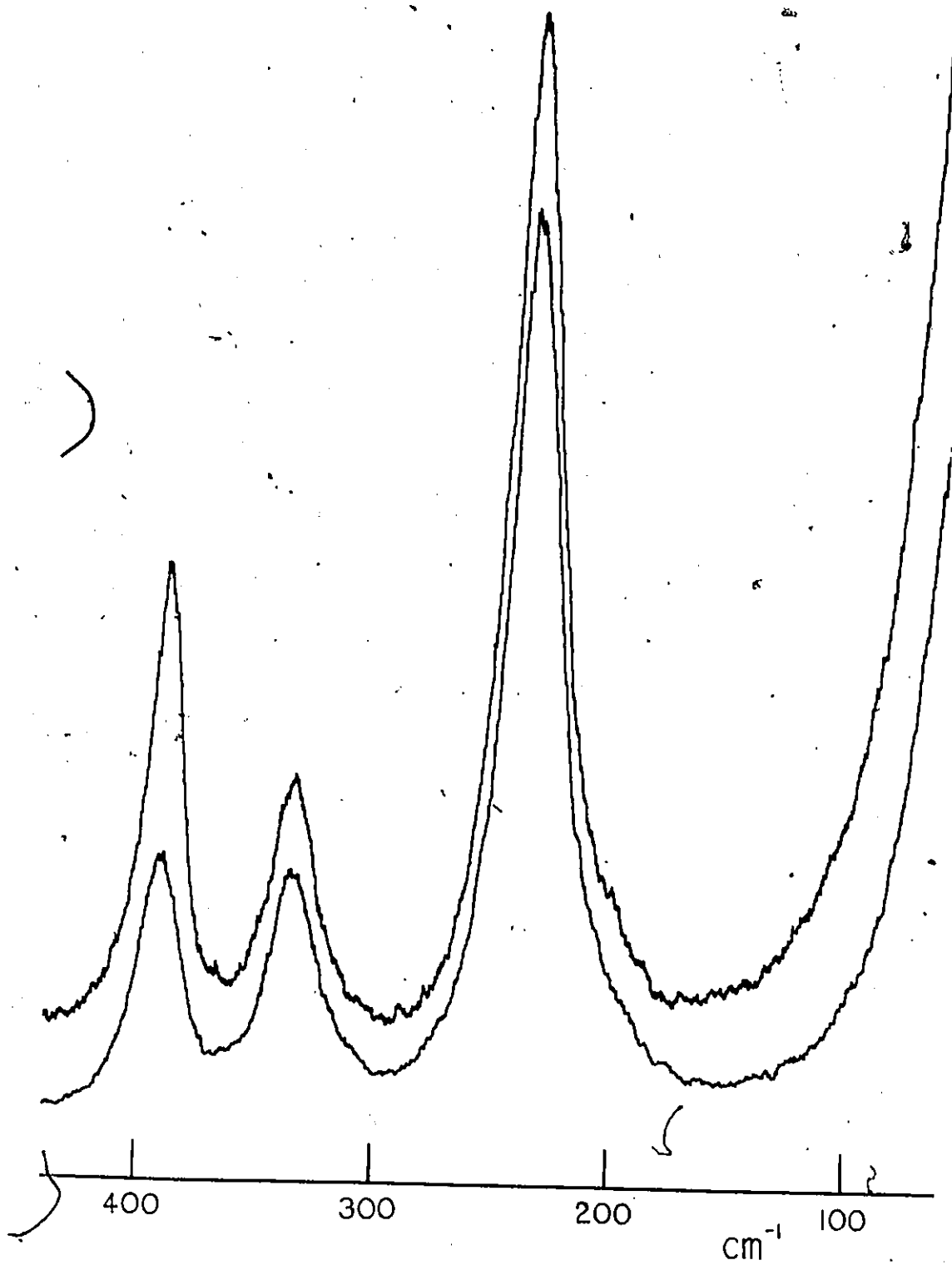
Figure I.2.3 Raman spectrum of the skeletal deformation region in CH_3SiF_3

assumed to be due to CD_3SiF_3. Application of the results from CH_3SiF_3 in the NCA calculations on the CH_3SiX_3 series to the "heavy" molecule produced approximate frequencies for CD_3SiF_3, which were then used as a basis for selecting the real frequencies from the two sets of spectra. Bands from CD_3 group vibrations were picked out fairly readily, the only slightly surprising observation (at first) being that of the two bands in the CD_3 deformation region (1050-1000 cm^{-1}), the higher was clearly polarised and the lower depolarised. This is a reversal of the order of the deformations compared to the methylsilanes, and the other CD_3 compounds studied in this work. However, it should be noted that in CD_3SiH_2F the asymmetric deformation was the higher of the two, and in CD_3SiHF_2 they were found to be coincident, so perhaps the reversal in CD_3SiF_3 is not so unusual after all. The most intense absorptions in the infrared spectrum, together with the CD_3 deformation envelope, are two bands at ca. 960 and 868 cm^{-1} (A-type), which have weak Raman counterparts, respectively broad and depolarised, and relatively sharp and virtually totally polarised, and are assumed to be the SiF_3 stretching modes. A strong, polarised band at 652 cm^{-1} is assumed to be ν_3, the SiC stretch, and three bands at 380 (pol.), 323 (dep.) and 214 cm^{-1} (dep.) the skeletal deformations. The remaining fundamental, the CD_3 rock, should be depolarised, and probably quite weak. The only features in the perpendicular scan between 380 and 956 cm^{-1} are the polarised portion of ν_3, and a shoulder to low

wavenumber of this band. In the parallel scan this is seen as a broadening at the base of the peak, and is estimated at 630 cm^{-1}. The transference of force constant values from CH_3SiF_3 to CD_3SiF_3 gave a value for this mode of 596 cm^{-1}, in fair agreement taking into account anharmonicity effects. A corresponding medium/weak feature is observed in the infra-red spectrum centred at 642 cm^{-1}.

The spectra for the two homologues are presented in Table I.2.3. The assignments will be discussed later.

iii) $\underline{CH_3SiI_3}$

In contrast to the Raman spectra of the trifluoro-methylsilanes, that of CH_3SiI_3 is extremely intense. Minimum laser power and low sensitivity settings still provided a strong spectrum. The intensity of the vibrations which involved iodine atoms can be seen from Figure I.2.4, where the sensitivity has been adjusted so that all bands can be shown. The low volatility of the compound necessitated a liquid infrared spectrum, as a gas spectrum showed only a few weak features. The liquid spectrum is shown in Figure I.2.5, and shows the expected good frequency correlation with the Raman spectrum, except for the bands at 1274 and 615 cm^{-1}, for which the only explanation is that they are due to hydrolysis products. The relevant region is not shown, but there are two bands at ca. 1030 and 1125 of approximately the same intensity, indicating the presence of some siloxane from hydrolysis in the cell.

There is no doubt as to the assignment of the triiodide,

Table I.2.3 Vibrational spectra (cm^{-1}) of CH_3SiF_3 and CD_3SiF_3

CH_3SiF_3			Assignment	CD_3SiF_3		
i.r.(gas)	Ra (liq)	calc.†		calc.†	Ra (liq)	i.r.(gas)
3008 2998 vw 2991	2999.9 mw dp	3005.4	ν_7	2239.6	2242 mw dp	∿2240 vw
	2979 wsh p 2930 vs p 2849 vw p 2809 w p	2957.1	ν_1	2128.0	2142 vs p	
			$2\nu_8$		2037 w p	
2816 vw			$2\nu_2$		2060 vw p	
1418 vw	1416 w dp	1420.3	ν_8	1026.7	1035 vw dp	1037 s
1294 1286 m 1277	1288 vw p	1303.2	ν_2	1041.1	1047 vw p	1052 s
988 983 vs	972 wbr dp	975.7	ν_{10}	950.7	956 wbr dp	∿965 s
911 901 s 894	893 w p	902.6	ν_4	852.2	862 m p	878 868 s 860
791 w	786 vw dp	800.2	ν_9	618.2	631 wsh dp	
711 701 w 691	704 vs p	690.5	ν_3	664.6	652 vs p	∿640 w
572 vw	578 vw p		$\nu_{11}+\nu_{12}$?			
400 391 mw 380	390 mw p	383.9	ν_5	373.2	380 m p	
	336 w dp	331.5	ν_{12}	330.2	323 w dp	
	235 m dp	228.3	ν_{11}	215.0	214 m dp	

† see following section for details
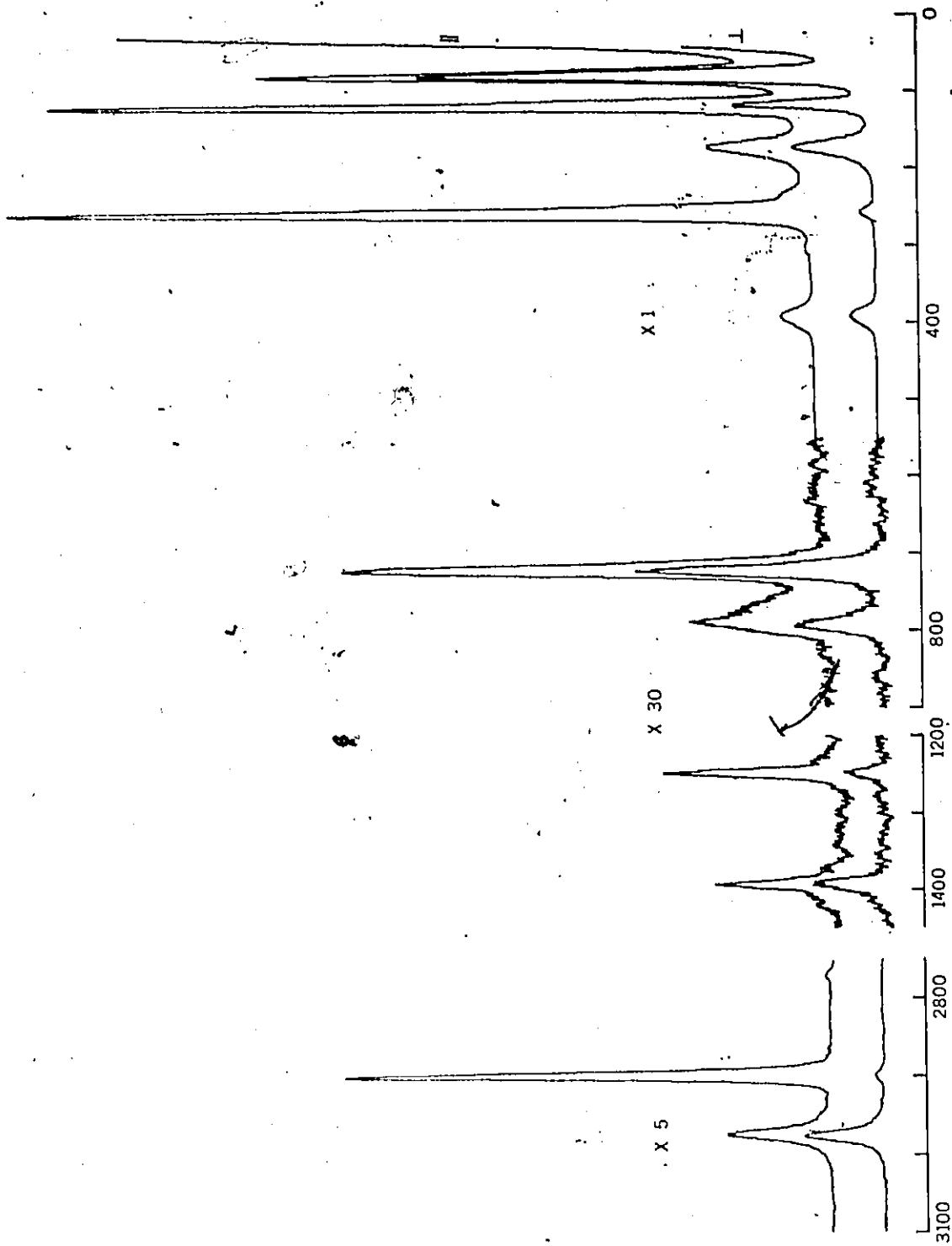
Figure I.2.4   Partial Raman spectrum of CH_3SiI_3
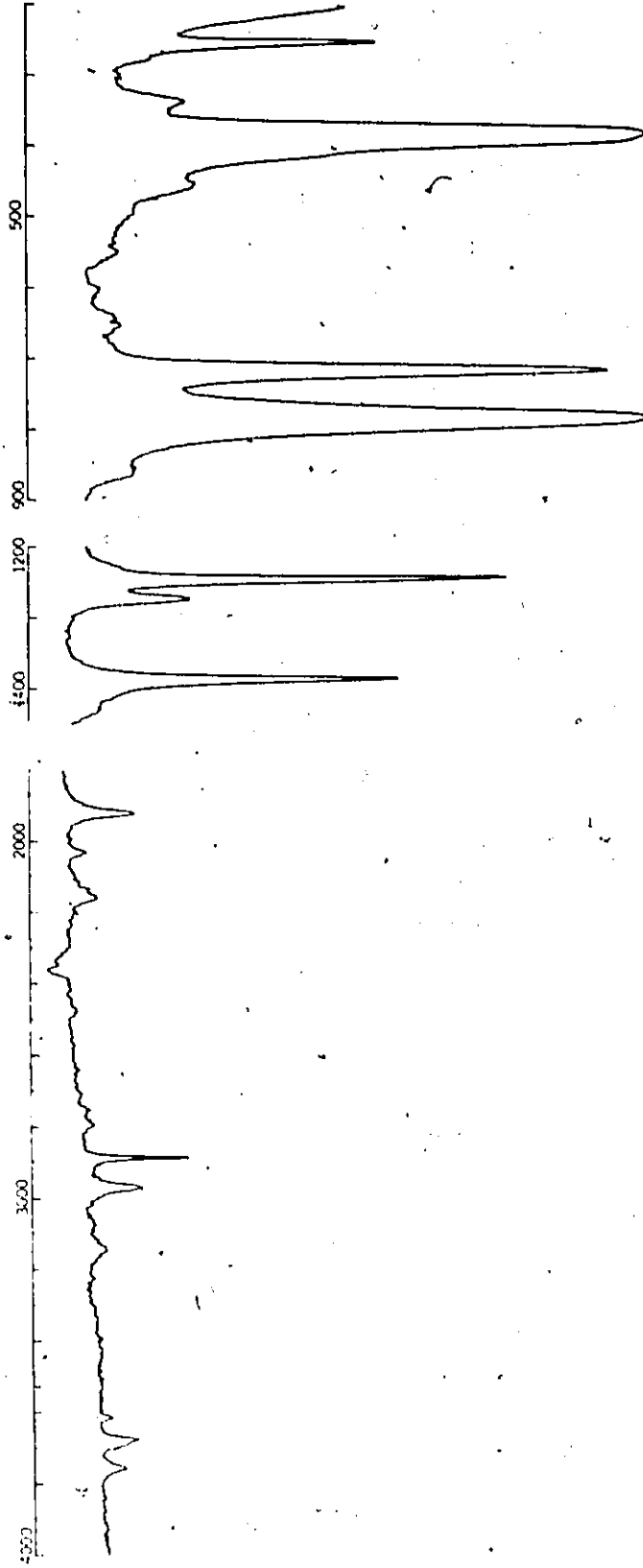
Figure I.2.5   Partial infrared spectrum of liquid CH_3SiI_3

the spectra of which are displayed in Table I.2.4, and so will be presented here. The large mass difference between the CH_3- and SiI_3- groups is responsible for the separation of their frequencies, and means that there is negligible mixing of the modes, except within the groups themselves. The CH_3 vibrations are in typical regions, and all vibrations of the SiI_3 group occur below 400 cm^{-1}. The only possible query of the assignment would be about the ordering of the skeletal modes, shown in Figure I.2.6. The polarised band at 116 cm^{-1} must be ν_5, the symmetric deformation. The lowest frequency band is assigned as ν_{12}, the asymmetric deformation, which results from deformation of ISiI angles, as opposed to ν_{11}, the SiI_3 rock, resulting from CSiI angle deformation. This assignment can be confidently made on mass and intensity grounds as well as comparison with deformations in SiI_4 [59] (94 and 63 cm^{-1}) and Me_3SiI [60] (198 and 164 cm^{-1}) which involve only ISiI and CSiI angle deformations respectively.

I.2.4 Normal Co-ordinate Analysis and Discussion

As was seen in Chapter 1.5 in the reassignment of CH_3GeF_3, an NCA involving all members of the CH_3SiX_3 series should provide additional evidence to help in the assignment of CH_3SiF_3, where frequency comparisons are not conclusive. Structures of the compounds, where available, were taken from the literature of from similar compounds. The values are listed in Table I.2.5. Vibrational frequencies used were from liquid Raman data, as found in the literature, and are used with one change.   In CH_3SiCl_3, where ν_5, the symmetric

Table I.2.4. The vibrational spectra of CH_3SiI_3

i.r.(liq)	Ra (liq)	calc.[†]	Assignment
3765 w			$\nu_7+\nu_9$
3690 wbr			$\nu_3+\nu_7$
~3620 vw			$\nu_1+\nu_9$
3228 vw			$\nu_1+\nu_3$
3145 vwbr			$\nu_4+\nu_7$
			$\nu_1+\nu_4$
			$\nu_7+\nu_{11}$
2975 mw	2976 w dp	2976.0	ν_7
2896 mw	2898 m p	2898.0	ν_1
2805 vw			$\nu_7-\nu_{11}$
2765 vw	2765 vw p		$2\nu_8$
2168 w			$\nu_8+\nu_9$
2038 w			$\nu_2+\nu_9$
1966 mw			$\nu_2+\nu_3$
1436 mw			$2\nu_3$
1390 s	1392 w dp	1392.0	ν_8
1274 mw			*?
1247 s	1248 w p	1248.0	ν_2
~1125 mw			*
~1030 mw			*
864 vw			$\nu_9+\nu_{12}$
790 vs	794 vw dp	794.0	ν_9
	769 vwsh dp		$2\nu_{10}$
721 vs	721 w p	721.0	ν_3
640 wbr			$\nu_4+\nu_{10}$
615 vw			*?
554 vw			$\nu_{10}+\nu_{11}$
	490 vw p		$2\nu_4$
458 w	464 vw p		$\nu_{10}+\nu_{12}$
~420 vwsh			$\nu_4+\nu_{11}$
388 vs	388 mw dp	388.0	ν_{10}
334 w	328 w p		$2\nu_{11}$
			$\nu_4+\nu_{12}$
252 m	253 vs p	253.0	ν_4
	228 wsh p		$2\nu_5$
	171 m dp	171.0	ν_{11}
	116 vs p	116.0	ν_5
	76 s dp	76.0	ν_{12}

[†] force constants and p.e.d. in following section

* hydolysis products
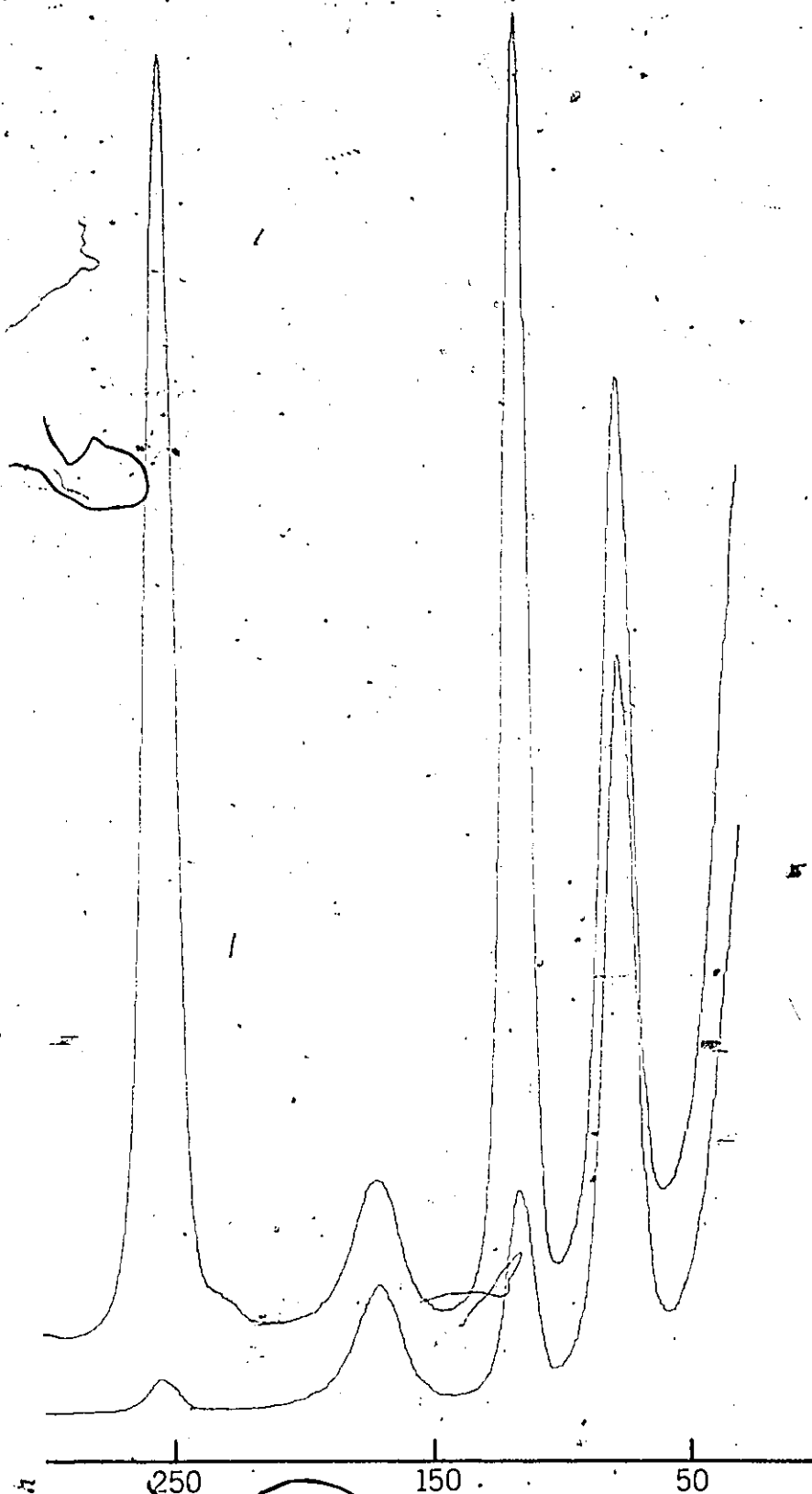
Figure I.2.6 Raman spectrum (30-300 cm^{-1}) of CH_3SiI_3.

Table I.2.5 Structural parameters[*] used in NCA of $MeSiX_3$

X	F^a	Cl	Br	I
r CH	110.0	110.0	110.0	110.0
r SiC	188.0	188.0	190.0	193.0
r SiX	156.0	202.1	217.0	243.0
∠ CSiX ∠ HCSi		109.45° (assumed)		

[*]ref. 61   a) ref. 62

$SiCl_3$ deformation and ν_{11}, the $SiCl_3$ rock were reported as accidently degenerate [33,34] from photographic data, that portion of the spectrum was rerun on our apparatus, and with a narrow slit width (4 cm^{-1}) and relatively high laser power (~500 mW) the tracing shown in Figure I.2.7 was obtained. Although this scan does not completely resolve the two modes, it can be seen that the high wavenumber side has relatively less intensity in the perpendicular scan, compared with the low wavenumber side. This suggests that ν_5 is at higher wavenumber than ν_{11}, and that the crossover point in the ordering of these fundamentals as the halogen changes from iodine to fluorine has already occured at chlorine, as was observed for the $MeGeX_3$ series.

At first, the calculations were performed as for the methylgermane series as described in Chapter 1.5, but neither of the alternate assignments for the fluoride (with the two possible orderings for ν_{11} and ν_{12}, taking ν_5 as the polarised band at 390 cm^{-1}) produced force constant values for f CSiF and f FSiF which continued the trend from the other three molecules at least fairly smoothly. Moreover
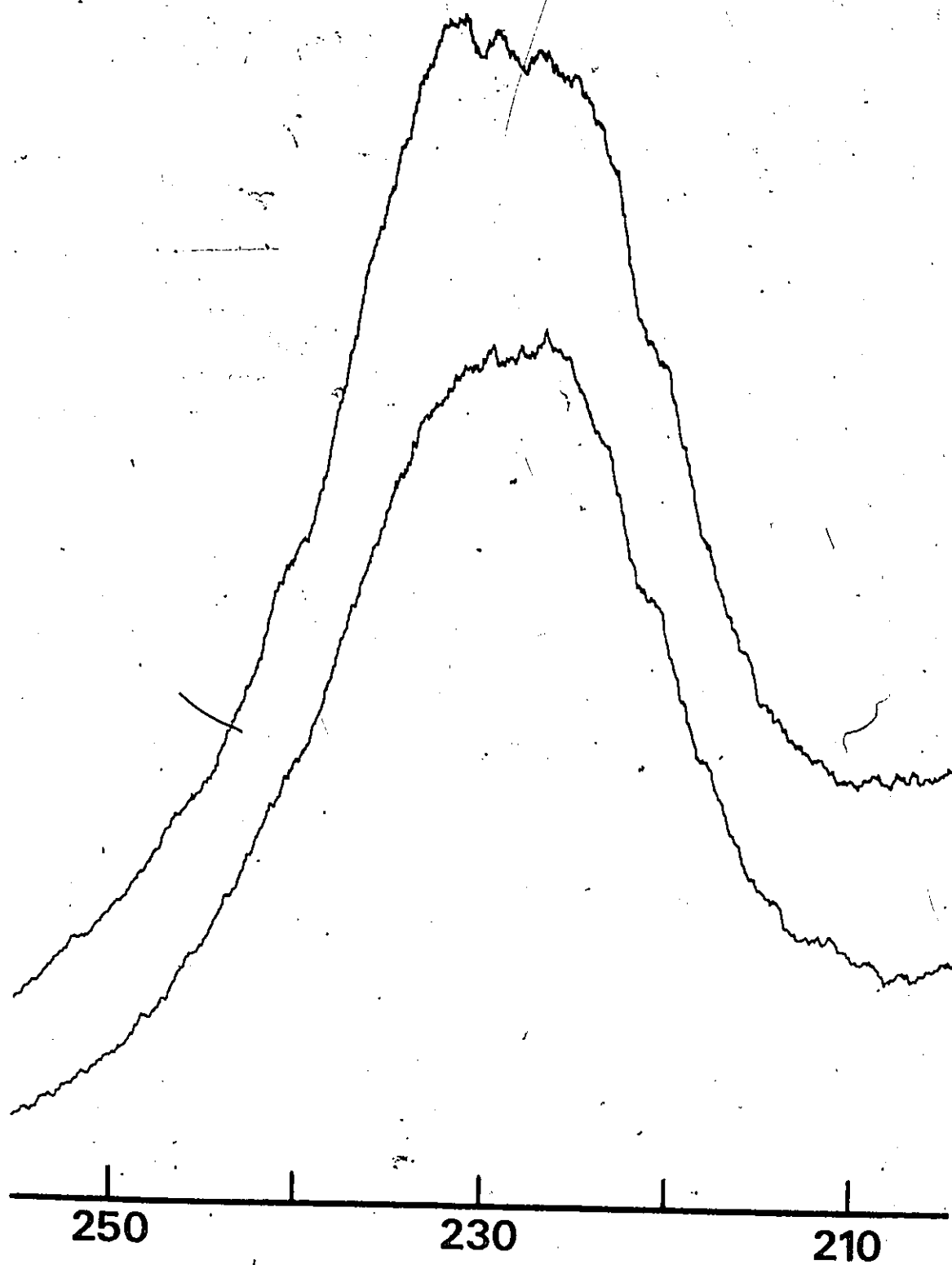
Figure I.2.7   Partial Raman spectrum of skeletal deformation region in CH_3SiCl_3

it was again found that a variety of values for the four constants describing the skeletal deformations ($\underline{f}$ CSiX, $\underline{f}$ XSiX, $\underline{f}$ CSiX/CSiX and $\underline{f}$ XSiX/XSiX) could be obtained depending on the starting values, or by fixing one and allowing the other three to change. This is really not too surprising, since these four force constants are used to calculate three frequencies. So a different approach was attempted, in which the two interaction terms were set to zero, and one constant, $\underline{f}$ CSiX/XSiX (where there is a common SiX bond), introduced, thus reducing the number of force constants to calculate the three skeletal deformations to three. The force constants from both approaches for the series are shown in Table I.2.6, and some sample results for the two assignments in MeSiF$_3$ in Table I.2.7. It can be seen from the latter data how the values varied widely when the two interaction terms were used, but refined to almost constant values when only one such term was used. It is evident from these results, however, that there is little to suggest which of (a) or (b) is the correct assignment based on force constant trends. In these calculations, as for MeGeX$_3$, the frequencies were reproduced exactly, and the resultant p.e.d.'s are listed in Tables I.2.8 and I.2.9. There is little help from these data as well. From Table I.2.8 it can be seen that the proportion of the potential energy of ν_{11} and ν_{12} contributed to by $\underline{f}$ CSiX and $\underline{f}$ XSiX respectively increases from the triiodide to the trichloride (presumably as the Si-X stretching frequency becomes further from this region). But in both

Table I.2.6 Force constant listings for MeSiX$_3$

Force constant	F (a)	F (b)	Cl	Br	I
1 CH	484.41	484.26	478.44	475.65	475.47
2 SiC	367.33	378.66	325.52	327.80	302.21
3 SiX	540.02	533.90	269.47	192.71	134.22
4 HCH	51.64	51.79	50.54	49.11	49.09
5 HCSi	42.10	41.63	41.50	41.72	41.50
6 CSiX	76.90	125.17	87.73	80.32	82.40
7 XSiX	98.93	58.89	70.91	60.70	75.46
8 CH/CH	5.17	5.23	5.02	4.07	4.20
9 SiX/SiX	27.72	24.14	34.99	28.87	21.27
10 HCH/HCH	−0.90	−0.71	−0.85	−1.59	−1.33
11 HCSi/HCSi	−0.97	−1.24	−1.53	−1.44	−1.25
12 CSiX/CSiX	21.50	8.36	4.75	5.48	4.36
13 XSiX/XSiX	5.26	13.94	4.21	2.35	4.37
14 CSiX/XSiX	−	−	−	−	−
15 SiC/SiX	18.46	17.88	5.59	5.52	−1.36

Force constant	F (a)	F (b)	Cl	Br	I
1 CH	483.87	483.74	478.45	475.65	475.47
2 SiC	368.64	375.95	320.49	328.75	303.71
3 SiX	548.38	543.36	273.72	195.75	138.94
4 HCH	51.13	51.04	50.54	49.27	49.07
5 HCSi	42.33	42.19	41.63	41.57	41.57
6 CSiX	60.68	113.24	81.76	73.55	73.82
7 XSiX	89.51	47.70	65.96	58.06	70.68
8 CH/CH	5.28	5.33	5.02	4.07	4.19
9 SiX/SiX	23.85	22.06	34.58	26.84	17.47
10 HCH/HCH	−1.08	−1.15	−0.83	−1.43	−1.34
11 HCSi/HCSi	−1.10	−1.05	−1.53	−1.63	−1.25
12 CSiX/CSiX	−	−	−	−	−
13 XSiX/XSiX	−	−	−	−	−
14 CSiX/XSiX	−19.74	−16.96	−9.34	−6.34	−8.21
15 SiC/SiX	18.04	17.59	3.03	6.47	0.30

Table I.2.7   Some force constant values from NCA
calculations for MeSiF$_3$.

Force constant	I*		II		III	
	(a)	(b)	(a)	(b)	(a)	(b)
1 CH	484.41	484.26	484.41	484.27	483.87	483.74
2 SiC	367.33	378.66	375.56	373.61	377.22	374.42
3 SiF	540.42	533.90	536.78	535.84	539.24	538.59
4 HCH	51.64	51.79	51.58	51.80	50.97	51.13
5 HCSi	42.10	41.63	42.06	41.69	42.52	42.19
6 CSiF	76.90	125.17	59.45	138.34	69.21	132.33
7 FSiF	98.93	58.89	116.25	45.77	105.62	50.76
8 CH/CH	5.17	5.23	5.16	5.24	5.26	5.33
9 SiF/SiF	27.72	24.14	24.48	26.08	23.38	25.16
10 HCH/HCH	−0.90	−0.71	−0.96	−0.70	−1.26	−1.04
11 HCSi/HCSi	−0.97	−1.24	−1.03	−1.18	−1.10	−1.18
12 CSiF/CSiF	21.50	8.36	4.03	21.53	13.84	16.98
13 FSiF/FSiF	5.26	13.94	22.58	0.85	13.12	5.77
14 CSiF/FSiF	−	−	−	−	−	−
15 SiC/SiF	18.46	17.88	17.97	18.05	17.54	17.67

Force constant	IV*		V		VI	
	(a)	(b)	(a)	(b)	(a)	(b)
1 CH	483.86	483.74	483.86	483.73	483.87	483.74
2 SiC	381.28	381.65	379.93	385.65	368.64	375.95
3 SiF	543.44	541.17	543.96	539.68	548.38	543.36
4 HCH	50.99	51.04	51.07	50.98	51.13	51.04
5 HCSi	42.31	42.10	42.25	42.10	42.33	42.19
6 CSiF	60.68	113.26	60.68	113.29	60.80	113.24
7 FSiF	89.61	47.67	89.61	47.65	89.51	47.70
8 CH/CH	5.26	5.33	5.27	5.32	5.28	5.33
9 SiF/SiF	18.98	19.91	19.49	18.44	23.85	22.06
10 HCH/HCH	−1.22	−1.15	−1.15	−1.22	−1.08	−1.15
11 HCSi/HCSi	−1.14	−1.14	−1.18	−1.12	−1.10	−1.05
12 CSiF/CSiF	−	−	−	−	−	−
13 FSiF/FSiF	−	−	−	−	−	−
14 CSiF/FSiF	−19.56	−16.88	−19.58	−16.83	−19.74	−16.96
15 SiC/SiF	17.43	17.43	17.46	17.40	18.04	17.59

*
calculations I,II,III; IV,V,VI are sample results from
NCA calculations using various starting values for main
force constants. They differ in the use of skeletal inter-
action terms (force constants 12, 13, 14). The assignments
(a) and (b) are described in the text.

Table I.2.8 Potential energy distribution among the force constants for $MeSiX_3$ compounds (X=Cl,Br,I)

$MeSiCl_3$			obs[1],calc.	p.e.d.*
CH_3 str.		ν_7	2983	101(1)
CH_3 str.	ν_1		2912	98(1)
CH_3 def.		ν_8	1405	95(4)
CH_3 def.	ν_2		1265	51(4)+42(5)+11(2)
CH_3 rock		ν_9	805[2]	88(5)+4(3)
SiC str.	ν_3		761	73(2)+9(3)+5(4,5)
SiX_3 str.		ν_{10}	576	97(3)−12(9)+6(6)
SiX_3 str.	ν_4		450	65(3)+17(9)+12(2)
SiX_3 rock		ν_{11}	227[3]	92(6)+7(3)
SiX_3 def.	ν_5		232[3]	40(6)+32(7)+18(14)
SiX_3 def.		ν_{12}	164	96(7)+6(3)
torsion	ν_6		−	

$MeSiBr_3$			obs[4],calc.	p.e.d.*
CH_3 str.		ν_7	2977	100(1)
CH_3 str.	ν_1		2898	98(1)
CH_3 def.		ν_8	1396	94(4)
CH_3 def.	ν_2		1249	51(4)+43(5)+12(2)
CH_3 rock		ν_9	800[5]	90(5)
SiC str.	ν_3		746	81(2)+7(4)+6(5)
SiX_3 str.		ν_{10}	453	90(3)+14(6)−12(9)
SiX_3 str.	ν_4		314	57(3)+16(9)+9(6)+7(7)
SiX_3 rock		ν_{11}	186	85(6)+15(3)
SiX_3 def.	ν_5		153	36(6)+28(7)+18(3)+12(14)
SiX_3 def.		ν_{12}	98	92(7)+10(3)
torsion	ν_6		−	

$MeSiI_3$			obs[6],calc.	p.e.d.*
CH_3 str.		ν_7	2976	100(1)
CH_3 str.	ν_1		2898	98(1)
CH_3 def.		ν_8	1392	94(4)
CH_3 def.	ν_2		1248	51(4)+43(5)+11(2)
CH_3 rock		ν_9	794	92(5)
SiC str.	ν_3		721	83(2)+6(4)+5(5)
SiX_3 str.		ν_{10}	388	80(3)+21(6)+11(7)−10(9)
SiX_3 str.	ν_4		253	45(3)+15(6,7)+11(9)+7(14)
SiX_3 rock		ν_{11}	171	78(6)+19(3)+3(14)
SiX_3 def.	ν_5		116	25(6)+24(7)+32(3)+11(14)
SiX_3 def.		ν_{12}	76	88(7)+15(3)
torsion	ν_6		−	

* contributions of at least 10%

1) ref. 34 2) ref. 35 3) this work; see text 4) ref. 36
5) calc., ref. 63 6) this work; ref. 45

Table I.2.9 Potential energy distribution among the force constants for MeSiF₃

Table I.2.9 Potential energy distribution among the force constants for $MeSiF_3$

Assignment (a)[*]		obs.,calc.	p.e.d.
CH_3 str.	ν_7	2999	101(1)
CH_3 str.	ν_1	2930	98(1)
CH_3 def.	ν_8	1416	95(4)
CH_3 def.	ν_2	1287	49(4)+41(5)+14(2)
CH_3 rock	ν_9	786	88(5)+6(3)
SiC str.	ν_3	704	43(2)+40(3)+6(12)
SiF_3 str.	ν_{10}	972	94(3)+5(5)-4(9)
SiF_3 str.	ν_4	893	49(3)+33(2)-6(12)+4(4,5,7,9,14)
SiF_3 rock	ν_{11}	235	101(6)-23(14)+19(7)
SiF_3 def.	ν_5	390	34(7)+23(6)+30(14)+10(2)
SiF_3 def.	ν_{12}	336	85(7)+9(14)+4(6)
torsion	ν_6	140†	–

Assignment (b)[*]		obs.,calc.	p.e.d.
CH_3 str.	ν_7	2999	101(1)
CH_3 str.	ν_1	2930	97(1)
CH_3 def.	ν_8	1416	94(4)
CH_3 def.	ν_2	1287	49(4)+40(5)+15(2)
CH_3 rock	ν_9	786	86(5)+8(3)
SiC str.	ν_3	704	40(2)+43(3)+6(12)
SiF_3 str.	ν_{10}	972	92(3)+5(5,6)-4(9)
SiF_3 str.	ν_4	893	47(3)+35(2)-5(12)
SiF_3 rock	ν_{11}	336	87(6)+6(14)
SiF_3 def.	ν_5	390	43(6)+26(14)+18(7)+10(2)
SiF_3 def.	ν_{12}	235	102(7)-16(14)+12(6)
torsion	ν_6	140†	–

†from microwave study

*from calculation VI in Table I.2.7.

assignments for the fluorides (Table I.2.9) one of these contributions increases and one decreases, again favouring neither assignment.

Following the apparent success of the central force field calculations for the $MeGeX_3$ series in Chapter 1.5, this approach was used for the methylsilane analogues. The data used for these calculations (see equation 5.2) are given in Table I.2.10, and the results presented in Table I.2.11, where again the arbitrary correction of 10^0 was made to the calculated β. There is not sufficient structural data for this series for a direct comparison, but if the same trend is expected as for the $MeGeX_3$ series, i.e. decreasing α' (XSiX) angle with lighter halogen, then the results point to assignment (a) as the most likely version, as the decrease calculated for assignment (b) is a bit unrealistic, if the assumptions inherent in this approach are valid.

As far as the NCA involving just the two trifluorides is concerned, the agreement in both the frequency matching and the force constant values (with respect to the $MeSiX_3$ calculations) indicates that the frequencies deduced for CD_3SiF_3 are probably quite close to the real ones. The calculated frequencies are listed in Table I.2.3 with the observed spectra. The force constants are listed in Table I.2.12, where the first column for the trifluoride is from the $MeSiX_3$ calculation, and the second from the two homologues. They present evidence as to why comparison of force constants from different sources is usually unreliable

Table I.2.10 Frequencies (cm^{-1}) used in the central force field calculations for $MeSiX_3$

X =	F (a)	F (b)	Cl	Br	I
$\nu_1 \equiv SiX_3$ sym. str.	901	901	450	314	253
$\nu_2 \equiv SiX_3$ sym. def.	390	390	232	153	116
$\nu_3 \equiv SiX_3$ asym. str.	985	985	576	453	388
$\nu_4 \equiv SiX_3$ asym. def.	336	235	164	98	76

Table I.2.11 Calculated values of central force field calculations for $MeSiX_3$

			β	α	$\beta+10$	α'
$MeSiF_3$	(a)	i)[†]	59.6	96.7	69.6	108.5
		ii)	58.7	95.5	68.7	107.6
	(b)	i)	46.2	77.3	56.2	92.0
		ii)	43.2	72.8	53.2	87.9
$MeSiCl_3$		i)	59.4	96.4	69.4	108.3
		ii)	58.7	95.4	68.7	107.5
$MeSiBr_3$		i)	60.8	98.2	70.8	109.8
		ii)	60.5	97.8	70.5	109.4
$MeSiI_3$		i)	63.2	101.2	73.2	112.0
		ii)	63.0	101.0	73.0	111.8

† i) and ii) refer to the calculations assuming the mass of the apical "atom" as 28 and 43 (Si+Me), respectively

Table I.2.12   Force constant values for CH_3SiF_3 and CH_3SiI_3

CH_3SiF_3		No†	Force constant	CH_3SiI_3
483.87	488.38	1	f CH	475.47
368.64	347.14	2	f SiC	303.71
548.38	519.90	3	f SiX	138.94
51.13	55.77	4	f HCH	49.07
42.33	46.45	5	f HCSi	41.57
60.68	57.07	6	f CSiX	73.82
89.51	87.54	7	f XSiX	70.68
5.28	7.78	8	f CH/CH	4.19
23.85	28.41	9	f SiX/SiX	17.47
-1.08	2.87	10	f HCH/HCH	-1.34
-1.10	-1.23	11	f HCSi/HCSi	-1.25
-19.74	-18.94	14	f CSiX/XSiX	-8.21
18.04	8.12	15	f SiX/SiC	0.30
-	22.35	16	f SiC/HCSi	-
-	11.84	17	f c-SiX/HCSi	-

* units: $N.m^{-1}$ for stretching, $N.m.rad^{-2}$ for bending force constants

† numbering consistent with Tables I.2.6 and I.2.7

(unless they are uniquely determined) in all but the most approximate manner. The most noticable differences in the main (diagonal) force constants are for $\underline{f}$ SiC, $\underline{f}$ SiX and $\underline{f}$ HCSi, but these also represent the motions involved in the extra interaction terms used; in the case of $\underline{f}$ SiC/HCSi to keep the methyl deformations in the correct order. The other additional interaction term was introduced to indicate the mixing between the SiF$_3$ stretching and methyl rocking modes. Other differences in the force constant values reflect the difference in anharmonicities as can be seen for $\underline{f}$ CH and $\underline{f}$ CH/CH which represent "pure" modes. The p.e.d.'s for the trifluorides, shown in Table I.2.13 indicate expected variations as various modes change frequencies through deuteration. Thus ν_2 becomes more mixed with $\underline{f}$ SiC on dropping to $\underline{ca}$. 1000 cm^{-1}, and the SiF$_3$ stretches becoming less mixed with both $\underline{f}$ SiC and $\underline{f}$ HCSi as ν_3 and ν_9 decrease in wavenumber.

Table I.2.13 Potential energy distribution[*] among the force constants for CH_3SiF_3 and CH_3SiI_3

Mode		CH_3SiF_3	CD_3SiF_3
ν_1	CH_3 str.	97(1)	96(1)
ν_2	CH_3 def.	55(4)+46(5)-10(16)	40(4)+33(5)+32(2)-20(16)
ν_3	SiC str.	46(2)+47(3)	48(2)+36(3)
ν_4	SiX_3 str.	41(3)+5(9)+42(2)	47(3)+15(4)+12(5)+11(2)
ν_5	SiX_3 def.	35(7)+23(6)+30(14)	33(7)+22(6)+29(14)+12(2)
ν_6	torsion	–	+10(2) –
ν_7	CH_3 str.	101(1)	100(1)
ν_8	CH_3 def.	102(4)	102(4)
ν_9	CH_3 rock	71(5)+30(3)	87(5)+9(3)
ν_{10}	SiX_3 str.	72(3)+19(5)-4(9)	92(3)-5(9)
ν_{11}	SiX_3 rock	102(6)-23(14)+18(7)	102(6)-21(14)+15(7)
ν_{12}	SiX_3 def.	86(7)+9(14)	88(7)+7(14)

[*] contributions at least 10%

Mode		CH_3SiI_3
ν_1	CH_3 str.	98(1)
ν_2	CH_3 def.	51(4)+43(5)+11(2)
ν_3	SiC str.	83(2)+6(4)+5(5)
ν_4	SiX_3 str.	45(3)+15(16,17)+11(9)
ν_5	SiX_3 def.	25(6)+24(7)+32(3)+11(14)
ν_6	torsion	–
ν_7	CH_3 str.	100(1)
ν_8	CH_3 def.	94(4)
ν_9	CH_3 rock	92(5)
ν_{10}	SiX_3 str.	80(3)+21(6)+11(7)-10(9)
ν_{11}	SiX_3 rock	78(6)+19(3)
ν_{12}	SiX_3 def.	88(7)+15(3)

[*] contributions at least >10%

CHAPTER I.3

MONOHALOMETHYLSILANES

I.3.1 Introduction

.In a dissertation which is supposed to cover original work, it may be surprising to note that of the twelve parent silane derivatives described in these next three chapters, only one had not been the subject of at least a partial vibrational study (not including numerous studies on correlations of Si-H stretching frequencies[63]). However, many of these studies were not complete, did not assign all the modes or only used one technique. Only one included data for isotopically substituted molecules[65]. Previous studies of the halogen derivatives of the mono- and di-methylsilanes are listed in Table I.3.1.

Table I.3.1 Survey of vibrational studies for halogen derivatives of the methylsilanes

Compound	Infrared	Raman
CH_3SiH_2F	fairly complete (64)	
CH_3SiH_2Cl	" " (64) .	
	complete (65,66)	complete (65,66)
CH_3SiH_2Br	fairly complete (64)	
CH_3SiH_2I	partial (67)	
	fairly complete (64)	
CH_3SiHF_2		
CH_3SiHCl_2		fairly complete (68,69)
		complete (66)
CH_3SiHBr_2		
CH_3SiHI_2	partial (67)	
$(CH_3)_2SiHF$	complete (70)	complete (70)
$(CH_3)_2SiHCl$	" (71)	complete (71)
$(CH_3)_2SiHBr$	" (70)	complete (70)
$(CH_3)_2SiHI$	" (70)	complete (70)

*includes deuterated homologues

As can be seen, data for the chloro- derivatives are fairly complete, while except for the dimethylsilane compounds the data are sparse. The first study of a complete series (of all four halo- derivatives) was in the infrared only[64], and contained some queries and blanks. With the benefit of hindsight this is understandable, as a comparison with the corresponding Raman spectra reveal a band in the latter which is unobserved in the infrared, precluding a correct assignment. The only other such systematic study is on the dimethyl derivatives[70], but the proposed assignments are not consistent with the data obtained from this work for the deuterated compounds. Even so, some of these assignments are considered dubious based on the evidence from the "normal" compounds alone. The only study of a deuterated series is for chloromethylsilane[65], which includes all four possible homologues (considering deuteration of all the methyl and silylene groups only) and a normal co-ordinate analysis. However, there is one frequency in each of the three compounds in common with this study which is not observed here, and at least one frequency which is observed here, but not in the other study, including the same Raman line that was missed in the earlier infrared investigation[64]. The NCA affords little chance of discussing differences in force constant values as the p.e.d.'s are not given.

For the discussion and presentation of the vibrational spectra which follow, only those overtones and combinations which are relatively intense or which appear in all three

molecules, or are used as an aid to assignment are reported.
Bands due to residual hydrogen in the deuterated species
are omitted, although for residual Si-H stretch, for
example, the band may be relatively strong. In most of the
infrared spectra an absorption at 1080-1100 cm^{-1} is observed,
due to the asymmetric Si-O-Si stretching mode from hydrolysis
of the sample. While not usually detectable in the ^1H n.m.r.
spectra (recorded on the fresh product), this trace of
siloxane is probably the result of repeated manipulations
on and off the vacuum line. These bands, however, do not
affect the assignment of the spectra.

Assignments which are considered to be unambiguous
are made in the description of the vibrational spectra,
while those that are open to question are discussed in the
section on the NCA.

I.3.2 Preparation of $MeSiH_2X$ and $MeSiHX_2$

Although the vibrational spectra of both series of
compounds will be discussed separately, the preparative
routes were generally chosen so that a variation of the
reaction conditions could enable both mono- and di- subst-
ituted derivatives to be produced in the same reaction, so
they will be discussed together. It happened that in most
cases the compounds were prepared more than once, and often
different synthetic routes were taken depending on available
materials and experience. In every case the starting point
in any scheme was the parent methylsilane, the preparation
of which is described in Chapter I.1.

i) Iodomethylsilanes

These were the most important derivatives from a preparative point of view, as they could be used in heavy salt exchange reactions to produce the lighter halogen derivatives. The simplest procedure was the iodination of methylsilane by hydrogen iodide,[72] as-described in the previous Chapter for CH_3SiI_3. Since less substitution was required, the ratio of reactants was reduced to approximately equimolar, the temperature reduced by immersing the reaction vessel in an ice bath and the reaction terminated after $1-1\frac{1}{2}$ hours. These conditions were found to produce approximately equal amounts of the mono- and di- substituted compounds according to the idealised equation

$$2CH_3SiH_3 + 3HI \xrightarrow[0^{\circ}C]{AlI_3} CH_3SiH_2I + CH_3SiHI_2 + 3H_2 \quad (I)$$
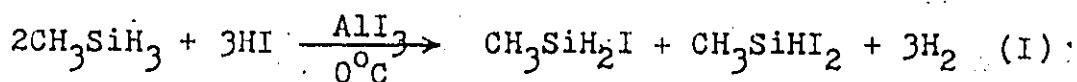
The products could be separated by passing through traps at -45°, -95° into one at $-196^{\circ}C$, which respectively condensed CH_3SiHI_2, CH_3SiH_2I and excess CH_3SiH_3. As a deficit of HI was used (with respect to equation I) excess HI was not found in the reaction mixture. A polar mechanism has been proposed[73] involving the nucleophilic attack of AlX_4^- ions on silicon, which does not require the hydrogen from HX to participate directly in the reaction. This is supported by the observation that in the reaction between CH_3SiD_3 and HI there is no evidence of deuterium-hydrogen exchange.

ii) Bromomethylsilanes

The most widely used method for these compounds

was the reaction between CH_3SiH_3 and BBr_3[74], in a reaction vessel similar to that used for the HI reaction above. The reactants were distilled into the vessel with a 4:1 molar excess of CH_3SiH_3 and were allowed to warm to $0°C$ for about 2h, when a mixture of products was formed according to the idealised equation

$$2CH_3SiH_3 + BBr_3 \longrightarrow CH_3SiH_2Br + CH_3SiHBr_2 + \text{"}BH_3\text{"}$$
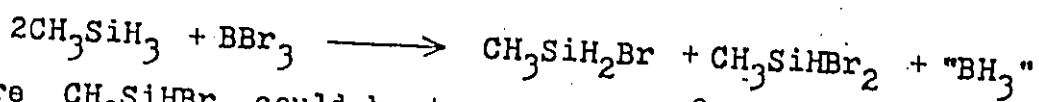
Pure CH_3SiHBr_2 could be trapped at $-63°C$, a small portion passing through this trap with a mixture of CH_3SiH_2Br, CH_3SiH_3 and B_2H_6. The CH_3SiH_3 and B_2H_6 were separated from the brominated species by passing the mixture through a trap at $-126°C$, which retained the halogenated compounds. Pure CH_3SiH_2Br could be obtained by holding the resultant mixture at $-78°C$ and pumping out into a trap at $-196°C$, which then contained the mono- brominated compound. By reducing the reaction temperature to $-78°C$, a reaction mixture consisting of approximately 85% CH_3SiH_2Br could be produced.

Salt exchange reactions using $HgBr_2$ and $AgBr$[75] and the respective iodomethylsilane were attempted, but not used, in the former because of no reaction and in the latter for reasons of expense.

A reaction analogous to that of HI for the iodomethyl-silanes was attempted with HBr and $AlBr_3$, and with suitable experimentation to determine reactant ratios, reaction time and temperature could have been a useful route. The same could be said of the reaction of CD_3SiH_3 and bromine, which

was attempted but left too long to react, and produced
mainly CD_3SiBr_3, although some evidence of the dimethyl
derivative was found from Raman spectra. The reaction of
SiH_4 with Br_2 is very vigorous - it has been reported to
explode at $20^{\circ}C$[76] and did so in one of the reactions in this
laboratory, although the other time careful monitoring and
low reaction temperatures ($-78^{\circ}C$) produced SiH_3Br only, with
no evidence of SiH_2Br_2 - but becomes more moderate with a
decreasing number of Si-H bonds.

iii) Chloromethylsilanes

Dichloromethylsilane was used as received from
commercial sources after distillation to remove possible
CH_3SiCl_3. Preparation of CH_3SiH_2Cl was attempted first by react-
ion with BCl_3 using a 4:1 molar excess of CH_3SiH_3 as for the
bromide reaction, at -78° for approx. 2h. However, it was
difficult to separate diborane from CH_3SiH_2Cl and after
standing for a few days a sealed sample of the chloro compound
with a trace of diborane was found to have disproportionated,
to the extent that after four days, such a tube contained
40% CH_3SiHCl_2. Far more satisfactory was the salt exchange
reaction of CH_3SiH_2I and other deuterated iodo compounds with
$HgCl_2$,[75] which produced the chloro compound after 2-4 double
passes. In the case of the almost involatile diiodo compounds
some local heating was necessary to increase its local vapour
pressure.

$$2CH_3SiH_2I + HgCl_2 \longrightarrow 2CH_3SiH_2Cl + HgI_2$$

white $\qquad\qquad\qquad\qquad\qquad$ orange

Complete exchange was checked by the absence of the strong Si-I stretching bands in the Raman effect.

iv) Fluoromethylsilanes

The fluoromethylsilanes were made exclusively by the exchange reaction between SbF_3 and the corresponding iodo, bromo or chloro compound[48], although in the latter case, some heating, using a hot air gun, was necessary. The column, packed alternately with SbF_3 and glass wool, was heated locally under vacuum to dry the SbF_3 before exchange. However, siloxane compounds were found in most cases to varying degrees, probably due to Sb_2O_3 formed before packing the column. This was not a serious problem as the fluoride could be recovered by treatment with BF_3[77] according to the approximate equation

$$3(CH_3SiH_2)_2O + 3BF_3 \longrightarrow 3CH_3SiH_2OBF_2 + 3CH_3SiH_2F$$
$$\longrightarrow 3CH_3SiH_2F + BF_3 + B_2O_3$$
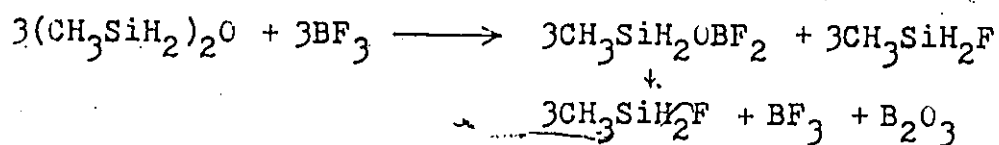
The fluoride could then be distilled from the solid boron compound. In the preparation of the difluoro compound, however, the BF_3 was found not to convert all the $(CH_3SiHF)_2O$ formed back to CH_3SiHF_2, but fortunately they could be separated using a -112° C trap, which retained the siloxane (see Chapter 1.2.4).

I.3.3 Vibrational Spectra

These molecules are assigned assuming C_s symmetry, which results in 18 vibrations, eleven of which are a' and seven a". All fundamentals are active in both effects. The

approximate description and numbering of the modes are
shown in Table I.3.2. The infrared spectra and representative
Raman spectra are displayed in Figures I.3.1-5.

All the molecules have the largest moment of inertia
perpendicular to the plane of symmetry and thus all the
C-type bands will belong to the a" species. The intermediate
moment of inertia is only a little smaller, so some hybrid
B/C bands may be expected. All bands with A, B or a hybrid
of these will be a' modes. Because of the uncertainties in
applying the band contour principle to asymmetric top mole-
cules, a more empirical method in general is to note the
band shape for unambiguously symmetric modes – the symmetric
methyl deformation usually had structure – and use that as a
guide. This was done for each series of compounds. In the
present case of monohalomethylsilanes, the SiH_2 scissoring
vibration at $\underline{ca}$. 950 cm^{-1} was also used, as the major com-
ponent of this motion is perpendicular to the CSi bond, and
together with the symmetric methyl deformation gave the
probable limits of the band shapes. In this series, the
latter bands were A-type for the fluoride and A/B for the
others, while SiH_2 scissors had a B-type contour throughout
the series.

i) <u>3000-1000 cm^{-1}</u>

The CH_3 stretching modes, ν_1, ν_2 and ν_{12}, are very
weak in the infrared spectra, with the asymmetric stretch,
ν_2, appearing as an A-type band in all cases, at $\underline{ca}$. 2920
cm^{-1}. Of the two asymmetric stretches at $\underline{ca}$. 2980 cm^{-1}, ν_{12}

CH_3SiH_2F

CD_3SiH_2F

CH_3SiD_2F

Figure I.3.1 Infrared spectra of the fluoromethylsilanes

CH$_3$SiH$_2$Cl

CD$_3$SiH$_2$Cl

CH$_3$SiD$_2$Cl
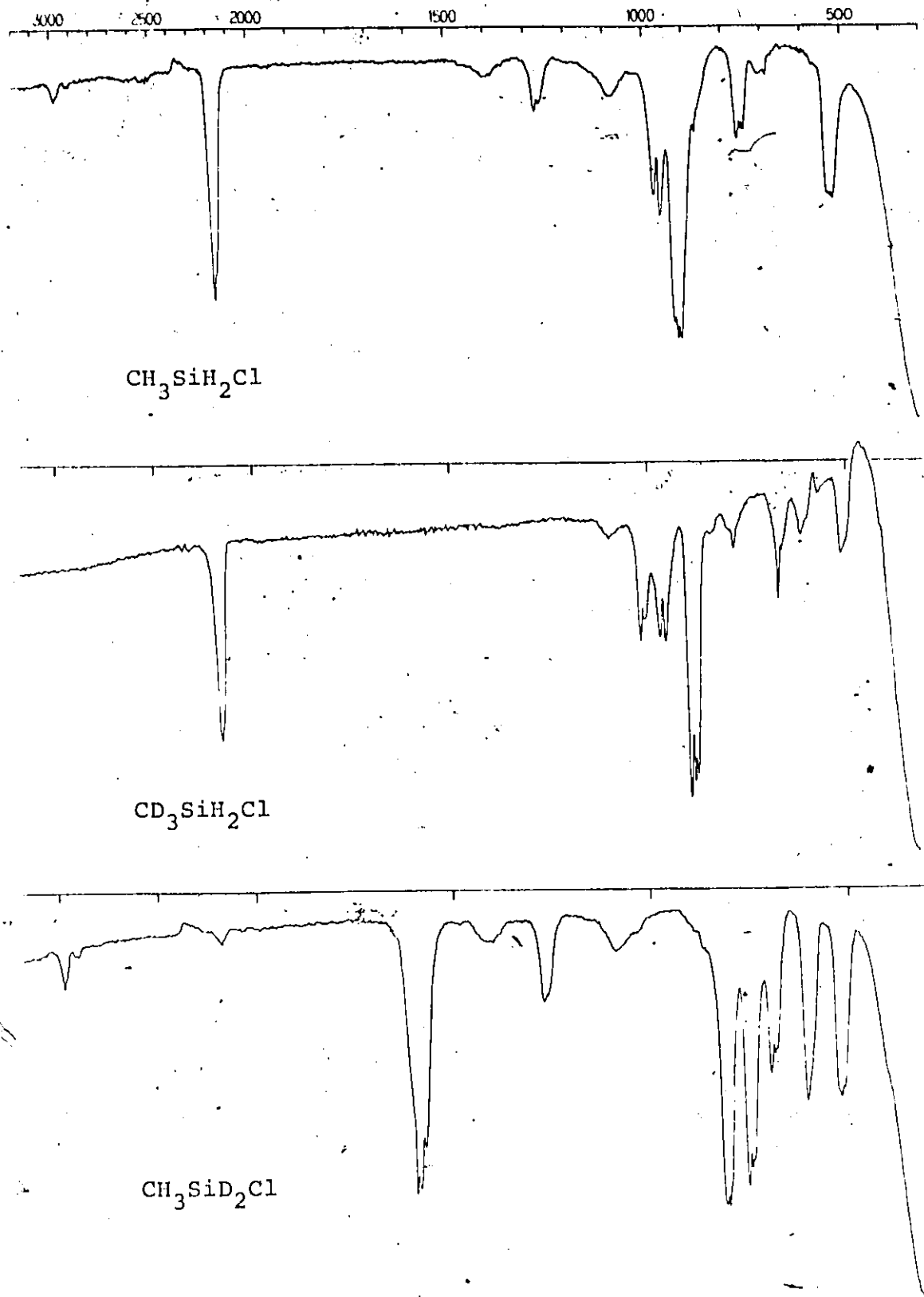
Figure I.3.2 Infrared spectra of the chloromethylsilanes
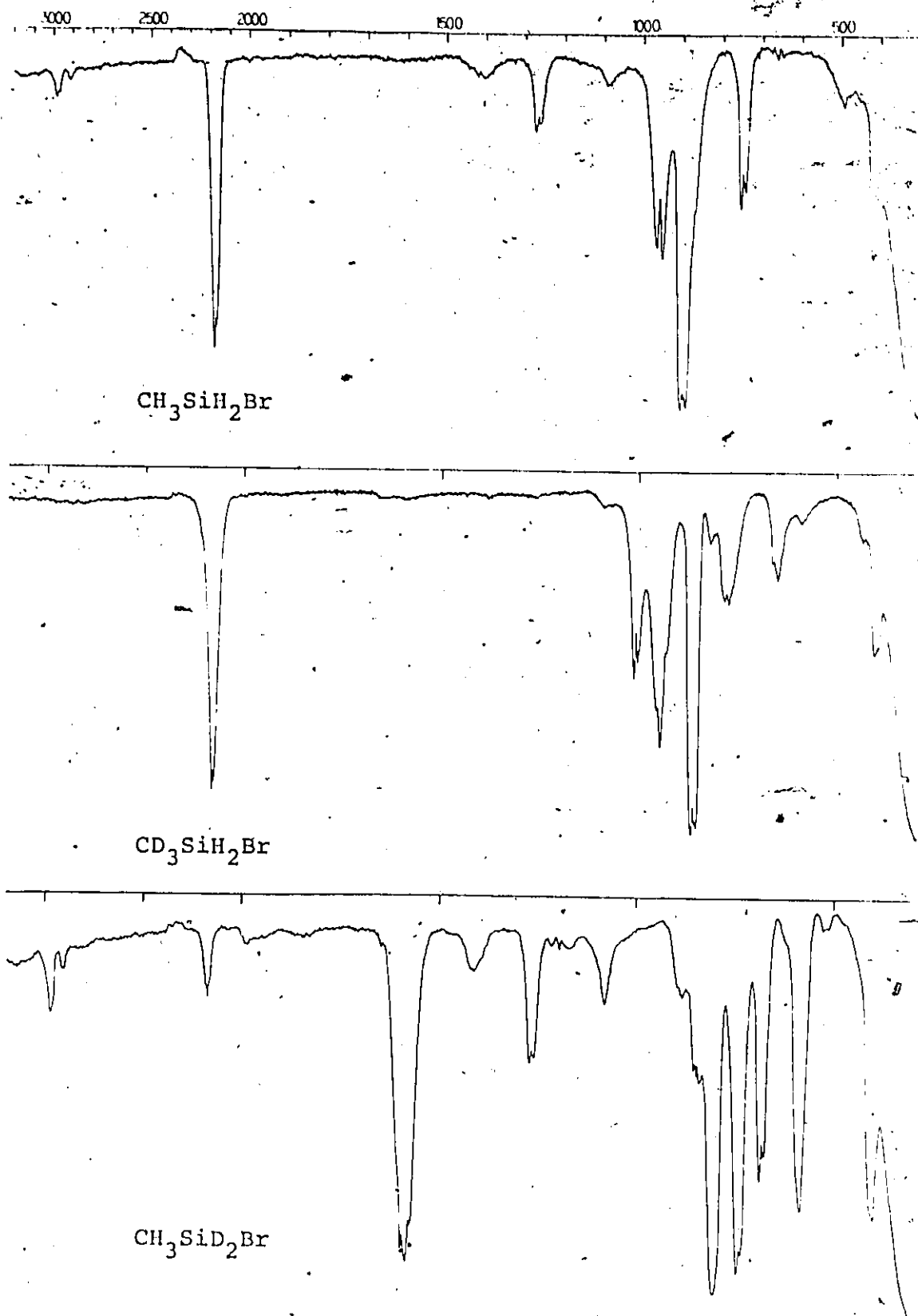
Figure I.3.3 Infrared spectra of the bromomethylsilanes

CH$_3$SiH$_2$I

CD$_3$SiH$_2$I

CH$_3$SiD$_2$I
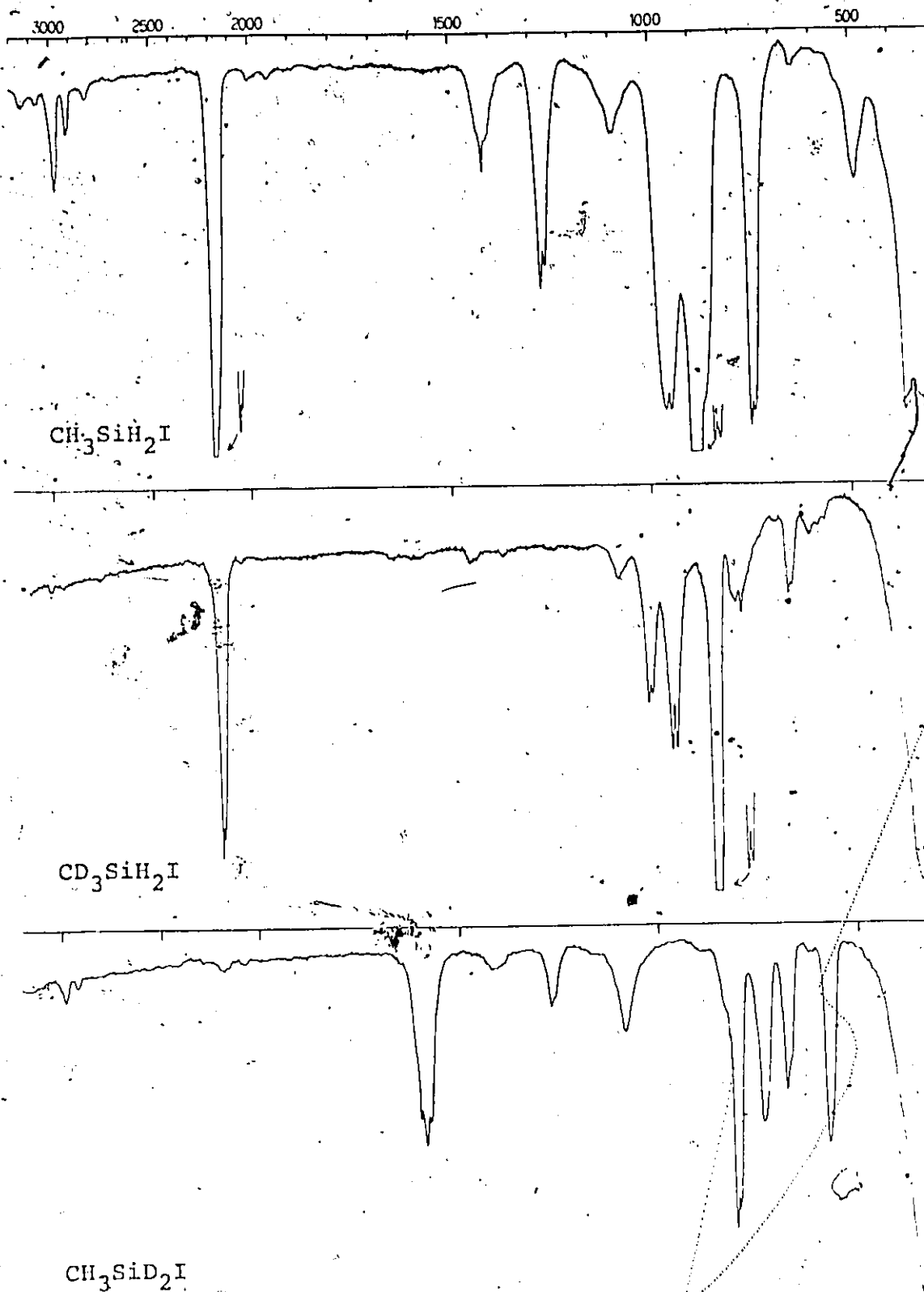
Figure I.3.4   Infrared spectra of the iodomethylsilanes
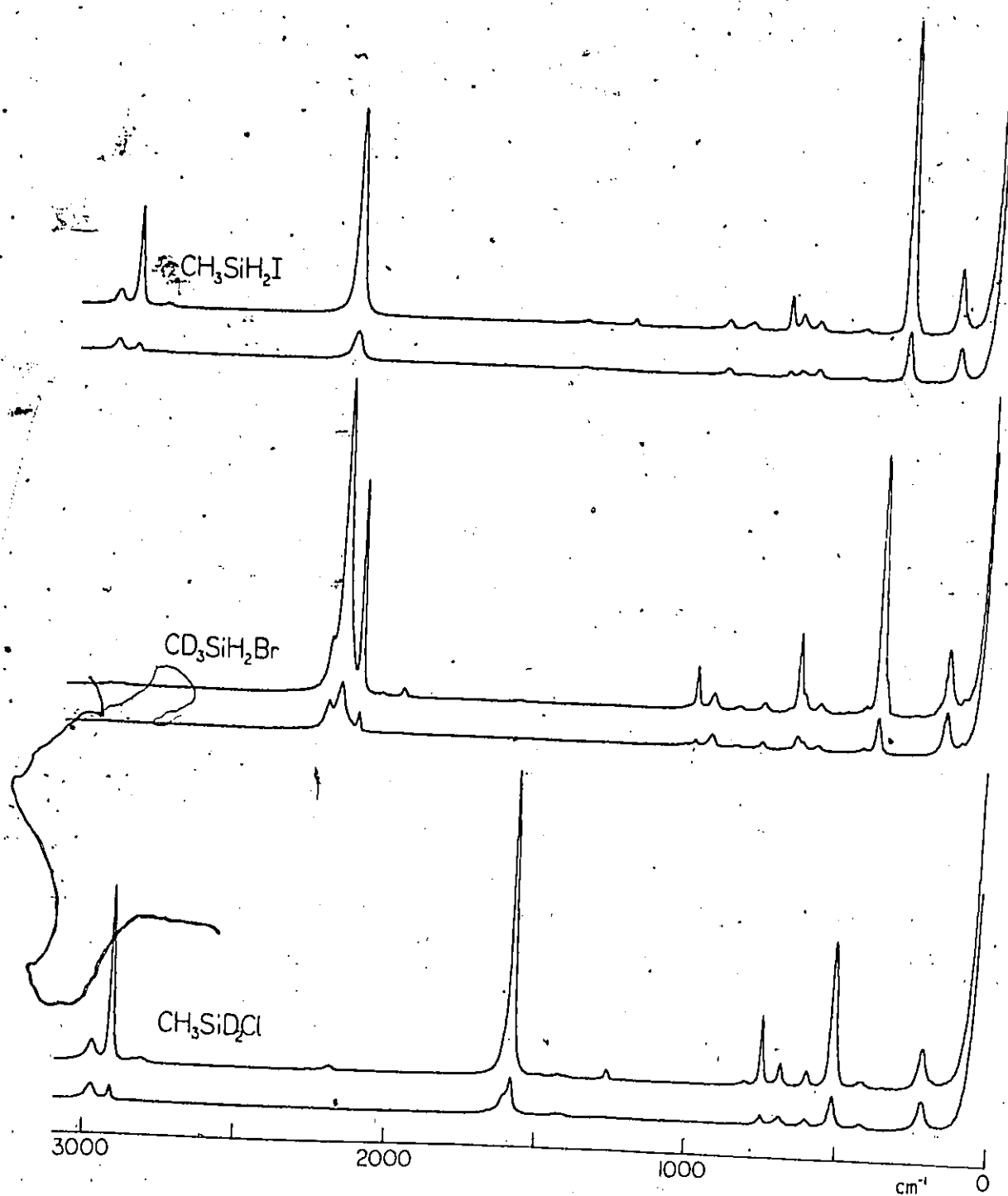
Figure I.3.5 Raman spectra of some halomethylsilanes

Table I.3.2. Fundamental modes and approximate descriptions for CH_3SiH_2X molecules.

Description	a'	a"
CH_3 str.(asym)	ν_1	ν_{12}
CH_3 str.(sym)	ν_2	
SiH_2 str.	ν_3	ν_{13}
CH_3 def.(asym)	ν_4	ν_{14}
CH_3 def.(sym)	ν_5	
CH_3 rock	ν_6	ν_{15}
SiC str.	ν_7	
SiH_2 def.	ν_8 (scissor)	
SiH_2 def.	ν_9 (wag)	ν_{16} (twist)
SiH_2 def.		ν_{17} (rock)
SiX str.	ν_{10}	
CSiX def.	ν_{11}	
CH_3 torsion		ν_{18}

appears as a C-type band to the high wavenumber side of ν_1, which is a hybrid band (B-type in the fluoride). In the Raman spectra, the symmetric stretch is strong and highly polarised, but no distinction between ν_1 and ν_{12} can be made. The CD_3 stretches are overlapped by the strong SiH_2 stretching absorption in the infrared, ν_1 and ν_{12} appearing as noticeably weak shoulders on the high wavenumberside. In the Raman spectra, however, they are both well-defined (Figure I.3.6).

The two SiH_2 stretching vibrations, ν_3 and ν_{13}, are at almost identical frequencies, as was observed for the
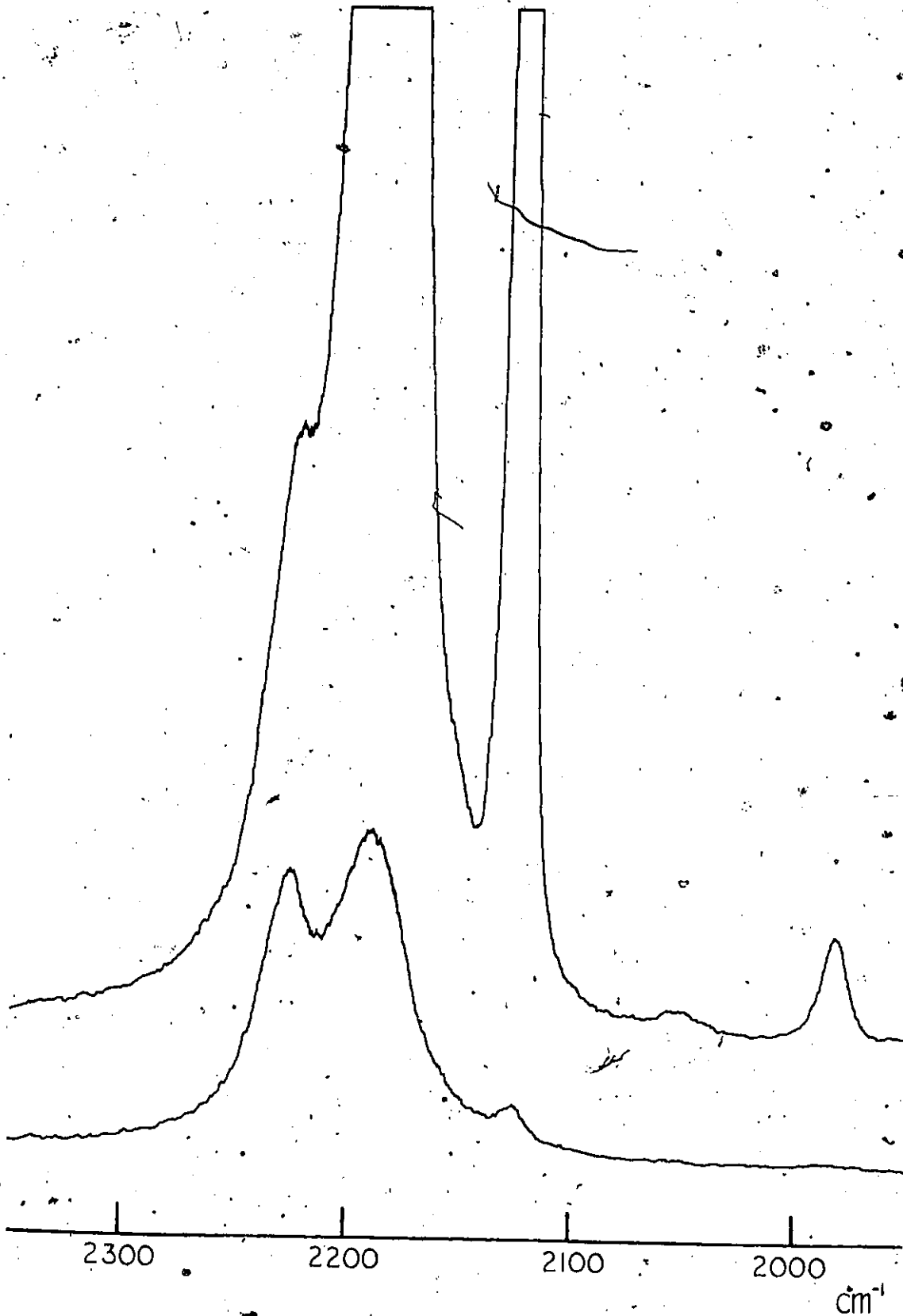
Figure I.3.6   The CD_3 and SiH_2 stretching region in the Raman spectrum of CD_3SiH_2Br

methylsilanes[2-4], appearing as B and C type bands respectively in the infrared spectra. For the fluoride and chloride (and CD_3SiH_2Br) the proximity of the two produces an apparent single A-type band, but for the heavier halides ν_{13} shifts to slightly higher wavenumber. Needless to say, the Raman envelope appears almost symmetrical. As is observed for the methyl group stretches, the splitting in the deuterated group is much greater, and increases with increasing mass of halide (11 cm^{-1} for F; 22 cm^{-1} for I). Thus the two band contours overlap in the fluoride but become separate in the iodide.

The CH_3 deformations appear at ca. 1420 and 1260 cm^{-1}, with the former bands diffuse and relatively weak in both effects. The only distinctive feature, if resolved, is a narrow "spike" in the infrared envelope assumed to be the expected C-type band of ν_{14}. The symmetric mode appears as a medium intensity band in the infrared spectra with an A-type contour for the fluoride, gradually acquiring more B character with increasing mass of halide.

The symmetric CD_3 deformations ν_5 appear at ca. 1000 cm^{-1} and have the same appearance as the CH_3 bands, (with more intensity in the Raman effect) but the asymmetric deformations are not observed in the infrared spectra, and only with any confidence in the Raman spectrum of the iodide. They are estimated, however, from the position of their overtones, observed in the Raman spectrum and enhanced by Fermi resonance with the CD_3 stretches[28]. The data are shown in

Table I.3.3 Observed and calculated frequencies from methyl deformation overtones.

	obs.$2\nu_5$[a]	2.obs.ν_5[b]	Δ[c]	obs.$2\nu_4$[a]	2.obs.ν_4[b]	Δ[c]	"obs.ν_4"
CD_3SiH_2I	1975	2000	25	2050	2066	16	1033
CD_3SiH_2Br	1983	2004	19	2052	$(2068)^d$	(16)	(1034)
CD_3SiH_2Cl	1991	2016	25	2056	$(2072)^d$	(16)	(1036)
CD_3SiH_2F	2011	2036	25	2060	$(2076)^d$	(16)	(1038)

a) obs. overtone b) twice obs. fundamental c) difference between (a) and (b) d) estimated from assumed Δ (from iodide)

Table I.3.3. The following assumptions are made; the anharmonicity and repulsion effects are the same for each molecule, and are as observed in the iodide; and the two combination bands are $2\nu_5$ and $2\nu_{4,14}$. (Although $\nu_4 + \nu_5$ also has character a' and thus can be expected to be relatively strong for an overtone, this combination is not large enough for the high wavenumber band, and is assumed to be weaker than $2\nu_5$ and so the more unlikely candidate for the lower, more intense combination).

ii) Below 350 cm^{-1}

The lowest frequency in each Raman spectrum is assigned as the CSiX deformation, which although an a' mode, appears only slightly polarised. The frequency is about 20 cm^{-1} lower in the CD_3- compounds than in the CH_3- homologues. In the fluoride spectra, additional weak bands are observed, at ca. 225 and 183 cm^{-1} for the CH_3- and CD_3- compounds respectively. If they are not impurities, which is thought unlikely, they may be the torsional modes, in which case the

decrease in frequency upon deuteration of the methyl group is in line with expectations. However, the frequencies are higher than for both CH_3SiH_3 and CH_3SiF_3, where it has been variously estimated from microwave and overtones (the torsion is inactive in C_{3v} molecules) at 190[27,29] and 208[4] cm^{-1} for the hydride and 140[32] and 156[62] cm^{-1} for CH_3SiF_3.

iii) <u>1000-350 cm^{-1}</u>

The Raman spectra for the region below 1000 cm^{-1} are shown in Figures I.3.7-10. The most prominent feature in the spectra of the iodide, bromide and chloride is the strong, polarised band of the Si-X stretch, at about 330, 400 and 500 cm^{-1} respectively. The Si-F stretch is a weak, broad band at about 900 cm^{-1} with a corresponding intense absorption of approximately A-type contour in the infrared spectra. This is considered to be the Si-F mode rather than the methyl rocking mode(s) by the position of a similar absorption in CD_3SiH_2F, where it cannot be due to a rock. In CH_3SiH_2F and CD_3SiH_2F, this overlaps with the distinctive B-type contour of ν_8, the SiH_2 scissoring mode at <u>ca</u>. 975 cm^{-1}, assigned by comparison with the HSiH deformation in SiH_4[78], which is also overlapped to the high wavenumber side by the CD_3 deformation bands. This latter mode appears to be depolarised in all the Raman spectra, despite being an a' mode. The other bands are more easily described in terms of the isotopically similar species since several bands were found not to be observed through accidental overlapping with stronger bands. This is particularly true for the chlorides,
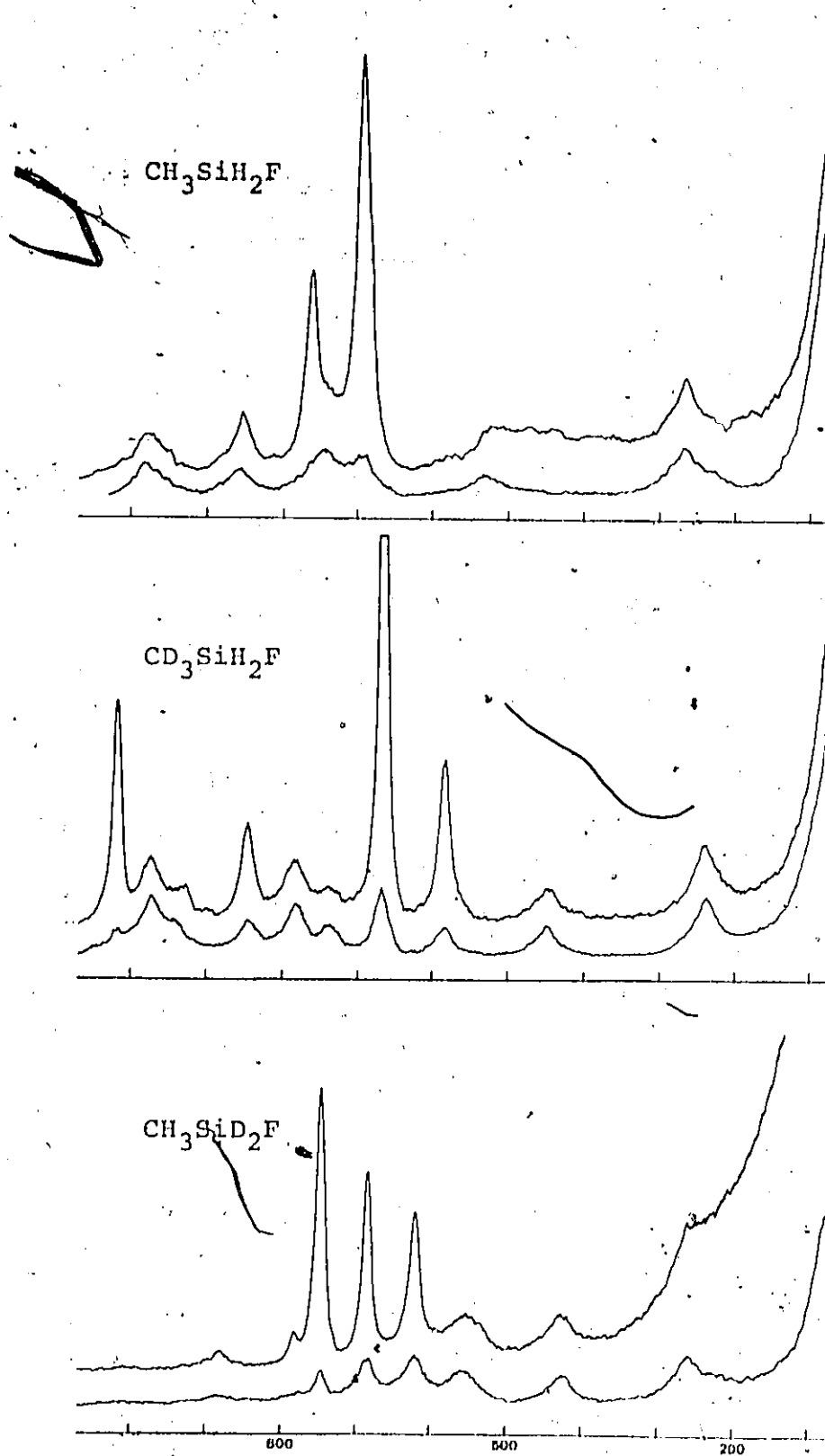
Figure I.3.7   Partial Raman spectra of the
fluoromethylsilanes

CH$_3$SiH$_2$Cl

CD$_3$SiH$_2$Cl

CH$_3$SiD$_2$Cl

800   600   200
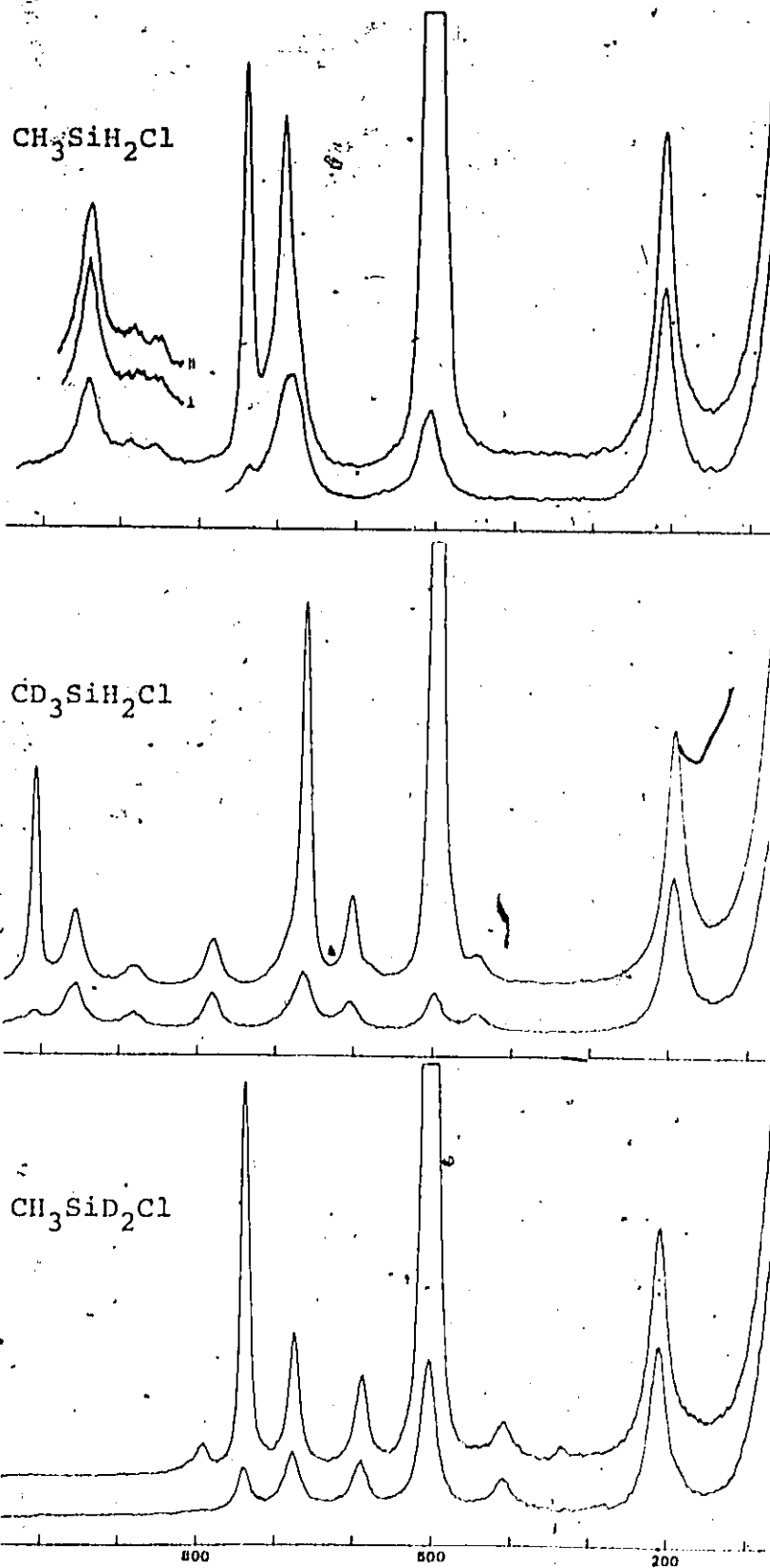
Figure I.3.8   Partial Raman spectra of the
chloromethylsilanes
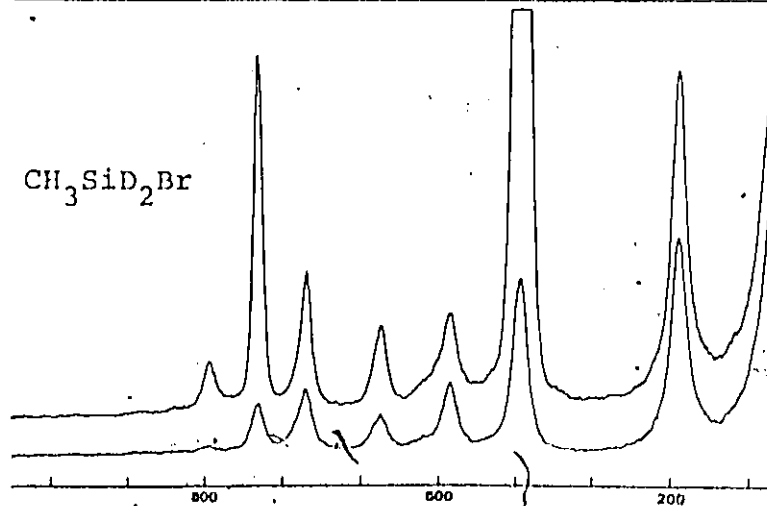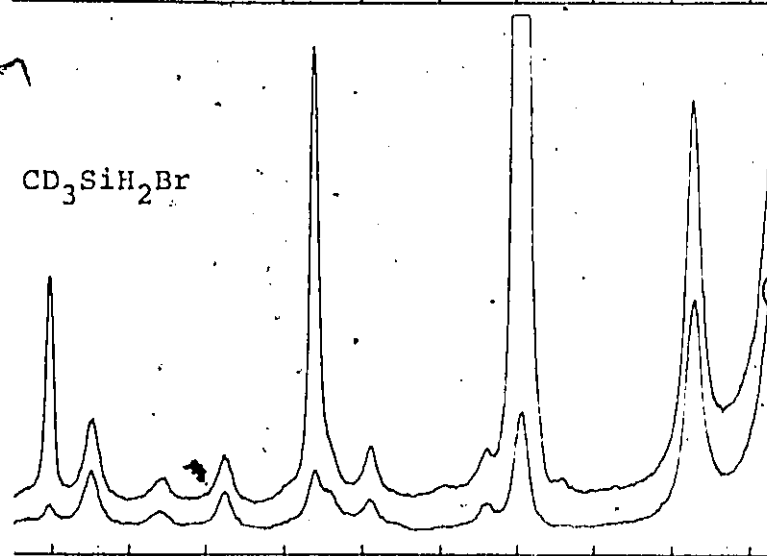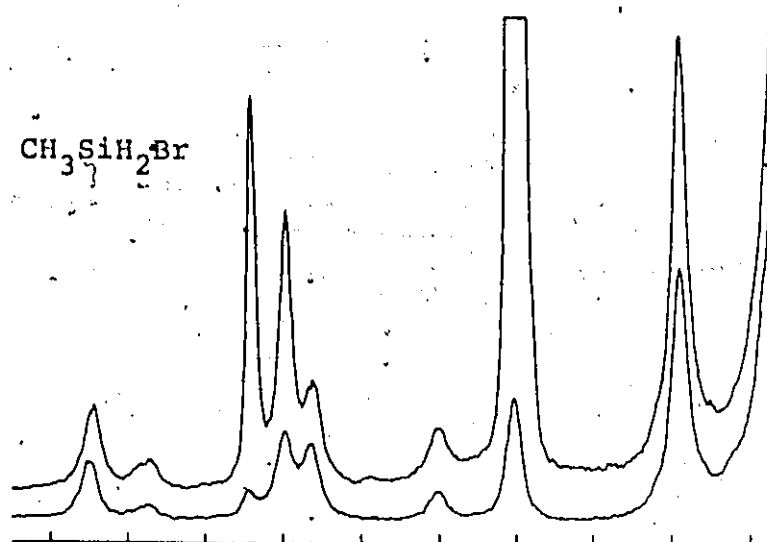
Figure I.3.9 Partial Raman spectra of the
bromomethylsilanes
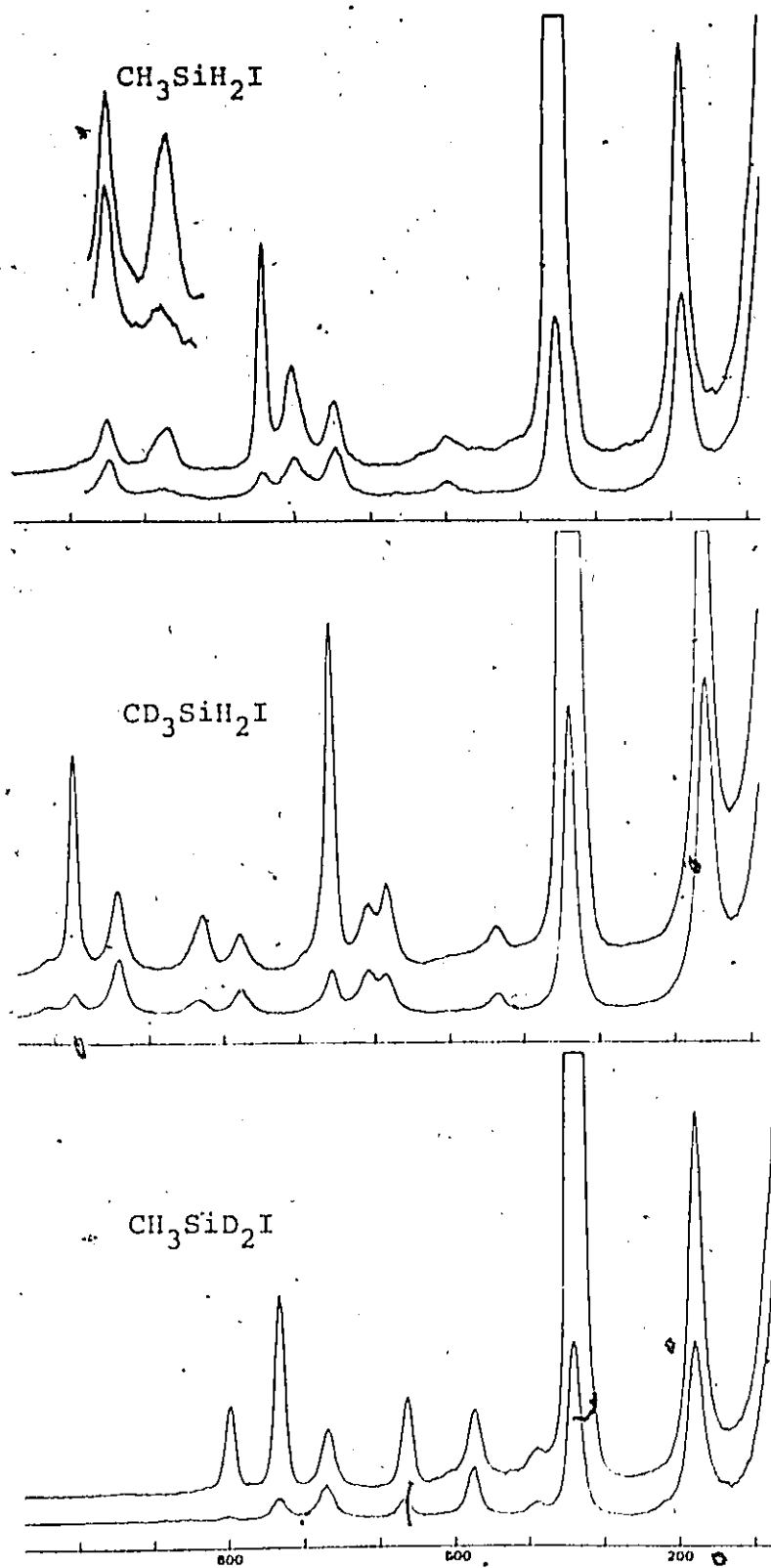
Figure I.3.10 Partial Raman spectra of the
iodomethylsilanes

and is probably one of the reasons for the disagreement in assignment with the only other report on deuterated derivatives[65]. These bands are only discovered through comparison of the whole series.

Starting at the low wavenumber region of the CH_3SiH_2X series, there appears a weak, depolarised band at about 500 cm^{-1}, which in the chloride should be located under the Si-Cl band. This must be the lowest frequency SiH_2 mode. At around 700 cm^{-1} in the iodide is a group of three medium intensity bands, with the separation between the lowest (depolarised) and middle one (polarised) decreasing with lighter halogen substitution. These two merge in the chloride, where they can only be distinguished by the different position of the envelope maxima in the normal and polarised scans. In the fluoride there are three bands in the same region, but in this case it is the higher two that are almost coincident, and hence the depolarised band is now the middle band instead of the lowest. It is this polarised band in the middle of the three (lowest in the fluoride) which is not observed in the infrared spectrum of these compounds, and by its absence prevented the authors of the original infrared study of the series[64] from making a correct assignment. The other two bands are seen quite clearly, the higher of the two displaying progressively more A character from its A/B hybrid shape in the iodide, and less intensity as the halogen becomes lighter. The former effect appears to be a typical transformation in this series. The lower band is weak and featureless

except in the fluoride where the sharp C-type contour is clearly visible to low wavenumber in the same envelope. In the three heavier halides, the strongest infrared absorption is an A/B type band with a low wavenumber shoulder, and with corresponding weak bands in the Raman effect is expected to contain the two methyl rocking modes. In the fluoride the remaining bands appear as a C and A-type band almost coincident at $\underline{ca}$. 865 cm^{-1} with a single weak band as their Raman counterpart.

Deuteration of the methyl group leaves the B-type ν_8 and a strong A/B band at only slightly lower wavenumber, but whereas the similar band was tentatively assumed to be the methyl rock in the CH_3- series, it is highly improbable that it can be the CD_3 rock in this case. Moreover, from the Raman spectra it would appear that there is only one band present since there are no other fundamentals unaccounted for. A band similar to that at $\underline{ca}$. 500 cm^{-1} in the CH_3- series is found about 70 cm^{-1} lower, this time managing to avoid being overlapped by either the Si-Br or Si-Cl modes. A similar pattern is again observed for the remaining bands located about the strong polarised band at $\underline{ca}$. 660 cm^{-1}, which is assumed to be ν_7, the Si-C stretching mode. Starting with the iodide, a pair of weak bands is observed to slightly lower wavenumber of ν_7, the higher of them appearing depolarised, and another pair on the high wavenumber side, the higher of which is polarised. With lighter halogen substituent all four increase in wavenumber with the higher band in both pairs

doing so more rapidly than the others. The highest of the
four, which is the Raman band corresponding to the intense
intrared absorption mentioned already; also appears more
depolarised, although presumably an a' mode from the A/B
contour of the infrared band. The fluoride continues the
general trend as far as relative position is concerned
although not the trend of increasing wavenumber.

This is also the case for the CH_3SiD_2X series, where the
four band pattern in the iodide, appearing below the stronger
polarised band at about 740 cm^{-1} (again assumed to be v_7),
at 388 (dep.), 472 (dep.), 562 (pol.) and 668 cm^{-1} (pol.)
is maintained throughout the four compounds. The lowest band
in the bromide, and the next lowest in the chloride are over-
lapped by the strong Si-X band. This time not only are the
relative positions maintained in the fluoride, but the wave-
numbers all continue the gradual increase as well. There
appears to be only one band above v_7, a weak polarised band
at about 800 cm^{-1}, where two methyl rocks are expected.
Closer examination at high sensitivity reveals extremely weak
bands which may be considered for the other (a") rock.
There is some confidence about assigning this band as a
fundamental in the fluoride as there is an infrared counter-
part at almost the same position. Weak shoulders are observed
to the high frequency side of the intense absorptions in the
other three compounds, with that in the iodide being at almost
the same wavenumber as a very weak Raman feature. These bands
in the bromide and chloride were tested by application of the

product rule, but produced unacceptably high ratios, and are thus considered dubious candidates as fundamentals.

I.3.4 Assignment and Normal Coordinate Analysis

Before an attempt at an assignment is made, it is obviously essential to confirm that the frequencies under consideration are in fact all fundamentals. While for most observed features this is a simple process based on intensities and expected band positions, there are some fundamentals that are of very low intensity, unobserved, or overlapped by a stronger feature. Examples in the compounds studied here are mostly in the CD_3- derivatives, and in the case of the monohalomethylsilanes are the a' CD_3 stretches in the infrared spectra and the asymmetric deformations in both effects. In the former case the frequency has been estimated at 100 cm^{-1} lower than the asymmetric stretching vibration, by comparison with the Raman spectra, and in the latter from the methyl deformation overtone region, as described above (see Table I.3.3). There still remain several unobserved fundamentals, and these are estimated, and the remaining observed frequencies tested, by application of the product rule. The results of these calculations using the best estimates for the missing frequencies are shown in Table I.3.4. The agreement, while not overwhelming, is sufficient to indicate that the frequencies chosen in each class are probably fundamentals, given the sensitivity of the calculations to the input data. Although separate calculations are shown for infrared and Raman frequencies, some values have been trans-

Table I.3.4 Calculated and observed product rule ratios
for the monohalomethylsilanes

ratio	species	calc.	obs. i.r.	obs. Ra
$\dfrac{CH_3SiD_2F}{CH_3SiH_2F}$	a'	0.372	0.387	0.383
	a"	0.416	0.422	0.419
$\dfrac{CD_3SiH_2F}{CH_3SiH_2F}$	a'	0.198	0.215	0.212
	a"	0.400	0.409	0.414
$\dfrac{CD_3SiH_2F}{CH_3SiD_2F}$	a'	0.533	0.555	0.552
	a"	0.962	0.968	0.989
$\dfrac{CH_3SiD_2Cl}{CH_3SiH_2Cl}$	a'	0.369	0.379	0.374
	a"	0.405	0.405	0.411
$\dfrac{CD_3SiH_2Cl}{CH_3SiH_2Cl}$	a'	0.194	0.210	0.207
	a"	0.400	0.396	0.404
$\dfrac{CD_3SiH_2Cl}{CH_3SiD_2Cl}$	a'	0.526	0.553	0.552
	a"	0.987	0.978	0.982
$\dfrac{CH_3SiD_2Br}{CH_3SiH_2Br}$	a'	0.366	0.375	0.372
	a"	0.400	0.419	0.402
$\dfrac{CD_3SiH_2Br}{CH_3SiH_2Br}$	a'	0.191	0.204	0.199
	a"	0.400	0.412	0.399
$\dfrac{CD_3SiH_2Br}{CH_3SiD_2Br}$	a'	0.522	0.545	0.534
	a"	0.997	0.980	0.994
$\dfrac{CH_3SiD_2I}{CH_3SiH_2I}$	a'	0.366	0.370	0.368
	a"	0.400	0.431	0.413
$\dfrac{CD_3SiH_2I}{CH_3SiH_2I}$	a'	0.190	0.200	0.194
	a"	0.400	0.420	0.416
$\dfrac{CD_3SiH_2I}{CH_3SiD_2I}$	a'	0.519	0.528	0.527
	a"	1.001	0.975	1.007

ferred from one effect to the other where they have not been observed. For example in the infrared frequencies the skeletal deformation frequencies were necessarily taken from the Raman spectra. Because of this and other adjustments just commented upon, the infrared ratios for the a' class in CD_3SiH_2X contain three values not directly observed out of the eleven frequencies, and so must be considered less accurate than the others. The effect of leaving the torsional mode out of the calculation of the a" ratios is not known, but if significant should affect the ratios involving CD_3SiH_2X most.

All three ratios were calculated because, since they are not independent of each other, any product containing an incorrect frequency will affect both of the ratios it is involved in, and thus should be more easily singled out. Thus if there are, say, two possible frequencies under consideration as fundamentals in one compound, all the ratios can be calculated and the assignments for those which are either significantly too high or too low can be rejected. In cases where there are two possible frequencies for each of two of the homologues, the ratio involving those two would have four possible values. Consideration of these, together with the two other pairs of possible values from the other two ratios was in all cases sufficient to select the better fitting frequencies. It was reassuring to note that whichever ratio was used as the starting point in this comparison, the same frequencies ended up being the best candidates from the list

of possible frequencies. The observed frequencies used in the calculation of the ratios are listed in Tables I.3.5-8, together with the preferred assignment.

The assignment was approached in two ways, as for the methylsilanes (chapter I.1) and the trihalomethylsilanes (chapter I.2); empirically, and with help from the NCA. The light compound was first assigned by inspection, with the SiH_2 wag and twist, the only two modes whose frequencies could not be easily predicted beforehand, assigned to features in the Raman spectra at about 700 cm^{-1}, approximately halfway between the SiH_2 scissors and rock. The deuterated compounds were then assigned fairly straightforwardly once the assignment of the light compound was assumed, although at first the increase in the SiH_2 wag and twist in the CD_3- compounds compared to the CH_3- homologues was a little surprising. Even more surprising was that once the NCA was underway, it was found to be very difficult to reproduce the assignment of the light compounds, while in general the deuterated compounds whose assignment was based on the light compound, produced a good match.

One of the major problems in an NCA of these compounds is the number of force constants necessary to describe all the motions, especially the number of interaction terms. Compared to the C_{3v} molecules reported in the previous two chapters, the descent in symmetry to C_s increases the number of diagonal terms from seven to eleven, but more significantly doubles the number of diagonal and interaction terms

Table I.3.5   The vibrational spectra of the fluoromethylsilanes

	CH₃SiH₂F i.r.(gas)	Ra (liq.)	CH₃SiD₂F i.r.(gas)	Ra (liq.)	CD₃SiH₂F i.r.(gas)	Ra (liq.)	Assignment
	C 2987 w A {2978 w {2970	2980 mw dp	C 2986 w 2978 w	2983 mw dp	~2233 mwsh	2230 sh dp	ν_{12} ν_1
	2922 vw	2917 s p	{2931 A{2919 vw {2908	2916 s p	—	2130 s p	ν_2
	2826 vw	2822 w p				~2060 vw dp 2011 w p	$2\nu_{4,14}$ $2\nu_5$
	B {2202 vs {2182 vs C 2188 vs	2188 vs p	B{1598 vs {1582 vs C 1601 vs	1585 vs p 1594 wsh dp	B{2197 vs {2183 C 2187	2188 vs p	ν_3 ν_{13}
	1416 w	1418 vw dp	C{1416 w {1410 w	1422 vw dp	—	~1043*	ν_{14} ν_4
	A{1278 {1266 mw {1256	1265 w p	A{1276 {1266 m {1257	1263 w p	A{1028 {1018 s {1008	1018	ν_5
	B{982 ms {974	978 w dp	B{691 {679 w	687 m p	B{982 {967 ms	973 mw dp	ν_6
	A{962 {954 vs {948	950 vw	A{906 {895 vs {884	~885 vw	A{945 {934 vs {924	927 w p	ν_{10}
	C 872 m	—	C? 817 w	~822 vw	C 731 m	737 vw dp	ν_{15}
	A{866 {859 w {851	851 w p	792 w	~781 wsh p	B{585 {570 w	583 m p	ν_7

177

Table I.3.5   (continued)

CH₃SiH₂F		CH₃SiD₂F		CD₃SiH₂F		Assignment
i.r.(gas)	Ra (liq.)	i.r.(gas)	Ra (liq.)	i.r.(gas)	Ra (liq.)	
A { 769, 759 m, 750	760 mw p	A { 760, 750 s, 740	750 m p	670 mw	666 s p	ν_8
C 734 m	744 vw dp	C 555 m	556 w dp	C 783 w	784 w dp	ν_{16}
~685 vvsh	691 m p	A { 631, 620 m, 608	622 mw p	A/B { 866, 857 m, 848	846 mw p	ν_9
525 w	530 vw dp	428 w	431 w dp	436 w	448 w dp	ν_{17}
	263 w dp?		260 w dp?		241 mw dp	ν_{11}
	225 wsh dp?		224 wsh dp?		183 wsh dp?	ν_{18}?

* estimated

Table I.3.6 The vibrational spectra of the chloromethylsilanes

	CH_3SiH_2Cl		CH_3SiD_2Cl		CD_3SiH_2Cl		Assignment
	i.r.(gas)	Ra (liq.)	i.r.(gas)	Ra (liq.)	i.r.(gas)	Ra(liq.)	
	C{2988 w A{2978 w 2971	2977 w dp	C{2988 mw A{2978 mw 2972	2978 mw dp	~2239 wsh	2227 msh dp	ν_{12} ν_1
	2928 A{2920 vw 2913	2915 s p	2928 A{2920 w 2911	2914 s p	–	2128 ms p	ν_2
	2820 vw	2810 vw p	2820 vw	2811 vw p		2056 vw p 1991	$2\nu_{4,14}$ $2\nu_5$
	C 2192 vs B{2198 vs 2183	2192 sh dp 2188 vs p	C 1604 vs B{1592 vs 1580	1606 sh dp 1583 vs p	C 2191 vs B{2197 vs 2183	2188 s p	ν_{13} ν_3
	~2020 vw		~2020 vw		1597 vw	1595 vw p	$\nu_5+\nu_7$
	1409 w	1420 vw dp	1418 w 1405 w	1421 w dp	–	~1036*	ν_{14} ν_4
	A/B{1273 1264 mw 1257	1261 w p	A/B{1270 1263 m 1258	1262 w p	B{1017 ms 1005	1008 m p	ν_5
	B{968 s 953	958 w dp	A/B{694 685 ms 678	681 m p	B{970 ms 953	957 mw dp	ν_6
						~680 vvsh	$\nu_{10}+\nu_{11}$
	A{922 913 vs 905	906 vw	A{815 807 vs 800	800 vw p	~606 mw	602 mw p	ν_7
	873 wsh	875 vw	824 wsh	~820 vvw	C 667 m	662	ν_{15}

Table I.3.6   (continued)

CH₃SiH₂Cl i.r.(gas)	Ra.(liq.)	CH₃SiD₂Cl i.r.(gas)	Ra(liq.)	CD₃SiH₂Cl i.r.(gas)	Ra(liq.)	Assignment
A⎰757 ⎱750 m B 742	753 m p	A⎰755 ⎱747 vs B 739	745 m p	B⎰667 m ⎱661	662 ms p	ν_8
A⎰705 ⎱699 vw B 693	702 m p	A⎰604 ⎱595 s B 588	593 w p	A/B⎰895 ⎱885 vs 878	881 mw p	ν_9
C 686 vw	677 wsh dp	−†	−†	C 783 mw	781 w	ν_{16}
A⎰537 ⎱530 s B 521 ~505	512 s p ~523 wsh dp	A⎰530 ⎱523 s B 514 408 vw	506 s p 413 w dp	507 m 438 w	497 s p 444 w dp	ν_{10} ν_{17}
	213 m p		212 m p		193 m dp?	ν_{11}

* estimated from overtones
† estimated at 510 cm⁻¹

Table I.3.7   The vibrational spectra of the bromomethylsilanes

	CH_3SiH_2Br		CH_3SiD_2Br		CD_3SiH_2Br		Assignment
	i.r.(gas)	Ra (liq.)	i.r.(gas)	Ra (liq.)	i.r.(gas)	Ra (liq.)	
	C 2989 w		C 2988 w		~2240 wsh	2229 mw dp	ν_{12}
	A{2985 w, 2978 w, 2972}	2977 mw dp	A{2985, 2978 w, 2973}	2977 mw dp	—		ν_1
	A{2926, 2919 vw, 2913}	2911 s p	A{2927, 2920 w, 2914}	2911 s p		2124 s p	ν_2
	2840 vvw	2820 vw p				2052 vw p	$2\nu_{4,14}$
		2502 vw p		2505 vw p		1983 w p	$2\nu_5$
	C 2193 vs	2200 wsh dp	C 1604 vs	1602 wsh dp	C 2188 vs		ν_{13}
	B{2193 vs, 2182 vs}	2191 vs p	B{1591 vs, 1579}	1581 vs p	B{2188 vs, 2179 vs}	2184 vs p	ν_3
	2005 vvw		1993 vw		1665 vw		$\nu_5+\nu_8$
			1652 vw		1376 vw		$\nu_5+\nu_{10}$
	C{1423 w, 1419 w}	1421 w dp	1425 w, 1416 w	1420 w dp	—	1034*	ν_{14} , ν_4
	A/C{1269, 1262 m, 1257}	1260 w p	A/C{1271, 1263 m, 1259}	1261 w p	B{1013 s, 1003}	1002 mw p	ν_5
	B{962 s, 949}	952 w dp	A{686, 679 ms, 673}	677 w p	B{960 s, 948}	947 w dp	ν_6
	A{906, 899 vs, 892}	883 vw p?	806 vs	801 mw p	592 mw	588 w p	ν_7

Table I.3.7 (continued)

	CH_3SiH_2Br		CH_3SiD_2Br		CD_3SiH_2Br		Assignment
	i.r.(gas)	Ra (liq.)	i.r.(gas)	Ra(liq.)	i.r.(gas)	Ra(liq.)	
	871 wsh	~875 vw dp?	824 wsh	~837 vw	642 wsh	638 wsh dp	ν_{15}
	A/B {752, 744 vs, 738}	745 mw p	B {747 vs, 735}	738 mw p	657 m	659 m p	ν_8
	–	701 mw p	586 s	579 w p	867 vs	858 w dp?	ν_9
	C 659 vw	667 w dp	–	490 w dp	C 778 m	775 w dp	ν_{16}
		591 vw p					$\nu_{10}+\nu_{11}$
	498 w	503 w dp	B {411 ms, 401}	395 vs p	434 wsh	438 w dp	ν_{17}
	B {421 ms, 408}	402 vs p	521 vw	522 vw p	407 m	394 vs p	ν_{10}
						(341) vw p	$\nu_5-\nu_8(2\nu_{11})$
		192 mw p		191 mw p		173 mw p	ν_{11}

*estimated

Table I.3.8　The vibrational spectra of the iodomethylsilanes

Assignment	CH_3SiH_2I i.r.(gas)	CH_3SiH_2I Raman(liq)	CH_3SiD_2I i.r.(gas)	CH_3SiD_2I Raman(liq)	CD_3SiH_2I i.r.(gas)	CD_3SiH_2I Raman(liq)
ν_{12}	C{2984 A{2977 w 2971	2972 mw dp	C{2983 A{2979 w 2973	2971 mw dp	~2240 wsh	2223 mw dp
ν_1	{2922 A{2916 vw 2911	2906 ms p	{2925 A{2919 vw 2911	2908 ms p	–	2121 ms p
ν_2	2825 vw	2810 vw p	2820 vw	2816 vw p		2001 vw p
$2\nu_{4,14}$	C 2189 s	2185 wsh dp	C 1602 vs	1596 wsh dp	C 2189 vs	2183 msh dp
ν_{13}	B{2189 s		B{1586 vs		B{2189 vs	
ν_3	{2170 s	2177 s p	{1575 vs	1576 s p	{2178 vs	2178 s p
$2\nu_5$	1995 vw		1994 vw			1977 vw p
$\nu_5+\nu_8$						
ν_{14}	C 1419 w 1413 w	1414 vw dp	C{1421 w 1414 w	1415 vw dp	~1028 vwsh	1033 vw dp
ν_4	B{1268 m 1256 m	1256 vw p	B{1267 m 1259 m	1256 vw p	B{1010 1002	1000 mw p
ν_5	954 ms 942	940 w dp	673 ms	668 w p	B{953 942	940 w dp
ν_6	B 888 880 vs	875 wsh dp?	804 vs	797 w p	B{591 w	581 w p
ν_7	856 msh	857 w p?	827 wsh	828 vw	C 607 w	607 w dp
ν_{15}	A{742 736 ms 731	735 mw p	A/B{741 737 s 733	731 mw p	B{661 m 651	655 mw p
ν_8	–	696 w p	575 s	562 w p	846 vs	827 w p
ν_9	640 vw	640 w dp	–	472 w dp	C 781 mw	776 w dp
ν_{16}	485 w	490 vw dp	510 vw	510 vw p		492 vvw
$\nu_{10}+\nu_{11}$			385 vw	388 xw p		434 vw p
ν_{17}	~355 wsh*	344 vs p	~345*	335 vs p	~346*	336 vs p
$2\nu_{10}$						309 vw p
ν_{11}		176 m p		176 m p		156 m p

* in KBr absorption shoulder

around the silicon atom, to four and eight respectively.
Bearing in mind the inability of the NCA for MeSiX$_3$ to pro-
duce a set of useful force constants when only two of the
four interaction terms about the silicon atom were used,
some problems might be expected because of this increase in
the number of terms that may be introduced. This is especial-
ly true for the molecules discussed in this chapter where
they will be accentuated by the increased anharmonicity
effects introduced by the two hydrogen atoms present in the
compounds studied here.

In the methylsilane analysis it was shown that there is
considerable interaction between the deformations of HCSi
and CSiH angles _trans_ to each other, but by introducing
substituents onto silicon the HCSi angles are no longer
equivalent. So for the following three series, the HCSi
angles have been separated into those whose deformation is
approximately in the plane of the molecule (HCSi$^{||}$) and those
that are approximately perpendicular to the symmetry plane
(HCSi$^{\perp}$). This makes for two HCSi interaction terms, of which
both were used in the dimethyl silane series (where there are
four rocks) and only one in the monomethyl- series.

Although initially the aim was to produce a consistent
set of calculations along the lines of those for the MeMX$_3$
(M =Si, Ge) compounds already described, this was soon
abandoned as the complexity of the analysis became apparent,
and the calculations were performed independently for each
molecule. The resulting force constants are listed in Table

I.3.9, where the absence of a smooth trend is apparent.

The monohalomethylsilane series turned out to be the least successful of the three series reported in this and the following two chapters, as far as the NCA was concerned. The poor agreement was mainly in the CH_3SiH_2X compounds, and this can be attributed to the inability of the quadratic field to account for the increased anharmonicity effects noted above, and probably more importantly, the interactions introduced by the close proximity of a number of the frequencies, an effect especially evident in the fluoride. This is not such a problem in the other homologues, where in both cases deuteration produces a greater separation of the frequencies. However, as can be seen from the p.e.d.'s in Tables I.3.10-13, satisfactory results are obtained for the heavier halogen derivatives, and for the two deuterated compounds throughout the series. While the overall frequency matching is not outstanding, the fit is close enough to suggest that the proposed assignments are reasonable, at least as far as these latter compounds are concerned. A noticeable feature in the heavier halides (Br, I) is the considerable mixing in CD_3SiH_2X, where the p.e.d. places the SiH_2 rock above the CD_3 rock (a") in a similar way to the ordering of the methyl and silyl rocks in CD_3SiH_3.

I.3.5 Discussion

Despite the lack of full support from the NCA for the CH_3SiH_2X compounds, the assignments as given in Tables I.3.5-8 are still preferred, on the basis of band intensities

Table I.3.9 Force constant values for $MeSiH_2X$

No.	Description	F	Cl	Br	I
1	CH	480.83	480.15	479.40	477.65
2	SiH	276.47	276.77	276.12	275.58
3	SiC	333	305	304	310
4	SiX	550	266.54	212.25	170.43
5	HCH	53.40	52.65	54.35	52.75
6	$HCSi^{\parallel}$	44.93	39.49	46.22	43.07
7	$HCSi^{\perp}$	46.55	52.84	42.02	47.27
8	HSiH	42.42	42.84	43.37	43.81
9	CSiH	56.86	51.52	58.37	58.88
10	HSiX	57.46	57.32	56.80	43.50
11	CSiX	59.18	60.43	66.51	64.93
12	CH/CH	6.70	7.00	6.55	6.51
13	SiH/SiH	−3.06	2.81	2.85	2.33
14	$HCSi^{\perp}/HCSi^{\perp}$	−3.20	1.44	−1.74	3.19
15	CSiH/CSiH	7.35	5.56	0.62	11.88
16	HSiX/HSiX	6.00	−2.11	2.40	−6.45
17	SiC/HCSi	17.07	17.30	19.06	21.74
18	SiC/CSiH	16.47	21.95	13.55	11.82
19	SiC/HSiX	−	−5.56	1.81	3.38
20	t-HCSi/CSiH	3.40	−6.72	12.33	7.14
21	c-HCSi/CSiH	−5.46	5.55	−2.66	−6.56
22	CSiH/HSiX	5.07	4.69	9.61	6.26
23	t-HCSi/HSiX	−5.45	0.10	−1.74	0.66
24	HSiH/CSiH	−2.43	0.25	3.26	2.79
25	HCH/HCH	−	−	1.57	−
26	SiX/HSiX	15.31	6.34	−	−
27	SiC/SiX	20*	−	−	−

* fixed

Units: $N.m^{-1}$ for stretching constants; $N.m.rad^{-2}$ for bending force constants

Tables I.3.10-13

Notes

The potential energy distribution is expressed as the percentage of the potential energy contributed by any force constant (in parentheses). See Table I.3.9 for the numbering of the force constants. All contributions in excess of 10% are listed. The compounds are listed in the order CH_3SiH_2X, CH_3SiD_2X, CD_3SiH_2X.

The major problem in the assignment, as discussed in the text, is the mixing between the methyl and $-SiH_2-$ groups. To indicate the extent of this in the Tables, the total contributions of the force constants describing the rocking motions (6 and 7) and those of the SiH_2 deformations (9 and 10) are given for the relevant modes, in (parentheses). When no separate total appears, the contribution is the same as that shown for the single force constant in the list. Where the total is different from the contribution of the single force constant, the contribution of the other constant was less than 10%. The amount of mixing is always indicated, even when the individual amounts are less than 10%, in which case the total is denoted by R (for rock) and D (for deformation) The modes markes by an asterisk in CD_3SiH_2X are those where the "empirical" assignment and that based on the p.e.d. are different.

Table I.3.10 Calculated frequencies and p.e.d. for MeSiH$_2$F

ν	mode	obs.	calc.	p.e.d.
1	CH$_3$ str(a)	2980	2985	101(1)
2	CH$_3$ str(s)	2917	2929	97(1)
3	SiH$_2$ str	2188	2173	101(2)
4	CH$_3$ def(a)	1421	1431	97(5)
5	CH$_3$ def(s)	1265	1272	55(5)+31(7)+10(6)
6	SiH$_2$ sc	978	993	65(8)+20(9)
7	CH$_3$ rock	859	771	33(6)+21(7) {54}+32(3)+15(10)+10(9) {25}
8	SiC str	760	739	69(3)+18(6)
9	SiH$_2$ wag	744	855	22(10)+12(9) {34}+45(4)+R{7}
10	SiX str	950	953	52(4)+20(10)+13(9)
11	CSiX def	263	262	81(11)
12	CH$_3$ str(a)	2980	2986	101(1)
13	SiH$_2$ str	2192	2222	99(2)
14	CH$_3$ def(a)	1421	1433	96(5)
15	CH$_3$ rock	8.72	897	72(7)+11(9)
16	SiH$_2$ twist	691	735	76(10)+45(9) {121}−10(22)+R{4}
17	SiH$_2$ rock	530	513	63(9)+38(10) {101}+18(7)

ν	mode	obs.	calc.	p.e.d.
1	CH$_3$ str(a)	2983	2985	101(1)
2	CH$_3$ str(s)	2916	2929	97(1)
3	SiD$_2$ str	1590	1559	100(2)
4	CH$_3$ def(a)	1422	1431	97(5)
5	CH$_3$ def(s)	1263	1270	56(5)+31(7)+17(6)
6	SiD$_2$ sc	687	702	57(8)+10(9,10)
7	CH$_3$ rock	786	805	45(6)+27(7) {72}+19(4)+D{2}
8	SiC str	750	755	82(3)+10(8)
9	SiD$_2$ wag	620	607	51(10)+36(9) {87}+R{11}
10	SiX str	895	929	78(4)
11	CSiX def	260	261	81(11)
12	CH$_3$ str(a)	2983	2986	101(1)
13	SiD$_2$ str	1601	1610	98(2)
14	CH$_3$ def(a)	1422	1433	96(5)
15	CH$_3$ rock	817	882	80(7)+D{4}
16	SiD$_2$ twist	555	535	80(10)+45(9) {125}−11(22)+R{1}
17	SiD$_2$ rock	430	412	70(9)+34(10) {104}+13(7)

ν	mode	obs.	calc.	p.e.d.
1	CD$_3$ str(a)	2230	2227	100(1)
2	CD$_3$ str(s)	2130	2108	96(1)
3	SiH$_2$ str	2187	2173	101(2)
4	CD$_3$ def(a)	1043	1039	78(5)
5	CD$_3$ def(s)	1018	1026	47(5)+16(8)+10(3,6)
6	SiH$_2$ sc	974	972	44(8)+20(5)+15(3)+12(7)
7	CD$_3$ rock	583	590	63(6)+29(7) {92}+D{7}
8	SiC str	666	681	68(3)+11(17)+10(7)
9	SiH$_2$ wag	857	846	37(10)+23(9) {60}+28(4)
10	SiX str	934	935	69(4)+17(10)+16(9)
11	CSiX def	241	247	79(11)
12	CD$_3$ str(a)	2230	2227	86(1)+14(2)
13	SiH$_2$ str	2190	2221	85(2)+14(1)
14	CD$_3$ def(a)	1043	1035	97(5)
15	CD$_3$ rock	735	698	38(7)+56(10)+10(23)
16	SiH$_2$ twist	784	759	63(9)+31(10) {94}+17(7)
17	SiH$_2$ rock	448	475	55(9)+27(10) {82}+41(7)

Table I.3.11 Calculated frequencies and p.e.d. for $MeSiH_2Cl$

ν	mode	obs.	calc.	p.e.d.
1	CH_3 str(a)	2977	2981	101(1)
2	CH_3 str(s)	2915	2927	97(1)
3	SiH_2 str	2188	2197	99(2)
4	CH_3 def(a)	1420	1424	95(5)
5	CH_3 def(s)	1260	1299	53(5)+38(7)+11(6)
6	SiH_2 sc	958	960	73(8)+11(9,10)
7	CH_3 rock	906	787	45(6)+20(7){65}+19(9)+10(10){29}
8	SiC str	753	714	92(3)
9	SiH_2 wag	702	813	40(10)+26(9){66}+19(6){25}
10	SiX str	512	517	87(4)
11	CSiX def	213	210	80(11)
12	CH_3 str(a)	2977	2981	101(1)
13	SiH_2 str	2192	2199	101(2)
14	CH_3 def(a)	1420	1428	95(5)
15	CH_3 rock	875	866	81(7)+D{10}
16	SiH_2 twist	677	732	65(10)+38(9){103}+21(7)
17	SiH_2 rock	523	522	80(9)+25(10){105}+R{4}
1	CH_3 str(a)	2978	2981	101(1)
2	CH_3 str(s)	2914	2927	97(1)
3	SiD_2 str	1586	1575	98(2)
4	CH_3 def(a)	1421	1424	95(5)
5	CH_3 def(s)	1262	1299	53(5)+38(7)+11(6)
6	SiD_2 sc	681	684	70(8)+16(10)
7	CH_3 rock	807	802	62(6)+26(7){88}+D{0}
8	SiC str	745	717	95(3)
9	SiD_2 wag	593	613	48(9)+35(10){83}+24(4)+R{0}
10	SiX str	506	486	65(4)+20(10)
11	CSiX def	212	209	80(11)
12	CH_3 str(s)	2978	2981	101(1)
13	SiD_2 str	1604	1592	101(2)
14	CH_3 def(a)	1421	1428	95(5)
15	CH_3 rock	824	850	98(7)+D{1}
16	SiD_2 twist	510	534	74(10)+38(9){112}+R{4}
17	SiD_2 rock	413	408	82(9)+23(10){105}+R{3}
1	CD_3 str(a)	2227	2222	100(1)
2	CD_3 str(s)	2128	2106	96(1)
3	SiH_2 str	2190	2197	99(2)
4	CD_3 def(a)	1036	1035	84(5)+11(7)
5	CD_3 def(s)	1008	1014	59(5)+25(7)+17(3)−12(17)+10(6)
6	SiH_2 sc	960	957	73(8)+12(10)+10(9)
7	CD_3 rock	602	612	56(6)+21(7){77}+18(4)+D{1}
8	SiC str	662	667	78(3)
9	SiH_2 wag	883	798	55(10)+50(9){105}+R{1}
10	SiX str	497	500	72(4)+13(6)
11	CSiX def	193	195	79(11)
12	CD_3 str(a)	2227	2221	100(1)
13	SiH_2 str	2191	2220	101(2)
14	CD_3 def(a)	1036	1033	95(5)
15	CD_3 rock	662	621	99(7)+D{16}
16	SiH_2 twist	781	762	64(10)+33(9){97}+R{5}
17	SiH_2 rock	444	520	80(9)+24(10){104}+R{4}

Table I.3.12 Calculated frequencies and p.e.d. for MeSiH$_2$Br

ν	mode	obs.	calc.	p.e.d.
1	CH$_3$ str(a)	2977	2981	101(1)
2	CH$_3$ str(s)	2911	2923	97(1)
3	SiH$_2$ str	2191	2194	99(2)
4	CH$_3$ def(a)	1421	1423	99(5)
5	CH$_3$ def(s)	1260	1277	56(5)+28(7)+17(6)
6	SiH$_2$ sc	952	959	73(8)+21(10)
7	CH$_3$ rock	892	887	31(6)+13(7) {44}+29(9)+17(10) {46}
8	SiC str	745	733	69(3)+12(9)+11(6) +10(20)
9	SiH$_2$ wag	701	699	32(9)+21(10) {53}+21(6)+13(7) {34}
10	SiX str	402	405	88(4) +27(3)−10(20)
11	CSiX def	192	192	75(11)
12	CH$_3$ str(a)	2977	2982	101(1)
13	SiH$_2$ str	2200	2197	101(2)
14	CH$_3$ def(a)	1421	1422	100(5)
15	CH$_3$ rock	877	906	49(7)+26(9) {30}+18(20)
16	SiH$_2$ twist	667	680	80(10)+28(9) {108}+23(7)−16(22)−13(20)
17	SiH$_2$ rock	503	517	60(9)+25(10) {85}+31(7)−21(20)+13(22)
1	CH$_3$ str(a)	2977	2981	101(1)
2	CH$_3$ str(s)	2911	2923	97(1)
3	SiD$_2$ str	1585	1572	99(2)
4	CH$_3$ def(a)	1420	1423	99(5)
5	CH$_3$ def(s)	1261	1277	56(5)+28(7)+17(6)
6	SiD$_2$ sc	677	693	71(8)+20(10)
7	CH$_3$ rock	806	836	52(6)+27(7) {79}+D{9}
8	SiC str	738	729	89(3)
9	SiD$_2$ wag	579	557	63(9)+31(10) {94}−15(22)+R{16}−11(20)
10	SiX str	395	384	81(4)+11(10)
11	CSiX def	191	191	75(11)
12	CH$_3$ str(a)	2977	2982	101(1)
13	SiD$_2$ str	1604	1592	101(2)
14	CH$_3$ def(a)	1420	1422	100(5)
15	CH$_3$ rock	837	856	72(7)+12(20)+D{8}
16	SiD$_2$ twist	490	502	74(10)+50(9) {124}−20(22)−12(20)+R{11}
17	SiD$_2$ rock	395	410	56(9)+33(10) {89}+19(7)−16(20)+14(22)
1	CD$_3$ str(a)	2229	2222	100(1)
2	CD$_3$ str(s)	2124	2103	96(1)
3	SiH$_2$ str	2184	2194	99(2)
4	CD$_3$ def(a)	1033	1029	100(5)
5	CD$_3$ def(s)	1002	1000	50(5)+26(7)+23(3)−17(17)+14(6)
6	SiH$_2$ sc	954	959	73(8)+21(10)
7	CD$_3$ rock	588	582	55(6)+32(7) {87}+12(9,10) {24}−10(20)
8	SiC str	659	666	77(3)+10(17)
9	SiH$_2$ wag	858	822	59(9)+34(10) {93}−15(22)+R{10}
10	SiX str	393	397	88(4)
11	CSiX def	170	176	75(11)
12	CD$_3$ str(a)	2229	2223	99(1)
13	SiH$_2$ str	2184	2197	100(2)
14	CD$_3$ def(a)	1033	1028	101(5)
15	CD$_3$ rock*	638	639	23(7)+81(10) {82}
16	SiH$_2$ twist	775	803	59(9)+17(10) {76}+17(7)+16(20)−11(22)
17	SiH$_2$ rock*	438	460	54(9) {63}+64(7)−29(20)

Table I.3.13 Calculated frequencies and p.e.d. for MeSiH$_2$I

ν	mode	obs.	calc.	p.e.d.
1	CH$_3$ str(a)	2972	2976	101(1)
2	CH$_3$ str(s)	2906	2918	97(1)
3	SiH$_2$ str	2180	2190	101(2)
4	CH$_3$ def(a)	1414	1422	96(5)
5	CH$_3$ def(s)	1256	1278	54(5)+33(7)+14(6)
6	SiH$_2$ sc	948	963	59(8)+29(9)
7	CH$_3$ rock	856	859	30(6)+15(7){45}+22(10){28}+20(8)
8	SiC str	735	740	64(3)+17(6)+13(10)+12(9)
9	SiH$_2$ wag	696	709	24(9)+23(10){47}+33(3)+16(6)
10	SiX str	344	347	85(4)+10(11)
11	CSiX def	176	175	74(11)+12(4)
12	CH$_3$ str(a)	2972	2976	101(1)
13	SiH$_2$ str	2189	2197	101(2)
14	CH$_3$ def(a)	1414	1419	97(5)
15	CH$_3$ rock	884	889	62(7)+23(9){26}+10(20)
16	SiH$_2$ twist	640	649	67(10)+32(9){99}+26(7)-11(22)+10(16)
17	SiH$_2$ rock	490	478	86(9)+18(10){104}±27(7)-17(15)+10(22) -12(20,21)
1	CH$_3$ str(a)	2971	2976	101(1)
2	CH$_3$ str(s)	2908	2918	97(1)
3	SiD$_2$ str	1581	1569	99(2)
4	CH$_3$ def(a)	1415	1422	96(5)
5	CH$_3$ def(s)	1256	1276	55(5)+34(7)+14(6)
6	SiD$_2$ sc	668	674	74(8)+12(9)
7	CH$_3$ rock	804	843	52(6)+25(7){77}+D{8}
8	SiC str	731	740	91(3)
9	SiD$_2$ wag	562	558	46(9)+41(10){87}-11(22)+R{11}
10	SiX str	335	328	79(4)+11(10)
11	CSiX def	176	175	74(11)+12(4)
12	CH$_3$ str(a)	2971	2976	101(1)
13	SiD$_2$ str	1602	1591	100(2)
14	CH$_3$ def(a)	1415	1419	97(5)
15	CH$_3$ rock	827	849	84(7)+D{7} /-10(15)+10(16)
16	SiD$_2$ twist	472	476	67(10)+49(9){116}-14(22)+13(7)
17	SiD$_2$ rock	388	375	83(9)+22(10){105}+18(7)-17(15)+11(22) -10(20,21)
1	CD$_3$ str(a)	2223	2218	100(1)
2	CD$_3$ str(s)	2121	2099	96(1)
3	SiH$_2$ str	2184	2190	99(2)
4	CD$_3$ def(a)	1033	1029	94(5)
5	CD$_3$ def(s)	1000	1000	44(5)+22(7)+13(3,6)-14(17)
6	SiH$_2$ sc	947	947	60(8)+21(9)
7	CD$_3$ rock	581	587	60(6)+19(7){79}+12(10)+11(9){23}
8	SiC str	655	675	72(3)
9	SiH$_2$ wag	827	805	46(10)+32(9){78}-10(22)+R{7}
10	SiX str	336	341	86(4)
11	CSiX def	156	160	75(11)+10(4)
12	CD$_3$ str(a)	2223	2219	99(1)
13	SiH$_2$ str	2189	2197	100(2)
14	CD$_3$ def(a)	1033	1026	98(5)
15	CD$_3$ rock*	607	606	64(10)+35(7)
16	SiD$_2$ twist	776	771	58(9)+17(10){75}+23(7)-12(15)+10(20)
17	SiD$_2$ rock*	434	437	81(9){89}+58(7)-18(20,21)-16(15)

and comparison with other, non-hydridic, compounds, for methyl rocking frequencies. This opinion is shared by the authors of the only other normal coordinate treatment of any of the monohalo- derivatives, that for the chloride[65], and also by Durig and Hawley[66] for the same compound. The assignments in this work and the latter report are very similar, the only difference being in the ordering of the two methyl rocking modes. From the observed frequencies reported for the former study it seeme likely that the workers relied more on infrared than Raman data, which would explain why the 702 cm^{-1} band observed in the Raman spectrum in this work and by Durig and Hawley[66] was not reported. The SiH_2 wag, which is assigned to this band, was assigned to the lower of the two methyl rocking absorptions, at 857? cm^{-1} (their query), presumably influenced by the tendency of the NCA to calculate the SiH bends to high wavenumber.

The non-appearance of the 702 cm^{-1} band in the infrared spectrum is obviously a handicap for an infrared study, but the choice of frequencies for the SiH_2 modes in the first study of this whole series[64] is another example of a dubious choice of comparative molecules, although admittedly there was not much of an alternative. In this case the SiH_2X_2 compounds were used, and apart from the SiH_2 scissoring mode, (the result in both compounds of an HSiH angle deformation) the comparison for the three lowest SiH_2 modes is of an HSiX deformation (in SiH_2X_2) with one involving varying contributions of HSiX and CSiH deformations. With the substantial

degree of mixing with the HCSi motions in the methyl derivat-
ives, it would be fortuitous to observe these vibrations at
the similar wavenumber.

CHAPTER I.4

DIHALOMETHYLSILANES

I.4.1 Vibrational Spectra

Preparative details are given in Chapter I.3.2. The infrared and representative Raman spectra - showing the dichlorides - are shown in Figures.I.4.1-5. For those bands in the infrared spectra with distinctive contours, those with B, C or hybrid B/C shapes in the CH_3SiHX_2 (X = Cl, Br, I) compounds will be a' modes, and those with A-type contours a" modes. For the fluoro- derivatives these are expected to change to A, C or A/C, and B-type contours respectively, as the moment of inertia along the axis approximately in the direction of the Si-C bond changes from the intermediate value to the lowest. The approximate description and numbering of the modes is shown in Table I.4.1. With the lack of

Table I.4.1 Description and numbering of fundamental modes in CH_3SiHX_2

Description	a'	Mode	a"
CH_3 str. (asym)	ν_1		ν_{12}
CH_3 str. (sym)	ν_2		
SiH stretch	ν_3		
CH_3 def. (asym)	ν_4		ν_{13}
CH_3 def. (sym)	ν_5		
CH_3 rock	ν_6		ν_{14}
SiC stretch	ν_7		
SiH bend	ν_8		ν_{15}
SiX_2 stretch	ν_9		ν_{16}
CSiX def.	ν_{10}		ν_{17}
SiX_2 def.	ν_{11}		
torsion			ν_{18}

CH$_3$SiHF$_2$

CD$_3$SiHF$_2$

CH$_3$SiDF$_2$

<u>Figure I.4.1</u> Infrared spectra of the difluoromethylsilanes

CH₃SiHCl₂

CD₃SiHCl₂

CH₃SiDCl₂
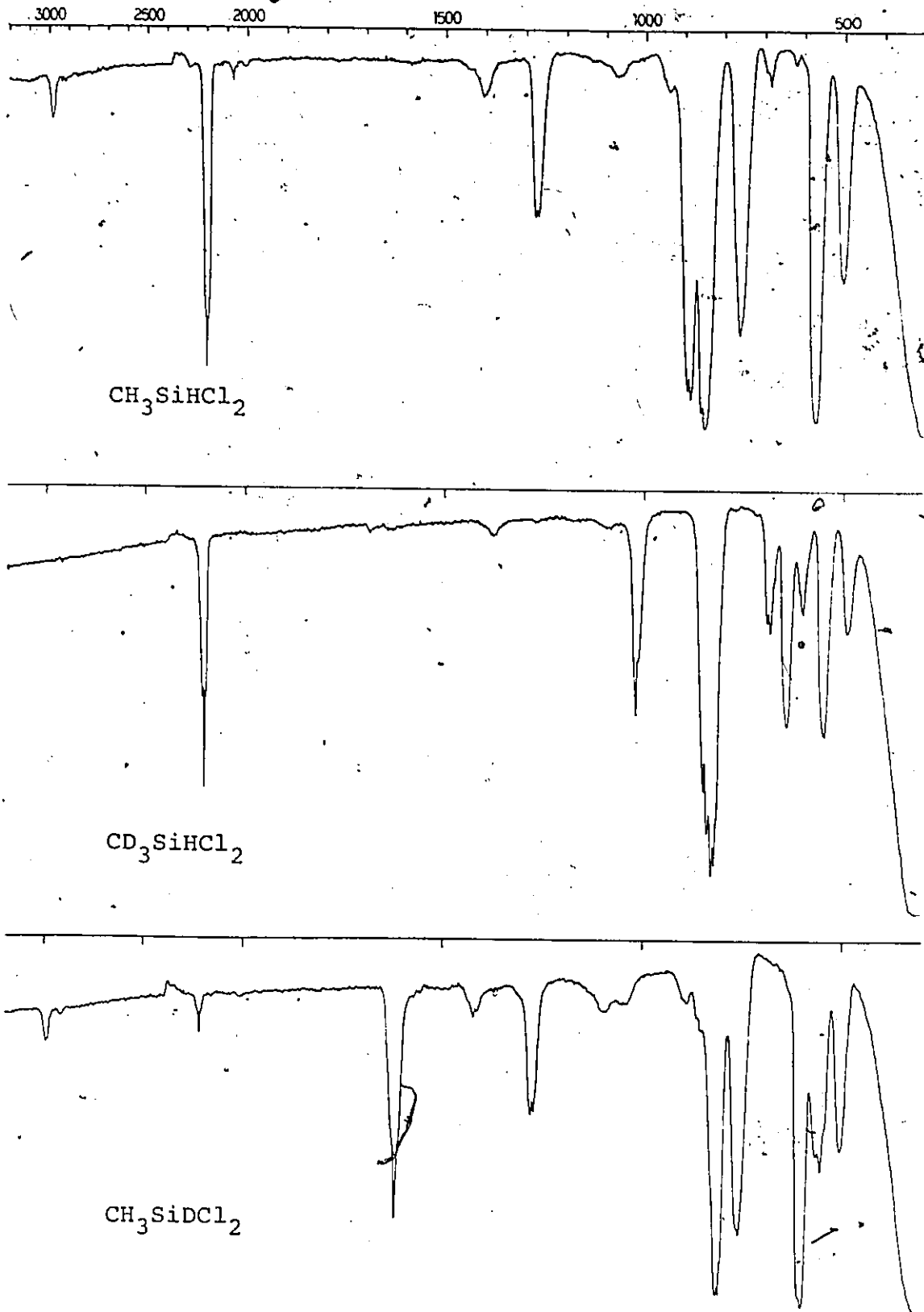
<u>Figure I.4.2</u>   Infrared spectra of the dichloromethylsilanes

CH_3SiHBr_2

CD_3SiHBr_2

CH_3SiDBr_2
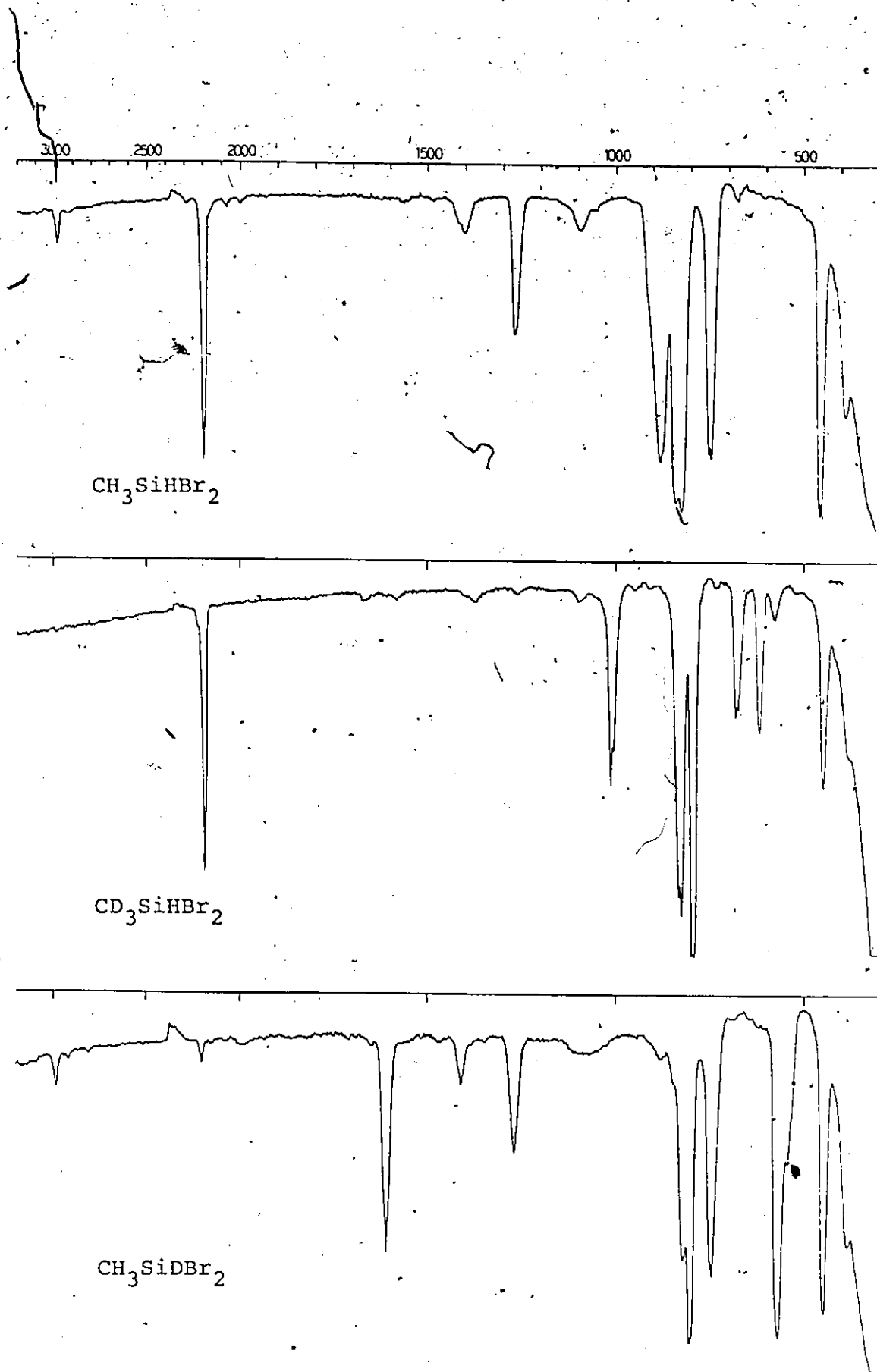
Figure I.4.3 Infrared spectra of the dibromomethylsilanes
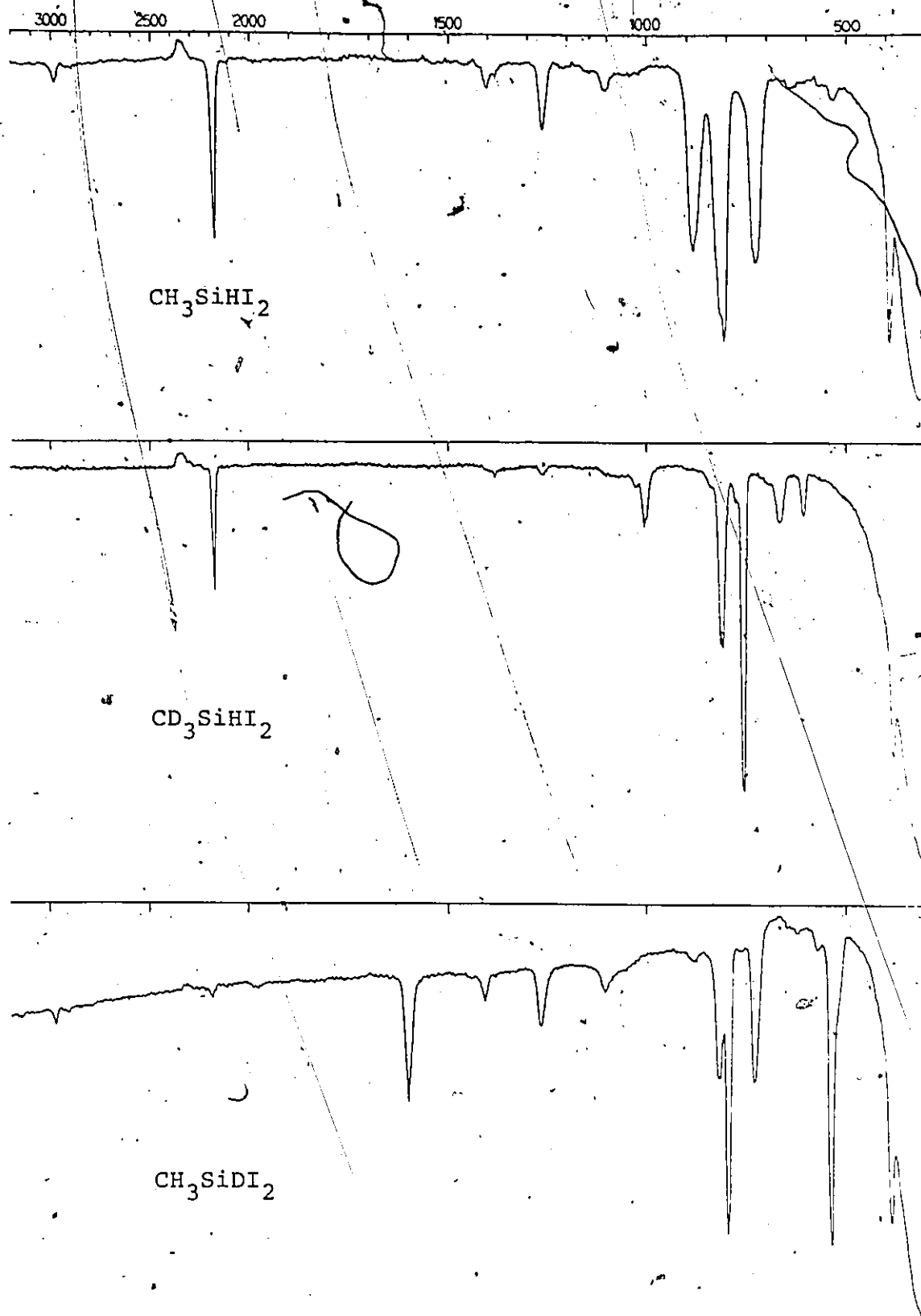
Figure I.4.4   Infrared spectra of the diiodomethylsilanes

CH₃SiHCl₂

CD₃SiHCl₂

CH₃SiDCl₂

3000   2000   1000   cm⁻¹ 0
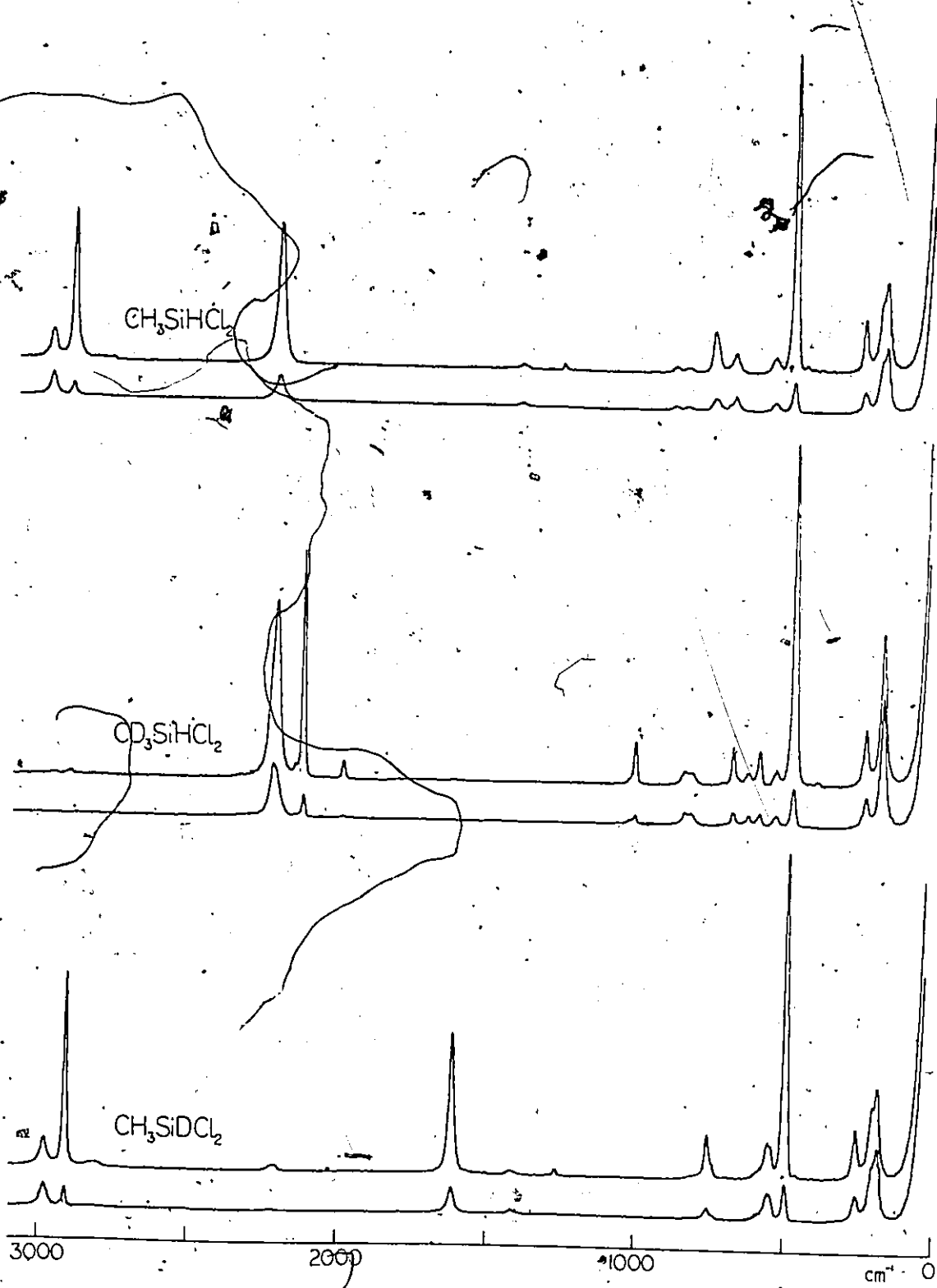
Figure I.4.5   Raman spectra of the dichloromethylsilanes

volatility of the diiodide (saturated vapour pressure $\sim$5 mm Hg) it was not possible to obtain all the bands at full scale in the gas phase for more accurate measurement. Use was made of the absorption expansion facility, but while this allowed for a better estimate of band position, the extra background noise effectively wiped out any contours present.

i) 3000 - 1000 cm^{-1}

The CH$_3$ stretching modes appear as weak bands in the infrared spectra, with only the fluoride showing distinctive contours, for the envelope containing ν_1 and ν_{12}. These appear as an A-type band, which suggests that these two modes are directly superimposed. The asymmetric CD$_3$ stretching modes can be seen as a spike on the high wavenumber side of ν_3, the SiH stretching mode, while the symmetric CD$_3$ stretch is barely observable in the low wavenumber tail of ν_3. The corresponding Raman features are fairly strong, with the CD$_3$ stretching modes being better defined than for the monohalo- derivatives as there is now only one SiH stretch, which appears as a strong, broad, and polarised band, as do the SiD stretches. In all infrared spectra ν_3 has a prominent Q branch, except for CH$_3$SiDF$_2$ where a doublet of almost equally intense bands appears, at 1634.1 and 1619.3 $\pm$ 0.5 cm^{-1}. The corresponding Raman band, centred at 1633 cm^{-1}, has a moderately strong shoulder to low wavenumber, estimated by approximate curve fitting plots to be at 1612 cm^{-1}. Both are polarised. The two features are shown in Figure I.4.6. No hydrogen or fluorine containing impurities
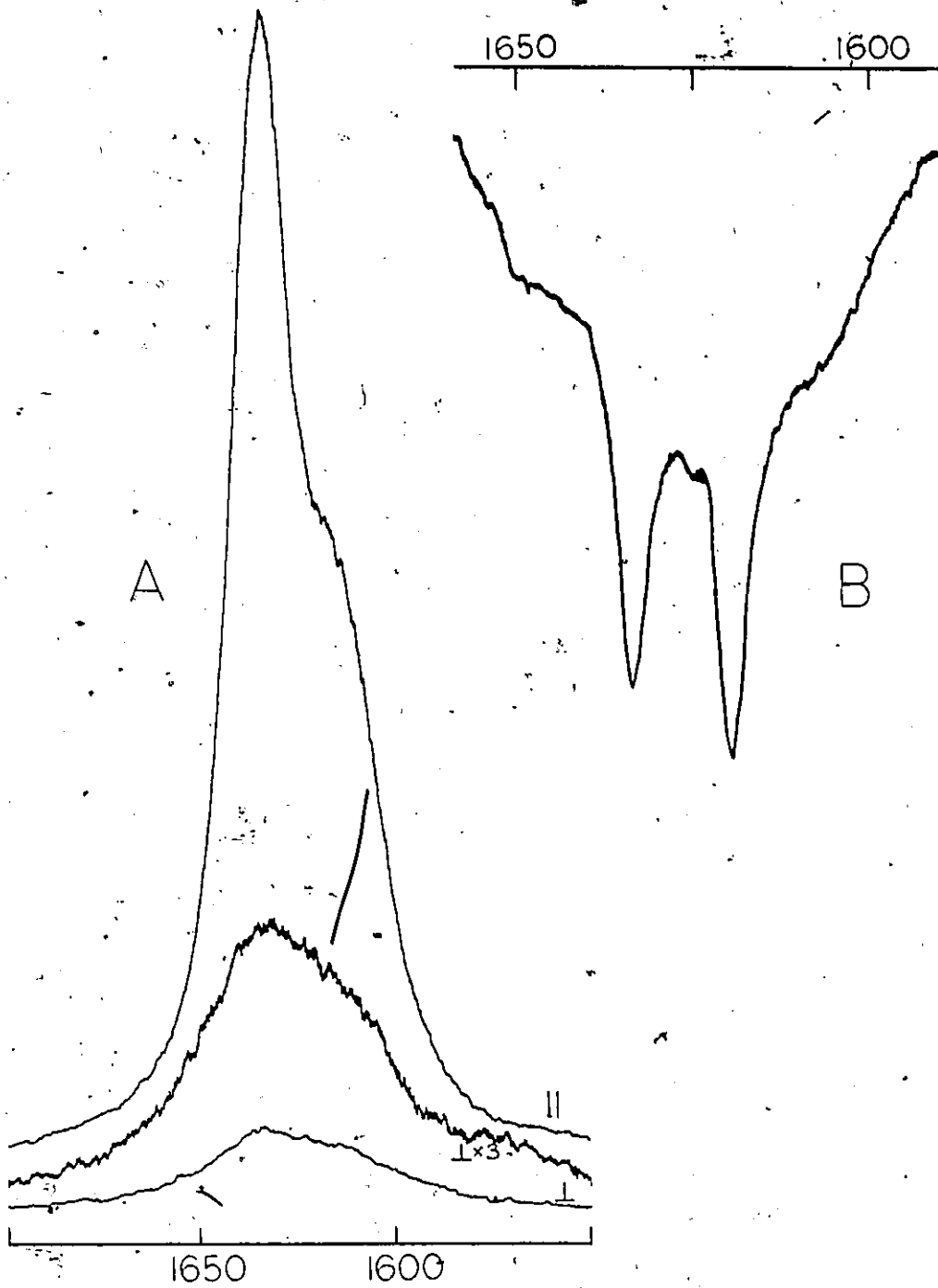
Figure I.4.6 Raman (A) and infrared (B) spectra of Si-D
stretching region in CH_3SiDF_2

were detected in ^{1}H or ^{19}F n.m.r. spectra except for $\sim$5%
$(CH_3SiDF)_2O$, which could not produce the band with such
intensity. The mass spectrum (at 70eV) showed no significant
peaks greater than the parent ion, and the other major peaks
could be attributed to CH_3SiDF_2 itself. The only plausible
alternative was Fermi resonance, since no other SiD stretch-
ing vibration is expected to be of such high frequency[79].
The fact that it appears only in the difluoride suggests
that a vibration involving a fluorine atom is involved, and
$\nu_7 + \nu_9$, the SiC and symmetric SiF_2 stretching mode respect-
ively, is found to be the combination band involved. The SiC
mode appears as a distorted A-type band at 733 cm^{-1}, while
ν_9 gives rise to a complicated contour, the strongest feat-
ure of which is at 897 cm^{-1}, for a sum of 1630 cm^{-1}. The
corresponding Raman sum is 1619 cm^{-1}, from the value of
733 cm^{-1} for ν_7 and 884 cm^{-1} for ν_9, although the latter is
less accurate due to its being weak and broad. The greater
difference in intensities in the Raman spectrum is presum-
ably because of a "lesser" coincidence, and so allows for
the stronger band at 1673 cm^{-1} to be designated as the "SiD
stretch", whereas the similarity of the intensities in the
infrared spectrum make such a tenuous distinction even more
so.

The asymmetric CH_3 deformations ν_4 and ν_{13} are generally
weak and featureless in both effects. The symmetric deform-
ations, ν_5, appear as medium bands in the infrared spectra
with A-type contours for the difluorides and B-types for the

other compounds, and as weak, polarised bands in the Raman spectra. In the CD_3- counterparts, the band shape changes to C and B/C types respectively. Whereas ν_4 and ν_{13} were mainly overlapped by ν_5 in the monohalo- derivatives, the distinction can be made for these molecules in all but the difluoride, but a comparison of the observed decreasing separations between ν_5 and ($\nu_{4,14}$) as the halogen becomes higher suggests that the two modes should be almost coincident in the difluoride. This is supported by the detection of only one band in the "deformation-overtone" region around 2000 cm^{-1} instead of the two due to $2\nu_5$ and $2\nu_{4,14}$ as observed in the monohalo- derivatives and the other three dihalo- analogues.

ii) Below 350 cm^{-1}

Three bands are expected in this region; ν_{10} and ν_{17}, the symmetric and asymmetric CSiX deformations, and ν_{11}, the SiX_2 scissoring mode. Since ν_{11} is the only vibration having an angle change involving both halogen atoms, it is expected to be the most sensitive to change in mass of halogen. Polarisation data fixes the assignment of ν_{17}, and ν_{11} is assigned to the lowest frequency in the diiodide on the basis of mass and intensity. However, this lowest band increases in wavenumber more than either ν_{10} and ν_{17} and is almost coincident with ν_{17} in the dichloride (and is in fact so for CD_3SiHCl_2). The polarisation data for the difluorides are inconclusive, but continuing with the trend of larger increase in wavenumber, and also decrease in intensity

relative to the CSiX deformations. ν_{11} is assigned to the highest band at ca. 340 cm^{-1} in these molecules. The assignment of this band to an a' mode is supported by the infrared spectrum of CD_3SiHF_2 recorded in the CsI region (> 200 cm^{-1}), which shows an A-type band at 333 cm^{-1} and an apparent B-type band at 274 cm^{-1}. (An absorption maximum was also observed at 203 cm^{-1}, but as this is at the limit of the instrument's range, it is not a reliable figure). If the band at 274 cm^{-1} is really an asymmetric mode, this conflicts with another trend in relative intensities, which has ν_{10} decreasing in intensity relative to ν_{17} as the halogen becomes lighter, the changeover from stronger to weaker coming at the dichloride. This assignment will be discussed later.

As with the monofluoro- compounds, additional weak bands are observed in the difluorides at about 200 cm^{-1}, on the low wavenumber side of the deformation envelope. The only explanation that can be offered is that they are the torsions. If the frequencies are expected to be intermediate between CH_3SiH_3 and CH_3SiF_3, then it appears that they are too high, in spite of displaying a reasonably consistent set, as shown in Table I.4.2.

Table I.4.2 Comparison of possible torsional modes (cm^{-1}) for fluoromethylsilanes

CH_3SiH_3	190[a] 208[b]	CH_3SiH_2F	225	CH_3SiHF_2	208	CH_3SiF_3	140[c] 156[d]
		CH_3SiD_2F	224	CH_3SiDF_2	206		
		CD_3SiH_2F	183	CD_3SiHF_2	183		

a) ref. 29 b) ref. 4 c) ref. 32 d) ref. 62

iii) <u>1000-350 cm^{-1}</u>

The Raman spectra of this region are shown in Figures I.4.7 - 10. The symmetric SiX$_2$ stretch, ν_9, is immediately apparent as a strong, polarised band at its characteristic position of about 310 cm^{-1} for Si-I, 375 for Si-Br and 500 cm^{-1} for Si-Cl. The asymmetric stretch appears as a medium/weak depolarised band about 65 cm^{-1} higher than ν_9. This difference is almost identical (± 3 cm^{-1}) for each of the diiodides and dibromides and CH$_3$SiHCl$_2$, but drops by up to 20 cm^{-1} in the other two dichlorides, presumably as the Si-Cl mode mixes with vibrations of deuterated groups in the same frequency range. The SiF$_2$ stretches are typically weak bands, with corresponding intense absorptions of mixed contours in the infrared spectra, overlapping in CH$_3$SiHF$_2$.

There remain five fundamentals to be determined; ν_7, the Si-C stretching vibration, and two each of methyl rocking and SiH(D) deformation modes. The patterns for each of the isotopic derivatives are quite similar on going from iodide to chloride, showing a gradual increaese in wavenumber for all bands. In the Raman spectra, the middle band of the five is the strongest and polarised. This might therefore be expected to be ν_7, since in the main stretching modes are more intense than bending modes. The band contours, where they can be made out, are of the appropriate type. For the CH$_3$- compounds, it seems reasonable that the two bands higher than ν_7 are the methyl rocks, and the two lower bands the SiH' bends, especially since these latter two decrease in

CH₃SiHF₂

CD₃SiHF₂

CH₃SiDF₂

800　　　600　　　400　　　200
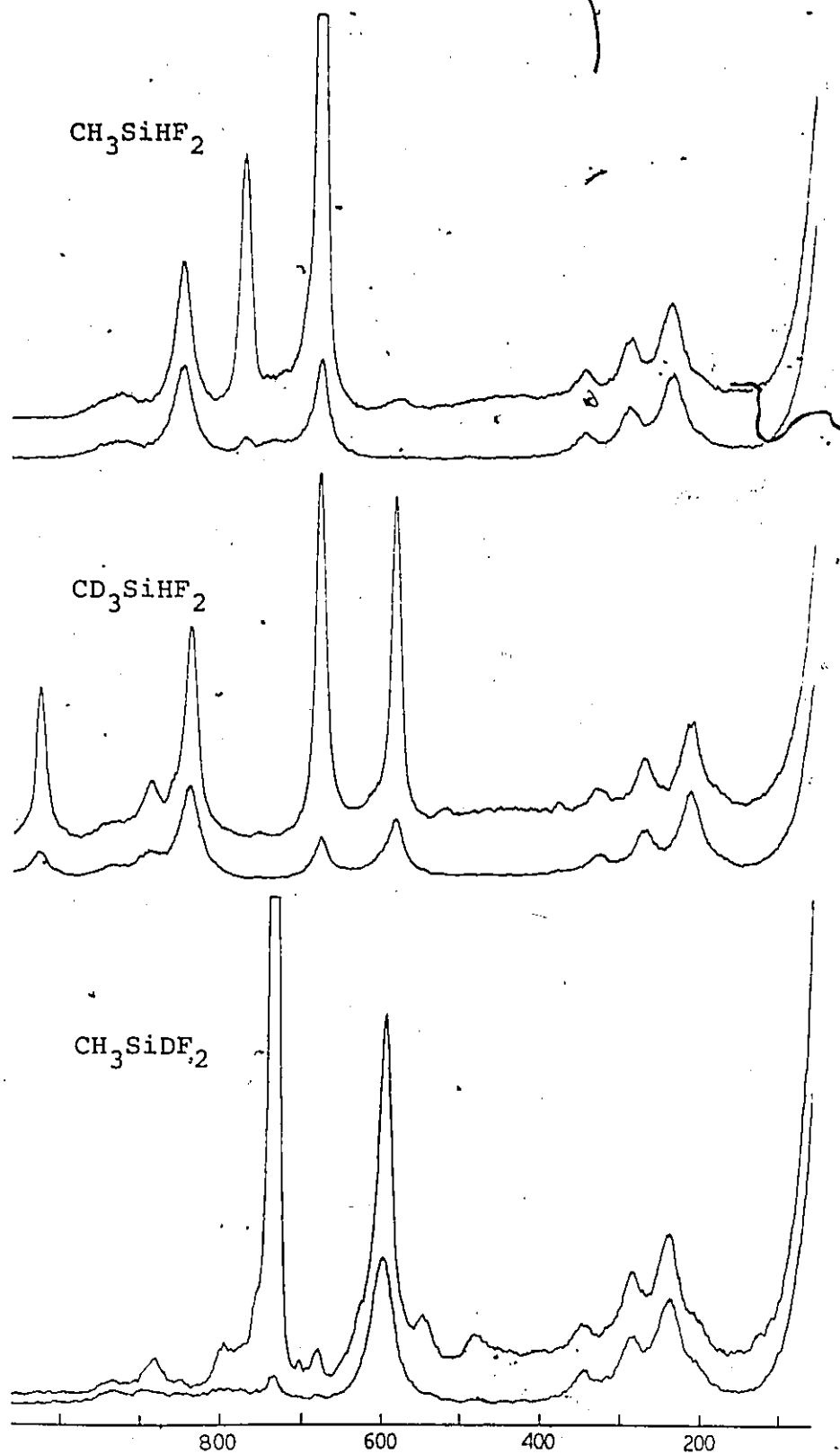
<u>Figure I.4.7</u> Partial Raman spectra of the
difluoromethylsilanes

CH$_3$SiHCl$_2$

CD$_3$SiHCl$_2$

CH$_3$SiDCl$_2$

900   700   500   300   100
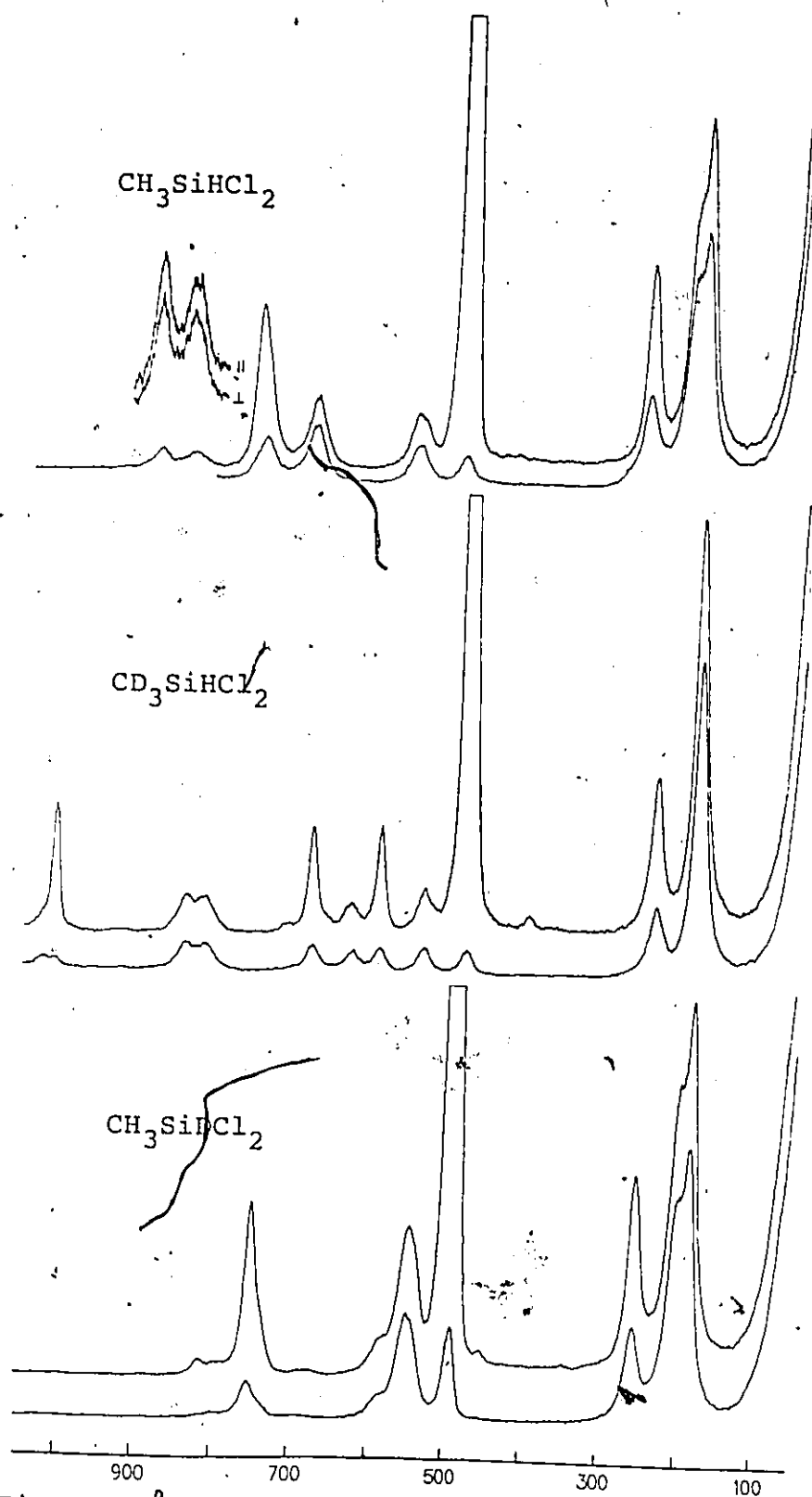
Figure I.4.8   Partial Raman spectra of the
dichloromethylsilanes

CH₃SiHBr₂

CD₃SiHBr₂

CH₃SiDBr₂

900   700   500   300   100
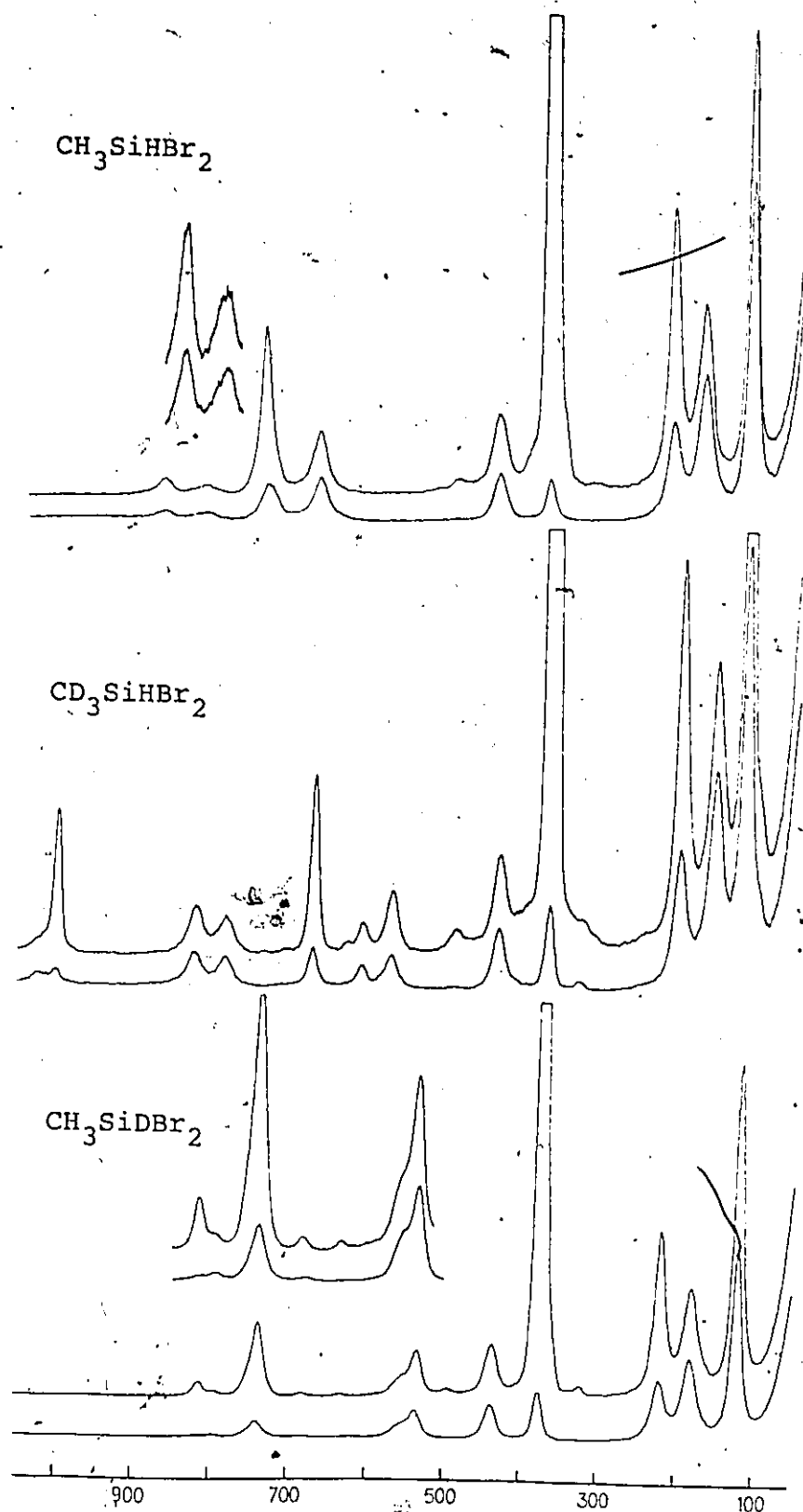
Figure I.4.9   Partial Raman spectra of the
dibromomethylsilanes
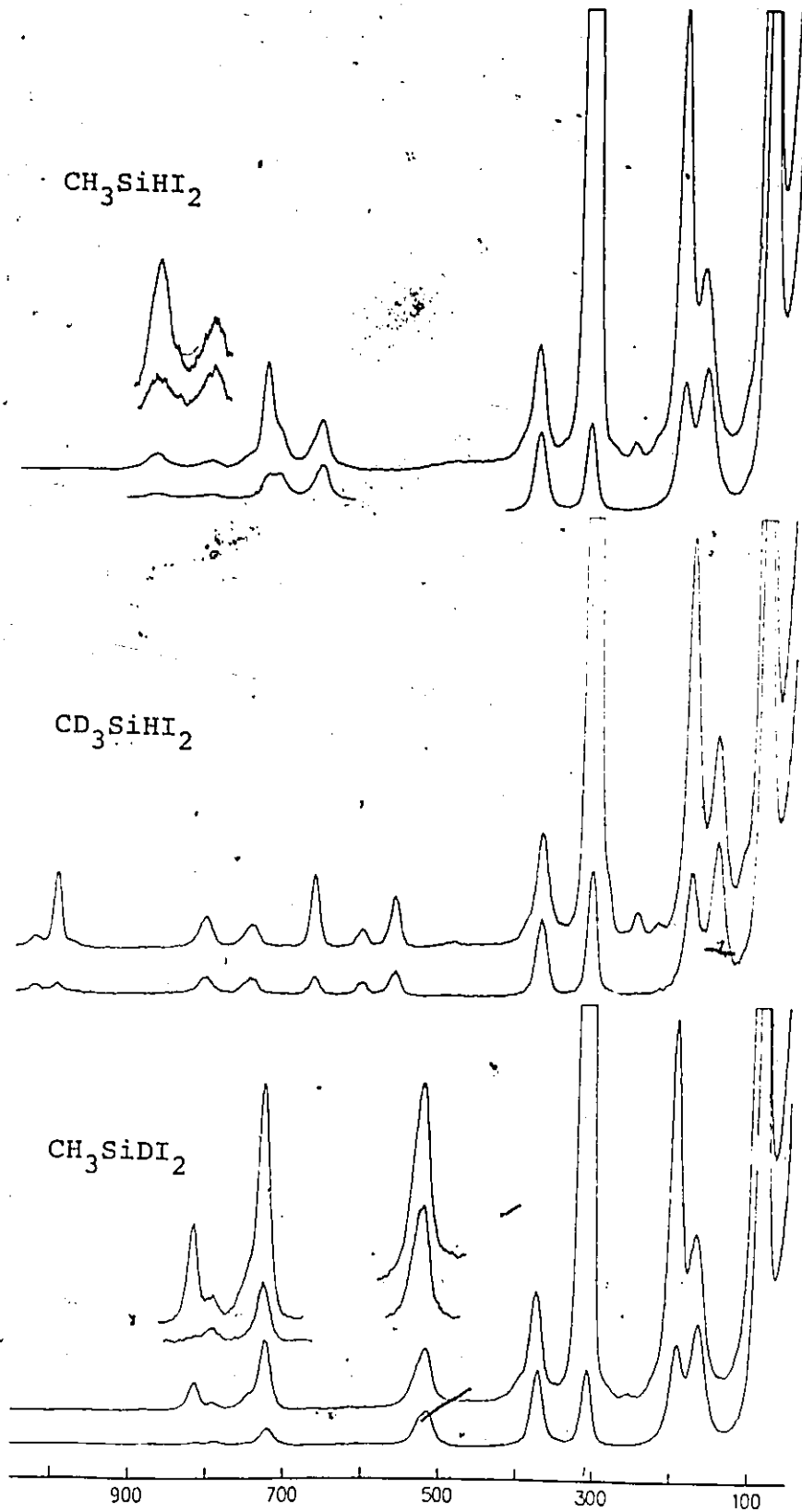
Figure I.4.10 Partial Raman spectra of the diiodomethylsilanes

wavenumber by about 150 cm^{-1} on deuteration at silicon. In the CD$_3$SiHX$_2$ molecules, this order is probably reversed, since keeping the methyl rocks higher implies almost no change in frequency for the four bending vibrations compared to the CH$_3$SiDX$_2$ species. The symmetric and asymmetric modes in each pair also change order. This argument applied to the difluoride is not so convincing, however, as the spectra are quite unlike those of the heavier halide derivatives.

I.4.2   Assignment and NCA

Of all the compounds reported in this study, the difluoromethylsilanes were the most difficult to assign. The problem was not only in matching the frequencies to fundamental modes but determining the frequencies themselves because of the lack of sufficient bands. Even allowing one's imagination a free rein could not produce the required number whereas in all but CD$_3$SiHCl$_2$ the seven fundamentals expected in the 1000-350 cm^{-1} region (Figures I.4.7-10) are observed as individual bands. Comparison of the two kinds of specta was helpful although the prediction of actual wavenumbers was not possible, as a continuation of trends present in the other three derivatives was not followed. However, some relative trends were found to be useful. For example, the observed splitting of the a' and a" methyl rocks in the CH$_3$SiHX$_2$ compounds decreases from the diiodide, where it is 74 cm^{-1}, to 49 cm^{-1} in the dibromide and 35 cm^{-1} in the dichloride. Thus it was thought not too unreasonable to assign both rocks to the same feature in the difluoride.

Eventually a list of possible candidates was drawn up from both spectra, which included at most two uncertain frequencies, and these values tested by application of the product rule. By again calculating all the possible ratios for the three compounds it was hoped to be able to determine in which compound the product was either too high or too low. Thus after a series of comparative calculations, a set of frequencies which produced the best fit to all three ratios, and was compatible with the observed spectra, was obtained. The most common decision thus arrived at involved assigning an uncertain mode as coincident with another band, or to a weaker feature nearby. The calculated and observed product rule ratios are listed in Table I.4.3, where again separate ratios have been calculated for infrared and Raman frequencies.

Most of the a" ratios involving CD_3SiHX_2 make use of two or even three estimated frequencies out of the six, and so not too much emphasis should be placed on these results. This series can be considered simpler than the previous one by virtue of having only two SiH bending modes, and the NCA reflects this with slightly better agreement, although by no means totally convincing for all the light compounds. The observed frequencies along with the preferred assignment, are listed in Table I.4.4-7. It appeared at first that these calculations would converge relatively easily, and in fact those for the diiodide and dibromide were found to do so. As is usual when a close agreement has been attained, all of the force constants were allowed to vary at the same time in

Table I.4.3 Calculated and observed product rule ratios for the dihalomethylsilanes

ratio	species	calc.	obs. i.r.	Obs. Ra
$\dfrac{CH_3SiDF_2}{CH_3SiHF_2}$	a'	0.517	0.532	0.527
	a"	0.728	0.733	0.737
$\dfrac{CD_3SiHF_2}{CH_3SiHF_2}$	a'	0.200	0.217	0.210
	a"	0.380	0.385	0.390
$\dfrac{CD_3SiHF_2}{CH_3SiDF_2}$	a'	0.387	0.408	0.399
	a"	0.522	0.526	0.529
$\dfrac{CH_3SiDCl_2}{CH_3SiHCl_2}$	a'	0.514	0.528	0.527
	a"	0.717	0.730	0.723*
$\dfrac{CD_3SiHCl_2}{CH_3SiHCl_2}$	a'	0.197	0.209	0.210
	a"	0.371	0.401	0.402
$\dfrac{CD_3SiHCl_2}{CH_3SiDCl_2}$	a'	0.383	0.395	0.399
	a"	0.517	0.549	0.556*
$\dfrac{CH_3SiDBr_2}{CH_3SiHBr_2}$	a'	0.511	0.535	0.531
	a"	0.712	0.713	0.717
$\dfrac{CD_3SiHBr_2}{CH_3SiHBr_2}$	a'	0.194	0.208	0.199
	a"	0.364	0.369	0.365
$\dfrac{CD_3SiHBr_2}{CH_3SiDBr_2}$	a'	0.380	0.390	0.374
	a"	0.510	0.518	0.509
$\dfrac{CH_3SiDI_2}{CH_3SiHI_2}$	a'	0.510	0.521	0.528
	a"	0.711	0.694	0.721
$\dfrac{CD_3SiHI_2}{CH_3SiHI_2}$	a'	0.193	0.196	0.198
	a"	0.360	0.366	0.361
$\dfrac{CD_3SiHI_2}{CH_3SiDI_2}$	a'	0.379	0.376	0.374
	a"	0.507	0.526	0.500

* half of the frequencies estimated

Table I.4.4 The vibrational spectra of the difluoromethylsilanes

CH$_3$SiHF$_2$		CH$_3$SiDF$_2$		CD$_3$SiHF$_2$		Assignment
i.r.(gas)	Ra (liq.)	i.r.(gas)	Ra (liq.)	i.r.(gas)	Ra (liq.)	
Γ 2997 / B 2987 C w / L 2983	2989 mw dp	Γ 2993 / B 2987 C w / L 2979	2988 mw dp	–	2235 s p	ν_1, ν_{12}
2919 vw	2922 vs p	2923 vw	2920 vs p	2138 vvw	2136 vs p	ν_2
	2802 w p / 2530 vw p		2844 w p		2026 vw p	$2\delta_{Me}$
A{ 2246 / 2232 s / 2217 }	2236 vs p			A{ 2244 / 2238 Q vs / 2230 Q / 2219 }	2235 s p	$\nu_3+\nu_9$ / $\nu_7+\nu_9$ FR†
1700 vvw / 2188 vw	2184 wsh	C 1634 s / C 1619 s	1633 s p / 1613 msh p		1036 vw	$\nu_7+\nu_9$ / $\nu_5+\nu_9$
B{ 1410 C w / 1397 }	1403 vw dp	C{ 1419 w / 1414 } B	1419 w dp	–		ν_4 / ν_{13}
A{ 1284 / 1273 m / 1267 }	1267 w p	A{ 1285 / 1274 s / 1267 }	1273 w p	A/C 1032 vs	1030 m p	ν_5
~960 vs	–	949 vs	931 vw dp?	B{ 959 / 951 } vs	940 vw dp?	ν_{16}
932 vs	931 vw p	901 vs	883 w p	A/C{ 913 / 904 vs / 895 }	891 w p	ν_9
A?{ 870 / 858 mw / 847 }	853 w p?	A{ 807 / 795 m / 784	800 w p	598 / 585 s / 572	588 s p	ν_6
		775 wsh }	774 vw			ν_{14}

Table I.4.4. (continued)

CH$_3$SiHF$_2$		CH$_3$SiDF$_2$		CD$_3$SiHF$_2$		Assignment
i.r.(gas)	Ra (liq.)	i.r.(gas)	Ra (liq.)	i.r.(gas)	Ra (liq.)	
A$\begin{cases}785\\773 \text{ s}\\766\end{cases}$	775 mw p	A$\begin{cases}745\\733 \text{ s}\\723\end{cases}$	734 vs p	A/C$\begin{cases}690\\679\\669\end{cases}$	681 s p	ν_7
734 wsh	734 vw dp?		679 w p			2ν_{11}
687		602.s	~612 ? sh	852 msh	864 wsh dp?	ν_{15}
A$\begin{cases}675 \text{ w}\\668\end{cases}$	683 w p		596 m p	840	843 m p	ν_8
	578 vw p		544 w p			$\nu_{11}+\nu_{17}$
			479 vw p?			2ν_{10} / 2ν_{17}
	350 vw dp?		345 mw dp?	A$\begin{cases}344\\333 \text{ m}\\322\end{cases}$	335 mw dp?	ν_{11}
	293 w dp?		287 mw dp?	B?$\begin{cases}280\\266\end{cases}$	275 mw dp?	ν_{10}
	243 w dp?		242 w dp?		218 w dp?	ν_{17}
	208 wsh dp?		206 vw dp?		184 vwsh	ν_{18}?

† Fermi resonance; see text

215

Table I.4.5   The vibrational spectra of the dichloromethylsilanes

CH$_3$SiHCl$_2$ i.r.(gas)	CH$_3$SiHCl$_2$ Ra (liq.)	CH$_3$SiDCl$_2$ i.r.(gas)	CH$_3$SiDCl$_2$ Ra (liq.)	CD$_3$SiHCl$_2$ i.r.(gas)	CD$_3$SiHCl$_2$ Ra (liq.)	Assignment
C{2992 w, A{2986 w, 2981	2986 mw dp	2990 w, 2983 w	2984 m dp	~2239 sh	~2235 msh dp	ν_1, ν_{12}
2923 vw	2916 s p	2920 vw	2915 s p	2133 vw	2130 s p	ν_2
	2781 vw p		2820 w p		2044 vw, 1955.5 w p	2ν_4, 2ν_5
2216 vs	2220 vs p	C 1615 s	1618 s p	C 2218 s	2222 s p	ν_3
2026 vw, 1777 vw		2017 vw		1688 w, 1174 w, 1637 w	1620 vw	$\nu_5{+}\nu_7$, 2ν_6, $\nu_5{+}\nu_{14}$
C{1411 w, A{1403 w, 1397	1404 w dp	1420 w, 1415 w	1416 w dp	-	1027 wsh dp	ν_4, ν_{13}
B{1273 ms, 1265	1265 w p	B{1272 ms, 1264	1265 w p	1016 ms	1010 m p	ν_5
B{892 vs, 885	887 w dp?	820 wsh	816 w	595 ms	593 m p	ν_6
A{860, 853 vs, 846	842 w dp?	A{808, 800 vs, 795	~784 w	634 s	631 w dp	ν_{14}
759 s	759 m p	B{755 s, 748 w	753 m p	B{682 ms, 673	681 m p	ν_7
~744 wsh	~747 wsh dp?	B{599 vs, 594	~585 wsh dp?	823 vs	818 w dp	ν_{15}

Table I.4.5   (continued)

CH₃SiHCl₂		CH₃SiDCl₂		CD₃SiHCl₂		Assign-
i.r.(gas)	Ra (liq.)	i.r.(gas)	Ra (liq.)	i.r.(gas)	Ra (liq.)	ment
683 vw	688 mw dp	A { 560, 548 m, 539	$\sim$547 m dp	845 vs	844 w dp?	ν_8
569 vs	556 mw dp			544 s	535, w dp	ν_{16}
504 ms	493 vs p	501 m	492 vs p	487 ms	481 vs p	ν_9
	430 vw p		452 vw p		400 w p	$\nu_{10}+\nu_{17}$
			426 vw p			$\nu_{10}+\nu_{11}$
	257 m p		256 m p		238 m p	ν_{10}
	199 mssh		199 ms			ν_{17}
	187 ms p?		186 ms		185 ms	ν_{11}

Table I.4.6   The vibrational spectra of the dibromomethylsilanes

	CH_3SiHBr_2		CH_3SiDBr_2		CD_3SiHBr_2		Assignment
	i.r.(gas)	Ra (liq.)	i.r.(gas)	Ra (liq.)	i.r.(gas)	Ra (liq.)	
	2985 mw	2982 mw dp	2984 mw	2982 mw dp	2239 vwsh	2228 msh dp	ν_1, ν_{12}
	2920 vw	2910 s p	2919 vw	2910 s p	2131 vvw	2123 s p	ν_2
		2784 vw p	2812 vw	2797 w p		2041 vw p	$2\nu_4$
		2498 vw p				1979 w p	$2\nu_5$
	C 2212 s	2211 s p	1609 s	1611 s p	2210 s	2208 s p	ν_3
	2082 vw				1615 vw	1609 vw	$\nu_5+\nu_{14}$
	2011 vw		2000 vw		1675 vw		$\nu_5+\nu_7$
	1484 vw		1469 vw				$2\nu_7$
	1422 mw	1419 vw dp	1414 mw	1409 w dp	—	1023 wsh dp	ν_{13}
	1401 mw	1398 vw dp					ν_4
	B{1267 / 1262} m	1260 w p	1265 m	1259 w p	B{1010 / 1004} m	1000 m p	ν_5
	880 s	874 vw p	B{820 / 813} s	814 w p	588 w	572 mw p	ν_6
			682 vw	684 w p	903 vw		$\nu_{11}+\nu_{15}$
	B{838 / 825} vs	822 vw dp	A{800 / 796 / 791} vs	785 vw dp?	615 m	610 w dp	ν_{14}
	B{750 / 742} s	746 m p	B{742 / 735} s	739 m p	B{676 / 670} m	672 m p	ν_7
		~738 wsh dp	563 vs	~560 msh dp?	B{797 / 791} vs	783 w dp	ν_{15}
	674 w	678 mw p?	540 msh	537 m p?	B{833 / 826} s	825 w p?	ν_8

Table I.4.6   (continued)

CH₃SiHBr₂		CH₃SiDBr₂		CD₃SiHBr₂		Assignment
i.r.(gas)	Ra (liq.)	i.r.(gas)	Ra (liq.)	i.r.(gas)	Ra (liq.)	
540 w				523 vw		$\nu_9+\nu_{17}$
496 vw	498 vw p		498 vw p		489 w p	$\nu_9+\nu_{11}$
457 vs	446 mw dp	444 vs	439 m dp	445 s	434 mw dp	ν_{16}
	427 vwsh p		416 vw p		399 vwsh p	$2\nu_{10}$
387 mw*	380 vs p	383 mw*	376 vs p	380 mw*	370 vs p	ν_9
	~305 vw p		300 vw p			$\nu_{11}+\nu_{17}$
	222 ms p		222 ms p		203 ms p	ν_{10}
	181 m dp		182 m dp		159 ms dp	ν_{17}
	122 s p?		123 s dp?		121 s p	ν_{11}

* in KBr absorption

Table I.4.7   The vibrational spectra of the diiodomethylsilanes

CH$_3$SiHI$_2$		CH$_3$SiDI$_2$		CD$_3$SiHI$_2$		Assignment
i.r.(gas)	Ra(liq.)	i.r.(gas)	Ra(liq.)	i.r.(gas)	Ra(liq.)	
2983 w	2977 mw dp	2979 w	2975 mw dp	−	2225 m dp	ν_1, ν_{12}
2915 vw	2902 ms p	2920 vw	2903 ms p	2126 vvw	2115 ms p	$2\nu_2$
	2773 vw p		2787 vw p		2033 vw p	$2\nu_{4,13}$
2196 s	2190 ms p	1598 ms	1596 ms p	2196 ms	2188 ms p	ν_3
1407 w	1400 vw dp	1409 w	1402 vw dp	1024 vw	1020 vw dp	ν_{13}
1385 vw		1402 w		B{1004 m, 998 m	992 m p	ν_4
1262 m	1253 vw p	1262 m	1255 w p	−	561 m p	ν_5
884 s	872 vw p	B{820 ms, 814	814 w p	608 m	602 w dp	ν_6
810 vs	803 vw dp	793 vs	792 mw dp	665 m	662 m p	ν_{14}
~731 s	729 m p	B{727 ms, 723	725 mw p	B{760 vs, 756	744 w dp?	ν_7
~720 s	717 wsh dp	535 vs	~532 wsh dp			ν_{15}
668 vw	660 w dp	~523 mwsh	520 mw p	B{816 ms, 810	803 w p	ν_8
408 vw	403 vw p		399 vw p		393 vw p	$\nu_9 + \nu_{11}$
394 ms	382 m dp	383 m	376 m dp	383 mw	371 m dp	ν_{16}
~320*	316 vs p	~315*	312 vs p	~308*	308 vs p	ν_9
	283 vw p		285 vw p		251 vw p	$\nu_{10} + \nu_{11}$
	258 vw p		256 vw p		224 vw p	$\nu_{11} + \nu_{17}$
	196 ms p		196 ms p		180 ms p	ν_{10}
	170 m dp		170 m dp		149 m dp	ν_{17}
	89 s p		89 s p		88 s p	ν_{11}

* in KBr absorption

order to achieve the best possible fit. In the case of the
diiodide, some of the f-c's. varied markedly, then eventually
settled down and converged to a final result. While the
frequency agreement was found to be as good as with the
previous refinement, the force constant values were in some
cases quite different, as can be seen from Table I.4.8,
where the values from the other compounds are included.
Such behaviour lessens the benefits of comparison with other
members of the series if the analyses are not performed in
a completely similar manner. The p.e.d.'s produced by these
force constant values are listed in Tables I.4.9-13. It can
be seen that, compared to the monohalo- derivatives, the
frequencies in the "heavy" compounds are well reproduced with
an acceptable confirmation of the approximate description of
all the modes. For the light homologues, however, the mixing
between the methyl rocking and SiH bending force constants is
extensive, the a' CH_3 rock designated so only because of all
the modes with contributions from these force constants, that
frequency has the highest proportion of methyl rocking con-
tribution, even though it is only about 40%, and less than
the total of $\underline{f}CSiH$ and $\underline{f}HSiX$, which together define the a'
SiH bend. In CH_3SiHF_2 the agreement is even poorer, even
though in the deuterated molecules the agreement is not only
good for the ordering of the frequencies, but the numerical
agreement averages less the 8 cm^{-1}. While this may be
thought to be indicative of a "true" assignment for CH_3SiHF_2,
the assignments thus proposed are difficult to reconcile with

Table I.4.8 Force constant values for MeSiHX$_2$

No.	Description	F	Cl	Br	I(1)	I(2)
1	CH	480.71	481.38	479.30	478.13	478.09
2	SiH	289.87	285.42	283.45	276.60	276.58
3	SiC	325.00	310.73	297.51	290.24	291.59
4	SiX	527.51	283.30	197.85	170.49	142.29
5	HCH	51.18	51.73	46.80	46.90	47.17
6	HCSi	35.97	37.03	41.10	34.67	34.81
7	HCSi	50.66	56.57	53.22	54.25	53.72
8	CSiH	69.72	69.08	54.56	41.10	42.06
9	HSiX	65.74	53.30	50.94	70.67	63.17
10	CSiX	60.18	75.39	79.17	62.04	80.04
11	XSiX	89.19	73.56	80.20	83.25	74.59
12	CH/CH	5.54	6.78	6.58	5.90	5.94
13	SiX/SiX	33.58	25.30	11.88	-4.62	13.53
14	HCH/HCH	-1.39	-0.21	-4.74	-4.24	-3.99
15	HCSi /HCSi	6.62	9.26	10.51	11.18	11.24
16	HSiX/HSiX	6.61	-0.51	0.66	24.87	18.38
17	CSiX/CSiX	2.19	13.63	10.11	2.79	2.79
18	SiC/HCSi	24.65	14.97	13.93	25.50	26.79
19	SiC/CSiH	9.88	22.79	2.94	6.10	4.83
20	SiX/HSiX	10.72	16.73	14.10	13.86	7.71
21	SiX/CSiX	–	–	-1.30	25.77	5.39
22	t-HCSi/CSiH	3.59	7.17	-17.05	7.19	6.41
23	c-HCSi/CSiH	8.62	-8.30	2.87	-13.91	-13.84
24	CSiH/HSiX	6.51	5.77	1.01	2.43	0.65
25	HCSi /HSiX	5.38	-7.32	3.46	2.50	2.26
26	t-HCSi/SiX	–	4.06	–	–	–
27	SiC/SiX	20.00*	–	–	–	–

*fixed

Units: N.m^{-1} for stretching constants, N.m.rad^{-2} for bending force constants

Table I.4.9 Calculated frequencies and p.e.d. for MeSiHF$_2$

ν	mode	obs.	calc.	p.e.d.
1	CH$_3$ str(a)	2989	2989	101(1)
2	CH$_3$ str(s)	2922	2921	98(1)
3	SiH str	2236	2251	100(2)
4	CH$_3$ def(a)	1422	1421	93(5)
5	CH$_3$ def(s)	1267	1280	50(5)+39(7)
6	CH$_3$ rock	853	703	29(6)+15(7) {44}+34(3)+17(8) {25}
7	SiC str	775	757	49(3)+19(6)+11(7) {30}+12(9) {19}
8	SiH def	683	940	39(8)+13(9) {52}+23(4)+18(6)+10(3)
9	SiX$_2$ str	932	852	58(4)+12(8) {20}
10	SiX$_2$ wag	293	296	52(10)+24(11)
11	SiX$_2$ sc	350	344	58(11)+18(9)+10(8)
12	CH$_3$ str(a)	2989	2988	101(1)
13	CH$_3$ def(a)	1422	1421	94(5)
14	CH$_3$ rock	853	768	91(7)+29(8)−12(15)
15	SiH def	734	841	54(9)+38(4)+R {7}
16	SiX$_2$ str	963	971	65(4)+29(9)+13(7)
17	SiX$_2$ twist	243	242	101(10)

ν	mode	obs.	calc.	p.e.d.
1	CH$_3$ str(a)	2988	2989	101(1)
2	CH$_3$ str(s)	2920	2921	98(1)
3	SiD str	1635	1624	99(2)
4	CH$_3$ def(a)	1419	1421	93(5)
5	CH$_3$ def(s)	1273	1271	52(5)+40(7)
6	CH$_3$ rock	800	800	47(6)+13(7) {60}+13(4)+D {5}
7	SiC str	734	737	74(3)+14(4)
8	SiD def	596	586	61(8)+35(9) {96}−13(24)+11(6,7) {22} −11(23)
9	SiX$_2$ str	897	898	62(4)+16(3)+11(6)
10	SiX$_2$ wag	287	295	52(10)+23(11)
11	SiX$_2$ sc	345	343	60(11)+18(9)+10(8)
12	CH$_3$ str(a)	2988	2988	101(1)
13	CH$_3$ def(a)	1419	1421	94(5)
14	CH$_3$ rock	774	790	90(7)−12(15)+18(4)+D {1}
15	SiD def	612	608	106(9)−11(16)+R {8}
16	SiX$_2$ str	949	951	86(4)+13(7)
17	SiX$_2$ twist	242	242	101(10)

ν	mode	obs.	calc.	p.e.d.
1	CD$_3$ str(a)	2235	2228	99(1)
2	CD$_3$ str(s)	2136	2101	97(1)
3	SiH str	2235	2251	99(3)
4	CD$_3$ def(a)	1030	1028	90(5)
5	CD$_3$ def(s)	1030	1020	36(5)+25(7)+17(8)
6	CD$_3$ rock	588	570	56(6)+27(7) {83}+11(9) {16}
7	SiC str	683	684	60(3)+12(18)
8	SiH def	843	832	30(8)+21(9) {51}+40(4)+R {6}
9	SiX$_2$ str	904	905	43(4)+29(3)+20(8)+13(5)−13(18)
10	SiX$_2$ wag	275	283	52(10)+15(11)+10(9)
11	SiX$_2$ sc	335	338	67(11)+14(9)
12	CD$_3$ str(a)	2235	2227	100(1)
13	CD$_3$ def(a)	1030	1028	94(5)
14	CD$_3$ rock	600	592	108(7)−14(15)+D {8}
15	SiH def	864	835	77(9)+26(4)+R {0}
16	SiX$_2$ str	955	958	76(4)+30(9)
17	SiX$_2$ twist	218	226	99(10)

Table I.4.10 Calculated frequencies and p.e.d. for MeSiHCl$_2$

ν	mode	obs.	calc.	p.e.d.
1	CH$_3$ str(a)	2986	2987	101(1)
2	CH$_3$ str(s)	2916	2931	97(1)
3	SiH str	2220	2233	100(2)
4	CH$_3$ def(a)	1404	1421	88(5)+10(7)
5	CH$_3$ def(s)	1265	1348	54(5)+33(7)
6	CH$_3$ rock	888	890	36(6){43}+36(8){45}+10(22)
7	SiC str	746	752	83(3)
8	SiH def	688	703	58(8)+28(9){86}+32(6)+12(7){44}
9	SiX$_2$ str	504	516	73(4) −18(24)−12(22)−10(23)
10	SiX$_2$ wag	257	256	51(10)+22(9)
11	SiX$_2$ sc	187	186	78(11)
12	CH$_3$ str(a)	2986	2987	101(1)
13	CH$_3$ def(a)	1404	1414	96(5)
14	CH$_3$ rock	853	864	67(7)+28(9)+12(21)−11(15)
15	SiH def	759	766	75(9)+48(7)−16(21)
16	SiX$_2$ str	569	576	102(4)
17	SiX$_2$ twist	199	201	114(10)−21(17)

ν	mode	obs.	calc.	p.e.d.
1	CH$_3$ str(a)	2984	2987	101(1)
2	CH$_3$ str(s)	2915	2931	97(1)
3	SiD str	1618	1610	99(2)
4	CH$_3$ def(a)	1416	1420	88(5)+10(7)
5	CH$_3$ def(s)	1265	1347	54(5)+33(7)
6	CH$_3$ rock	818	842	57(6)+15(7){72}+D{9}
7	SiC str	752	748	86(3)
8	SiD def	547	552	75(8)+21(9){96}−18(24)+11(6){17}
9	SiX$_2$ str	501	502	58(4)+16(9)+13(8) +16(4)
10	SiX$_2$ wag	256	255	52(10)+22(9)
11	SiX$_2$ sc	186	185	78(11)
12	CH$_3$ str(a)	2984	2987	101(1)
13	CH$_3$ def(a)	1416	1414	96(5)
14	CH$_3$ rock	800	835	110(7)−18(15)+D{1}
15	SiD def	596	609	55(9)+63(4)−16(20)+R{1}
16	SiX$_2$ str	547	538	42(4)+47(9)+12(20)
17	SiX$_2$ twist	199	201	114(10)−21(17)

ν	mode	obs.	calc.	p.e.d.
1	CD$_3$ str(a)	2235	2227	92(1)
2	CD$_3$ str(s)	2130	2110	96(1)
3	SiH str	2235	2233	92(2)
4	CD$_3$ def(a)	1027	1020	96(5)
5	CD$_3$ def(s)	1010	1071	40(5)+38(7)+18(3)−11(18)
6	CD$_3$ rock	594	590	52(6)+14(7){66}+17(9)+15(8){32}
7	SiC str	678	697	64(3)+11(4)
8	SiH def	845	815	76(8)+23(9){99}+R{9}
9	SiX$_2$ str	487	501	66(4)
10	SiX$_2$ wag	238	240	48(10)+21(9)
11	SiX$_2$ sc	185	185	78(11)
12	CD$_3$ str(a)	2222	2226	100(1)
13	CD$_3$ def(a)	1027	1022	97(5)
14	CD$_3$ rock	634	640	84(7)+32(4)−14(15)+D{7}
15	SiH def	823	807	95(9)+R{2}
16	SiX$_2$ str	544	554	74(4)+31(7)
17	SiX$_2$ twist	185	184	112(10)−20(17)

Table I.4.11 Calculated frequencies and p.e.d. for MeSiHBr$_2$

ν	Mode	obs.	calc.	p.e.d.
1	CH$_3$ str(a)	2982	2980	101(1)
2	CH$_3$ str(s)	2910	2923	97(1)
3	SiH str	2211	2225	100(2)
4	CH$_3$ def(a)	1411	1416	85(5)
5	CH$_3$ def(s)	1260	1262	49(5)+42(7)
6	CH$_3$ rock	880	882	26(6)+10(7){36}+24(8)+14(9){38}
7	SiC str	746	751	62(3)+24(6)−13(22)+14(8).\+18(22)
8	SiH def	678	680	41(8)+13(9){54}+31(6){34}+27(3)
9	SiX$_2$ str	380	380	66(4)+11(11) −26(22)
10	SiX$_2$ wag	222	220	60(10)+16(9)+10(4)
11	SiX$_2$ sc	122	122	74(11)+16(4)
12	CH$_3$ str(a)	2982	2981	101(1)
13	CH$_3$ def(a)	1411	1407	88(5)
14	CH$_3$ rock	831	828	67(7)+37(9)−13(15)
15	SiH def	738	743	67(9)+51(7)−10(15)
16	SiX$_2$ str	446	448	91(4)+14(10)
17	SiX$_2$ twist	181	180	98(10)+15(4)−13(17)
1	CH$_3$ str(a)	2982	2980	101(1)
2	CH$_3$ str(s)	2910	2923	97(1)
3	SiD str	1611	1603	100(2)
4	CH$_3$ def(a)	1409	1415	85(5)
5	CH$_3$ def(s)	1259	1260	49(5)+43(7)
6	CH$_3$ rock	816	820	63(6)+17(7){80}+D{3}
7	SiC str	739	741	87(3)
8	SiD def	537	540	75(8)+26(9){101}−24(22)+15(6){16}
9	SiX$_2$ str	376	373	65(3)+11(11)
10	SiX$_2$ wag	222	219	60(10)+16(9)+10(4)
11	SiX$_2$ sc	123	122	74(11)+16(4)
12	CH$_3$ str(a)	2982	2981	101(1)
13	CH$_3$ def(a)	1409	1407	88(5)
14	CH$_3$ rock	796	802	112(7)−22(15)+D{2}
15	SiD def	563	560	98(9)+R{7}
16	SiX$_2$ str	439	437	83(4)+13(10)
17	SiX$_2$ twist	182	180	98(10)+15(4)−13(17)
1	CD$_3$ str(a)	2208	2220	96(1)
2	CD$_3$ str(s)	2123	2103	96(1)
3	SiH str	2228	2225	96(2)
4	CD$_3$ def(a)	1023	1025	83(5)
5	CD$_3$ def(s)	1000	998	44(5)+34(7)+21(3)−12(18)
6	CD$_3$ rock	572	567	76(6)+10(7){86}−31(22)+24(8){28}
7	SiC str	672	665	60(3)+15(7)
8	SiH def	825	818	53(8)+27(9){80}+10(3)+R{2}
9	SiX$_2$ str	370	374	65(4)+11(11)
10	SiX$_2$ wag	203	207	58(10)+16(9)+10(4)
11	SiX$_2$ sc	121	122	74(11)+16(4)
12	CD$_3$ str(a)	2228	2221	100(1)
13	CD$_3$ def(a)	1023	1018	88(5)
14	CD$_3$ rock	610	604	103(7)−20(15)+D{6}
15	SiH def	783	785	97(9)+R{4}
16	SiX$_2$ str	434	433	87(4)+14(7)
17	SiX$_2$ twist	159	162	99(10)+13(4)−13(17)

Table I.4.12 Calculated frequencies and p.e.d. for $MeSiHI_2(1)$

ν	mode	obs.	calc.	p.e.d.
1	CH_3 str(a)	2977	2979	101(1)
2	CH_3 str(s)	2902	2915	97(1)
3	SiH str	2190	2197	100(2)
4	CH_3 def(a)	1400	1406	86(5)
5	CH_3 def(s)	1253	1260	46(5)+42(7)
6	CH_3 rock	884	881	37(6){37}+24(8)+13(9){37}+16(5)
7	SiC str	731	731	76(3) +10(22)
8	SiH def	660	659	26(8)+24(9){50}+29(6)+14(7){43}
9	SiX_2 str	316	318	77(4)+24(10) +16(3)-16(23)
10	SiX_2 wag	196	195	59(10)+16(4)+15(8)
11	SiX_2 sc	89	89	69(11)+18(4)
12	CH_3 str(a)	2977	2979	101(1)
13	CH_3 def(a)	1400	1402	89(5)
14	CH_3 rock	810	808	96(7)-20(15)+22(9)
15	SiH def	720	720	120(9)-35(16)+24(7)
16	SiX_2 str	382	385	77(4)+24(10)
17	SiX_2 twist	170	168	77(10)+33(4)

ν	mode	obs.	calc.	p.e.d.
1	CH_3 str(a)	2975	2980	101(1)
2	CH_3 str(s)	2903	2915	97(1)
3	SiD str	1596	1583	100(2)
4	CH_3 def(a)	1402	1405	86(5)
5	CH_3 def(s)	1255	1248	49(5)+45(7)
6	CH_3 rock	817	819	62(6){68}+14(5)+D{8}
7	SiC str	725	724	96(3)
8	SiD def	521	521	48(8)+40(9){88}-20(23)+12(6,7){24}
9	SiX_2 str	312	314	57(4)+13(11) +12(16)
10	SiX_2 wag	196	194	59(10)+16(8)+15(4)
11	SiX_2 sc	89	89	69(11)+18(4)
12	CH_3 str(a)	2975	2979	101(1)
13	CH_3 def(a)	1402	1402	89(5)
14	CH_3 rock	793	797	116(7)-24(15)+D{2}
15	SiD def	534	535	134(9)-38(16)+R{4}
16	SiX_2 str	376	373	71(4)+23(10)
17	SiX_2 twist	170	168	77(10)+34(4)

ν	mode	obs.	calc.	p.e.d.
1	CD_3 str(a)	2225	2221	99(1)
2	CD_3 str(s)	2115	2096	97(1)
3	SiH str	2188	2197	100(2)
4	CD_3 def(a)	1020	1014	90(5)
5	CD_3 def(s)	992	992	45(5)+26(7)+12(23)
6	CD_3 rock	561	561	56(6)+21(7){76}+17(9){26}-11(23)
7	SiC str	662	662	63(3)+15(18)
8	SiH def	803	805	32(8)+23(9){55}+32(3)+20(5)-20(18)
9	SiX_2 str	308	308	58(4)+13(11)+10(8)+12(6){20}-13(23)
10	SiX_2 wag	180	181	59(10)+16(8)+13(4)
11	SiX_2 sc	88	89	69(11)+18(4)
12	CD_3 str(a)	2225	2220	100(1)
13	CD_3 def(a)	1020	1018	76(5)+12(7)
14	CD_3 rock	602	600	108(7)-23(18)+10(9)
15	SiH def	744	743	132(9)-38(16)+R{5}
16	SiX_2 str	374	371	79(4)+18(10)
17	SiX_2 twist	149	152	80(10)+29(4)

Table I.4.13 Calculated frequencies and p.e.d. for $MeSiHI_2(2)$

ν	mode	obs.	calc.	p.e.d.
1	CH_3 str(a)	2977	2979	101(1)
2	CH_3 str(s)	2902	2915	97(1)
3	SiH str	2190	2197	100(2)
4	CH_3 def(a)	1400	1406	85(5)
5	CH_3 def(s)	1253	1260	46(5)+43(7)
6	CH_3 rock	884	881	37(6)+23(8)+15(9) {38}+16(5)+11(22)
7	SiC str	731	730	79(3)
8	SiH def	660	660	28(9)+25(8) {53}+31(6)+16(7) {48}+18(3)
9	SiX_2 str	316	316	74(4)+16(11)+10(8) −17(23)−11(22)
10	SiX_2 wag	196	196	51(10)+27(8)
11	SiX_2 sc	89	89	70(11)+28(4)+10(10)
12	CH_3 str(a)	2977	2979	101(1)
13	CH_3 def(a)	1400	1402	88(5)
14	CH_3 rock	810	808	97(7)+23(9)−20(15)
15	SiH def	720	724	134(9)−47(16)+23(7)
16	SiX_2 str	382	382	105(4)−18(21)+13(10)
17	SiX_2 def	170	169	98(10)
1	CH_3 str(a)	2975	2979	101(1)
2	CH_3 str(s)	2903	2915	97(1)
3	SiD str	1596	1583	100(2)
4	CH_3 def(a)	1402	1405	86(5)
5	CH_3 def(s)	1255	1248	49(5)+46(7)
6	CH_3 rock	817	819	62(6) {68}+14(5)+D{8}
7	SiC str	725	725	95(3)
8	SiD def	521	521	47(9)+45(8) {92}+12(6,7) {24}−19(23)
9	SiX_2 str	312	313	100(4)−17(21)+12(10) +16(16)
10	SiX_2 wag	196	195	51(10)+29(8)−10(23)
11	SiX_2 sc	89	89	70(11)+27(4)+10(10)
12	CH_3 str(a)	2975	2979	101(1)
13	CH_3 def(a)	1402	1402	88(5)
14	CH_3 rock	793	798	117(7)−24(15)+D{2}
15	SiD def	534	531	156(9)−55(16)+R{3}
16	SiX_2 str	376	374	100(4)−17(21)+12(10)
17	SiX_2 def	170	169	98(10)
1	CD_3 str(a)	2225	2221	99(1)
2	CD_3 str(s)	2115	2096	97(1)
3	SiH str	2188	2197	100(2)
4	CD_3 def(a)	1020	1014	89(5)
5	CD_3 def(s)	992	992	48(5)+25(7)+11(23)
6	CD_3 rock	561	561	57(6)+21(7) {78}+19(9) {27}−11(23)
7	SiC str	662	663	62(3)+14(18)
8	SiH def	803	805	31(8)+26(9) {57}+32(3)+12(6) {19}
9	SiX_2 str	308	308	73(4)+16(11)+10(8) −18(18)−13(23)
10	SiX_2 wag	180	181	49(10)+29(8)−10(23)
11	SiX_2 sc	88	89	70(11)+27(4)+11(10)
12	CD_3 str(a)	2225	2220	100(1)
13	CD_3 def(a)	1020	1019	72(5)+13(7)
14	CD_3 rock	602	598	113(7)−23(15)+D{8}
15	SiH def	744	745	150(9)−53(16)+R{4}
16	SiX_2 str	374	376	103(4)−16(21)+10(10)
17	SiX_2 def	149	151	98(10)

trends in the other analogues and the deuterated homologues.
(Also one asymmetric mode is matched to an a' frequency and
vice-versa).

I.4.3   Discussion

The only complete study reported for any of these
compounds is for the dichloride, by Durig and Hawley[66]. An
early report on the diiodide[67] listed five infrared frequen-
cies and assigned the "SiH bend" to an absorption at 887 cm^{-1}.
There have been no previous reports for the difluoride and
dibromide. The spectra reported for the dichloride[66] are in
excellent agreement with those recorded in this work, and the
assignments similar. The differences are in the ordering of
the two SiH bends, and the skeletal deformation modes.
Polarisation data for the former two bands are not conclusive,
a point noted in the other study, where it was even suggested
that the order may in fact be reversed. The fact that it is
in the assignment proposed here is from more definite polar-
isation data collected from the other analogues, and from the
NCA, where, again, polarisation and band contour data are
more distinctive. This ordering is also that observed in
the analogous germanium compounds[80], where once more polar-
isation data supports this ordering more convincingly.
Because of the lower range of frequencies for these modes in
the germanium compounds, the GeH bends were not found to be
mixed with the methyl rocking modes and so a comparison of
frequencies is not too meaningful. Suffice it to note that
they are 50-70 cm^{-1} lower in these compounds except for the

difluoride, where extensive mixing with the GeF force constant was observed.

A less satisfactory comparison was used by Durig and Hawley[66] for the ordering of the deformation modes. Analogy with CH_3CHCl_2[81] led to placing the $SiCl_2$ scissoring mode at the highest wavenumber and the a' CSiCl bend to the lowest (the middle band is the most depolarised, and is assigned as the a" CSiCl mode). The benefit of having the whole series to compare again is seen, as the lowest band can be seen to correspond to the lowest band in the dibromide and diiodide, which in these heavier compounds is without doubt the XSiX mode.

Such comparisons are not so clear in the difluoride, where the polarisation data is of little diagnostic use. The best use that can be made of the frequency data is to note that in the other three analogues, the SiX_2 deformation is the one least affected by deuteration, whereas the two CSiX modes understandably decrease significantly with deuteration at carbon. Thus the bands at ca. 340 cm^{-1} might be expected to be the SiF_2 scissors mode. This is supported by the spectrum of the fluoromethylsilanes from the previous chapter, where the single CSiF mode appears at ca. 260 for the CH_3-derivatives and at 241 cm^{-1} for the CD_3- compounds; almost exactly midway between the two remaining frequencies. The choice as shown in Table I.4.4 is arrived at from the observation from the other three analogues that the separation between the two CSiX modes increases (both in absolute

and relative terms) with lighter halogen, and thus the order
is likely to be maintained rather than reversed in the
difluoride. This is supported by the force constant values,
where $\underline{f}$CSiF/CSiF has a positive value, as does the similar
interaction in the other compounds, and in CH_3SiF_3.

Comparison of force constant values results in a good
agreement with the monofluoro- compound for $\underline{f}$CSiF (60.2 versus
59.2 N.m.rad^{-2} for CH_3SiH_2F) and an amazing agreement for both
$\underline{f}$CSiF and $\underline{f}$FSiF with CH_3SiF_3 (60.2 and 89.2 as against 60.7
and 89.6 N.m.rad^{-2} respectively)! This is of course highly
fortuitous, since the agreement between Tables I.2.6 and
I.4.8 for the other halogen derivatives is not nearly as good.

CHAPTER I.5

HALODIMETHYLSILANES

I.5.1 Preparation

In general, the methods used for the halogenation of dimethylsilane were the same as described previously for the monomethylsilanes. The protonated species were also prepared by a facile synthetic route starting with tetramethyldisilazane.

i) Dimethylsilanes

The dimethylsilanes Me_2SiH_2 and Me_2SiD_2 were prepared by the reduction of Me_2SiHCl and Me_2SiCl_2 by the lithium tetrahydroaluminates $LiAlH_4$ and $LiAlD_4$, respectively, in dibutyl ether in a similar manner to that described for the methylsilanes (Chapter I.1). They were separated from unreacted and partially reduced starting material by passage of the volatile products through a trap at $-95^{\circ}C$ which retained any chloromethylsilanes and allowed for collection of dimethylsilane in a $-196^{\circ}C$ following trap. Purity was checked by ^1H n.m.r., infrared[30] and Raman spectroscopy, for the detection of unreacted Si-Cl.

ii) Halogenation reactions

For the halogenation of Me_2SiD_2, the more efficient reactions used for the monomethyl derivatives were applied. For the iodo- and bromo- species, this was the reaction of the parent silane with HX (X = I, Br) in the presence of AlX_3 catalyst under fairly severe reaction conditions (viz. $0^{\circ}C$ for 1 hour, and $-78^{\circ}C$ for 1 hour, respectively) in order to reduce the proportion of dihalogen substitution. The volatile products from the HI(HBr) reaction were passed

through traps at -45(-63)°C, -78(-95)°C into a trap at -196°C;
the first trapped any dihalogen species, the second the
desired product, excess HX passing into the following trap.
Salt exchange reaction of the iodo- or bromo- species so
formed with $HgCl_2$ and SbF_3 afforded the chloro- and fluoro-
derivatives.

The fully protonated homologues Me_2SiHX (X = I, Br)
were also made by the cleavage of $(Me_2SiH)_2NH$ with excess
HX, in a clean and facile reaction[75] which has the advant-
age of producing only the monohalogenated species and an
involatile co-product.

$$(Me_2SiH)_2NH + 3HX \longrightarrow 2Me_2SiHX + NH_4X$$
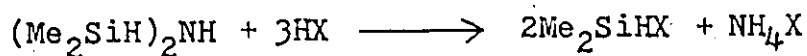
Excess HI(HBr) was recovered by passing the volatile products
through a trap at -78(-95)°C which retained the silane
compound.

I.5.2 Vibrational Spectra

The numbering and description of the modes are shown in
Table I.5.1, and the Raman and infrared spectra shown in
Figures I.5.1 - 11. These include some liquid infrared
spectra of the less volatile compounds which were recorded
with the hope of resolving the envelope containing the
methyl rocking bands. For the chloride, bromide and iodide,
the expected band contours are A and/or C for the a' modes,
and B for the a" modes. Me_2SiHF is almost a symmetric top
and although A type bands are predicted for a' modes, the
band shapes will probably be hybrids.

$(CH_3)_2SiHF$

$(CH_3)_2SiDF$
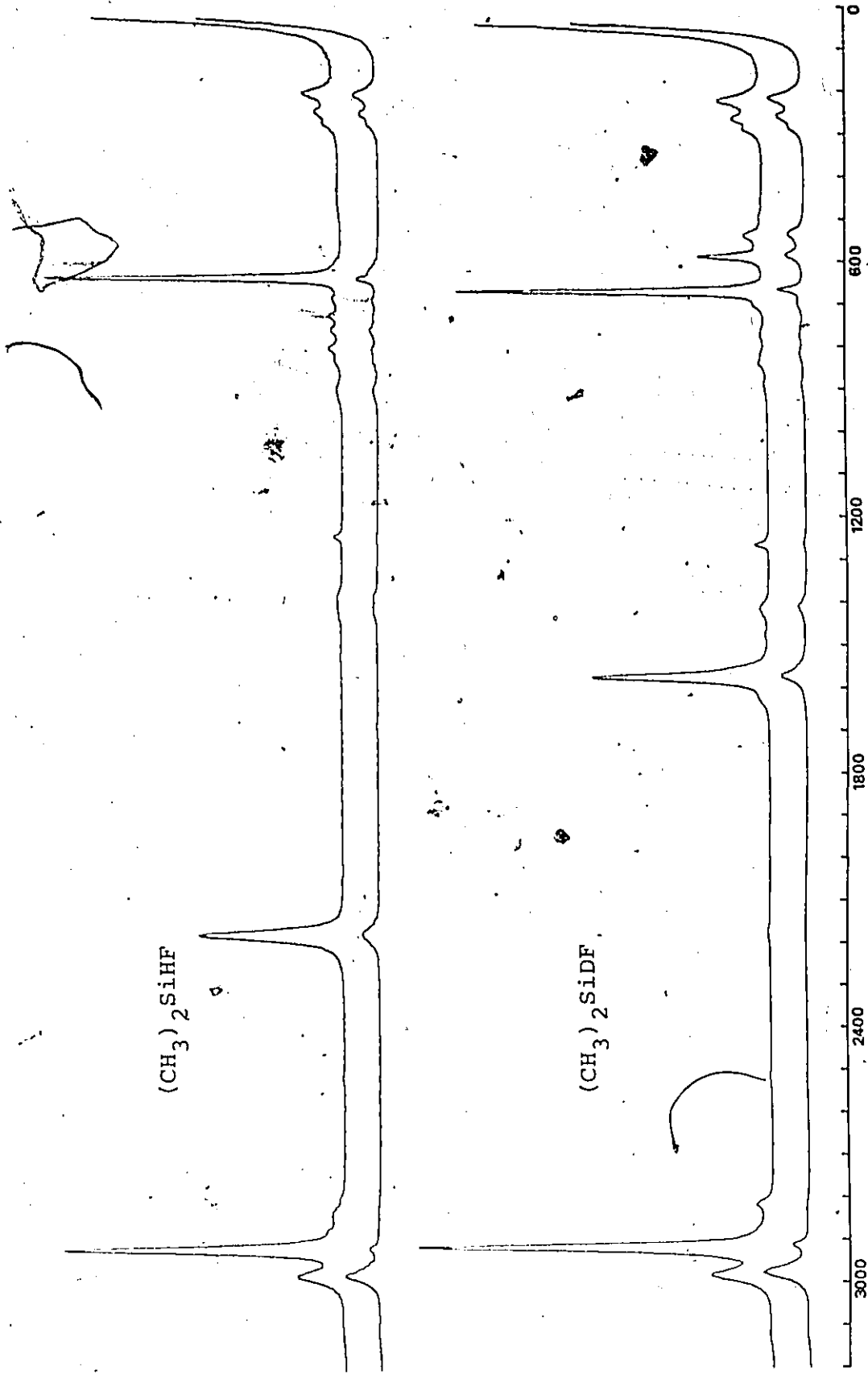
Figure I.5.1   Raman spectra of the fluorodimethylsilanes

(CH$_3$)$_2$SiHCl.

(CH$_3$)$_2$SiDCl
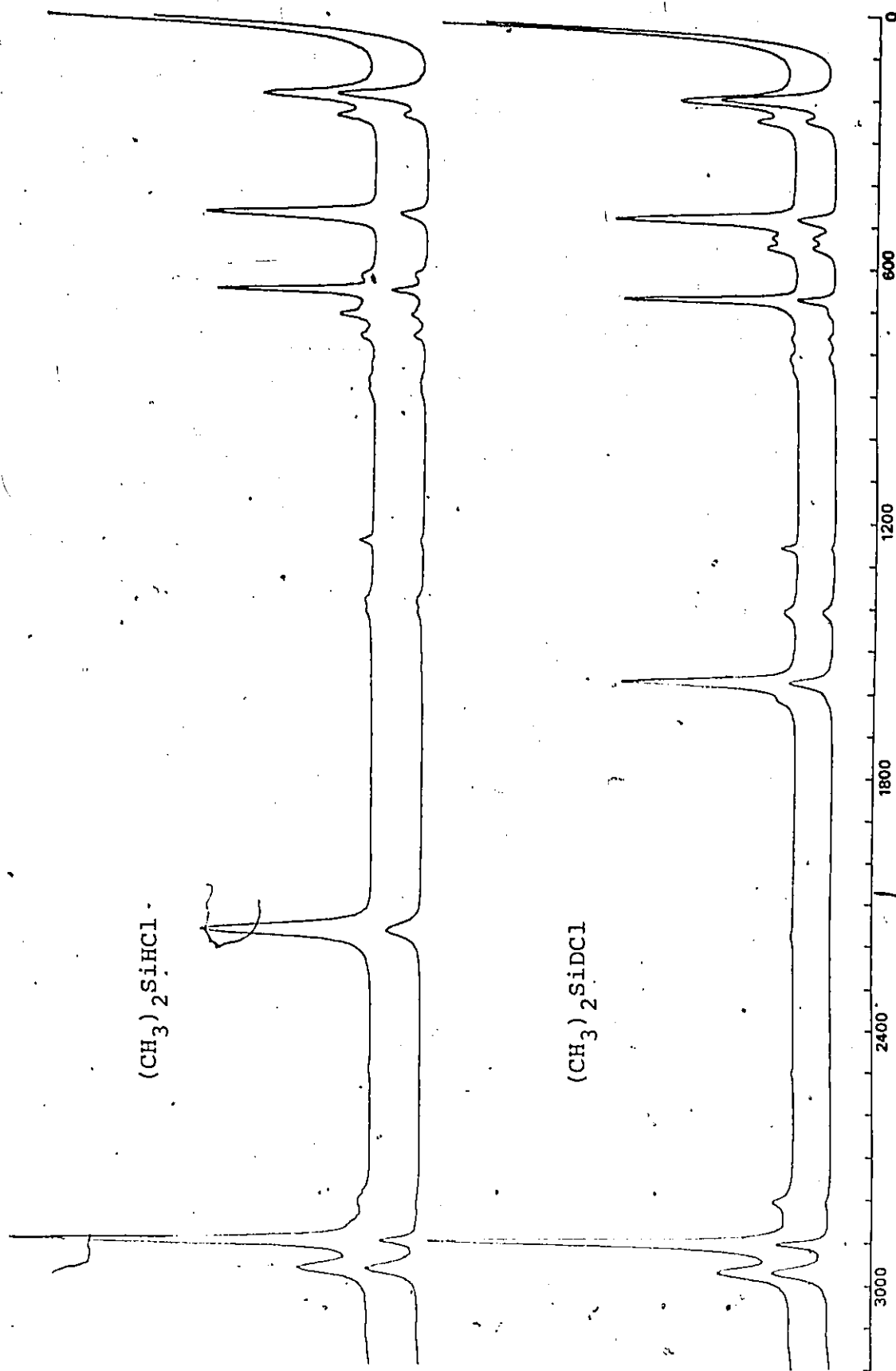
Figure I.5.2   Raman spectra of the chlorodimethylsilanes

$(CH_3)_2SiHBr$

$(CH_3)_2SiDBr$
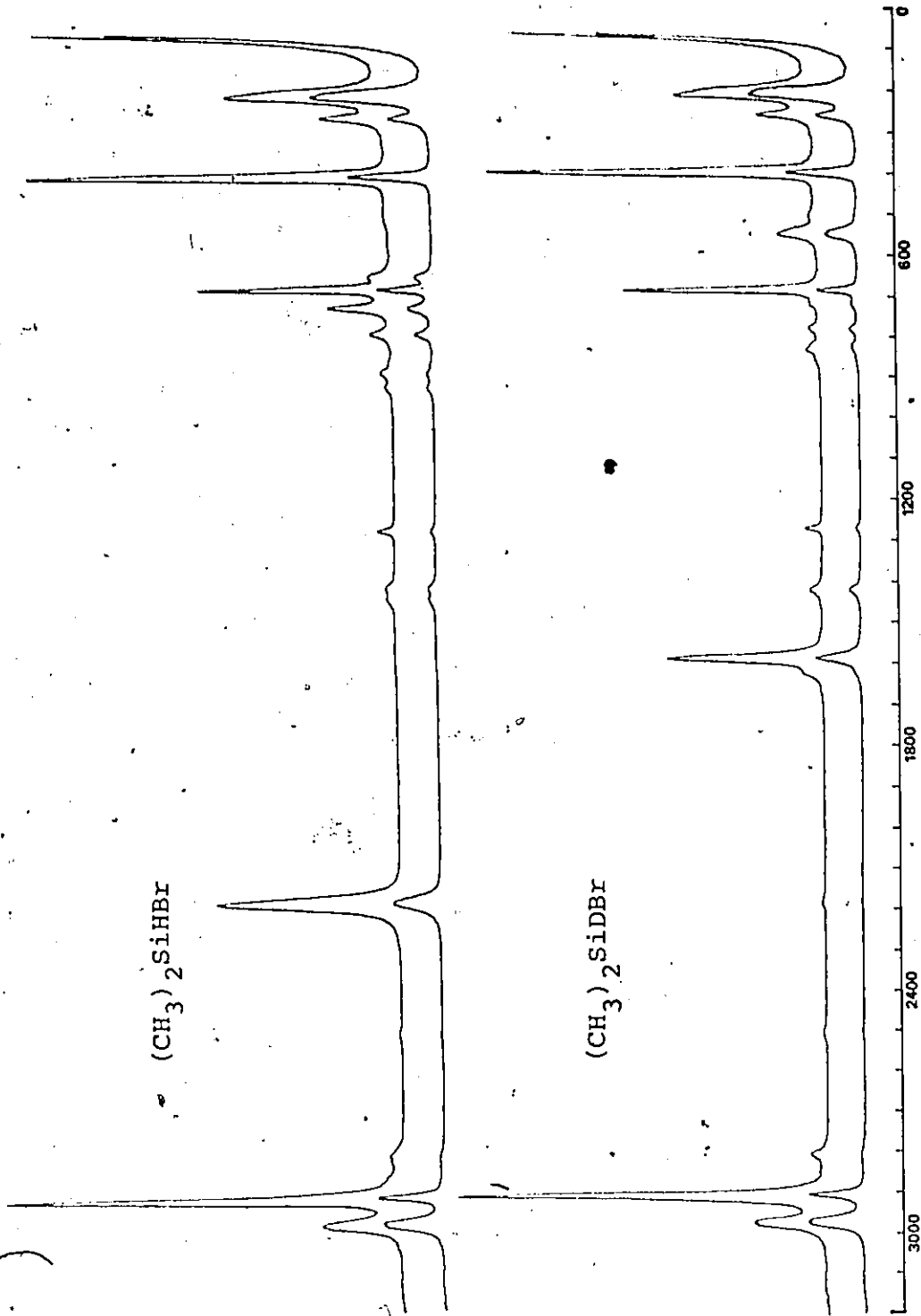
Figure I.5.3   Raman spectra of the bromodimethylsilanes
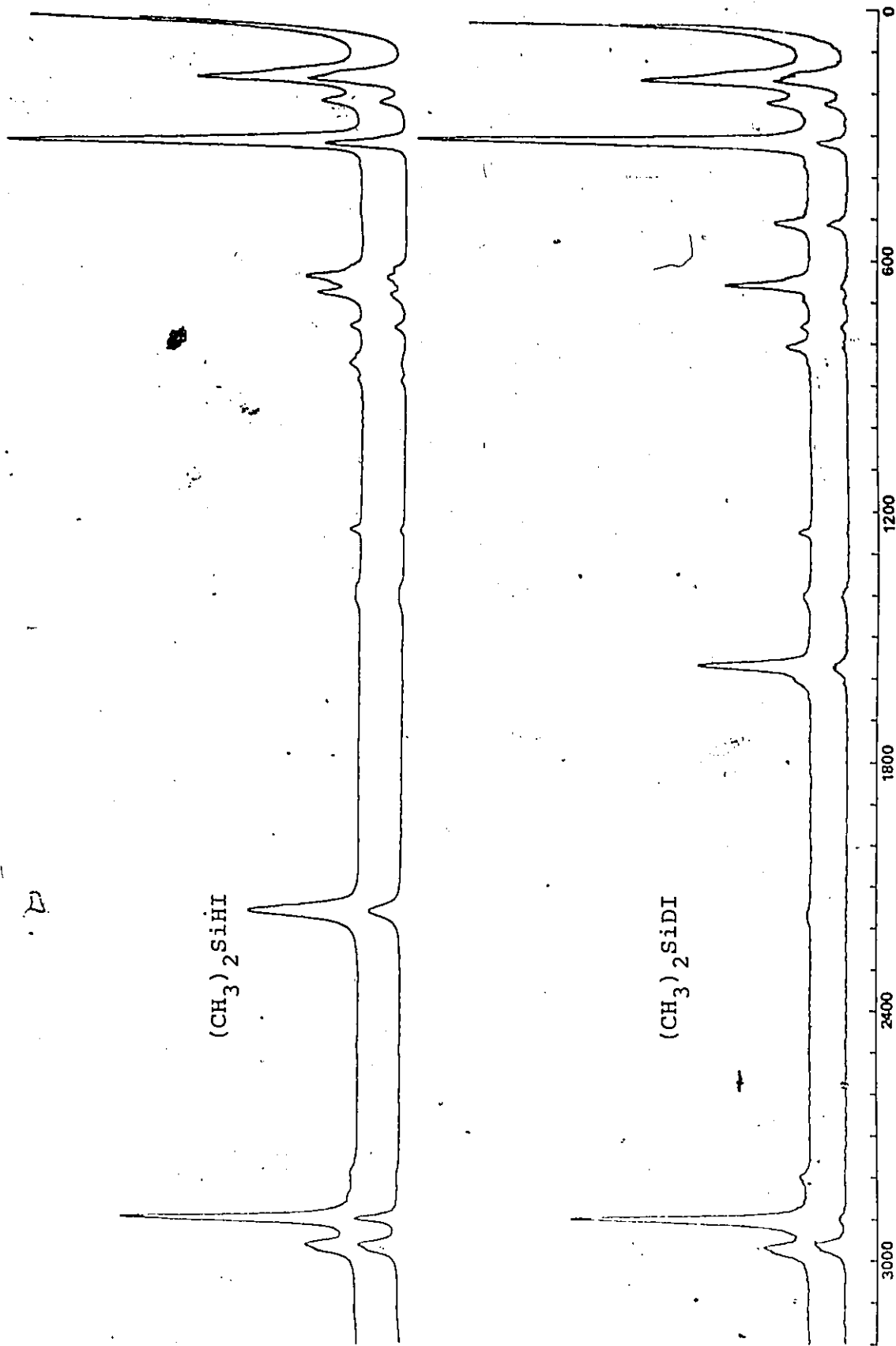
Figure I.5.4   Raman spectra of the iododimethylsilanes

$(CH_3)_2SiHI$

$(CH_3)_2SiDI$

$(CH_3)_2SiHF$

$(CH_3)_2SiDF$
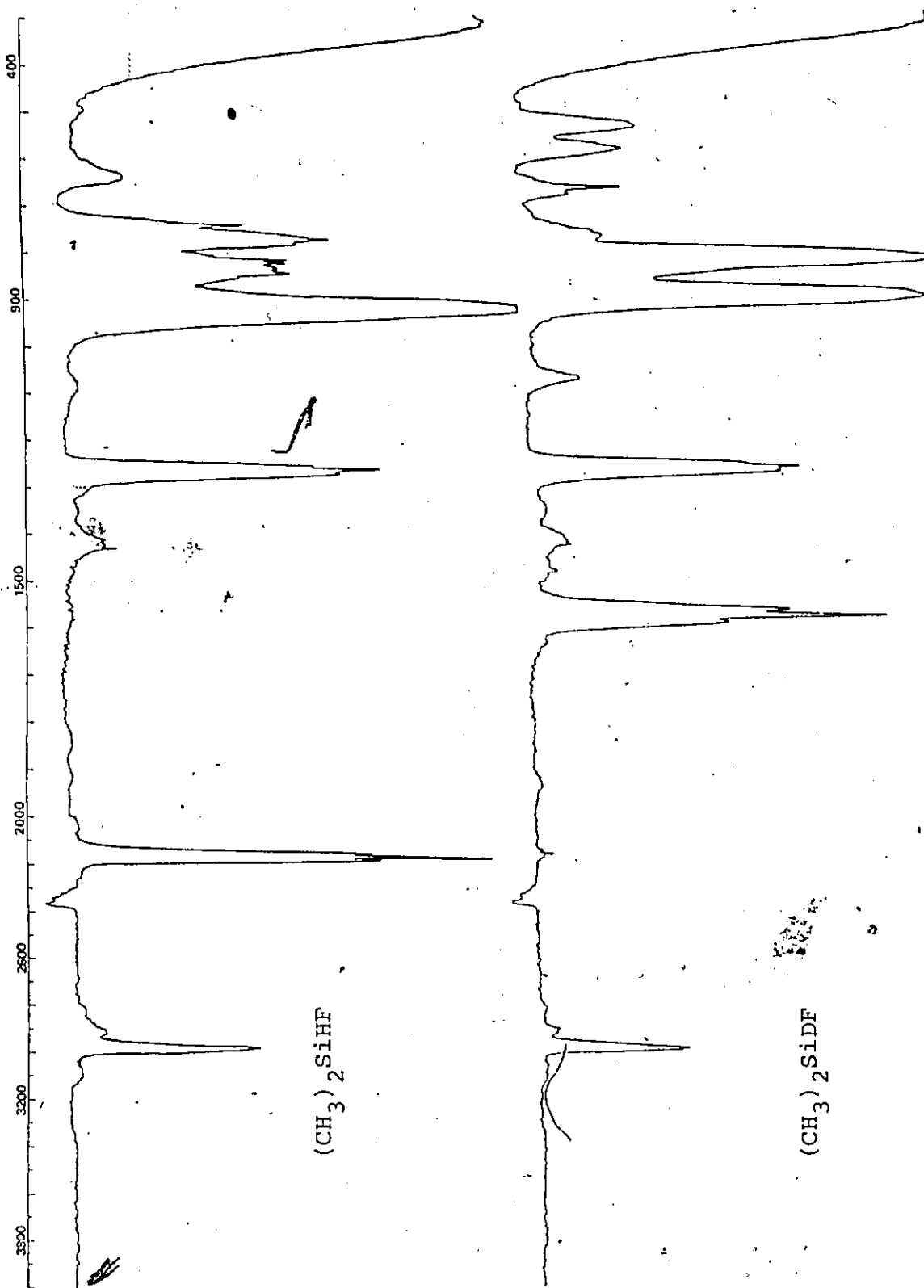
Figure I.5.5   Gas infrared spectra of the fluorodimethylsilanes

(CH$_3$)$_2$SiHCl

(CH$_3$)$_2$SiDCl
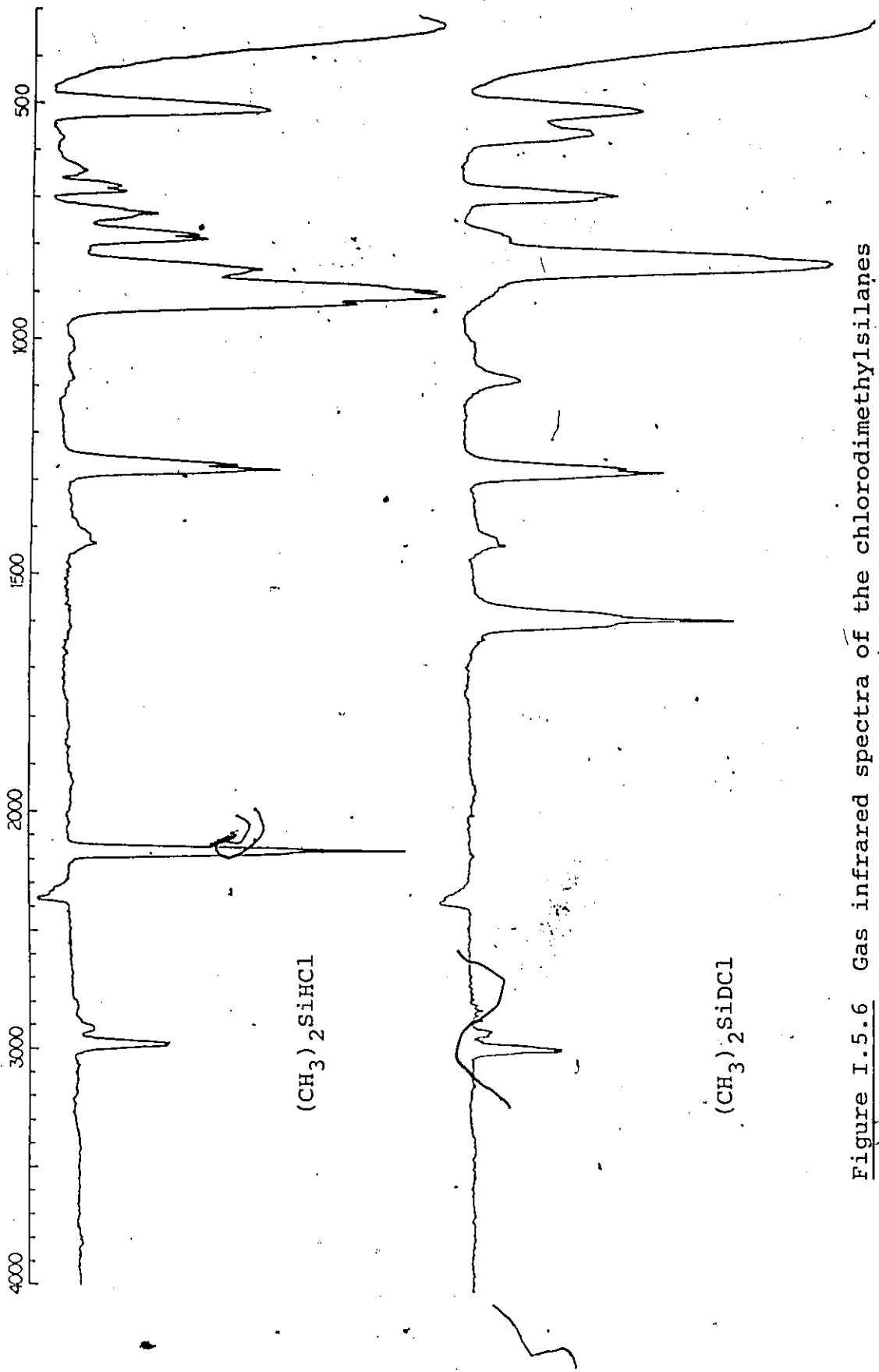
Figure I.5.6   Gas infrared spectra of the chlorodimethylsilanes

(CH$_3$)$_2$SiHBr

(CH$_3$)$_2$SiDBr
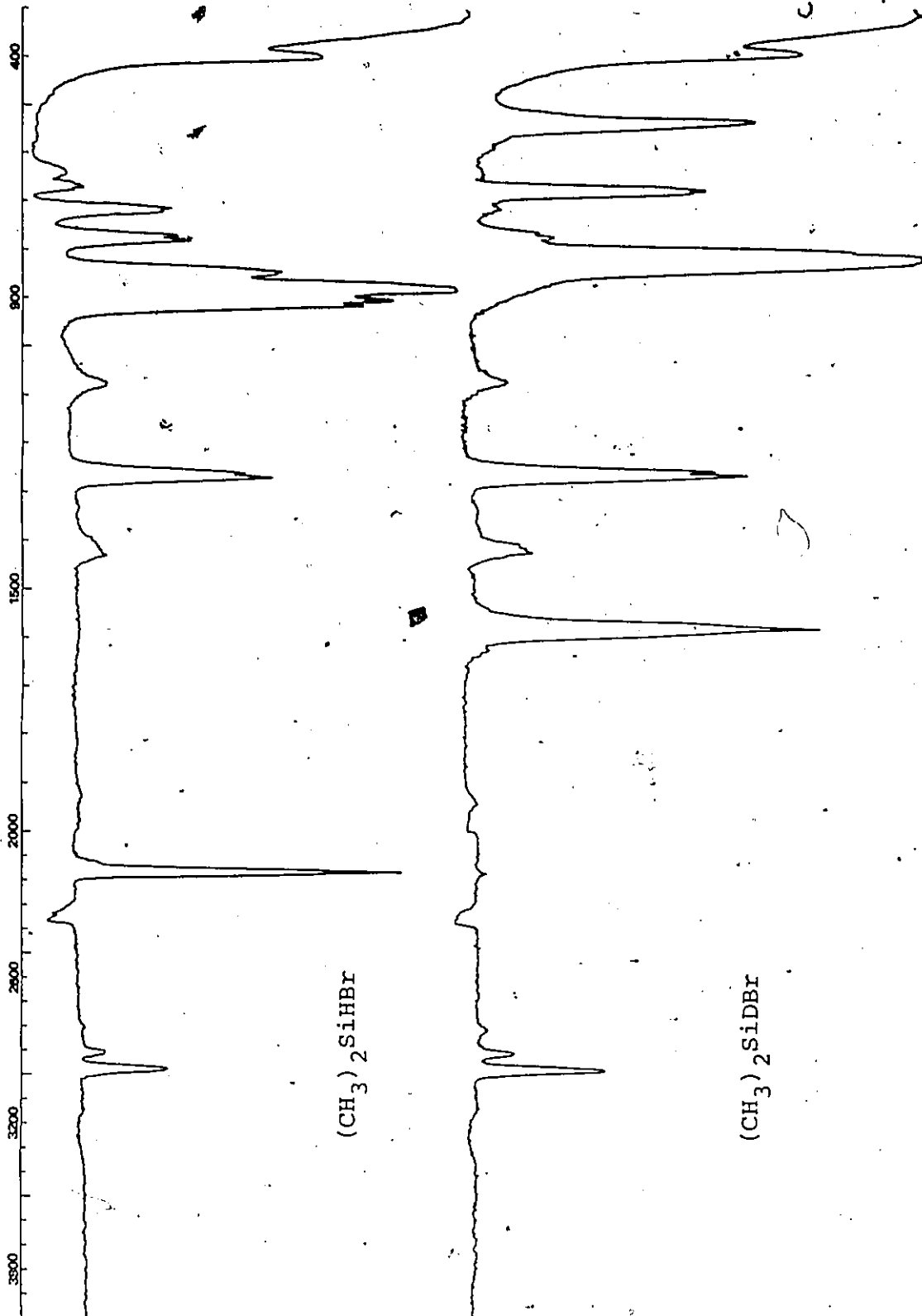
Figure I.5.7. Gas infrared spectra of the bromodimethylsilanes
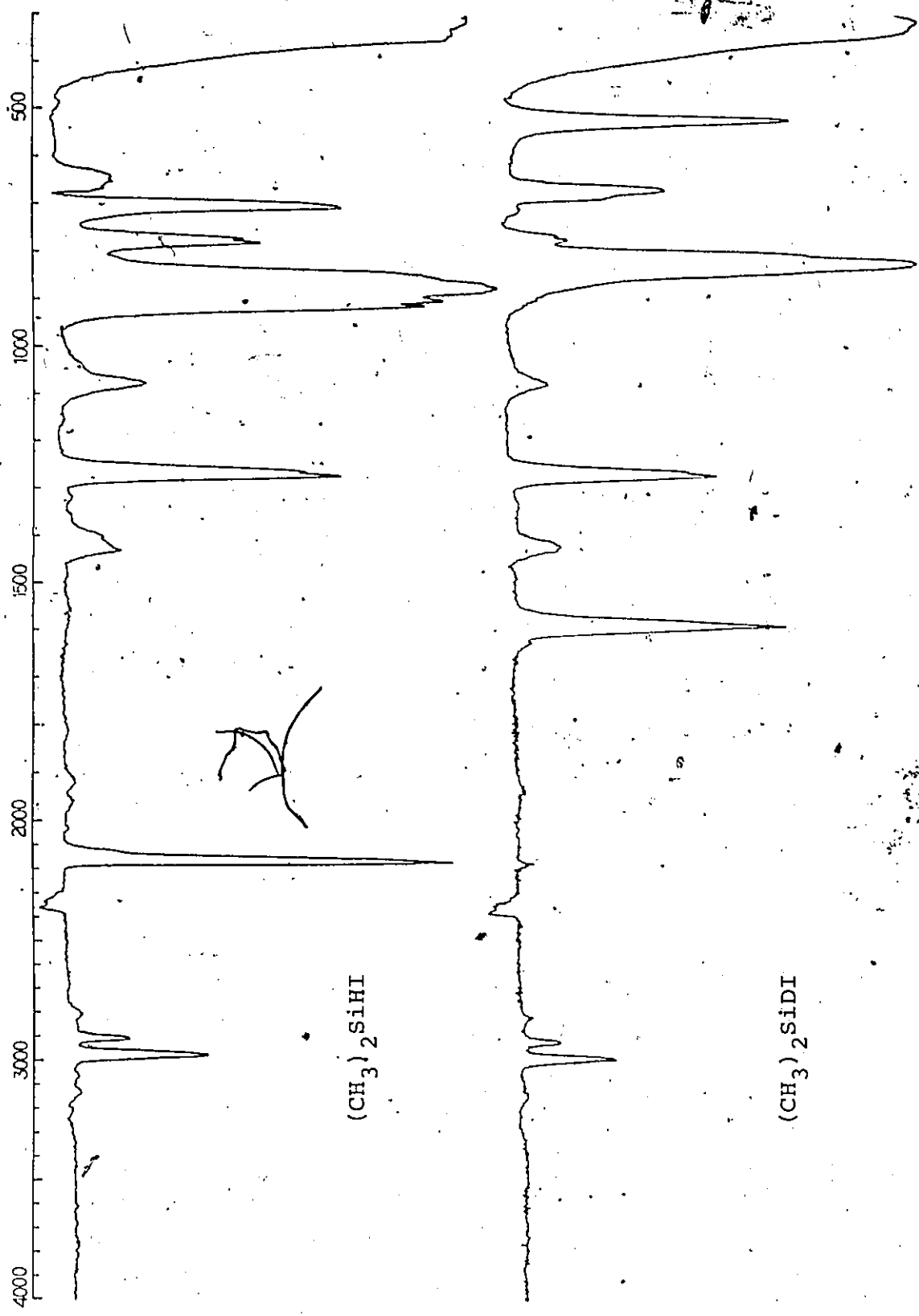
$(CH_3)_2SiHI$

$(CH_3)_2SiDI$

Figure I.5.8 Gas infrared spectra of the iododimethylsilanes

$(CH_3)_2SiHBr$ (gas)

$(CH_3)_2SiHBr$ (liquid)
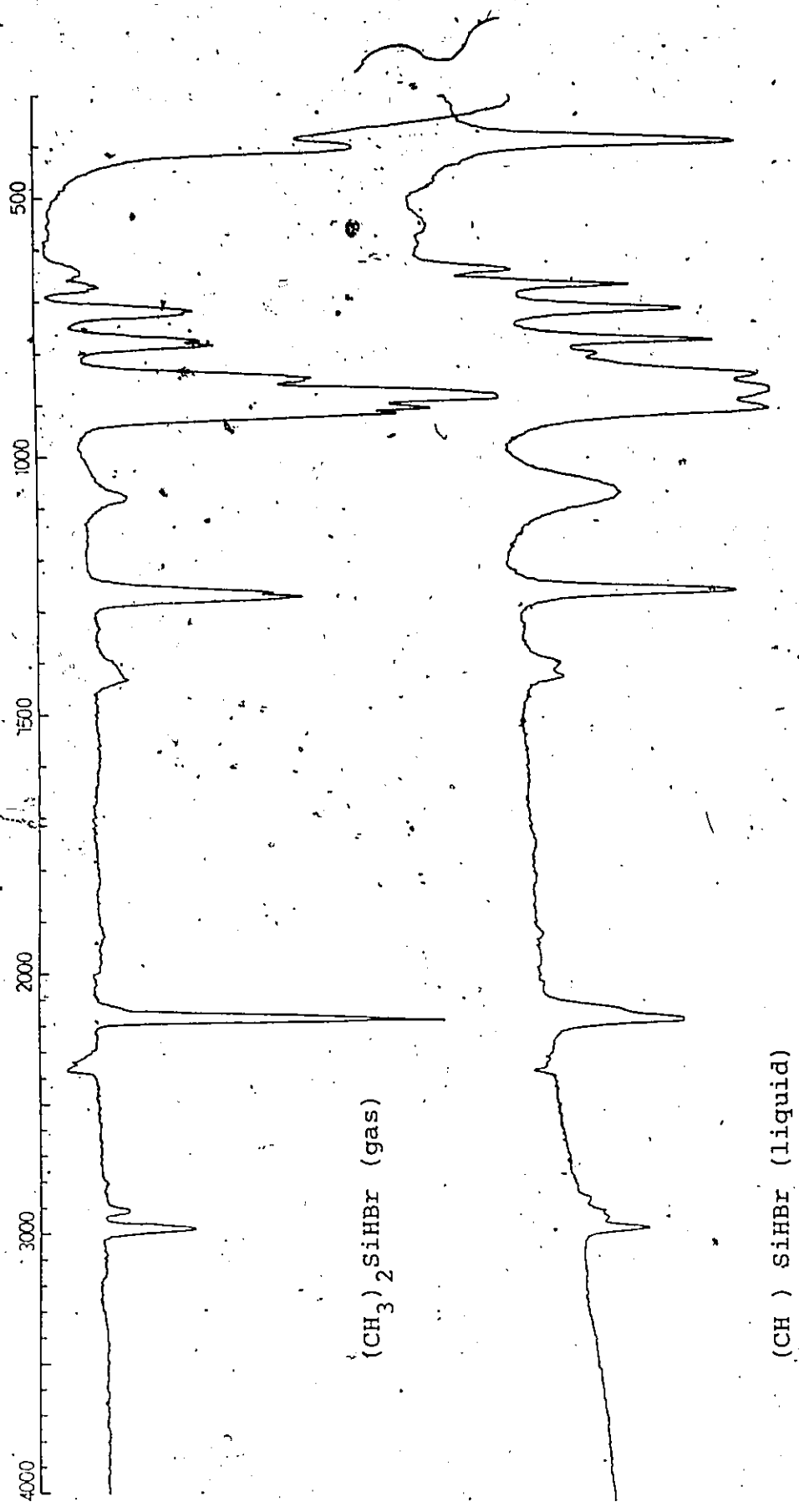
Figure I.5.9   Infrared spectra of $(CH_3)_2SiHBr$

(CH$_3$)$_2$SiHI (gas)

(CH$_3$)$_2$SiHI (liquid)
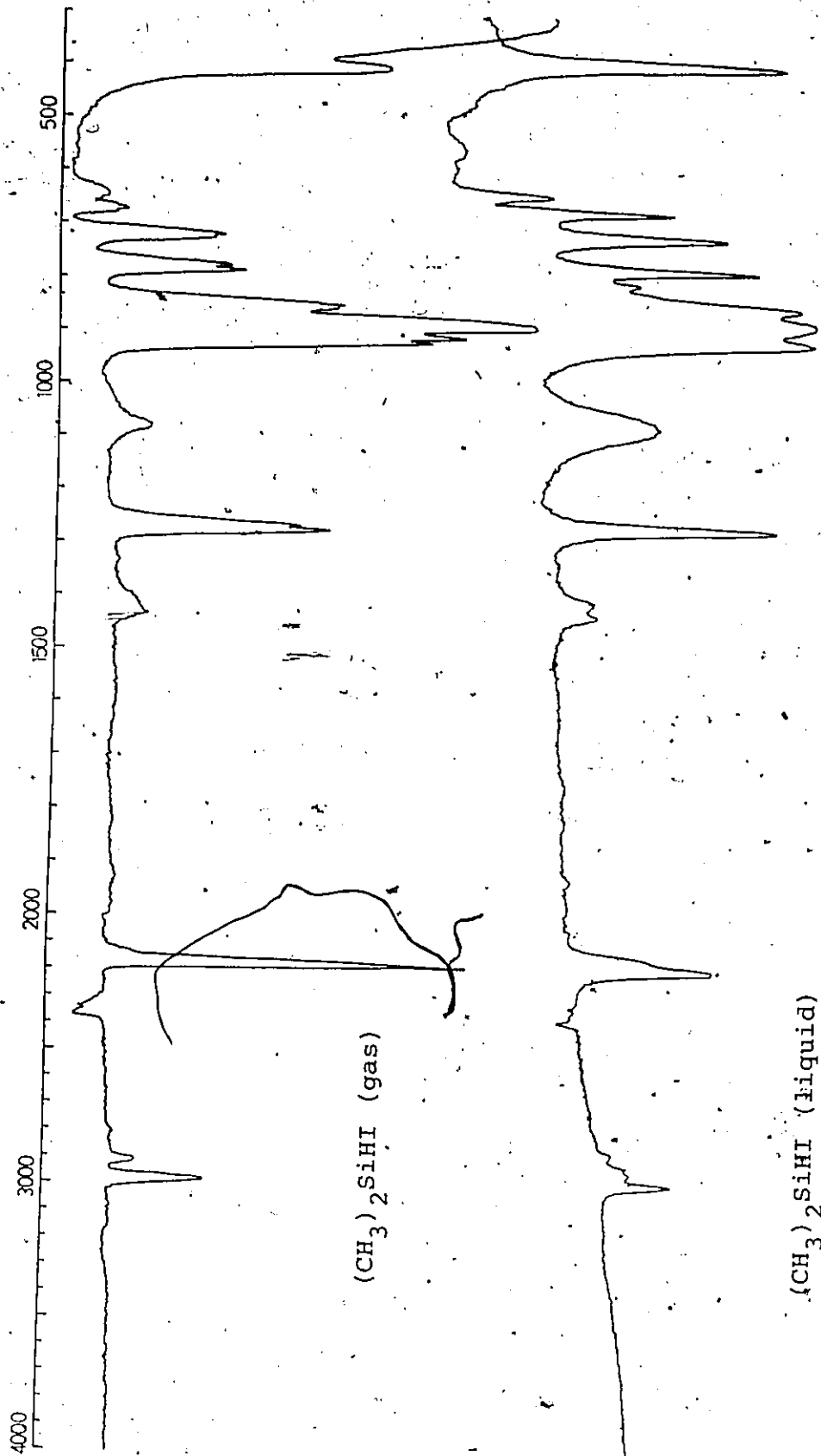
Figure I.5.10 Infrared spectra of (CH$_3$)$_2$SiHI
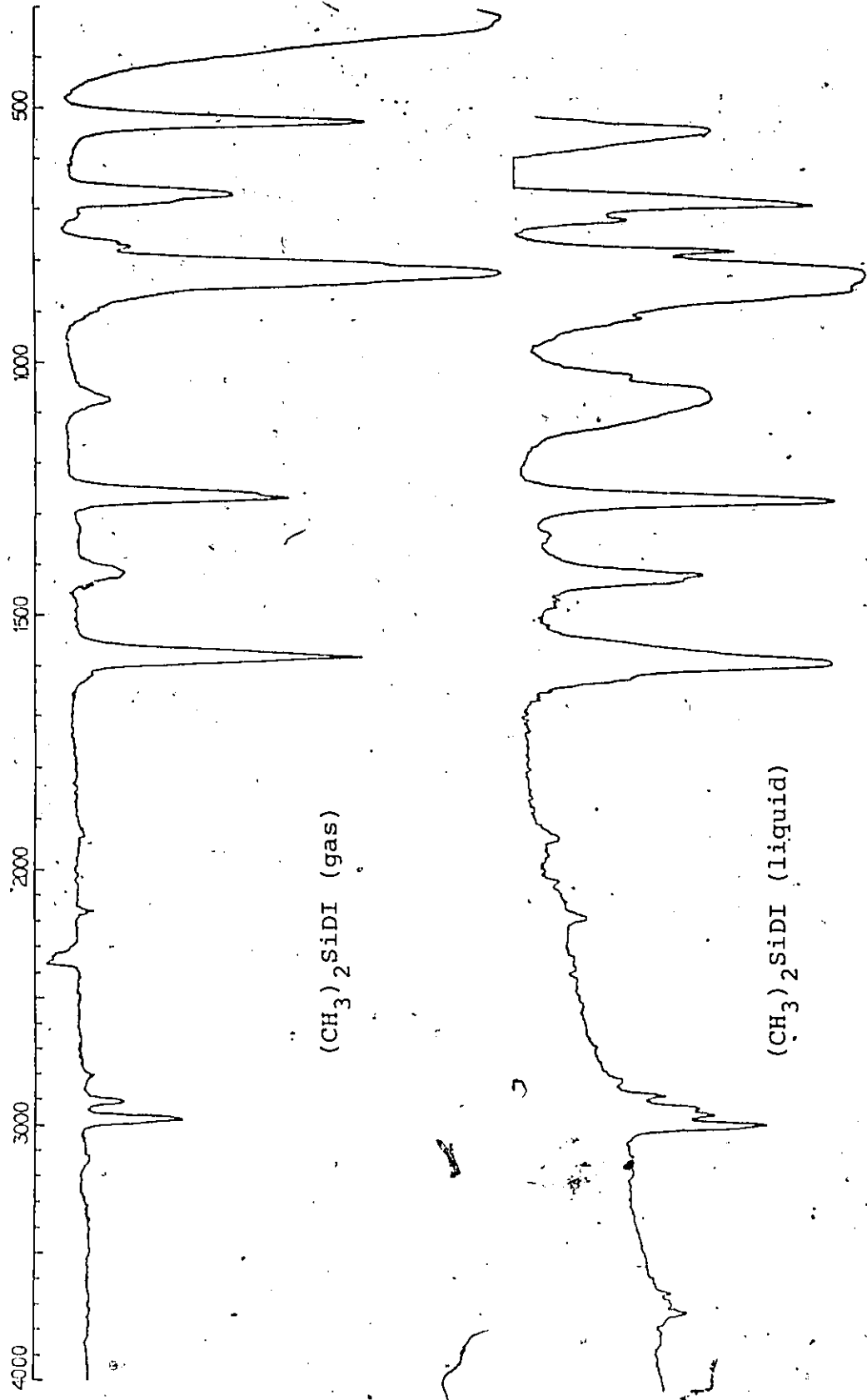
Figure I.5.11   Infrared spectra of (CH$_3$)$_2$SiDI

$(CH_3)_2$SiDI (gas)

$(CH_3)_2$SiDI (liquid)

Table I.5.1. Fundamental modes and approximate descriptions for $(CH_3)_2SiHX$ molecules.

Description	a'		a"	
CH_3 str.(asym)	ν_1	ν_2	ν_{16}	ν_{17}
CH_3 str.(sym)	ν_3		ν_{18}	
SiH str.	ν_4			
CH_3 def.(asym)	ν_5	ν_6	ν_{19}	ν_{20}
CH_3 def.(sym)	ν_7		ν_{21}	
CH_3 rock	ν_8	ν_9	ν_{22}	ν_{23}
SiC_2 str.	ν_{10}		ν_{24}	
SiH def.	ν_{11}		ν_{25}	
SiX str.	ν_{12}			
SiC_2 def.	ν_{13}			
CSiX def.	ν_{14}		ν_{26}	
torsion	ν_{15}		ν_{27}	

The liquid spectra are useful where the infrared spectra of the gas produce weak or overlapping bands, and the corresponding Raman bands are weak. While the gas spectra provide information through band contours, the corresponding absorptions in the liquid spectra are narrower and have only one maximum. This allows for some weaker bands that may otherwise have been obscured in the tail of an absorption to be observed, and provides the possibility of resolving partially overlapping bands. Not too much attention should be paid to extra weak bands, however, because of the fairly rapid hydrolysis occuring in the cell.

i) $\underline{3000-1000\ cm^{-1}}$

The CH_3 stretching regions in both spectra are almost identical for both homologues. The only difference between these compounds and the monomethyl derivatives is that the asymmetric CH_3 stretches can be resolved into two bands in the Raman spectra. They appear as featureless weak to medium intensity bands in the infrared spectra.

The Si-H and Si-D stretches are strong bands in both effects, those in the fluoride having the expected A-type contours, the others a Q branch which could be from an A, C or hybrid band. A weak shoulder is observed to the high wavenumber side of the Si-D band in both spectra, but not for the Si-H band. It is thus probably an overtone or combination band enhanced by Fermi resonance with ν_3. Since it is present in all four compounds, it does not involve a vibration involving the halogen. If it is a binary combination, as is most probable, it is almost bound to involve the rocking modes (as combinations including the methyl deformations can be ruled out for lack of a consistent low-lying frequency to give the correct sum). The favoured candidate is $2\nu_9$, the highest rock at $\underline{ca}$. 820 cm^{-1}. This is moderately strong (for a rock) in the Raman spectra and the most intense absorption in the infrared spectra (except in the fluoride, where the Si-F stretch is the strongest).

The asymmetric deformations appear as two depolarised bands in the Raman spectra, and have what appear to be a C-type "spike" to the high frequency side of the infrared

envelope. The a' and a" symmetric deformations are both observed in the Raman spectra, where they are clearly distinguished in the polarised scan.

ii) Below 350 cm^{-1}

Each compound has three bands in this region, the SiC_2 deformation and the a' and a" CSiX deformations. These are more clearly seen in Figures I.5. 12-15. The two of lowest frequency are of medium intensity in the Raman spectra and appear in the same envelope for the iodide, bromide and chloride. The splitting between them decreases as the halogen becomes lighter until they are approximately coincident in the chloride. The highest wavenumber feature is a weaker, polarised band at ca. 250 cm^{-1} in these same three compounds. Polarisation data are inconclusive for the fluoride, and the infrared spectrum in the CsI region provided no band contours, so an assignment cannot satisfactorily be made by frequency comparison alone.

iii) 1000-350 cm^{-1}

This region is interpreted mainly from the Raman spectra (Figures I.5.12-15) and the liquid infrared spectra (Figures I.5.9-11). The Si-X stretches (X=Cl, Br, I) are intense, polarised bands at their characteristic frequencies. The rest of the Raman spectrum is typical of the Me_2SiH- group, and is almost identical to the pattern observed in the $(Me_2SiH)_2E$ series (E = S, Se, Te)[82] when the spectra of the two compounds containing "neighbouring" halogen and chalcogen are compared. The bands between 500-600 cm^{-1} in

(CH$_3$)$_2$SiHF

(CH$_3$)$_2$SiDF

800   500   200
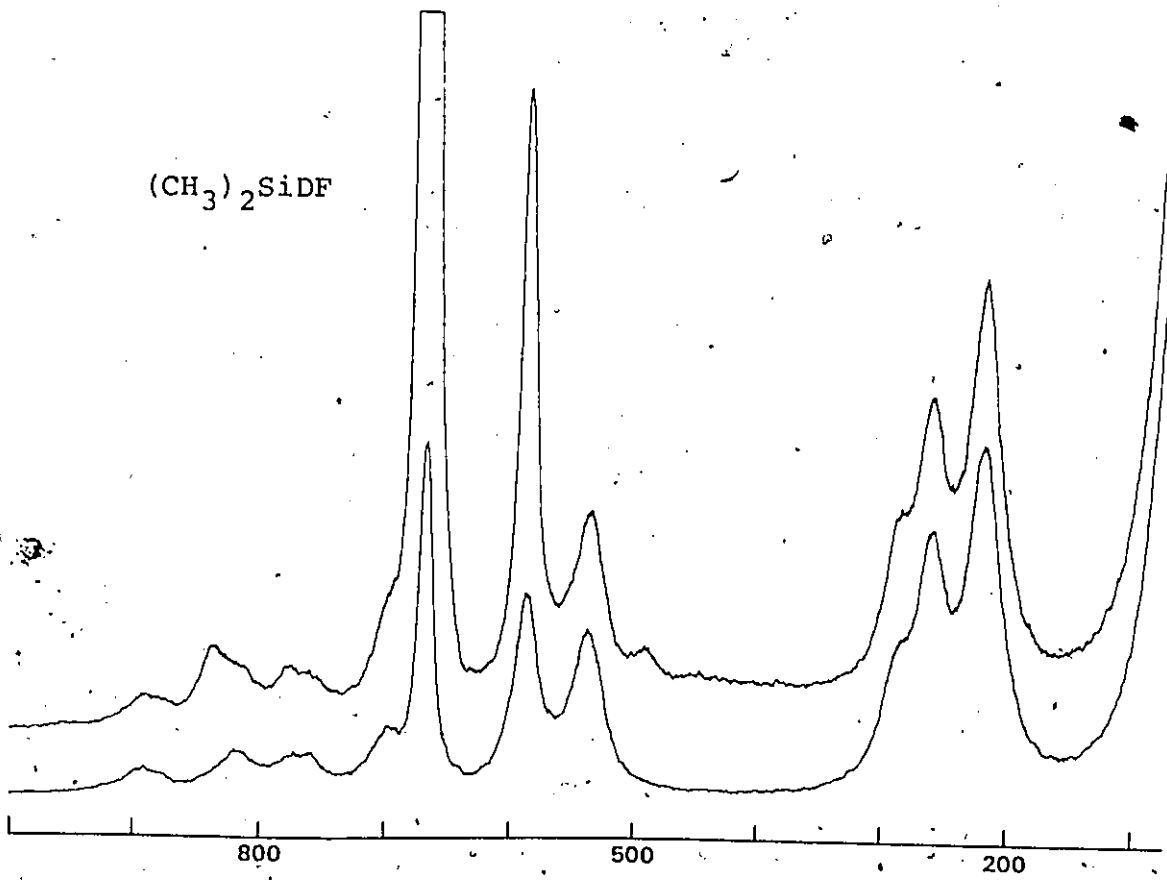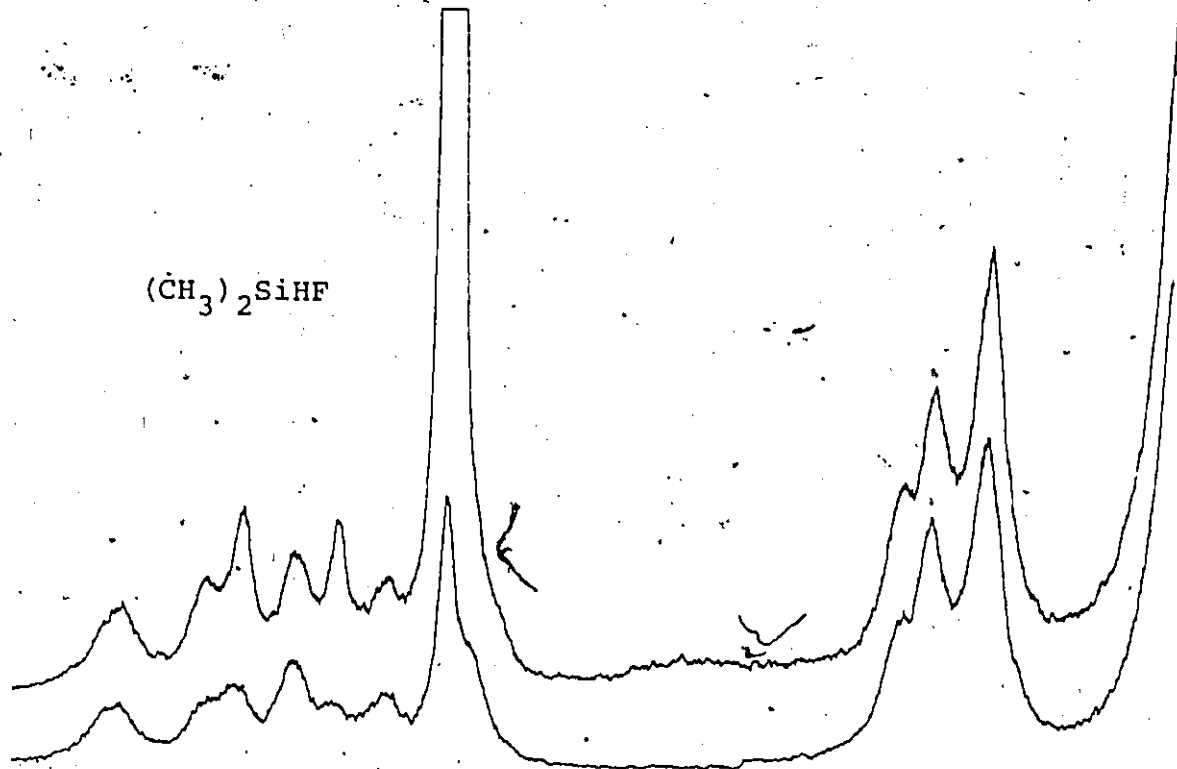
Figure I.5.12   Partial Raman spectrum of the fluoro-
dimethylsilanes
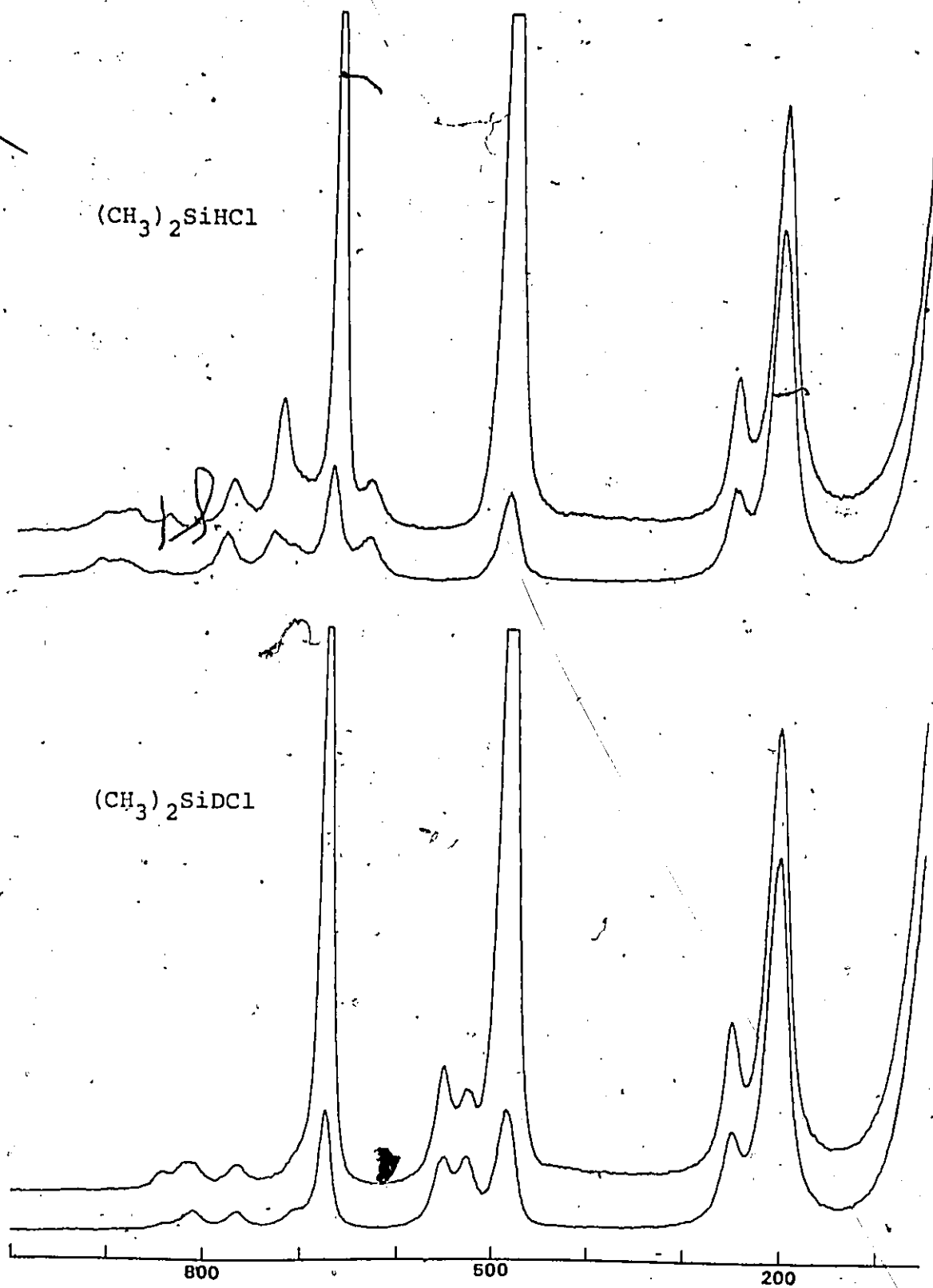
Figure I.5.13   Partial Raman spectra of the chlorodimethylsilanes

$(CH_3)_2SiHBr$

$(CH_3)_2SiDBr$

800   500   200
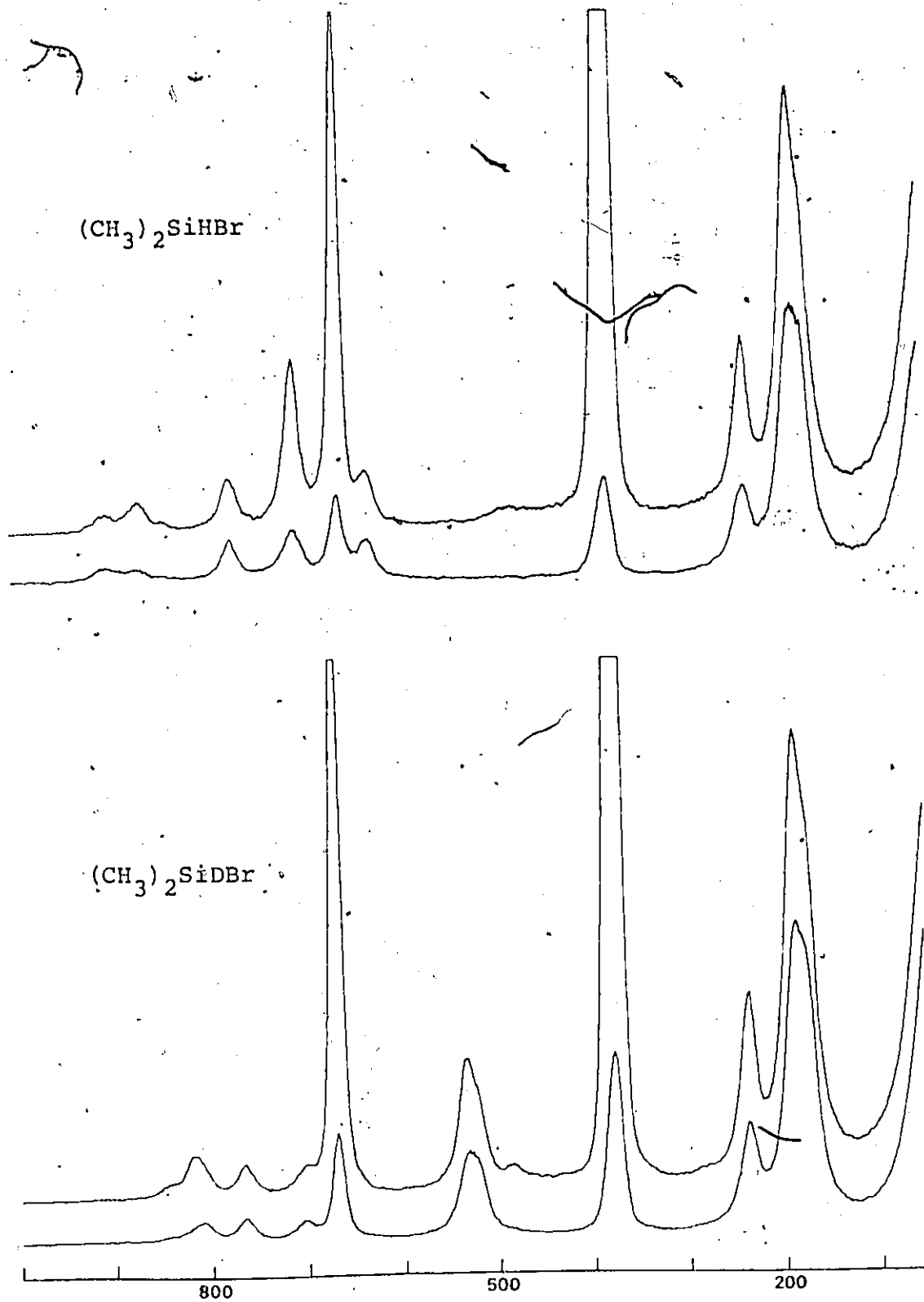
Figure I.5.14   Partial Raman spectra of the
bromodimethylsilanes
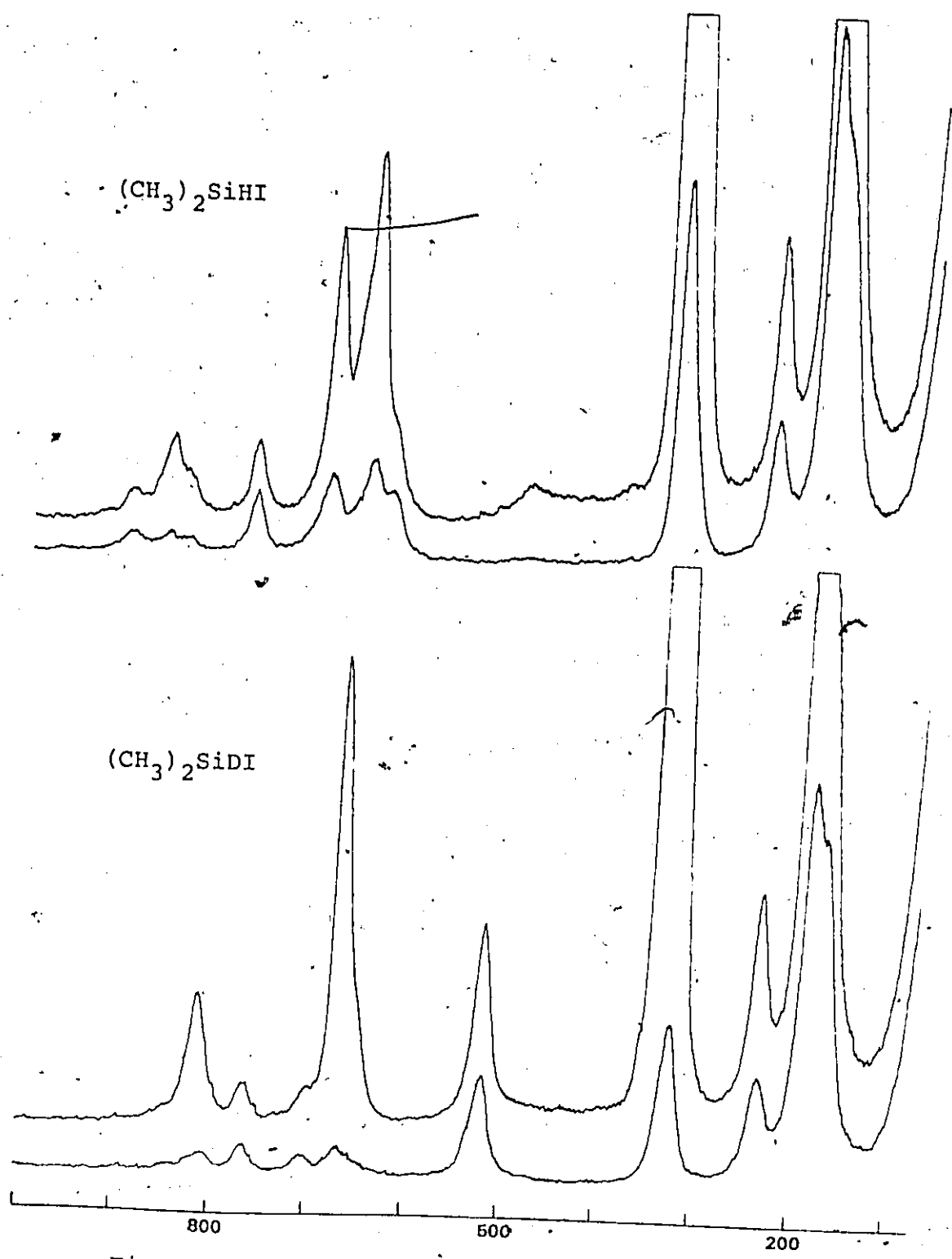
Figure I.5.15   Partial Raman spectra of the
iododimethylsilanes

the Raman spectrum of the "heavy" molecule are without doubt
the two Si-D bends, with an increasing separation as the
halogen becomes lighter, the two appearing exactly overlapped
in the iodide. The strongest remaining Raman band in both
spectra at about 665 cm^{-1} is expected to be the symmetric
Si-C stretch, but the rest of the assignment is not immed-
iately clear, although it is expected that the intense
absorption at ca. 850 cm^{-1} in the infrared spectra contains
some, if not all, the methyl rocking modes.

I.5.3. Assignment of Fundamentals

This series of compounds was the only one for which
a recent, complete study had been performed[66]. This however,
was thought to be in error in several respects. A discussion
of the differences in assignment will be given later. By
having the spectra of the d_1- derivatives at hand it was
hoped that there would be sufficient evidence for a clear-cut
assignment to be made, but the assignment process was not as
simple as had been anticipated.

Three different assignments were originally proposed,
and these are discussed with respect to the NCA and product
rule calculations. The first assignment considered both
series of light and heavy molecules independently. It was
assumed that the polarised and depolarised bands appearing
on each side of what was assumed to be the Si-C stretch in
the light compound were the a' and a" Si-H bends, and so
ν_{24}, the asymmetric Si-C stretch, was assigned to the
depolarised band at 775 cm^{-1}, which was a medium B-type band

(except for the fluoride) in the infrared effect. In the
deuterated compound, four bands (five for the fluoride) can
be picked out above 750 cm^{-1}, the top three of which were
assumed to be the methyl rocks. This left in each spectrum
a weak, depolarised band at about the same position as ν_{24}
for the light compound, and a similar feature at ca. 705 cm^{-1}.
The preferred assignment was that this latter band be assigned
as ν_{24} (since it could not be satisfactorily explained as an
overtone or combination) and the band at ca. 765 cm^{-1} then be
the remaining rocking mode, although all four bands need not
necessarily be observed. (It was originally thought that the
three maxima in the liquid spectra may represent all four
rocks). The result of this assignment was that the range of
frequencies for the rocking modes was 60 and 80 cm^{-1}, but that
the SiC$_2$ stretches were split by 100 and 30 cm^{-1} for the
light and heavy compound respectively. This large difference
in the SiC$_2$ stretching modes, however, could not be reproduced
in the NCA by any means, and produced a poor agreement with
the calculated product rule ratios. For example, for the
bromide, the calculated a" ratio is 0.726 and this assignment
produced a" ratios for the Raman data in the range of 0.562
to 0.656, depending on the choice of which band contained
the fourth methyl rocking mode. It was therefore rejected
as a possible assignment.

The product rule indicates that either one of the a"
frequencies in the normal molecule is too high or one in the
heavy molecule too low. In order to achieve an acceptable

match, an assignment where the SiC_2 stretches are at about the same wavenumber in each compound (or for the NCA, the ame splitting) is required. This leaves two alternatives, with ν_{24} either at ca. 770 cm^{-1} or at ca. 705 cm^{-1}, neither of which could be dismissed on the grounds of the product rule. There are objections to both of these. If the former assignment is accepted, then the bands at ca. 705 cm^{-1} in the deuterated compound and Me_2SiHF must be explained. This is not possible as a binary overtone or combination for the whole series, even considering the torsional modes[66], and assigning it as the fourth methyl rock is improbable (approx. 100 cm^{-1} below the other three, which are separated by about 40 cm^{-1}; 60 cm^{-1} in the fluoride) and not possible by NCA criteria, although this is not sufficient in itself to preclude this assignment. An objection to the second alternative is that while the 705 cm^{-1} band is present in the spectrum of Me_2SiHF, and possibly in Me_2SiHCl, it does not appear as a distinct band in the bromide or iodide. It should be noted, however, that this band is clearly seen in $(Me_2SiH)_2E$ where $E = S$, Te[82]. (In this series it appears to low wavenumber of the symmetric SiH deformation in the sulphide and to high wavenumber in the telluride, and so is probably coincident with this band in the selenide). The methyl rocks would then occur within a range of about 135 cm^{-1} for the light molecule and 80 cm^{-1} for the deuterated compound.

For a comparison with other molecules, there are several features that they should have in order to provide some help.

In addition to the $(Me_2SiH)_2E$ compounds, these could include

    i) Me_3SiX; for the effect of one halogen atom on the methyl rocks plus the possibility of some information on Si-C stretches.

    ii) $Me_2Si\lessdot$; for SiC_2 stretches and methyl rocks (effectively limiting the compounds to Me_2SiX_2).

    Both of these have the advantage of no SiH deformations to confuse with the rocks.

    iii) $MeSiHX_2$; a compound with one SiH deformation, which does not however escape the problems of mixing with the methyl rocks.

    Extensive data has been collected for trimethylsilyl compounds[60,83,84], much of it accompanied by NCA[83,84], and the consensus points to bands observed at ca. 760 and 690-710 cm^{-1} in these compounds to assigned as a methyl rock and the asymmetric Si-C stretch respectively. The symmetric Si-C stretch occurs at ca. 630 cm^{-1}, a little lower than for the dimethyl compounds studied here. The report on chlorotrimethylsilane[84] which included data on $(CD_3)_3SiCl$, studied all likely assignments and concluded that the asymmetric SiC_3 stretches were at 695 and 705 cm^{-1} respectively.

    The only complete spectrum reported recently for Me_2SiX_2 has been for the diiodide by Durig and Hawley[66], where weak, depolarised bands are again observed at 790,750 and 705 cm^{-1}, good candidates for two rocking modes and the asymmetric Si-C stretch, in agreement with frequencies for both Me_3Si- and the $(Me_2SiH)_2E$ compounds (although the authors chose a

different assignment). Much of the remaining data [34,36,85] for Me$_2$SiX$_2$ compounds are not considered to be very reliable, as the Raman spectra were recorded photographically and some weaker bands were consequently not observed. Thus in early reports on the Me$_n$SiX$_{4-n}$ series (n= 0-4; X= Br[36], Cl[34]) the asymmetric Si-C stretches for Me$_2$SiX$_2$ and Me$_3$SiX were both assigned at high wavenumber (ca. 800 and 760 cm^{-1} respectively) but the large splitting thus invoked was not reproducible in the calculations included in the reports (for which no force constant or p.e.d. data were included) which could only account for 1/3 to 1/2 of the observed splitting. Moreover, the results for Me$_3$SiX do not agree with the later (considered more reliable) studies on Me$_3$Si- compounds[60,83] Since only the skeletal stretching and bending frequencies were reported, it is not possible to consider alternative assignments for the observed bands. The other report on Me$_2$SiX$_2$ (X= H,F,Cl,Br)[85] also preferred the high frequency bands for the asymmetric SiC$_2$ stretch, but is somewhat confusing in the case of Me$_2$SiF$_2$ in which the 695 cm^{-1} band is observed, but assigned together with three other frequencies to the two SiC$_2$ stretches.

Using the MeSiHX$_2$ compounds discussed in the previous chapter to compare the SiH bending modes, it is seen that they occur in the 650-750 cm^{-1} range for SiH bends in CH$_3$SiHX$_2$ and between 520 and 630 cm^{-1} for SiD deformations in CH$_3$SiDX$_2$. (Notice, however, that in CD$_3$SiHX$_2$, the range for the SiH modes increases by about 100 cm^{-1}, indicating the effect of the mixing with the methyl rocking motions).

After trying the NCA with both alternatives, it was decided to use the latter assignment, the objection of assigning the 705 cm^{-1} band for the former alternative, along with its observation in the chalcogenide series, plus the support for this frequency as ν_{24} from other related compounds and the inability of the NCA to account for the required splitting of the methyl rocks all being deciding factors. The product rule ratios for this assignment are shown in Table I.5.2, and on the whole the agreement is reasonable. There are one or two striking anomalies; for example the difference in the a" values between the infrared and Raman results, especially for the chloride, even though corresponding frequencies were used for each ratio. Apart from confirming the possibility of this assignment, they helped sort out the methyl rocks in Me$_2$SiDF, where polarisation data and band contours did not offer conclusive evidence, after values of 0.55 (a') and 0.67 (a") were calculated

Table I.5.2   Product rule ratios for Me$_2$SiHX

		calc.	obs. Ra	obs. i.r.
Me$_2$SiDF / Me$_2$SiHF	a'	0.517	0.521	0.519
	a"	0.725	0.721	0.705
Me$_2$SiDCl / Me$_2$SiHCl	a'	0.512	0.501	0.502
	a"	0.726	0.727	0.752
Me$_2$SiDBr / Me$_2$SiHBr	a'	0.509	0.508	0.492
	a"	0.726	0.723	0.709
Me$_2$SiDI / Me$_2$SiHI	a'	0.508	0.509	0.511
	a"	0.726	0.741	0.742

from the initial assignment. A closer reinvestigation pro-
duced frequencies compatible with the ratio and both observed
spectra.

The observed frequencies with the preferred assignment,
along with the frequencies calculated by the NCA are listed
in Tables I.5.3 - 6.

I.5.4   Normal Coordinate Analysis

The following dimensions, taken from related molecules[61],
were assumed; C-H 110, Si-C 185, Si-H 148 and Si-X 160 (F),
203 (Cl), 224 (Br) and 246 pm (I). All angles were assumed to
be tetrahedral. The methyl groups were defined such that all
bonds were staggered when sighted along each C-Si bond, as
shown in Figure I.5.16. The HCSi bends were again separated
into those approximately perpendicular and parallel to the
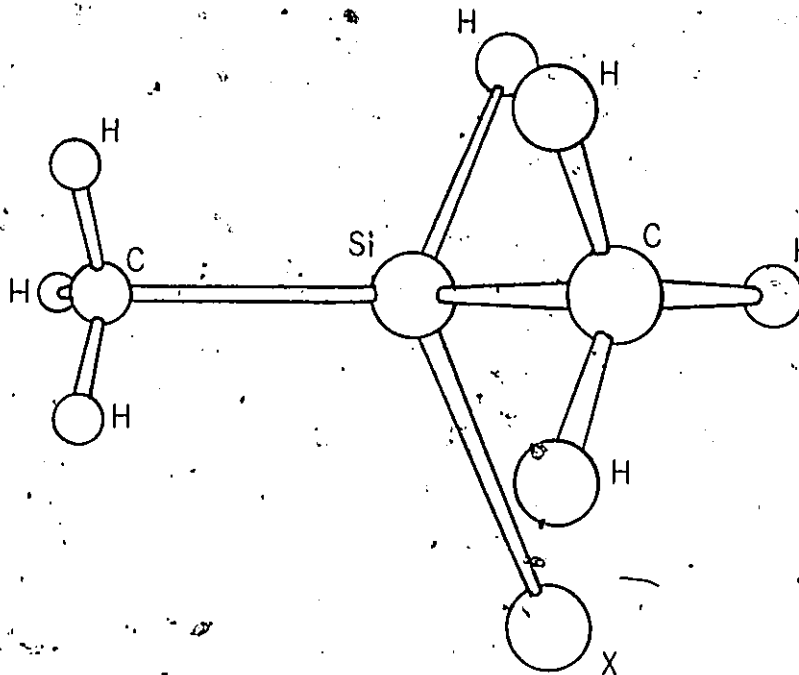
Figure I.5.16 Assumed geometry for Me_2SiHX

Table I.5.3   The vibrational spectra of the fluorodimethylsilanes

Me₂SiHF i.r.(gas)	Raman(liq.)	calc.	assignment	Me₂SiDF i.r.(gas)	Raman(liq.)	calc.
2981 mw	2974 mw dp	2978	ν_1, ν_{16}	2981 mw	2975 mw dp	2978
2974 mw		2977	ν_2, ν_{17}	2974 mw		2977
A { 2927 / 2917 w / 2909	2912 s p	2911	ν_3, ν_{18}	2914 w	2910 s p	2911
2624 vw			$2\delta_{Me}$	2821 vw	2805 vw p / 2505 vw	
A { 2184 / 2169 s / 2156	2166 s p	2177	ν_4	A { 1594 / 1582 s / 1568	1578 s p	1571
1436 w	1430 vw dp	1419	ν_5, ν_{19}	1430 w	1415 vw dp	1419
1422 w	1404 vw dp	1410	ν_6, ν_{20}	1422 w	1409 vw dp	1410
A { 1274 / 1266 ms / 1257	1262 vw p	1266	ν_7	A { 1272 / 1264 s / 1257	1262 vw p	1256
		1261	ν_{21}			1254
929 vs	917 vw dp	912	ν_{12}	902 vs	889 vw dp	896
921 vs		911	ν_{22}	821 vs	817 vw dp	841
844 m	848 vw dp	866	ν_8	840 msh	837 vw p	839
B { 828 / 821	819 vw p	770	ν_9	769 w	776 vw p?	770
A/C { 786 / 777 ms / 772	775 vw dp	793	ν_{23}	759 w	757 vw dp	793

Table I.5.3   (continued)

	Me$_2$SiHF		assign-ment	Me$_2$SiDF		
i.r.(gas)	Raman(liq.)	calc.		i.r.(gas)	Raman(liq.)	calc.
C? 742 m	742 vw p	756	ν_{11}	584 m	586 mw p	578
	703 vw dp	714	ν_{24}	680 mw	698 vw dp	690
C? 651 vwsh	653 vs p	659	ν_{10}	C 667 mw	668 vs p	659
638 mw	634 vwsh dp	635	ν_{25}	530 m	536 w dp	523
505 w			$\nu_{14}+\nu_{13}$			
A 287	288 w p?	288	ν_{13}		286 w p?	286
270.	262 mw dp?	261	ν_{26}		259 mw dp?	260
	218 mw dp?	218	ν_{14}		217 mw dp?	217

260

Table I.5.4   The vibrational spectra of the chlorodimethylsilanes

Me₂SiHCl i.r.(gas)	Raman(liq.)	calc.	assignment	Me₂SiDCl i.r.(gas)	Raman(liq.)	calc.
2983 m	2977 mw dp	2975	ν_1,ν_{16}	2984 mw	2979 mw dp	2975
2974 m	2971 mw dp	2974	ν_2,ν_{17}	2974 mw	2970 mw dp	2974
2916 w	2909 vs p	2909	ν_3,ν_{18}	A? 2916 w	2908 vs p	2909
2821 vw			$2\times\delta_{Me}$		2842 vw p	
					2807 w p	
2519 vw					2502 vw p	
2176 vs	2176 s p	2181	ν_4	A/C $\{$ 1591, 1581 s, 1572	1579 s p	1573
2041 vw			$\nu_{7,21}+\nu_{23}$			
1934 vw,			$\nu_{7,21}+\nu_{10}$			
1815 vw			$2\times\rho_{Me}$	1624 vw		
1765 vw						
1435 w	1427 w dp	1418	ν_5,ν_{19}	1429 w	1414 w dp	1418
1420 w	1402 w dp	1410	ν_6,ν_{20}	1419 w		1410
C $\{$ 1267 s	1263 w p	1271	ν_7	C $\{$ 1268 s	1263 w p	1254
B $\{$ 1262 s	1258 vw dp	1257	ν_{21}	B $\{$ 1263 s	1253 vw dp	1251
B $\{$ 913 mssh, 905?	905 vw dp	909	ν_{22}	808 s	812 w dp	847
A $\{$ 894?, 885 vs, 878	883 vw p?	873	ν_8	~840 msh	844 vw p	839
C 845 s	843 vw p	817	ν_9	825 vsbr	822 w p	813
B $\{$ 781 ms, 772	776 w dp	792	ν_{23}	B $\{$ 771 w, 762	765 w dp	787
A $\{$ 734, 726 m, 718	726 w p	729	ν_{11}	554 m	553 mw p?	554

261

Table I.5.4   (continued)

	Me₂SiHCl			assign-ment	Me₂SiDCl		
	i.r.(gas)	Raman(liq.)	calc.		i.r.(gas)	Raman(liq.)	calc.
	A $\left\{\begin{array}{l}679\\671\ \text{mw}\\663\end{array}\right.$	∿698 vw dp	707	ν_{24}	715 vw	705 vw dp	694
		670 s p	672	ν_{10}	A $\left\{\begin{array}{l}688\\680\ \text{ms}\\672\end{array}\right.$	676 s p	676
	636 w	633 w dp	644	ν_{25}	547 m	530 mw dp	522
	507 s	489 s p	492	ν_{12}	505 ms	486 s p	484
		258 mw dp	255	ν_{13}		252 mw p	254
		209 m dp	208	ν_{14}		207 m dp	208
		207 m dp	205	ν_{26}		202 m dp	204

262

Table I.5.5   The vibrational spectra of the bromodimethylsilanes

	Me₂SiHBr			assign-ment	Me₂SiDBr		
i.r.(gas)	i.r.(liq.)	Raman(liq.)	calc.		i.r.(gas)	Raman(liq.)	calc.
2980 m	2978 msh	2977 mw dp	2973	ν_1, ν_{16}	2980 m	2977 mw dp	2973
2974 m	2968 m	2967 mw dp	2972	ν_2, ν_{17}	2974 m	2969 mw dp	2973
2914 w	2905 w	2906 vs p	2906	ν_3, ν_{18}	2913 w	2906 mw dp	2906
2814' vw				2×δMe	2819 vw	2802 w p	
2176 s	2170 s	2173 s p	2182	ν_4	1581 s	1580 s p	1573
2036 vw				+ν_{23}			
1971 vw				δ_sMe+ν_{11}	1938 vw		
1928 vw				+ν_{10}	1624 vwsh	1618 wsh p	
1816 vw				2×ρMe			
1432 w	1428 w	1425 w dp	1417	ν_5, ν_{19}	1428 mw	1414 w dp	1417
~1417 wbr	1398 w	1401 w dp	1410	ν_6, ν_{20}	~1418 mw		1410
C{1266 ms	1257 vs	1260 w p	1283	ν_7	C{1266 s	1262 w p	1268
B{1261 ms		1252 vwshdp	1270	ν_{21}	B{1262	1252 vwshdp	1265
B{913 s	906 vs	905 w dp	861	ν_{22}	807 s sh	811 w dp	837
{903 s							
880 vs	872 vs	870 w p	900	ϑ_8	~843 sh	847 vwsh p	826
A{852	843 vs	842 vw dp?	778	ν_9	818 vsbr	821 w p	794
{846 ms							
{842							
B{780 m	775 s	775 w dp	801	ϑ_{23}	B{772 w	767 w dp	770
{770					{764		

Table I.5.5   (continued)

	Me₂SiHBr				assign-ment	Me₂SiDBr		
	i.r.(gas)	i.r.(liq.)	Raman(liq.)	calc.		i.r.(gas)	Raman(liq.)	calc.
A {	718 711 m 706	711 s	710 mw p	706	ν_{11}	537 s	536 mw dp?	535
				707	ν_{24}	710 w	706 w dp	699
A/B {	671 665 mw 661	665 s	665 s p	668	ν_{10}	A/B {680 674 s 668	672 s p	672
	637 w	635 m	635 w dp	624	ν_{25}	519 mwsh	524 m dp	505
			572 vw p		$\nu_{12}+\nu_{13}$			
	402 m	389 vs	385 vs p	386	ν_{12}	397 m	382 vs p	380
		242 w	244 m dp	242	ν_{13}		240 mw dp	241
			194 ms dp?	194	ν_{14}		191 ms dp	194
			186 ms dp?	183	ν_{26}		183 ms dp	183

Table I.5.6   The Vibrational spectra of the iododimethylsilanes

Me2SiHI				assign-	Me2SiDI			
i.r.(gas)	i.r.(liq)	*Raman(liq)	calc.	ment	i.r.(gas)	i.r.(liq)	Raman(liq)	calc.
3136 w				$\nu_{1,16}+\nu_{13}$	3138 vw			
2987 msh	2977 m	2978 mw dp	2973	ν_1,ν_{16}	2988 wsh	*2976 m	*2981 mw dp	2973
2974 m	2964 m	2965 mw dp	2972	ν_2,ν_{17}	2975 mw	*2964 mw	*2967 mw dp	2972
2913 mw	2903 w	2903 s p	2903	ν_3,ν_{18}	2913 w	*2901 w	2902 s p	2903
2860 vw		2849 vw p		$2\delta_a$ Me				
2813 w	2793 vw	2796 vw p		$2\delta_s$ Me	2814 vw		2799 w p	
2512 vw		2503 vw p		2δ Me				
1811 vw	1801 vw			2ρMe	1617 vw	†*1611 w	†1612 wsh p	
2172 vs	2167 vs	2170 m p	2180	ν_4	1579 s	*1574 vs	1578 m p	1571
2136 wsh				$\nu_8+\nu_{22}$	2028 vw			
2034 vw	2030 vw			δ_sMe$+\nu_{23}$				
1962 vw	1956 vw			ν_{11}	1929 vw	*1920 vw	*1920 vw	
1923 vw	1910 vw			ν_{10}				
1430 w	1425 m	1424 w dp	1413	ν_5,ν_{19}	1417 wbr	*1420 ms	1411 w dp	1413
~1401 wbr	1397 m	1396 w dp	1408	ν_6,ν_{20}		*1405		1408
1356 vw				$\nu_{10}+\nu_{24}$		†1365 w		
1320 vw				$2\nu_{10}$		*1328 vw		
C{1264 s	1255 vs	1258 w p	1261	ν_7	C{1265	*1254 vs	1257 w p	1254
B{1259		1253 wsh dp	1257	ν_{21}	B{1261 ms		1253 wsh dp	1253
B{909 s	900 vs	902 vw dp	893	ν_{22}	806 s sh †806	808 vs	808 vwshdp	840
899								
872 vsbr	862 vs	862 w p	848	ν_8	845 s sh †843	*843 vs		827
846 s sh	843 vs	843 vwsh	817	ν_9	822 vsbr †819	†819 vs	817 mw p	800

Table I.5.6   (continued)

Me₂SiHI i.r.(gas)	i.r.(liq)*	Raman(liq)	calc.	assignment	Me₂SiDI i.r.(gas)	i.r.(liq)	Raman(liq)	calc.
B{777 m / 768	772 m	773 w dp	783	ν_{23}	B{772 w / 763	*767 m	767 w dp	772
697 s	694 s	694 mw p	700	ν_{24}	708 wsh	*705 mw	706 vw dp	699
~710 wsh			711	-ν_{11}	526 s	*522 ms	522 mw p	524
		668 wsh		$2\nu_{12}$	682 mwsh†659 m		653 vwsh p?	
656 mw	655 m	656 mw p	652	ν_{10}	667 m	*671 s	762 m p	675
637 mw	634 m	634 wsh dp	643	ν_{25}	526 s	*522 ms	522 mw p	507
486 vw	~490 vwbr	490 vw p / 392 vvw		$\nu_{12}+\nu_{26}$ / $\nu_{13}+\nu_{26}$			488 vw p?	
~350 sh	335 s	337 vs p	336	ν_{12}	342	*329 m	327 vs p	327
	238 w	237 mw p	237	ν_{13}			236 mw p	236
		185 m p	184	ν_{14}			183 ms p	184
		167 sh dp	168	ν_{26}			166 msh dp	168

* neat liquid
† cyclohexane solution

266

symmetry plane. Note that in this case the two parallel bends are not equivalent with respect to the interaction term with the CSiH bending motion, one being _cis_ and the other _trans_.

The force constants are listed in Table I.5.7, and the p.e.d.'s in Tables I.5.8-11. Note that again the practice of bracketing the total contributions from the HCSi force constants (nos. 6 and 7) and the force constants defining the hydrogen deformation (nos. 8 and 9) is repeated. Generally, the agreement is quite good, except for the methyl rocks, where even with two interaction terms involving the rocking motions, it was not possible to reproduce the observed ordering of the a' and a" rocks. However, so much mixing is taking place (the perpendicular HCSi motion contributes more than 20% of the potential energy in eight or nine normal modes) that this is not too serious a drawback in the context of the overall assignment.

As with the two previous calculations and that for the methylsilanes themselves, there was extensive mixing of CSiH and HCSi motions, which produces an approximately equal mixture of both for the highest a' rocking mode and the symmetric SiH bend. In fact, if the refinement was allowed to continue to the mathematical "best fit", these assignments reversed, albeit marginally. The large value of the inter- action term between CSiH and the HCSi angle _cis_ to it was necessary to keep these assignments in the correct order. The fSiX/CSiX interaction term was used only for the heavier

Table I.5.7   Force constant values for the series Me$_2$SiHX

	Me$_2$SiHF	Me$_2$SiHCl	Me$_2$SiHBr	Me$_2$SiHI	
1	f CH	477.30	476.35	475.76	475.31	f CH
2	f SiH	271.37	272.46	272.67	272.02	f SiH
3	f SiC	277.96	272.51	278.39	273.57	f SiC
4	f SiX	482.00	241.54	183.19	129.28	f SiX
5	f HCH	47.90	49.46	50.46	49.68	f HCH
6	f HCSi⊥	34.19	35.00	34.88	39.76	f HCSi⊥
7	f HCSi‖	54.35	51.22	48.84	47.23	f HCSi‖
8	f CSiH	57.50	56.32	54.49	52.68	f CSiH
9	f HSiX	59.67	56.10	53.90	44.43	f HSiX
10	f CSiC	90.66	69.37	61.61	57.81	f CSiC
11	f CSiX	46.62	57.95	64.65	72.36	f CSiX
12	f CH/CH	5.56	5.63	5.48	5.13	f CH/CH
13	f SiC/SiC	25.02	15.13	15.50	19.85	f SiC/SiC
14	f HCH/HCH	-3.98	-2.44	-1.27	-1.80	f HCH/HCH
15	f HCSi‖/HCSi⊥	-1.97	-3.13	-1.99	-0.33	f HCSi‖/HCSi⊥
16	f HCSi‖/HCSi‖	11.19	9.50	9.50	7.75	f HCSi‖/HCSi‖
17	f CSiH/CSiH	2.60	0.90	1.45	3.42	f CSiH/CSiH
18	f CSiX/CSiX	-15.30	-3.83	2.86	14.70	f CSiX/CSiX
19	f c-HCSi/CSiH	-11.61	-13.36	-13.57	-10.69	f c-HCSi/CSiH
20	f t-HCSi/CSiH	-0.80	-2.60	-1.20	-0.07	f t-HCSi/CSiH
21	f CSiH/HSiX	3.26	2.70	3.01	0.85	f CSiH/HSiX
22	f SiC/CSiH	26.33	21.79	20.37	3.29	f SiC/CSiH
23	f SiX/HSiX	9.66	12.90	12.34	5.19	f SiX/HSiX
24	f SiX/CSiX	-	-	4.68	4.91	f SiX/CSiX
25	f SiC/SiX	12.70	-	-	-	f SiC/SiX
26	f SiC/HCSi	17.00*	17.00*	17.00*	17.00*	f SiC/HCSi

*fixed.   Units as in Table I.3.9

Table I.5.8 Potential energy distribution* among the force constants for Me$_2$SiH'F

Mode		Me$_2$SiHF	Me$_2$SiDF
ν_1	CH$_3$ str.	101(1)	101(1)
ν_2	CH$_3$ str.	101(1)	101(1)
ν_3	CH$_3$ str.	97(1)	97(1)
ν_4	SiH str.	100(2)	99(2)
ν_5	CH$_3$ def.	85(5)	85(5)
ν_6	CH$_3$ def.	89(5)	89(5)
ν_7	CH$_3$ def.	50(5)+43(7)	51(5)+43(7)
ν_8	CH$_3$ rock	27(6)+11(7){38}+23(4)+11(3)	38(7)+36(6){74}
ν_9	CH$_3$ rock	56(7)+22(6){78}+26(4)-10(16)	76(7)+25(6){101}-14(16)
ν_{10}	SiC str.	66(3)+6(13)	69(3)+6(13)
ν_{11}	SiH def.	57(9)+15(8){72}+28(7)+12(6){40}-12(23)	75(9)+27(8){102}
ν_{12}	SiX str.	43(4)+35(7)+16(9)+12(8)	66(4)+27(7)
ν_{13}	CSiC def.	72(10)+19(8)	72(10)+20(8)
ν_{14}	CSiX def.	71(11)+28(8)-23(18)+13(10)	71(11)+29(8)-24(18)+13(10)
ν_{15}	torsion	–	–
ν_{16}	CH$_3$ str.	101(1)	101(1)
ν_{17}	CH$_3$ str.	101(1)	101(1)
ν_{18}	CH$_3$ str.	98(1)	98(1)
ν_{19}	CH$_3$ def.	85(5)	86(5)
ν_{20}	CH$_3$ def.	89(5)	89(5)
ν_{21}	CH$_3$ def.	49(5)+40(7)	51(5)+44(7)
ν_{22}	CH$_3$ rock	34(7)+10(6){44}+45(8)+13(23)	46(7)+29(6){75}+13(23)+12(8)
ν_{23}	CH$_3$ rock	63(7)+32(6){96}-11(16)	76(7)+25(6){101}-14(16)
ν_{24}	SiC str.	61(3)+25(7)+11(8,20)	102(3)-9(13)
ν_{25}	SiH def.	66(8)+50(3)-33(23)+30(6)+21(7){51}	110(8)-36(23)+18(6)+16(7){34}-13(20)
ν_{26}	CSiX def.	71(11)+24(18) -24(20)+11(5)	71(11)+23(18) +10(5)
ν_{27}	torsion	–	–

* contributions >10%

Table I.5.9 Potential energy distribution[*] among the force constants for Me$_2$SiH'Cl

Mode		Me$_2$SiHCl	Me$_2$SiDCl
ν_1	CH$_3$ str.	101(1)	101(1)
ν_2	CH$_3$ str.	101(1)	101(1)
ν_3	CH$_3$ str.	97(1)	97(1)
ν_4	SiH str.	100(2)	99(2)
ν_5	CH$_3$ def.	89(5)+5(7)	89(5)
ν_6	CH$_3$ def.	92(5)+5(14)	92(5)
ν_7	CH$_3$ def.	52(5)+40(7)+7(16)-7(19)	53(5)+42(7)
ν_8	CH$_3$ rock	41(7)+16(6){57}+16(9)+15(8){31}+12(23)	42(6)+34(7){76}
ν_9	CH$_3$ rock	46(7)+36(6){82}	82(7)+15(6){97}-15(16)
ν_{10}	SiC str.	66(3)+4(13)+10(6)+8(4)	72(3)+4(13)+9(4)
ν_{11}	SiH def.	57(9)+18(8){75}+41(7)+5(6){46}-16(23)	65(9)+32(8){97}-14(23)+11(7){15}
ν_{12}	SiX str.	81(4)+7(3)	75(4)+8(9)+7(3)
ν_{13}	CSiC def.	71(10)+21(8)-8(23)	72(10)+21(8)
ν_{14}	CSiX def.	64(11)+17(8)+10(10)+9(4)	64(11)+17(8)+9(10)
ν_{15}	torsion	—	—
ν_{16}	CH$_3$ str.	101(1)	101(1)
ν_{17}	CH$_3$ str.	101(1)	101(1)
ν_{18}	CH$_3$ str.	97(1)	97(1)
ν_{19}	CH$_3$ def.	89(5)+5(7)	89(5)
ν_{20}	CH$_3$ def.	92(5)+5(14)	92(5)+5(14)
ν_{21}	CH$_3$ def.	49(5)+36(7)+8(6)+7(16,23)	53(5)+40(7)+8(6)
ν_{22}	CH$_3$ rock	33(7)+13(6){46}+41(8)+13(23)	37(6)+31(7){68}+12(23)+11(8)
ν_{23}	CH$_3$ rock	63(7)+30(6){93}-10(16)	90(7)+15(6){105}-16(16)
ν_{24}	SiC str.	74(3)-4(13)+18(7)	102(3)-6(13)
ν_{25}	SiH def.	69(8)-42(23)+32(3)+30(6,7){60}-16(20)+13(5)-10(19)	107(8)-43(23)+18(7)+17(6){35}
ν_{26}	CSiX def.	91(11)	91(11)
ν_{27}	torsion	—	—

[*] contributions >5%

Table I.5.10 Potential energy distribution* among the force constants for Me₂SiH'Br

Mode		Me₂SiHBr	Me₂SiDBr
ν_1	CH₃ str.	101(1)	101(1)
ν_2	CH₃ str.	101(1)	101(1)
ν_3	CH₃ str.	97(1)	97(1)
ν_4	SiH str.	100(2)	99(2)
ν_5	CH₃ def.	91(5)	91(5)
ν_6	CH₃ def.	94(5)	94(5)
ν_7	CH₃ def.	52(5)+37(7)	53(5)+38(7) {76}
ν_8	CH₃ rock	33(7)+12(6){45}+41(8)+13(23)	43(6)+33(7) {100}
ν_9	CH₃ rock.	55(7)+33(6){88}	86(7)+14(7){100}-16(16)
ν_{10}	SiC str.	65(3)+4(13)+11(6)	77(3)+4(13)
ν_{11}	SiH def.	53(9)+17(8){70}+45(7){47}-15(23) +13(3)	70(9)+34(8){104}-16(23)+12(7){16}
ν_{12}	SiX str.	77(4)+13(11)	75(4)+13(11)
ν_{13}	CSiC def.	69(10)+23(8)	69(10)+23(8)
ν_{14}	CSiX def.	52(11)+19(4)+10(8)	53(11)+19(4)+10(8)
ν_{15}	torsion	–	–
ν_{16}	CH₃ str.	101(1)	101(1)
ν_{17}	CH₃ str.	101(1)	101(1)
ν_{18}	CH₃ str.	98(1)	98(1)
ν_{19}	CH₃ def.	91(5)	91(5)
ν_{20}	CH₃ def.	94(5)	94(5)
ν_{21}	CH₃ def.	50(5)+33(7)	53(5)+37(7)
ν_{22}	CH₃ rock	40(7)+15(6){55}+16(9)+15(8){31}	36(6)+32(7){68}+12(23)+11(8)
ν_{23}	CH₃ rock	45(7)+37(6){82}+12(23)	88(7)+15(6){103}-16(16)
ν_{24}	SiC str.	86(3)-5(13)+15(7)	100(3)-6(13)
ν_{25}	SiH def.	75(8)-48(23)+46(7)+27(6){73}+16(3) +11(5)-11(20)	109(8)-46(23)+23(7)+17(6){40}+10(5)
ν_{26}	CSiX def.	102(11)	101(11)
ν_{27}	torsion	–	–

* contributions >10%

Table I.5.11 Potential energy distribution* among the force constants for Me₂SiH'I

Mode		Me₂SiHI	Me₂SiDI
ν_1	CH₃ str.	101(1)	101(1)
ν_2	CH₃ str.	101(1)	101(1)
ν_3	CH₃ str.	98(1)	98(1)
ν_4	SiH str.	100(2)	99(2)
ν_5	CH₃ def.	91(5)	91(5)
ν_6	CH₃ def.	93(5)	93(5)
ν_7	CH₃ def.	53(5)+36(7)+11(6)	53(5)+36(7)+11(6)
ν_8	CH₃ rock	46(7)+18(6){64}+14(8)+12(9){26}+10 (23)	57(6)+25(7){82}
ν_9	CH₃ rock	41(6)+37(7){78}	94(7){98}-15(16)
ν_{10}	SiC str.	57(3)+4(13)+12(9)	77(3)+6(13)
ν_{11}	SiH def.	34(9)+13(8){47}+44(7){44}+23(3)	54(9)+36(8){90}+12(7){15}-11(23)
ν_{12}	SiX str.	56(4)+27(11)	54(4)+26(11)
ν_{13}	CSiC def.	66(10)+18(8)	65(10)+18(8)+10(9)
ν_{14}	CSiX def.	34(11)+7(10,18)+41(4)	34(11)+7(10,18)+41(4)
ν_{15}	torsion	—	—
ν_{16}	CH₃ str.	101(1)	101(1)
ν_{17}	CH₃ str.	101(1)	101(1)
ν_{18}	CH₃ str.	98(1)	98(1)
ν_{19}	CH₃ def.	92(5)	92(5)
ν_{20}	CH₃ def.	93(5)	93(5)
ν_{21}	CH₃ def.	51(5)+34(7)+11(8)	53(5)+13(7)+11(6)
ν_{22}	CH₃ rock	29(7)+14(6){43}+41(8)+11(23)	40(6)+28(7){68}-10(3,8)
ν_{23}	CH₃ rock	60(7)+35(6){95}	92(7)+13(6){105}-14(16)
ν_{24}	SiC str.	86(3)-6(13)+12(6,7)	94(3)-7(13)
ν_{25}	SiH str.	63(8)+45(7)+10(6){55}-27(23)+13(3)	101(8)-26(23)+18(7){26}
ν_{26}	CSiX def.	123(11)-25(18)	123(11)-25(18)
ν_{27}	torsion	—	—

* contributions >10%

halides, where the Si-X stretch was heavily mixed with the skeletal deformations. This phenomenon is common for iodo-derivatives of the methylsilanes[50], but is thought not to be significant for the chloride and fluoride. The value for fSiC/HCSi was chosen from the value calculated for the methylsilanes.

I.5.5   Discussion

The assignment derived above from the comparison with other molecules and the NCA is in disagreement with the work of Durig and Hawley[66], and Kriegsmann and Engelhardt[71]. With respect to the former study, the differences is assign-ment are considerable; apart from the CH_3 stretching and deformation modes, two of the CH_3 rocking modes and the a' SiH bend, all other modes are in disagreement. The other report on Me_2SiHCl[71] agrees a little better in that the a' SiC_2 stretch is assigned to the strong, polarised band at 670 cm^{-1}, but the a" SiC_2 is again assigned to the 776 cm^{-1} band, and the a' SiH bend, is in this case assigned to the highest frequency band at 901 cm^{-1}. The polarised band at 722 cm^{-1}, to which this latter mode is assigned here, is reported without comment. This assignment will not be discussed further. The most immediately obvious disparity between this work and Durig's report is in the assignment of the strong, polarised bands at about 660 cm^{-1} in all compounds as methyl rocking modes. As can be seen from Me_nSiX_{4-n} (n = 1-4) compounds, methyl rocks are notoriously weak in the Raman effect. Indeed, the strongest rock in the Me_2SiI_2

spectrum in the same report is only about 2% of the intensity of the symmetric CH_3 stretching band. Yet in Me_2SiHI, the strongest band in the region (16% relative intensity) is assigned as a rock. This is taken to an extreme in the fluoride, where the second most intense band, 86% of the intensity of the symmetric CH_3 stretching band, is assigned as the rock, while the two Si-C stretches are assigned to equally intense weak bands (4% relative intensity). This chosen value for a methyl rock is also extremely low, being little higher than the CD_3 rocks observed in the deuteromethyl derivatives studied here, and in $(CD_3)_3SiCl$[84]. This assignment calls for a splitting of the rocks of over 240 cm^{-1}, compared to the reported splitting for Me_2SiI_2 of 140 cm^{-1}, although this in fact becomes less than 100 cm^{-1} if the assignment of the 705 cm^{-1} band is accepted as the asymmetric stretch. The argument given for this increased splitting is that it is consistent with the rocking frequencies observed for propane[31]. This seems a dubious choice indeed for a comparative molecule. Intuitively it also seems improbable that the replacement of of an iodine atom by hydrogen would cause the lowest frequency methyl rock to decrease in wavenumber by over 100 cm^{-1}. While the placement of ν_{24} at ca. 775 cm^{-1} is not too unreasonable considering there was no isotopic data available, and in fact was even considered in this study, the assignment of the symmetric SiH bend to a very weak Raman band (which is not reported in the Raman spectrum of Me_2SiHBr) and a strong infrared feature is perhaps a surprising choice on the grounds

of expected intensity. This band at 829 cm^{-1} in the iodide, was also not observed in either the infrared or Raman spectra recorded in this work.

The assignment of the strongest band in the 1000-500 cm^{-1} region to a methyl rock means that the a' SiC stretch must be assigned elsewhere. The polarised band assigned in this work as the a' SiH bend is chosen, and the SiH bend assigned to one of the weaker features above 800 cm^{-1}, although not to a consistent frequency throughout the series (viz. 829 cm^{-1} (I), 840 (Br), 842 (Cl) and 815 cm^{-1} (F)).

There is disagreement, too, in the ordering of the skeletal bending fundamentals, in which the two a' modes are reversed; in Durig's report, the CSiC deformation, ν_{13}, is placed between the two CSiX deformations (although there is some confusion over the ordering for the bromide where the text and the table are not consistent). The CSiC deformation in Me$_2$SiH$_2$ has a value of 223 cm^{-1} [30], and the CSiX deformation in MeSiH$_2$X, where these are the only skeletal deformations possible, occur at frequencies of 176 (I), 192 (Br), 213 (Cl) and 263 cm^{-1} (F). This, together with the observation that the lowest two bands increase in wavenumber more rapidly than does the highest, points to them probably involving the halogen atom, whereas ν_{13} is expected to be less sensitive to a change in substituent, and is thus assigned to the band at ca. 250 cm^{-1} in the iodide, bromide and chloride. On the basis of mass, it seems unlikely that in the iodide and bromide the two CSiX deformations should be at

higher wavenumber than the CSiC deformation. Moreover, from
the point of view of intensity, the a' CSiX deformation might
also be expected to give rise to a stronger band than the
CSiC band in the Raman effect. In the fluoride, the polar-
isation data give no firm clues, and the frequency agreement
is not convincing for any assignment, except to note that
with the more rapid increase in wavenumber of the a" CSiX
deformation with lighter halogen substituent, compared to its
a' mode, and their near coincidence in the chloride, these
two modes may be expected to be reversed in the fluoride.
Here the assignment is made on the basis of the NCA, where
for the preferred assignment, i.e. with the CSiC deformation
at highest frequency, the force constants $\underline{f}$CSiC, $\underline{f}$CSiF and
$\underline{f}$CSiF/CSiF all continue general trends from the other com-
pounds (Table I.3.7). Although a warning has been given
concerning the camparison of bending force constants of
chemically related though structurally different molecules
(Chapter 1.5), the value of $\underline{f}$CSiF is found to be only a little
lower than that in CH_3SiH_2F and CH_3SiF_3 and like the value of
$\underline{f}$CSiF/CSiF in the latter compound, the interaction term is
large (approximately 1/3 of $\underline{f}$CSiF) and negative. If the
observation of an A-type band in the infrared spectrum of
Me_2SiHF in the CsI region is taken as proof that the highest
frequency in this region is an a' mode, then placing the two
CSiF deformations above the CSiC mode, as Durig and Hawley[70]
did, calls for a reversal of the expected ordering of the two
CSiF modes, and changes in the force constant values which

then deviate significantly from those in the other compounds. In order to match this ordering, $\underline{f}$CSiC requires a value of 46.1 (cf. 69.4 (Cl), 61.6 (Br) and 57.8 (I)), $\underline{f}$CSiX becomes 70.4 (cf. 58.0 (Cl), 64.7 (Br) and 72.4 (I)), and $\underline{f}$CSiX/CSiX takes on a positive value of 8.5 (cf. -3.8 (Cl), 2.9 (Br) and 14.7 (I)).

REFERENCES

1. S. Kaye and S. Tannembaum, <u>J. Org. Chem.</u> <u>18</u>, 1750 (1953).

2. M. Randić, <u>Spectrochim. Acta</u> <u>18</u>, 115 (1962).

3. R.E. Wilde, <u>J. Mol. Spectrosc.</u> <u>8</u>, 427 (1962).

4. D.F. Ball, T. Carter, D.C. McKean and L.A. Woodward, <u>Spectrochim. Acta</u> <u>20</u>, 1721 (1964).

5. I.F. Kovalev, <u>Opt. i Spektr.</u> <u>8</u>, 315 (1960); <u>Opt. Spectry.</u> <u>8</u>, 166 (1960)

6. K. Ohno, M. Hayaslin and H. Murata, <u>J. Sci. Hiroshima Univ., Ser. A</u> <u>36</u>, 121 (1972).

7. R.J. Oullette, <u>J. Amer. Chem. Soc.</u> <u>94</u>, 7674 (1972).

8. J.L. Duncan, <u>Spectrochim. Acta</u> <u>20</u>, 1807 (1964).

9. I.F. Kovalev, <u>Opt. i Spektr.</u> <u>4</u>, 560 (1958); Yu. I. Ponomarev, I.F. Kovalev and V.A. Orlov, <u>ibid.</u> <u>23</u>, 483 (1967); <u>Opt. Spectry.</u> <u>23</u>, 258 (1967).

10. J.A. Lannon, G.S. Weiss and E.R. Nixon, <u>Spectrochim. Acta</u> <u>26A</u>, 221 (1970).

11. E.A. Clark and A. Weber, <u>J. Chem. Phys.</u> <u>45</u>, 1759 (1966).

12. A.E. Finholt, A.C. Bond, Jr., K.E. Wilzbach and H.I. Schlesinger, <u>J. Amer. Chem. Soc.</u> <u>69</u>, 1199, 2692 (1947).

13. G.W. Bethke and M.K. Wilson, <u>J. Chem. Phys.</u> <u>26</u>, 1107 (1956).

14. A. Stock, <u>Z. Elektrochem.</u> <u>32</u>, 341 (1926); A. Sujishi and S. Witz, <u>J. Amer. Chem. Soc.</u> <u>76</u>, 4631 (1954).

15. D.F. Shriver, "The Manipulation of Air-Sensitive Compounds", McGraw-Hill, New York, N.Y., (1969); p. 282.

16. R.W. Peterson and T.H. Edwards, <u>J. Mol. Spectrosc.</u> <u>38</u>, 1 (1971).

17. G.P. van der Kelen, O. Volders, H. van Onckelen and Z. Eeckhaut, <u>Z. anorg. allgem. Chem.</u> <u>338</u>, 106 (1965).

18. W.C. Steele, L.D. Nicholls and F.G.A. Stone, <u>J. Amer. Chem. Soc.</u> <u>84</u>, 4441 (1962); F.E. Saalfeld and H.J. Svec, <u>J. Phys. Chem.</u> <u>70</u>, 1753 (1966).

19. D.M. Golden and S.W. Benson, _Chem. Rev._ 69,125 (1969).

20. K.A. Gingerich, _J. Chem. Phys._ 54,3720 (1971).

21. P.L. Timms, R.A. Kent, T.C. Ehlert and J.L. Margrave, _J. Amer. Chem. Soc._ 87,2824 (1965).

22. R.L. Jenkins, A.J. Vanderwielen, S.P. Ruis, S.R. Gird and M.A. Ring, _Inorg. Chem._ 12,2968 (1973) and references therein.

23. D.I. Bradshaw, R.B. Moyes and P.B. Wells, _Can. J. Chem._ 54,599 (1976).

24. D.H. Liskow and H.F. Schaeffer, _J. Amer. Chem. Soc._ 94, 6641 (1972).

25. L. Pauling, "_Nature of the Chemical Bond_," 3rd. Ed., Cornell Univ. Press, Ithaca, N.Y., 1960.

26. A.P. Altshuller and L. Rosenblum, _J. Amer. Chem. Soc._ 77,272 (1955).

27. R.W. Kilb and L. Pierce, _J. Chem. Phys._ 27, 108 (1957).

28. D.C. McKean, _Spectrochim. Acta_ 29A,1559 (1973).

29. J.E. Griffiths, _J. Chem. Phys._ 38,2879 (1963).

30. D.F. Ball, P.L. Goggin, D.C. McKean and L.A. Woodward, _Spectrochim. Acta_ 16,1358 (1960).

31. T. Shimanouchi, "_Tables of Molecular Vibrational Frequencies, Consolidated Vol. I_," NSRDS-NBS 39, 1972, and references therein.

32. R.L. Collins and J.R. Nielsen, _J. Chem. Phys._ 23,351(1955)

33. J Goubeau, H. Siebert, and M. Winterwerb, _Z. anorg. allgem. Chem._ 259,240(1949).

34. T. Shimanouchi, I. Tsuchiya and Y. Mikawa, _J. Chem. Phys._ 18,1306 (1950).

35. A.L. Smith, _J. Chem. Phys._ 21,1997 (1953).

36. H. Murata and S. Hayashi, _J. Chem. Phys._ 19,1217 (1951).

37. J.R. Aronson and J.R. Durig, _Spectrochim. Acta_ 20,219 (1964).

38. D.F. Van de Vondel and G.P. Van der Kelen, _Bull. Soc. Chim. Belges_ 74,453 (1965).

39. D.F. Van de Vondel, G.P. Van der Kelen and G. Van Hooydonk, *J. Organomet. Chem.* 23,431 (1970).

40. J.W. Anderson, G.K. Barker, J.E. Drake and R.T. Hemmings, *Can. J. Chem.* 49,2931 (1971).

41. J.R. Durig, C.F. Jumper and J.N. Willis, *J. Mol. Spectry.* 37,260 (1971).

42. J.W. Anderson, G.K. Barker, A.J.F. Clark, J.E. Drake and R.T. Hemmings, *Spectrochim. Acta* 30A,1081 (1974).

43. H.H. Anderson, *J. Amer. Chem. Soc.* 73,2351 (1951).

44. E.V. Van den Berghe and G.P. Van der Kelen, *J. Organometal. Chem.* 59,175 (1973).

45. A.J.F. Clark and J.E. Drake, *Spectrochim. Acta* 32A,1419 (1976).

46. E.A. Jones, J.S. Kirby-Smith, P.J.H. Woltz and A.H. Nielsen, *J. Chem. Phys.* 19,242 (1951).

47. E.W. Kifer and C.H. Van Dyke, *Inorg. Chem.* 11,404 (1972).

48. L. Pierce, *J. Chem. Phys.* 29,383 (1958).

49. B. Glavinčevski, private communication (1979).

50. The author, unpublished observations.

51. L.G.L. Ward and A.G. MacDiarmid, *J. Amer. Chem. Soc.* 82,2151 (1960); M. Abedini and A.G. MacDiarmid, *Inorg. Chem.* 2,608 (1963).

52. E.A.V. Ebsworth and S.G. Frankiss, *Trans. Faraday Soc.* 59,1518 (1963).

53. E.A.V. Ebsworth and S.G. Frankiss, *Trans. Faraday Soc.* 63,1574 (1967).

54. H. Schmidbaur, *Ber.* 97,1639 (1964).

55. R.T. Hemmings, Ph.D. thesis, University of Windsor, 1973.

56. A.N. Egorochkin, A.I. Burov, V.F. Mironov, T.K. Gar and N. Vyazankin, *Dokl. Akad. Nauk SSSR* 180,861 (1968).

57. H. Schmidbaur and I. Ruidisch, *Inorg. Chem.* 3,599 (1964).

58. L.E. Levchuk, J.R. Sams and F. Aubke, *Inorg. Chem.* 11,43 (1972).

59. M.L. Delwaulle, J. Phys. Chem. 56,355 (1952); M.L. Delwaulle and F. François, J. Phys. Radium 15,206 (1954).

60. H. Bürger, Organometal. Chem. Rev. A 3,425 (1968); Spectrochim. Acta 24A,2013 (1968)

61. Tables of Interatomic Distances and Configuration in Molecules and Ions, Special Publications 11 and 18, The Chemical Society, London, 1958 and 1965.

62. J. Sheridan and W. Gordy, Phys. Rev. 77,719 (1950).

63. A.L. Smith and N.C. Angelotti, Spectrochim. Acta 15,412 (1959); H.W. Thompson, Spectrochim. Acta 16,238 (1960); C.F. Attridge, J. Organomet. Chem. 13,259 (1968); A.N. Egorochkin and N.S. Vyazankin, Dokl. Akad. Nauk SSSR 193,590 (1970); M.G. Voronkov, T.V. Kashik and N.I. Shergina, Dokl. Akad. Nauk SSSR 232,817 (1977) and refs. therein.

64. E.A.V. Ebsworth. M. Onyszchuk and N. Sheppard, J. Chem. Soc. 1958,1453.

65. Z. Meić, A. Braun, H. Knehr and W. Zeil, Ber. 78,1249 (1974).

66. J.R. Durig and C.W. Hawley, J. Chem. Phys. 59,1 (1973).

67. H. Eméleus, M. Onyszchuk and W. Kuchen, Z. anorg. allgem. Chem. 283,74 (1956).

68. H. Murata, Nippon Kagaku Zasshi 73,465 (1952).

69. R. Ulbrich, Z. Naturforsch. 9b,380 (1954).

70. J.R. Durig and C.W. Hawley, J. Chem. Phys. 58,237 (1973).

71. H. Kriegsmann and G. Engelhardt, Z. anorg. allgem. Chem. 310,320 (1961).

72. L.G.L. Ward and A.G. MacDiarmid, J. Amer. Chem. Soc. 82,2151 (1960); M. Abedini and A.G. MacDiarmid, Inorg. Chem. 2,608 (1963).

73. E. Wiberg and E. Amberger, "Hydrides of the Elements of Main Groups I-IV," Elsevier, Amsterdam, 1971; p.517.

74. J.E. Drake and J. Simpson, Inorg. Nucl. Chem. Letters 2,219 (1966).

75. E.A.V. Ebsworth and H.J. Eméleus, J. Chem. Soc. 1958, 2150.

76. A. Stock and C. Somieski, _Ber._ 50, 1739 (1917); A. Sujishi and S. Witz, _J. Amer. Chem. Soc._ 76, 4631 (1954).

77. H.J. Emeleus and M. Onyszchuk, _J. Chem. Soc._ 1958, 604.

78. D.F. Heath, J.W. Linnett and P.J.Wheatley, _Trans. Faraday Soc._ 46, 137 (1950); D.F. Ball and D.C. McKean, _Spectrochim. Acta_ 18, 1019 (1962).

79. H. Burger, private communication.

80. G.K. Barker, J.E. Drake, R.T. Hemmings and B. Rapp, _J. Chem. Soc._ A1971, 3291.

81. L.W. Baasch, C.Y. Liang and J.R. Nielsen, _J. Chem. Phys._ 22, 1293 (1954).

82. B. Glavincevski, Ph.D. dissertation, University of Windsor, 1978.

83. H. Burger, U. Goetze and W. Sawodny, _Spectrochim. Acta_ 24A, 2003 (1968).

84. F. Hofler, _Z. Naturforsch._ 27a, 760 (1972).

85. H. Kriegsmann, _Z. Elektrochem._ 62, 1033 (1958).

PART II

II.1 INTRODUCTION

Interest in the second and third row elements of Group V comes as a natural progression from the study of nitrogen compounds in many different areas of chemistry. Ammonia[1] and arsine[2], in fact were the first hydride compounds known, over three hundred years ago. As far as organo- and hydrido-derivatives of phosphorus and arsenic are concerned, interest is focussed in three main areas: their ability as Lewis bases to form addition compounds, principally with Group III compounds[3a,3b]; the spectroscopic determination of barriers to pyramidal inversion[4a,4b]; and their use as complexing agents, mainly as bridging groups, in transition metal compounds[5,6a,6b]. Methylated derivatives of Group V have been extensively used in these, and many other, areas of investigation. Indeed, recent studies have even found bacteria which produce dimethylarsine (anaerobically) and trimethylarsine (aerobically) from arsenic (V) compounds[7].

Prior to the beginning of this work, almost all of the methyl derivatives of the first three rows had been studied spectroscopically. In the case of the amines, several reports have appeared for monomethyl-[8,9] and trimethyl-amine[8,10,11], but mostly on dimethylamine[8,12-15], and it is clear that there was some confusion in assigning the modes involving the deformations of the hydrogen atom(s) attached to nitrogen. In contrast, for the corresponding phosphine and arsine compounds it was the methylphosphine[16-18] and

-arsine[19], and particularly the trimethylphosphine[11,20-25] and -arsine[11,20,22,26,27] derivatives which received most attention. The only vibrational study on the dimethyl derivatives was a relatively early report on dimethylphosphine[28], with an incomplete Raman spectrum, and with what now appears to have been an impure sample, due to the number of unexplained bands. In view of the fairly widespread use of dimethylarsine as starting material in the formation of complexes[29], it was indeed surprising that no vibrational study had appeared in the literature. Because of this, and since there was little correlation between the report on dimethylphosphine with spectra obtained here of dimethylarsine, it was decided to study the vibrational spectra of both dimethyl derivatives to complete the series. In order to properly assign the hydrogen deformation modes, which as in the case of dimethylamine were the least predictable, and probably the most important vibrations if studies of possible hydrogen bonding were to be carried out, it was thought necessary to include the deuterated forms $(CH_3)_2AsD$ and $(CH_3)_2PD$. The information derived from the frequency shifts in the $-d_1$ analogues enables a complete assignment to be made for both molecules thus completing the series of methylated amines, phosphines and arsines which have had their vibrational spectra satisfactorily described. (Towards the end of this work, a report of the vibrational spectra of $(CH_3)_2PH$ and $(CD_3)_2PH$ appeared[30], but on close examination this is also thought to be incorrect,
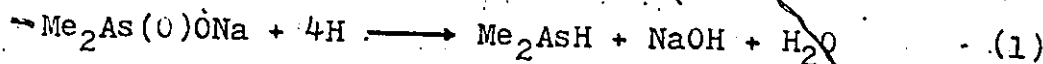
as it is attempted to show in the Discussion).

II.2 DIMETHYLARSINE

II.2.1 Preparation

Dimethylarsine was most conveniently prepared by the in situ reduction[31] of sodium dimethylarsonate (sodium cacodylate) (equation 1). A three-necked round-bottomed

$$Me_2As(O)ONa + 4H \longrightarrow Me_2AsH + NaOH + H_2O \qquad (1)$$

flask was charged with an aqueous solution of the cacodylate, a quantity of fine zinc powder and a Teflon covered magnetic stirring bar. A dropping funnel containing concentrated hydrochloric acid was added to the flask and the apparatus attached to the vacuum line. After the solution had been degassed, the mixture was stirred and a small quantity (ca. 1 ml) of acid added. The gases produced were allowed into the manifold and the tap to the reaction flask was closed. The gases were then passed through a train of U-traps held at $-45^{\circ}C$, $-78^{\circ}C$ and $-196^{\circ}C$. Any hydrogen formed was pumped out through the U-traps before the process was repeated. Water was found in the $-45^{\circ}C$ trap and dimethylarsine in the trap at $-78^{\circ}C$. The trap at $-196^{\circ}C$ was to prevent any dimethylarsine from being carried into the pump by entrainment with the hydrogen as it was being pumped away. Any water appearing in the $-78^{\circ}C$ fraction —water and dimethylarsine are immiscible— again by entrainment was removed by further fractional distillation.

The [1]H n.m.r. spectrum (Figure II.1A) shows the expected doublet and septet, at $\delta 0.98\pm0.01$ and $\delta 2.40\pm0.01$
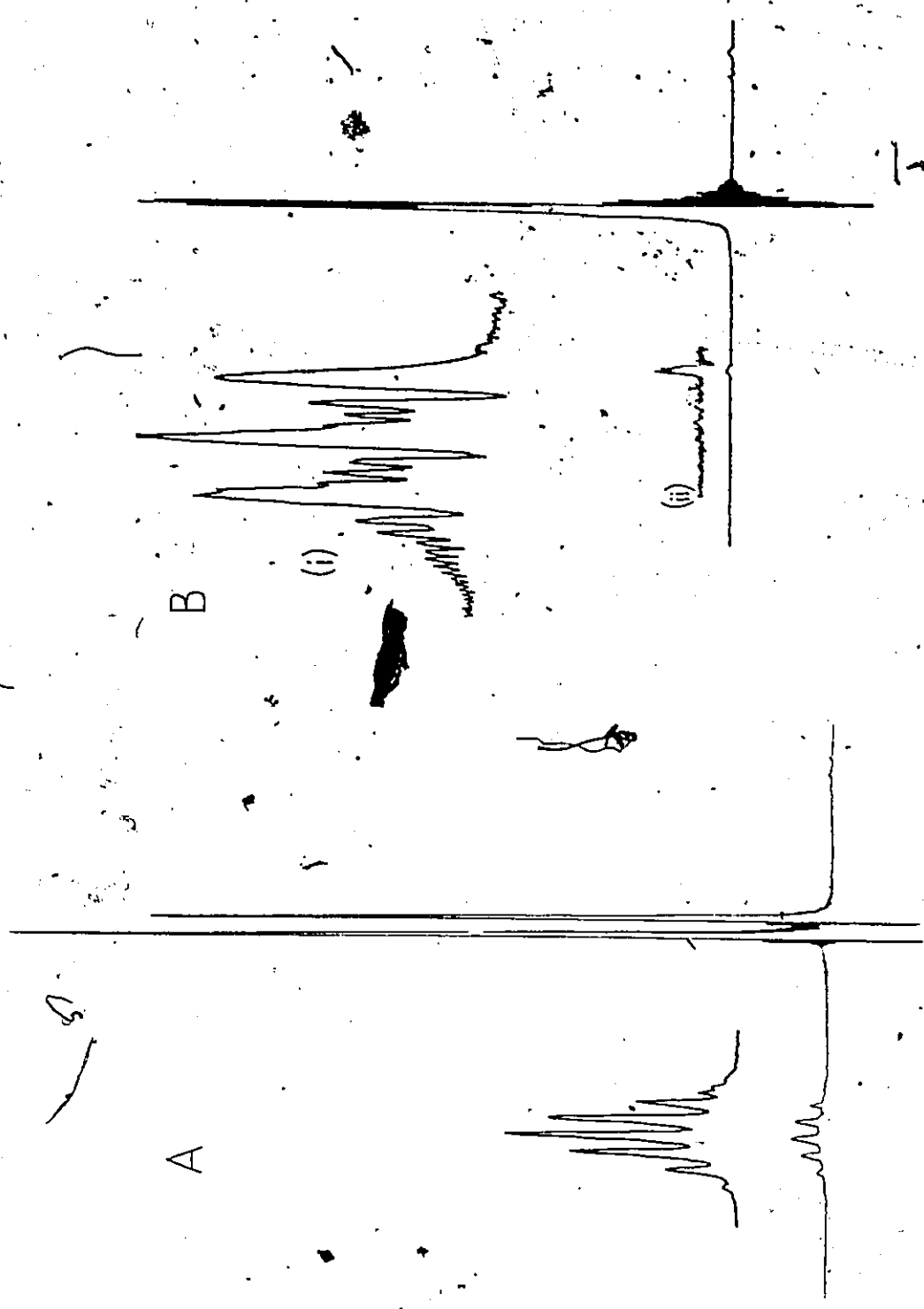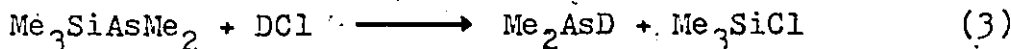
Figure II.1 ^1H n.m.r. spectra of (A) $(CH_3)_2AsH$ and (B) $(CH_3)_2AsD$

ppm respectively, with observed coupling constants J_{HH}: 6.95±0.02 Hz and J_{CH} 131.3±0.2 Hz (high field signal only; the low field signal is under the As$\underline{H}$ signal).

The d_1 analogue was prepared by two general methods: the cleavage of $Me_3SiAsMe_2$[32] (from another experiment) by D_2O or DCl[33], and the exchange equilibrium between dimethyl-arsine and KOD in D_2O[34]. In fact both were used, the latter to increase the deuterium content of products from the former reaction to more than 98.5 mol.% before recording spectra. Although the more convenient method was the first reaction with D_2O (equation 2), the similar volatilities of the

$$2Me_3SiAsMe_2 + D_2O \longrightarrow 2Me_2AsD + (Me_3Si)_2O \quad (2)$$
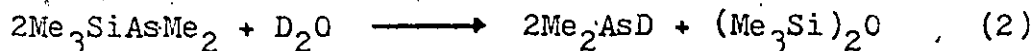
products made a clean separation by trap-to-trap distillation virtually impossible. This was overcome by using DCl (equation 3). Deuterium chloride was condensed onto a stoichio-

$$Me_3SiAsMe_2 + DCl \longrightarrow Me_2AsD + Me_3SiCl \quad (3)$$

metric excess of trimethylsilyldimethylarsine and the mixture allowed to warm. The products and excess starting material were then separated by trap-to-trap distillation.

The exchange equilibrium was set up by pouring about 1 ml (ca. 50 mmol) of deuterium oxide into a 100 ml two-necked, round bottomed reaction vessel. The liquid was degassed and the flask filled with a positive pressure of dry nitrogen through the manifold. The stopper in the second neck was removed and a small piece of potassium, washed in low boiling point petroleum ether, was held in the opening until dried by the nitrogen stream, and then dropped

into the water. The stopper was replaced, the resulting gases pumped off, and a sample of dimethylarsine (1-2 mmol) was condensed into the vessel. After shaking for a few minutes the flask was cooled in an ice/salt bath (to reduce the vapour pressure of the water), opened and the resulting vapours separated by trap-to-trap distillation. This process was repeated as necessary until a sufficiently high deuterium content (minimum 98 mol.%) was obtained.

The ^{1}H n.m.r. spectrum of dimethylarsine-d$_1$ showed the expected 1:1:1 triplet (Figure II.1B) expanded x20 in (i) at δ 0.98±0.01 ppm with a J_{HD} equal to 1.09±0.05 Hz. The insert (ii) in Figure II.1B shows the resonance due to residual AsH along with the low field ^{13}C satellite.

Mass spectra were recorded for both compounds at an ionising potential of 70 eV. The computer tracings are shown in Figures II.2 and II.3. Both showed a base peak at m/e 90 (MeAs$^-$) and fairly intense molecular ions; 50% of the base peak for Me$_2$AsH (m/e 106) and 34% for Me$_2$AsD (m/e 107). There was virtually no sign of an M-H(D) peak in either spectrum.

II.2.2 Vibrational Spectra

Infrared spectra were recorded at pressures ranging from 10 to 92 mm Hg, and Raman spectra on the neat liquid. The spectra are shown in Figures II.4 and II.5, and are assigned on the basis of C$_s$ symmetry, giving rise to 24 fundamentals, 13 of which are a' and eleven a" modes. All modes are both infrared and Raman active, with the a' modes

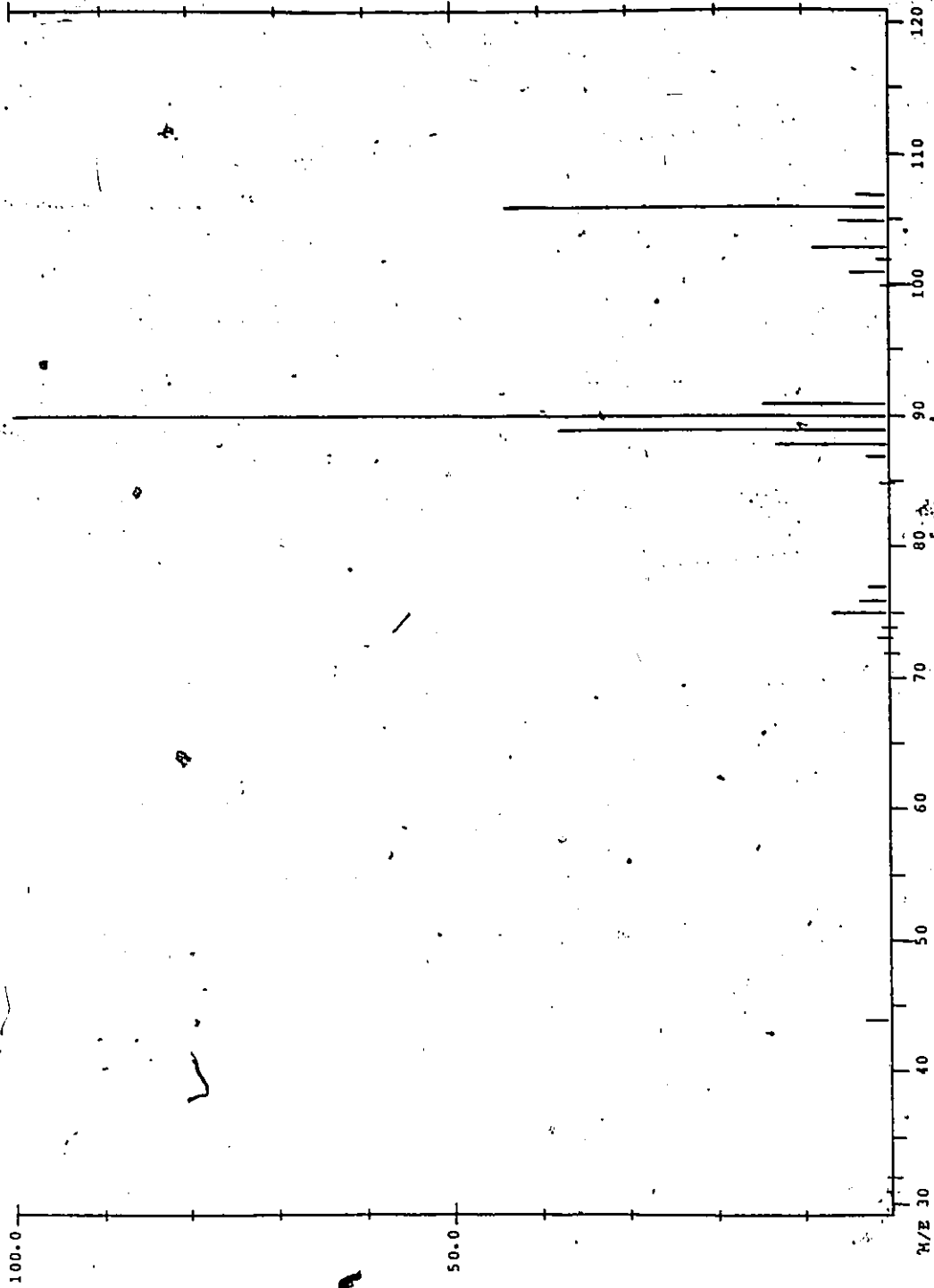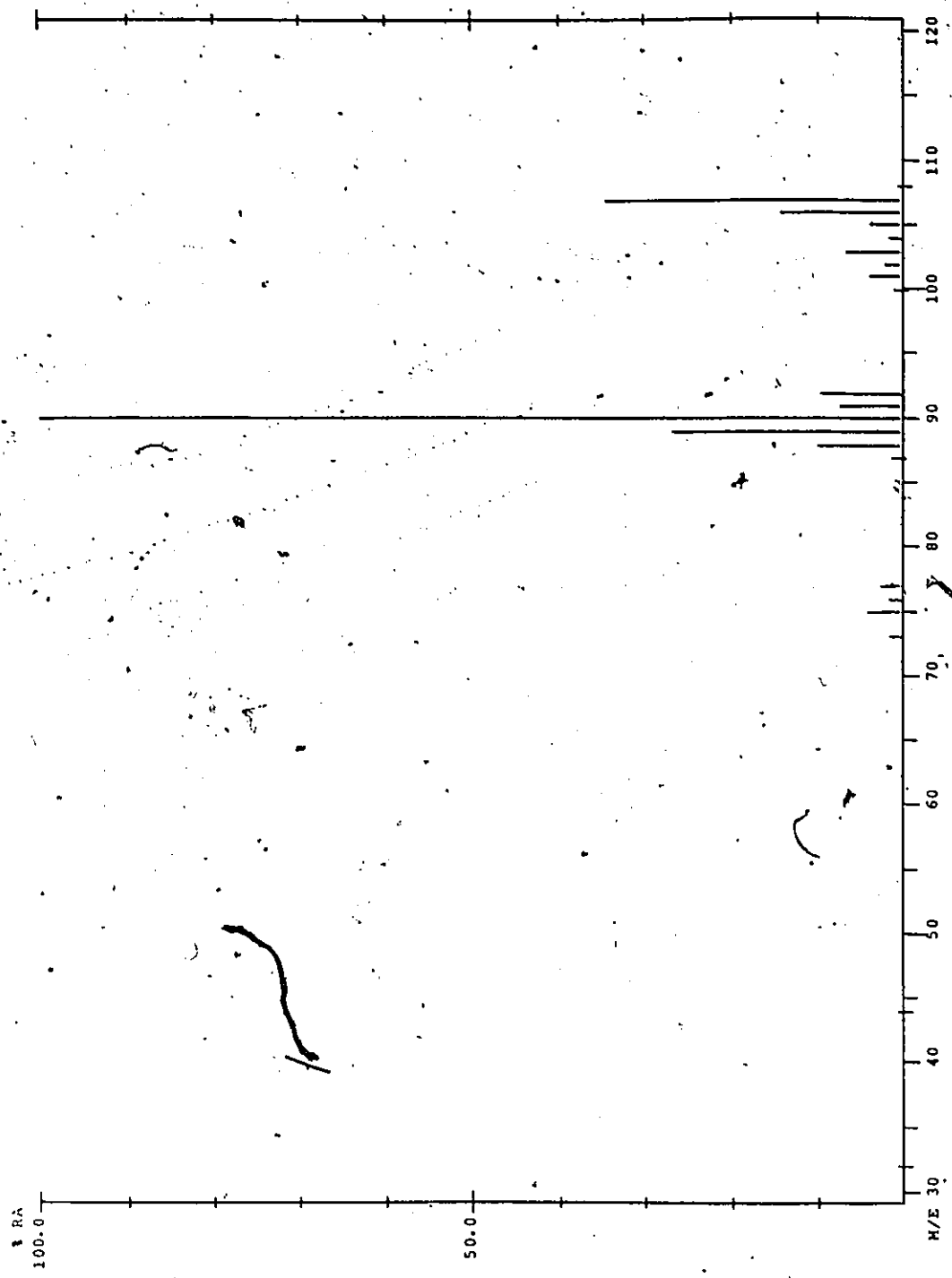Figure II.2 Mass spectrum (70 eV.) of Me_2AsH

Figure II.3   Mass spectrum (70 eV.) of Me$_2$AsD
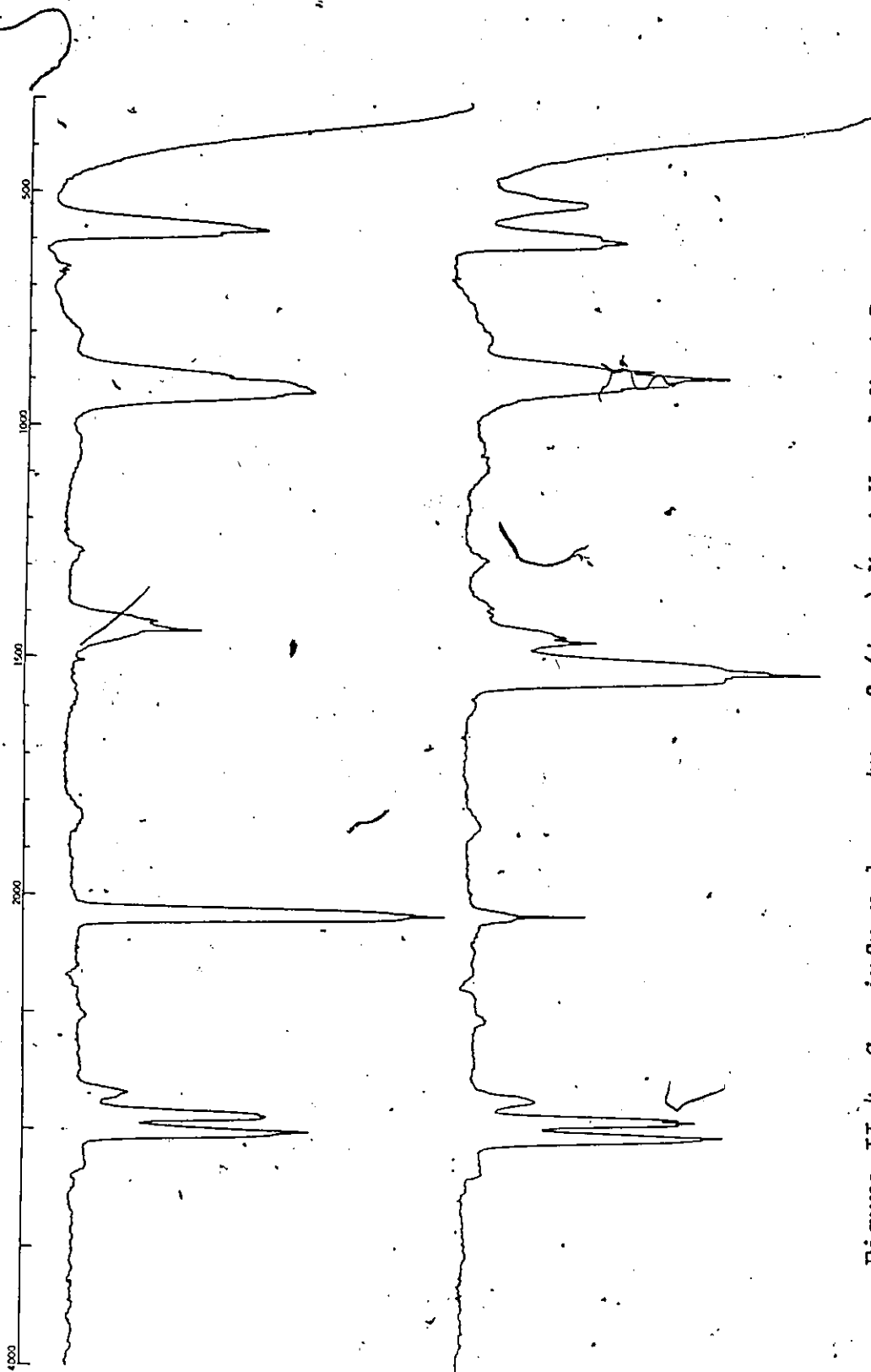
Figure II.4   Gas infrared spectra of (top) Me_2AsH and Me_2AsD
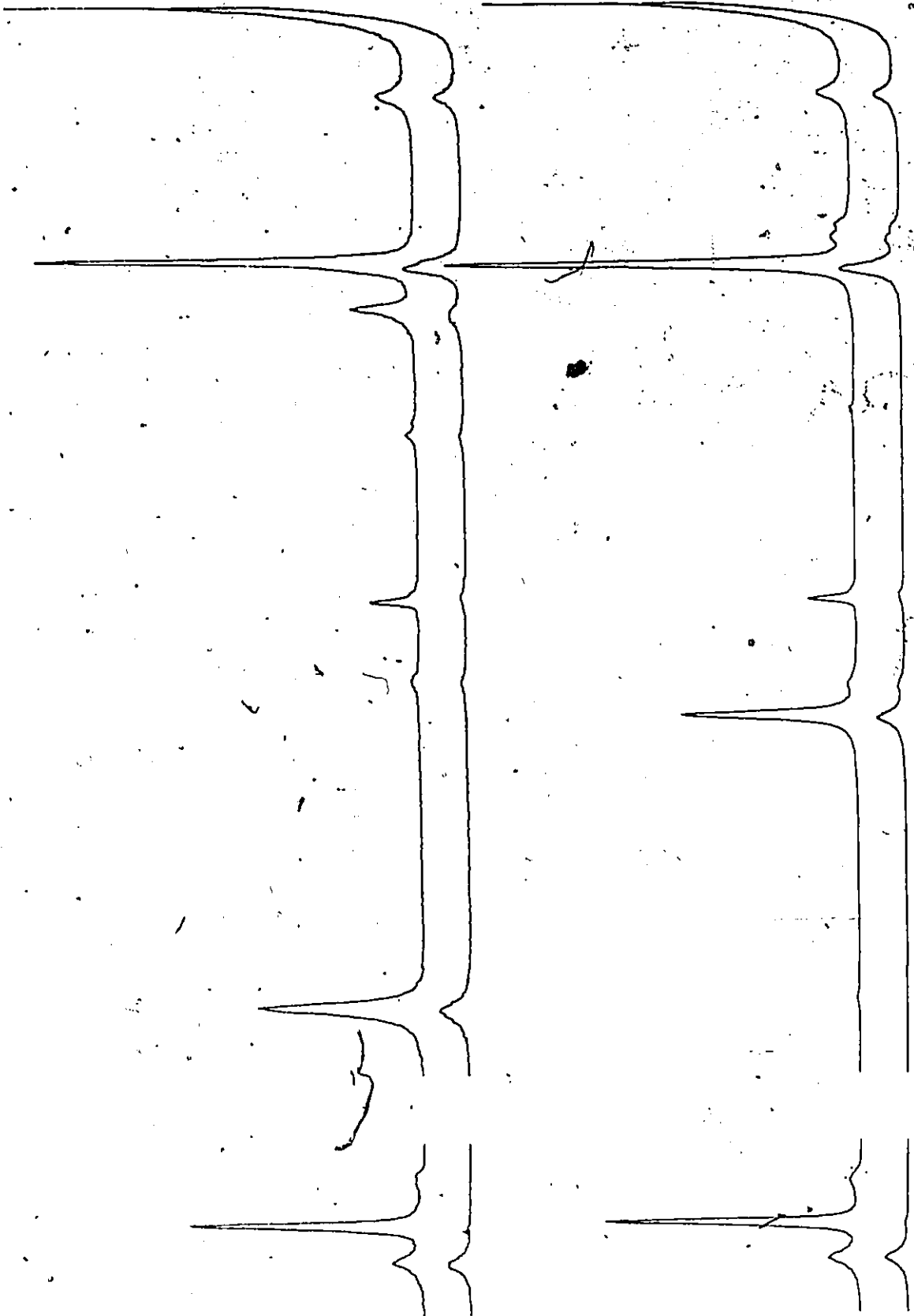
Figure II.5   Raman spectra of (top) Me$_2$AsH and Me$_2$AsD

3100   2750   2250   30

expected to give rise to B or C type bands in the gas infra-
red spectra and to be polarised in the Raman spectra, and the
a" modes to give A type infrared bands and depolarised Raman
lines. The numbering of these modes, for both dimethyl-
arsine and -phosphine, and their approximate descriptions
are given in Table II.1 and the observed frequencies in
Table II.2.

The methyl group vibrations appear in the expected regions,
and are straightforwardly assigned, except for the rocks
which appear in one envelope in the infrared spectra and as
weak, broad and generally featureless bands in the Raman
spectra. The Raman spectra however allow for separation of
the a' and a" symmetric deformations, ν_7 and ν_{19} because
ν_{19}, which appears as a weak shoulder in the parallel scan,
becomes more evident in the polarised spectrum.

The modes incorporating the isotopic substitution can
be seen to decrease in wavenumber as expected, the AsH
stretch, ν_4, falling from 2080 to 1500 cm^{-1}. The in- and
out-of-plane AsH deformations appear to higher wavenumber
of the C_2As stretches and the AsD deformations to lower
wavenumber. The C_2As stretches, ν_{11} and ν_{23}, appear in the
same envelope in the infrared spectra and are only separated
in the polarised scan of the Raman spectrum. The C_2As
deformation, ν_{12}, is unshifted at 229 cm^{-1} for both molecules.

There are several interesting observations about these
latter bands. The first is that the AsH bands are in the
same envelope, again only distinquishable in the two Raman

Table II.1 Numbering and approximate description of fundamentals for molecules $(CH_3)_2MH_r$ (M=As,P)

Description	a'		a"	
CH_3 stretch (asym)	ν_1	ν_2	ν_{14}	ν_{15}
CH_3 stretch (sym)	ν_3		ν_{16}	
MH stretch	ν_4			
CH_3 def. (asym)	ν_5	ν_6	ν_{17}	ν_{18}
CH_3 def. (sym)	ν_7		ν_{19}	
CH_3 rock	ν_8	ν_9	ν_{20}	ν_{21}
MH def.	ν_{10}		ν_{22}	
C_2M stretch	ν_{11}		ν_{23}	
CMC def.	ν_{12}			
CH_3 torsion	ν_{13}		ν_{24}	

Table II.2 The vibrational spectra (cm^{-1}) of the dimethylarsines*

	$(CH_3)_2AsH$			$(CH_3)_2AsD$			
i.r. (gas)	Raman (liq.)		calc.	i.r. (gas)	Raman (liq.)		calc	Assignment
3140 w				3141 w				
3012 s	2994	m dp	2993	3006 s	2992	m dp	2993	$\nu_3 + \nu_{12}$
2994 s				2994 s				ν_1, ν_{14}
2932 s	2920	s p	2920	2933 s	2920	s p	2920	ν_2, ν_{15}
2840 mw	2825	w p		2847 mw	2836	w p		ν_3, ν_{16}
2500 w				2508 w			}	} 2 × δMe
2080 vs	2073	s p	2086	1501 vs	1494	s p	1486	ν_4
1826 wbr				1843 wbr				
1577 wbr				1381 w				
				1367 w				} ρMe + δAsX
1434 m	1423	wbrdp	1428	1440 m	1430	wbrdp	1427	ν_5, ν_{17}
1415 m			1419	1429 m				ν_6, ν_{18}
1266 w	1261	m p	1265	1266 w	1260	m p	1241	ν_7
	1246	w dp	1253		1245	w dp	1239	ν_{19}
933 s	930	w p	932	875 s			872	ν_{20}
922 s	922	w p	919	862 s	~873	w p	865	ν_8
912 s	894	w p	891	901 s	~922	vw	903	ν_9
893 s			884	889 s	~895	vw	903	ν_{21}
796 w				793 w				
672 w	677	wshdp	682	513 m	526	w dp	522	νCAs + ν_{12}
659 w	663	m p	658	496 msh	501	w	504	ν_{22}
580 s	579	mshdp	578	588 ms	585	mshdp	586	ν_{10}
	565	vs p	570		579	vs p	574	ν_{23}
	229	m dp	229		229	m dp	229	ν_{11}
								ν_{12}

v = very, s = strong, m = medium, w = weak, sh = shoulder, br = broad, p = polarized, dp = depolarized, δ = deformation, ρ = rock.

*ref. 51

spectra, where ν_{22} appears as a depolarised high wavenumber tail on ν_{10}, whereas on deuteration the separation increases and they appear as two separate bands. The order is kept the same (ν_{22} higher than ν_{10}) although the depolarisation ratios are inconclusive. However, the higher wavenumber band appears slightly less polarised, is expected to be more intense in the infrared spectrum (which it is) and compares favourably with the $(CF_3)_2AsH$ analogues[35], where the order is maintained on deuteration. The second is the change in relative intensities on deuteration. The AsH bends are fairly strong in the Raman but quite weak in the infrared spectrum, whereas the AsD bends exhibit the opposite intensity relationship, being weaker in the Raman and of medium intensity in the infrared spectrum, as can be seen in Figure II.6 (in which the wavenumber scales are not the same for infrared and Raman scans). While the C_2As stretches, ν_{11} and ν_{23}, appear in one envelope in both the infrared spectra, the separation, as seen in the two Raman spectra (again in Figure II.6), decreases on deuteration; the position of the envelope and the average stretching frequency from the Raman spectra are seen to increase. These observations will be referred to again later.

II.2.3 Normal Co-ordinate Analysis

The molecular geometry was assumed from comparison with related molecules[36] to be C-H 110 pm, C-As 195 pm, As-H 152 pm; $\angle$CAsC, $\angle$CAsH 100° and $\angle$HCH 109.5°. The calculated frequencies were fitted to the Raman frequencies except

for the methyl rocks for which infrared data were used. The results of a product rule calculation are shown in Table II.3.

Table II.3   Product Rule Ratios

	calc.	obs. i.r.	obs. Ra.
a'	0.525	0.52	0.54
a"	0.724	0.73	0.75

These results are approximate due to uncertainties in resolving the rocking modes, but assuming that they are in the same order in both molecules, no deviation greater than that implied by the significant figures is observed. Apart from the infrared a' result they are all a little larger than calculated values as expected[37].

Initially a separate NCA was performed on each molecule, using SOTONVIB, which produced, not surprisingly, very good agreement for each. Considering the difference in anharmonicity the force constants were adequately transferable, except for $\underline{f}$ CAsH(D) which describes both in- and out-of-plane deformations, with values of 61 and 68 $N.m^{-1}$ respectively. Presumably because of the different vibrational amplitudes of the hydrogen and deuterium atoms, there is a difference in the interaction with the lone pair on arsenic in these motions, which these calculations do not reflect. For example, a UBFF calculation for ammonia was only able to fit the frequencies when a fifth "atom" of zero mass was included to represent the lone pair[38], whereas without it the fit was poor[39]. Subsequently a calculation was performed, using

LARMOL for both molecules together, which produced the force constants listed in Table II.4, and the frequencies they calculate in Table II.2. The p.e.d. is reproduced in Table II.5, where the main feature is the large interaction between the CAsH(D) and HCAs bends cis to each other. However, this may or may not be real because of the assumed geometry of the molecule. For the sake of simplicity, the three-fold axis of the methyl group was defined as coincident with the CAs bond, although it is well known that for molecules involving lone pairs the axis of the methyl group is tilted towards the lone pair by an angle $\epsilon = 1 - 5^o$ [40]. This is apparently due to an attraction between the lone pair and the methyl group, since methylamine has a larger tilt than trimethyl-amine[41]. In the latter case, and trimethylphosphine[42], this effect also produces significantly different C-H bond lengths and HCH (and so presumably HCM (M = N,P)) bond angles. That this effect has a significant influence on force constant calculations can be seen from such work as that on methyl-phosphine[18], where the assumed value of $\epsilon = 2^o$ from the microwave study[43] produced a poor fit and a reversal of two expected assignments, based on the p.e.d. Increasing ϵ to $2^o 30'$ however, resulted in much improved agreement and a correct order of assignment. Since no such refinement was included in the calculations for dimethylarsine, very little can be gained from comparison of force constants, for example with $(CF_3)_2AsH$[35] where the CF_3- lone pair interaction should be entirely dissimilar, even though here the diagonal force constants still agree within five percent.
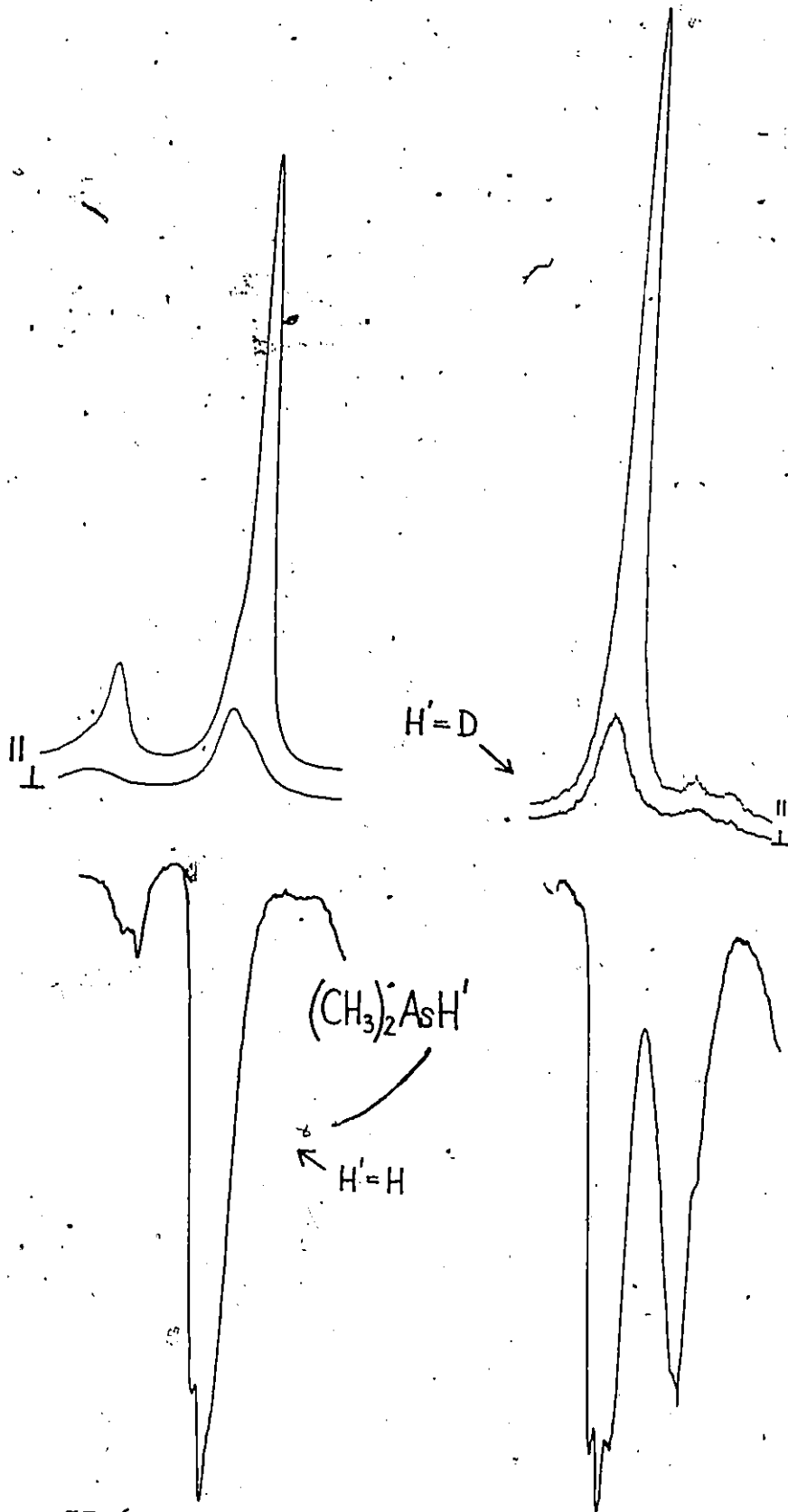
$H' = D$

$(CH_3)_2AsH'$

$H' = H$

Figure II.6 Raman and infrared spectra of C_2As stretching region in dimethylarsine

Table II.4. Force constant values for dimethylarsine

No.	Description	Value[*]
1	f CH	481.5
2	f AsH	255.
3	f CAs	259.
4	f HCH	45.
5	f HCAs $\perp$	62.
6	f HCAs $\parallel$	49.
7	f CAsH	85.
8	f CAsC	84.
9	f CH/CH	4.9
10	f CAs/CAs	2.5
11	f HCH/HCH	-7.4
12	f CAsH/CAsH	10.1
13	f cis-HCAs/CAsH	-18.3
14	f CAs/CasH	9.3

[*]Units are $N.m^{-1}$ for stretching and $N.m.rad^{-2}$ for bending force constants.

Table II.5 Description of vibrational modes and the potential energy distribution

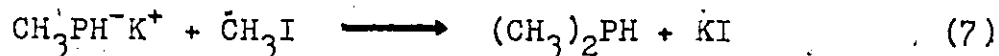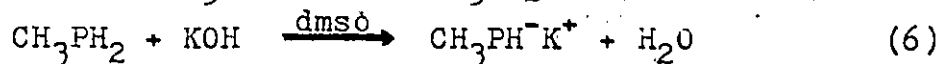| Mode description	Class	Potential energy distribution[*]	
		$(CH_3)_2AsH$	$(CH_3)_2AsD$
v_1 CH₃ asym. str.		101(1)	101(1)
v_2 CH₃ asym. str.		101(1)	101(1)
v_3 CH₃ sym. str.		98(1)	98(1)
v_4 AsH(D)str.		100(2)	100(2)
v_5 CH₃ asym. def.		80(4)+13(11)	80(4)+13(5)
v_6 CH₃ asym. def.		82(4)+14(11)	82(4)+14(5)
v_7 CH₃ sym. def.	a'	42(4)+25(5)+25(6)−13(11)+11(13)	47(4)+29(6)+28(5)−15(11)+6(3)
v_8 CH₃ rock (in)		58(6)+15(7)+10(5)+8(4)+7(13)	79(6)+6(5)+6(13)
v_9 CH₃ rock (out)		46(6)+41(5)+6(7)	45(5)+44(6)+7(4)
v_{10} AsH(D)def. (in)		76(7)+39(6)−36(13)+9(12)+6(5)	90(7)−34(13)+19(6)+11(12)+7(5)+6(4)
v_{11} C₂As sym. str.		88(3)	91(3)
v_{12} CAsC def.		98(8)	98(8)
v_{13} CH₃ torsion		—	—
v_{14} CH₃ asym. str.		101(1)	101(1)
v_{15} CH₃ asym. str.		101(1)	101(1)
v_{16} CH₃ sym. str.		98(1)	98(1)
v_{17} CH₃ asym. def.		80(4)+13(11)+6(5)	80(4)+13(11)
v_{18} CH₃ asym. def.		82(4)+14(11)	82(4)+14(11)
v_{19} CH₃ sym. def.	a"	44(4)+27(5)+27(6)−14(11)+7(13)	47(4)+29(5)+29(6)−15(11)+6(3)
v_{20} CH₃ rock (in)		54(6)+27(7)+11(4)+7(13)	75(6)+10(5)+6(7)+6(13)
v_{21} CH₃ rock (out)		47(5)+42(6)+6(7)	45(5)+42(6)+7(4)
v_{22} AsH(D)def. (out)		90(7)+49(6)−44(13)−11(12)+10(5)	109(7)−41(13)+21(6)−13(12)+9(5)+8(4)
v_{23} C₂As asym. str.		89(3)	88(3)+12(7)+6(6)
v_{24} CH₃ torsion		—	—

[*]Contributions greater than 5%, (in) = in plane; (out) = out-of-plane.

ref. 51

II.3 DIMETHYLPHOSPHINE

II.3.1 Preparation

The sample of dimethylphosphine used in this study had been prepared by Bro. B. Rapp in this laboratory for the preparation of phosphine-borane adducts. It was prepared starting from phosphine[44] by successive deprotonation and methylation[45]. Phosphine was introduced into a round-bottomed flask fitted with a dropping funnel, containing a slurry of potassium hydroxide in dimethylsulphoxide. On stirring, the mixture turned yellow indicating the formation (equation 4) of the PH_2^- ion. Enough iodomethane was added to decolourise the mixture (equation 5) and the process repeated (equations 6 and 7). The ^1H n.m.r. spectrum[46]

$$PH_3 + KOH \xrightarrow{dmso} K^+PH_2^- + H_2O \tag{4}$$

$$K^+PH_2^- + CH_3I \longrightarrow CH_3PH_2 + KI \tag{5}$$

$$CH_3PH_2 + KOH \xrightarrow{dmso} CH_3PH^-K^+ + H_2O \tag{6}$$

$$CH_3PH^-K^+ + CH_3I \longrightarrow (CH_3)_2PH + KI \tag{7}$$
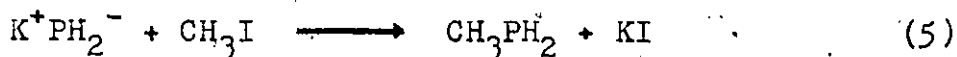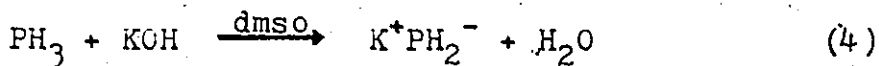
indicated a compound of sufficient purity for spectroscopic work.

The d_1 compound was prepared in > 98 mol.% by exchange of $(CH_3)_2PH$ with KOD as for the arsine compound (see Chapter II.2.1). The ^1H n.m.r. spectrum gave only the expected six line methyl resonance (a doublet of 1:1:1 triplets), with coupling constants $J_{HCP} = 3.40\pm0.02$ and $J_{HD} = 1.16\pm0.02$ Hz. These values compare with literature

values[46] of 3.77 ± 0.05 and 1.17 ± 0.01 Hz (calculated from J_{HH}) respectively.

II.3.2 Vibrational Spectra

The gas infrared and liquid Raman spectra of the d_1 compound are shown in Figures II.7 and II.8. The molecule is assigned on the basis of C_s symmetry, and the numbering and activity of the modes, similar to dimethylarsine, are shown in Table II.1. The observed frequencies of both "light" and "heavy" compounds are listed in Table II.6.

The CH_3 stretching and deformation modes, and PH(D) stretching modes were straightforwardly assigned. The remaining features in the Raman spectra of $Me_2PH(D)$ were weak bands

Table II.6 The vibrational spectra (cm^{-1}) of dimethylphosphine

(CH₃)₂PH*		(CH₃)₂PD**		Assignment
i.r. (gas)	Raman (liq.)	i.r. (gas)	Raman (liq.)	
3244		3253 vw		
3155		3168 vw		
2985	2975	2988 s	2978 m, dp	ν_1, ν_{14}
2975	(2969)**	2978 s	2974 m, dp	ν_2, ν_{15}
2923		2926 s	2911 vs, p	{ ν_{16}'
2918	2908	2920 s		ν_3
2862	2850	2853 m	2870 wsh	{
		2843 m		$2 \times \delta Me$
2830	2824	2832 m	2825 m, p	
2288	2282	2290 w	2281 w, p	$\nu_4(PH)$
2010		2000 vw		$\nu_9 + \nu_{23}$
1954		1951 vw		$\nu_6 + \nu_{11}$
		1667 C, s	1661 s, p	$\nu_4(P,D)$
1434		1434 ms	1428 wbr, dp	{ ν_5, ν_{17}
1423	1425	1424 ms		{ ν_6, ν_{18}
1297		1301 B, w	1294 mw, p	ν_7
	1294			
1284		1287 w	1285 wsh, dp	ν_{19}
1012	1003	910 s	910 vw	ν_{21}
~990	986	932 s	930 w, p	ν_9
947	950‡	949 B, s		ν_{10}
818	801‡ S	816-A, w	816 vw	ν_{22}
703 Q	704 S	709 A, m	708 m, dp	ν_{23}
660	657	670 B, w	669 s, p	ν_{11}
	729	584 m	590 w, dp	ν_{20}
714 R	714	567 B, mw	561 w, p	ν_8
261	267		269 m, dp	ν_{12}

* Ref. 30   ** this study;
‡ gas Raman spectrum;   § crystal Raman spectrum.
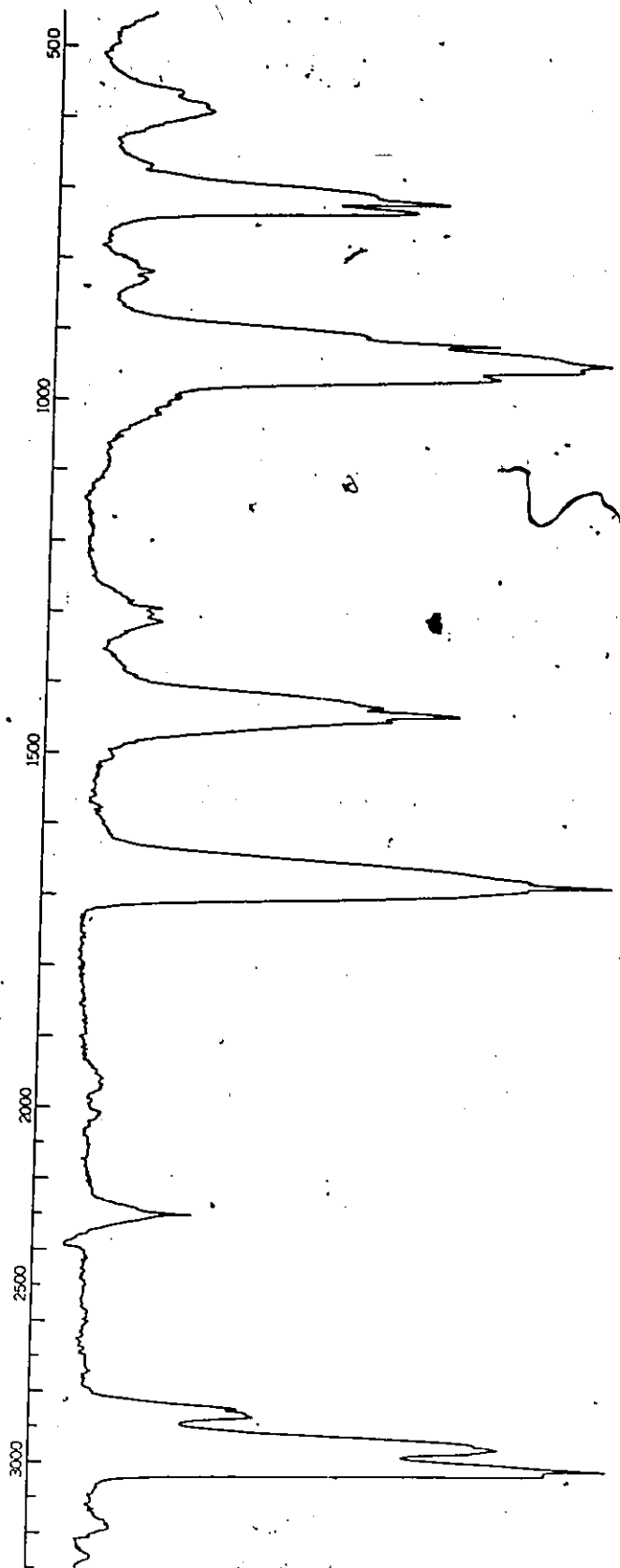
Figure II.7   Infrared spectrum of gaseous $(CH_3)_2PD$

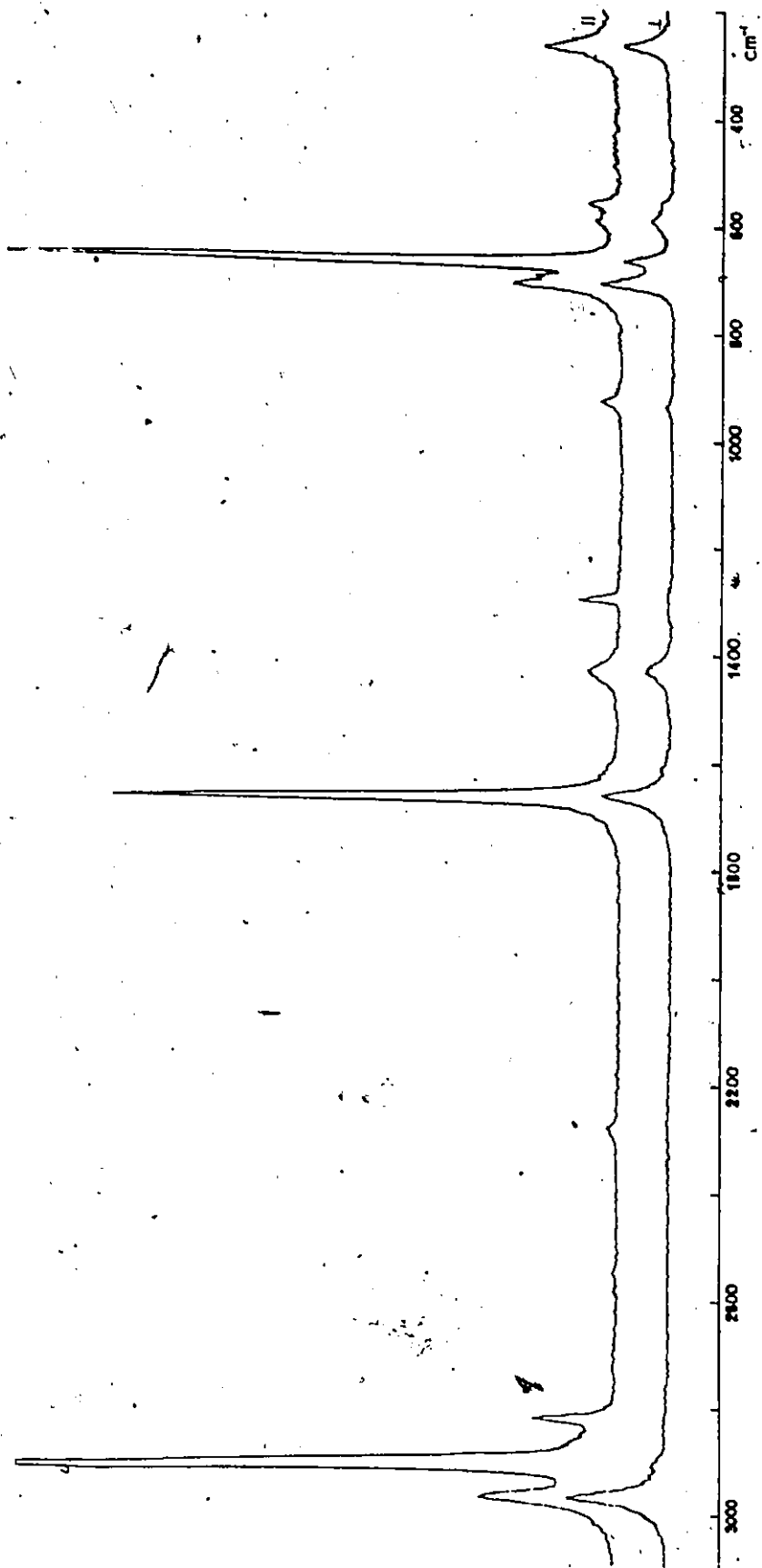Figure II.8   Raman spectrum of liquid $(CH_3)_2PD$

at $\sim 1000(\sim 930)$ cm^{-1}, some bands in the region of a strong, polarised band at ~ 650 cm^{-1}, assumed to be ν_{11}, the symmetric PC$_2$ stretch, and a medium intensity band at ~ 268 cm^{-1}, assigned as the PC$_2$ deformation mode ν_{12}.

The first obvious difference in the comparison of the Raman spectra of the two compounds was the appearance of two bands to low wavenumber of the PC$_2$ symmetric stretch in Me$_2$PD, as shown in Figure II.9 (N.B.-- intensities are not the same). These bands, at 590 (dep.) and 561 cm^{-1} (pol.) were assumed to be ν_{10} and ν_{22}, the symmetric and asymmetric PD bends, as these should be the only modes (other than ν_4, the PD stretch) most dramatically affected by deuteration. This left the band at 708 cm^{-1} (dep.) as ν_{23}, the PC$_2$ asymmetric stretch. Application of the rule of thumb isotope rule for deuteration (multiplying by $\sqrt{2}$) indicated that the corresponding modes in Me$_2$PH should be found below ~ 835 cm^{-1}. Close examination of the parallel and perpendicular scans of the middle envelope in Figure II.10 revealed three maxima; one in the parallel scan at 714 cm^{-1}, and two in the perpendicular scan at 704 and 729 cm^{-1} (shoulder). Thus the fundamentals in this region (two PH bends and two PC$_2$ stretches) were all accounted for. As for which band was which, the observations from dimethylarsine for the corresponding modes were found to be useful for an initial assignment, for if the assumption that the bends in both arsine and phosphine analogues were similarly affected by deuteration, which is not too unreasonable, then it should
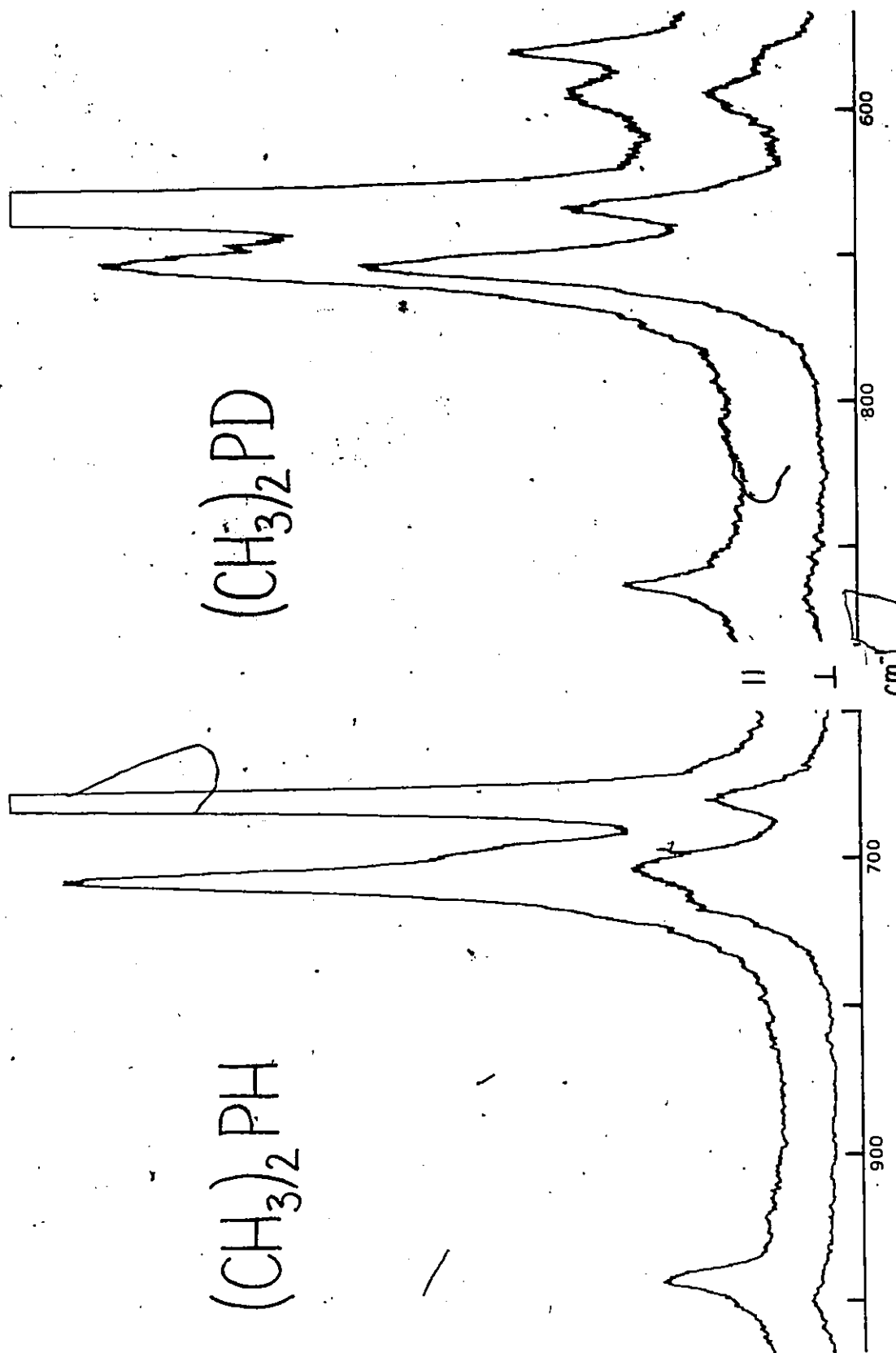
Figure II.9   Raman spectra of selected regions of dimethylphosphine

follow (from Figure II.5) that (i) both absolute values for the PC_2 stretches in the "light" molecule were lower than for the deuterated molecule, and with increased separation, (ii) the PH(D) bends should maintain the same order (asymmetric above symmetric) in both molecules, and be found in the same envelope for Me_2PH and separate for Me_2PD in the Raman spectra, and (iii) the observed Raman and infrared intensity relationships, again as seen in Figure II.6, should hold. These conditions are in fact thought to hold true, and so the PH bends, ν_{10} and ν_{22} were then assigned at 714 (pol.) and 729 cm^{-1} (dep.) respectively and the asymmetric PC_2 stretch ν_{23} at 704 cm^{-1} (dep.).

The bands at ~ 1000 and ~ 930 cm^{-1} in the light and heavy molecule repectively were assigned as two methyl rocks, each envelope having a polarised and a depolarised counterpart. The other two methyl rocks were assigned to features in the infrared spectra, at almost the same wavenumber in both molecules. This could imply that they are the a' and a" out-of-plane rocks, which might be expected to be the least affected by the motions of the (P)H atom. (This effect may be present in the dimethylarsine case where two values for the methyl rock are almost the same, but here the rocks are all in the same envelope and it is difficult to determine each mode separately).

II.4 DISCUSSION

As mentioned in the Introduction, a report on the vibrational spectra of $(CH_3)_2PH$ and $(CD_3)_2PH$ by Durig and Saunders[30] appeared towards the conclusion of this work, but their assignments do not compare at all well with this study and are believed to be in error as this discussion attempts to show. The assignment of dimethylarsine was fairly routine, as the AsH bends were found in a region not expected to be occupied by other fundamentals, which clearly shifted on deuteration, and so is not discussed further, except with reference to dimethylphosphine.

The principal difference in the spectra of Me_2PH from this work and the other two reports[28,30] is the absence of any bands in the 1250-1050 cm^{-1} range found by both other studies, and in which assignments of fundamentals were made. It may be noteworthy that it is in this region that the $P=0$ stretch is found; for example at 1146 cm^{-1} in Me_3PO[47]. These P(V) compounds are the products from oxidation by exposure to air of P(III) compounds[48]. Purity checks for the other studies consisted of a vapour pressure measurement for the earlier work[28] and a trap-to-trap distillation, followed by the production of the compound on a fractionation column for the later study[30], although should oxidation products be present, these would probably occur during the manipulation of the product after initial preparation. So many infrared lines were observed in the earlier work that

the presence of impurities is almost certain, and it is not discussed further.

Apart from assigning fundamentals to features not observed in our spectra, the results of Durig and Saunders[30] differ from this work in few respects. One of the major differences is in the ~ 730 cm^{-1} envelope in the Raman spectrum of $(CH_3)_2PH$ (Figure II.9) where in their assignment the depolarised band at 704 cm^{-1} is unassigned (it appears in the crystal Raman spectrum but is not reported in the liquid spectrum). The reason for the "asymmetric (shaped) polarised" band they report at 714 cm^{-1}, to which they assigned ν_{23} the asymmetric PC_2 stretch, is of course that it is in fact two bands. The symmetric PH bend, ν_{10}, is then assigned by Durig to the polarised band at 1003 cm^{-1} and the asymmetric bend, ν_{22}, to a line at 1124 cm^{-1} which is not observed in their Raman spectra, and is very weak in the infrared. It was these contradictions of the information from the parallel and perpendicular scans, by assigning an a" mode to an apparently polarised band and an a' mode to a depolarised band that was seen as the first evidence of an incorrect assignment. The remaining bands, spread over 260 cm^{-1} are assigned as the four methyl rocks.

In the spectrum of $(CD_3)_2PH$ most modes not involving the isotopically substituted atoms decrease somewhat in wavenumber, which is to be expected. Thus the PC_2 stretches are reported by Durig to drop from "714" and 657 cm^{-1} to 662 and 612 cm^{-1}, and the PC_2 deformation from 267 to 230 cm^{-1}. However, the

PH bends are reported to increase slightly, into the region of the CD_3 deformations, which incorporate six fundamentals and at least two bands, and again in the 1120 cm^{-1} region. However, if the assignments as proposed in this work for $(CH_3)_2PH$ and $(CH_3)_2PD$ are correct, they should also be able to explain the spectrum of $(CD_3)_2PH$. Assuming that the PH bends have been correctly assigned, and that, for lack of other comparison, the isotopic shift factor for them is the same as for the PC_2 stretches (taking symmetric and asymmetric modes separately), then on going from $(CH_3)_2PH$ to $(CD_3)_2PH$, ν_{22} and ν_{10} should be found at 686 and 665 cm^{-1} respectively. The reported spectrum of $(CD_3)_2PH$ contains unassigned features at ~ 690 cm^{-1} in the gas and crystal spectra, and the asymmetric PC_2 stretch is at 662 cm^{-1} which would overlap any weak feature in that region. However, a comparison of the shapes of the 662 cm^{-1} envelope from the infrared spectrum of $(CD_3)_2PH$ (Figure II.10 (iii); from a spectrum recorded by Bro. B. Rapp in this laboratory) and the 705 and 709 cm^{-1} bands from $(CH_3)_2PH$ and $(CH_3)_2PD$, (Figure II.10 (i) and (ii) respectively) which contain principally the asymmetric PC_2 stretch, points to the possibility of there being a feature (or features) in the high wavenumber portion of the envelope at those calculated positions, if, as is assumed, the change in moments of inertia for all three molecules is sufficiently small so as not to significantly affect the band contours, and thus enable a valid comparison. (It should be noted that the 705 cm^{-1} envelope for $(CH_3)_2PH$

(Figure II.10 (i)) also contains the two PH bends, but by comparison with dimethylarsine (Figure II.3, upper tracing) these are expected to be very weak in the infrared effect and not contribute significantly to the shape of the comparatively intense band due to ν_{23}).

These arguments, however, really only represent one personal interpretation, and perhaps more hard statistical evidence should be presented. Comparison with other related compounds shows the unlikeihood of the PH bends being found in the region proposed by Durig and Saunders (above 1000 cm^{-1}). For other compounds with AsH(D) or PH(D) deformations, it can be seen (Table II.7) that for the arsine derivatives, the

Table II.7 Summary of 'MH' deformations (cm^{-1})[*] in selected secondary phosphines and arsines

M		$(CF_3)_2MH^a$	Ph_2MH^b	$(CH_3)_2MH^c$	$(CF_3)_2MD^a$	$(CH_3)_2MD^c$
P	a"	855		(729)	643	590
	a'	800	800	(714)	∼ 643	561
As	a"	753		677	575	526
	a'	654	710	663	486	501

[*]All Raman frequencies
a) ref. 35; b) ref. 49; c) this work, M = P ref. 50; M = As ref. 51

trend is $(CF_3)_2 \sim Ph_2 > (CH_3)_2$ for AsH and $(CF_3)_2 > (CH_3)_2$ for AsD deformations. This indicates that if the same is true for the phosphines, the upper limits for PH and PD deformations are ∼ 800 and ∼ 640 cm^{-1} respectively.

It is also instructive to look at which angle changes are involved in these deformations. To take the series of

arsine derivatives, the deformations in arsine itself result from a change of the HAsH angles, the average of the symmetric and asymmetric modes being 971 cm^{-1}. In CH_3AsH_2 there are three AsH_2 deformation modes; AsH_2 scissors (HAsH angle change), wag (a') and twist (a") (both CAsH angle changes). The scissoring vibration occurs at 973 cm^{-1}, almost exactly the value in AsH_3, the others at 674 and 654 cm^{-1} respectively, an average of 664 cm^{-1}. The a' and a" AsH deformations in $(CH_3)_2AsH$, which can only be CAsH angle changes, occur at 672 and 659 cm^{-1} respectively for an average of 666 cm^{-1}, almost exactly the value from CH_3AsH_2. (Note also that the symmetric mode is still above the asymmetric mode). These similarities also exist for the molecules deuterated at arsenic. These values are gathered in Table II.8 along with

Table II.8   Comparison of average vibrational frequencies resulting from deformation of HMH and CMH angles for some phosphines and arsines

M =	P		As	
∠ change	HPH	CPH	HAsH	CAsH
MH_3	1079[a,b]	--	971[c]	--
$MeMH_2$	1092[d]	713	973[e]	664
Me_2MH	--	722[f]	--	666[g]
MD_3	768[a]	--	687[c]	--
$MeMD_2$	790[d]	563	697[e]	500
Me_2MD	--	575[f]	--	504[g]

a) ref. 52; b) ref. 53; c) ref. 54; d) ref. 18; e) ref. 19; f) this work, ref. 50; g) this work, ref. 51.

data from the phosphine analogues. It is immediately apparent that if these comparisons are valid, the values proposed by Durig and Saunders (and Beachell and Katlafsky[28]) are far too high. (N.B. These comparisons hold strictly only if, the contribution of the angle change to the total potential energy of the vibration is 100%, or at least the same in each case; they range from 65-116% for CH_3AsH_2[19], CH_3PH_2[18] and $(CH_3)_2AsH$, averaging 88%, so the comparison is fair). Beachell and Katlafsky compared the PH bending fundamentals to those of PH_3, which the foregoing has sought to prove invalid and Durig and Saunders appeared to have not considered any other region, possibly influenced by the former study.

This discussion has attempted to substantiate the assignments for dimethylarsine and dimethylphosphine, and show that these assignments are consistent with and related to similar vibrations in related arsenic and phosphorus hydrides for which data has appeared in the literature. It is also hoped that this has demonstrated the usefulness of the judicious use of comparisons of various kinds to the assigning of molecular vibrations.

REFERENCES

Part II

1. J. Priestley, cited in "A History of Chemistry", J.R. Partington, Vol. 3, Macmillan, London, 265,(1962).

2. C.W. Scheele, Svenska Akad. Handl., 36, 263,(1775).

3.a. P: see e.g. A.B. Burg, Inorg. Chem., 3, 1325,(1964); J. Davis and J.E. Drake, J. Chem. Soc., A1971, 2094; J.E. Drake, J.L. Hencher and B. Rapp, Inorg. Chem., 16, 2289,(1977); J.E. Drake, J.L. Hencher, L. Khasrou and B. Rapp, in press.

   b. As: see e.g. F.G.A. Stone and A. Burg, J. Amer. Chem. Soc., 76, 386,(1954); F. Hewitt and A.K. Holiday, J. Chem. Soc., 1953, 530; M.L. Denniston and D.R. Martin, J. Inorg. Nucl. Chem., 36, 2175,(1964); D.C. Mente, J.L. Mills and R.E. Mitchell, Inorg. Chem., 14, 123, (1975).

4.a. P: see e.g. A. Rauk, J.D. Androse, W.G. Frick, R. Tang and K. Mislow, J. Amer. Chem. Soc., 93, 6507,(1971).

   b. As: see e.g. C.C. Costain and G.B.B.M. Sutherland, J. Phys. Chem., 56, 321,(1952); J.D. Androse, A. Rauk and K. Mislow, J. Amer. Chem. Soc., 96, 6904,(1974).

5. see e.g. R.G. Hayter, J. Amer. Chem. Soc., 85, 3120, (1963).

6.a. P: see e.g. W. Ehrl and H. Vahrenkamp, J. Organomet. Chem., 63, 389,399,(1973).

   b. As: see e.g. W.R. Cullen, F.W.B. Einstein, R.K. Pomeroy and P.L. Vogel, Inorg. Chem., 14, 3017,(1975); E. Keller and H. Vahrenkamp, Chem. Ber., 109, 229,(1976) and refs. therein.

7. B.C. McBride, M.M. Reimer and W.R. Cullen, 175th, ACS Meeting, Anaheim CA, 1978.

8. J.R. Barceló and J. Bellanato, Spectrochim. Acta , 8, 27,(1956).

9. A.P. Gray and R.C. Lord, J. Chem. Phys., 26, 690,(1957).

10. J.N. Gayles, Spectrochim. Acta , 23A, 1521,(1967).

11. B. Beagley and A.R. Medwid, J. Mol. Struct., 38, 229, (1977).

12. J.-P. Perchard, M.-T. Forel and M.-L. Josien, J. Chim. Phys., 61, 652,(1964).

13. W.G. Fateley and F.A. Miller, Spectrochim. Acta, 18, 977, (1962).

14. M.J. Buttler and D.C. McKean, Spectrochim. Acta, 21, 465, (1965).

15. G. Gamer and H. Wolff, Spectrochim. Acta, 29A, 129, (1973).

16. H.R. Linton and E.R. Nixon, Spectrochim. Acta, 15, 146, (1959).

17. J.R. Neilsen and J.D. Walker, Spectrochim. Acta, 21, 1163, (1964).

18. J.A. Lannon and E.R. Nixon, Spectrochim. Acta, 23A, 2713, (1967).

19. A.B. Harvey and M.K. Wilson, J. Chem. Phys., 44, 3535, (1966).

20. E.J. Rosenbaum, D.J. Rubin and C.R. Sandberg, J. Chem. Phys., 8, 366, (1940).

21. F.J. Wagstaffe and H.W. Thompson, Trans. Faraday Soc., 40, 41, (1944).

22. G. Bouquet and M. Bigorgne, Spectrochim. Acta, 23A, 1231, (1967).

23. J.D. Park and P.J. Hendra, Spectochim. Acta, 24A, 2081, (1968).

24. M. Halmann, Spectrochim. Acta, 16, 407, (1960).

25. H. Rojhantalab, J.W. Nibler and C.J. Wilkins, Spectrochim. Acta, 32A, 519, (1976).

26. F. Fehér and W. Kolb, Naturwiss., 27, 615, (1939).

27. G. Petit, Compt. rend., 218, 414, (1944).

28. H.C. Beachell and B. Katlafsky, J. Chem. Phys., 27, 182, (1957).

29. see e.g. W.R. Cullen, P.S. Dhalival and G.E. Styan, J. Organomet. Chem., 6, 364, (1966).

30. J.R. Durig and J.E. Saunders, J. Raman Spectrosc., 4, 121, (1975).

31. W.H. Dehn, Am. Chem. J., 40, 88, (1908): CA 2; 2793.

32. E.W. Abel, R. Honigschmidt-Grossich and S.M. Illingworth, J. Chem. Soc., A1968, 2623.

33. E.W. Abel and S.M. Illingworth, J. Chem. Soc. A1969,1094.

34. cf. A.L. Allred and R.L. Deming, Inorg. Nucl. Chem. Letters 6, 39 (1970).

35. H. Bürger, J. Cichon, J. Grobe and R. Demuth, Spectrochim. Acta 29A, 47 (1973).

36. Tables of Interatomic Distances and Configuration in Molecules and Ions, Special Publications 11 and 18, The Chemical Society, London, 1958 and 1965.

37. G. Herzberg, Molecular Spectra and Molecular Structure II. Infrared and Raman Spectra of Polyatomic Molecules, Van Nostrand, Princeton, N.J., 1945, p.232.

38. M. Pariseau, E. Wu and J. Overend, J. Chem. Phys. 39, 217 (1963).

39. W.T. King, J. Chem. Phys. 36, 165 (1962).

40. J.E. Wollrab, Rotational Spectra and Molecular Structure, Academic Press, New York, N.Y., 1967.

41. J.E. Wollrab and V.W. Laurie, J. Chem. Phys. 51, 1580 (1969).

42. P.S. Bryan and R.L. Kuczkowski, J. Chem. Phys. 55, 3049 (1971).

43. T. Kojima, E.L. Breig and C.C. Lin, J. Chem. Phys. 35, 2139 (1961).

44. S.D. Gokhale and W.L. Jolly, Inorg. Synth. 9, 56 (1967); R.C. Marriott, J.D. Odom and C.T. Sears, Inorg. Synth. 14, 1 (1973).

45. W.L. Jolly, Inorg. Synth. 11, 124 (1968).

46. S.L. Manatt, G.L. Juvinall, R,I, Wagner and D.D. Elleman, J. Amer. Chem. Soc. 88, 2689 (1966).

47. F. Choplin and G. Kauffman, Spectrochim. Acta 26A, 2113 (1970).

48. C. Dorken, Ber. 21, 1505 (1888); M.M. Rauhaut and H.A. Currier, J. Org. Chem. 26, 2646 (1961); K.D. Berlin and G.B. Butler, Chem. Revs. 60, 243 (1960).

49. H. Stenzenberger and H. Schindlbauer, Spectrochim. Acta 26A, 1713 (1970).

50. A.J.F. Clark and J.E. Drake, Spectrochim. Acta 34A, 307 (1978).

51. A.J.F. Clark, J.E. Drake and Q. Shen, Spectrochim. Acta 34A, 307 (1978).

52. E. Lee and C.K. Wu, Trans. Faraday Soc. 35, 1366 (1939).

53. J.M. Hoffman, H.H.Nielsen and K.N. Rao, Z. Elecktrochem. 64, 606 (1960).

54. V.M. McConaghie and H.H. Nielsen, Phys. Rev. 75, 633 (1949).

APPENDICES

1. The Vacuum Line
2. Starting Materials
3. Instrumental Techniques
4. Computer Programmes
5. Additional NCA Data

APPENDIX I

THE VACUUM LINE

The general principles involved in vacuum line techniques have been fully described in some excellent books[1,2] and will only be briefly mentioned here as they pertain to the methods most widely used during the preparations described herein.

The general design of the vacuum line used in the course of this work and the pumping system are shown in Figures A.1 and A.2. The main manifold M was connected to the pumping system at stopcock P1, and contained outlets to four smaller manifolds, of which two are shown in the figure, and the head of a Pirani gauge (PG) to monitor the vacuum in the system. Manifolds A and B were connected to the main manifold by ball joints with Viton O-rings and stopcocks A1 and B1 and were equipped with greaseless stopcocks, either Teflon or glass barrelled, with Viton A O-rings. (The other two manifolds, on the other side of the rack, were fitted with ground glass stopcocks and used only for "dirty" preparations). Each manifold was equipped with simple mercury manometers. The manifolds A and B are also connected by a train of four removable U-traps, interconnected by greaseless stopcocks and ball joints with Viton A O-rings. Although some vacuum loss was inevitable with the extra joints (compared to a continuous train), this was not considered to be serious, and this disadvantage was more than offset by the ease of cleaning and extra versatility offered, for example by the
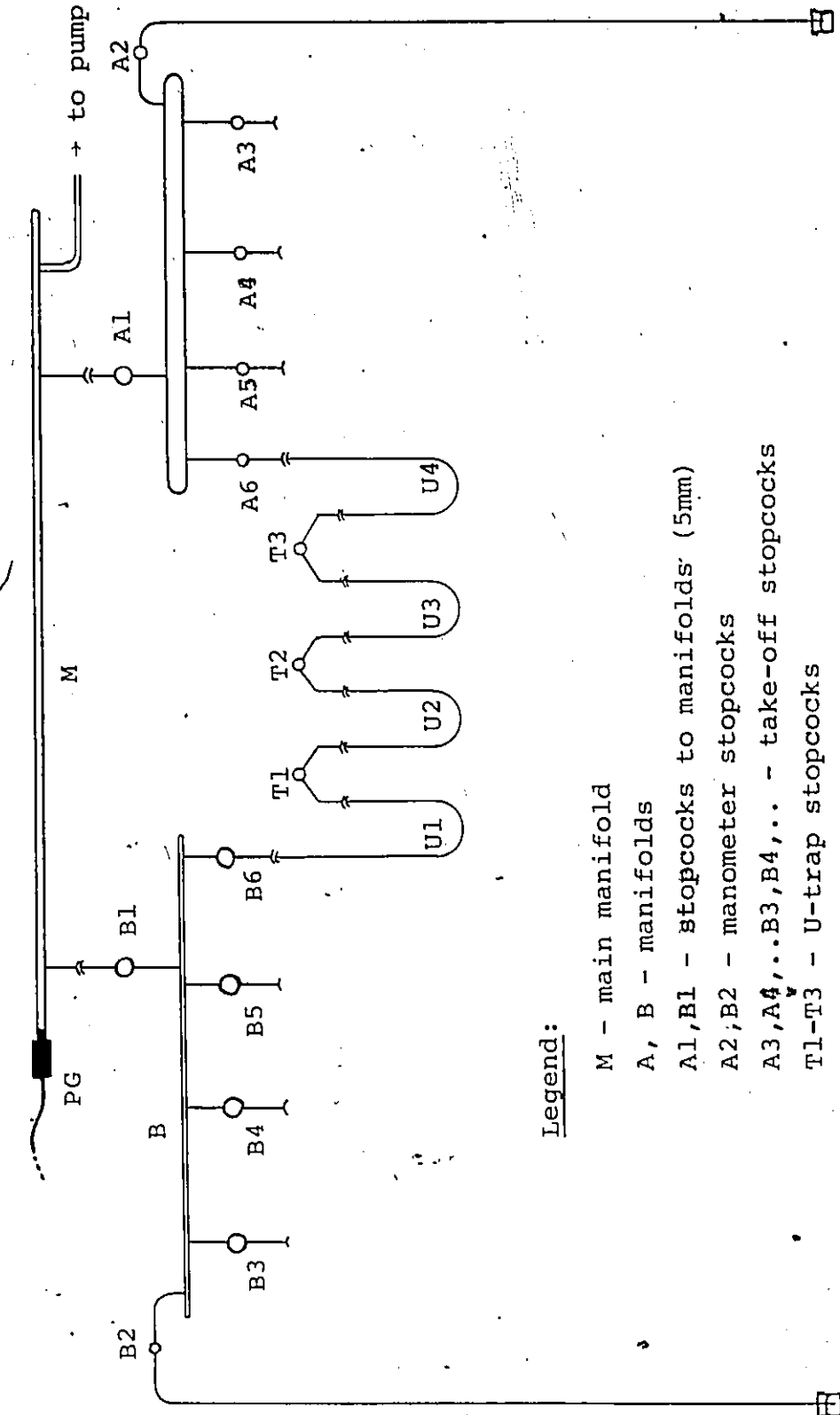
Legend:

M – main manifold

A, B – manifolds

A1,B1 – stopcocks to manifolds (5mm)

A2;B2 – manometer stopcocks

A3,A4,...B3,B4,.. – take-off stopcocks

T1-T3 – U-trap stopcocks

U1,U2,... – U-traps

PG – Pirani gauge head

Figure A1 The vacuum line
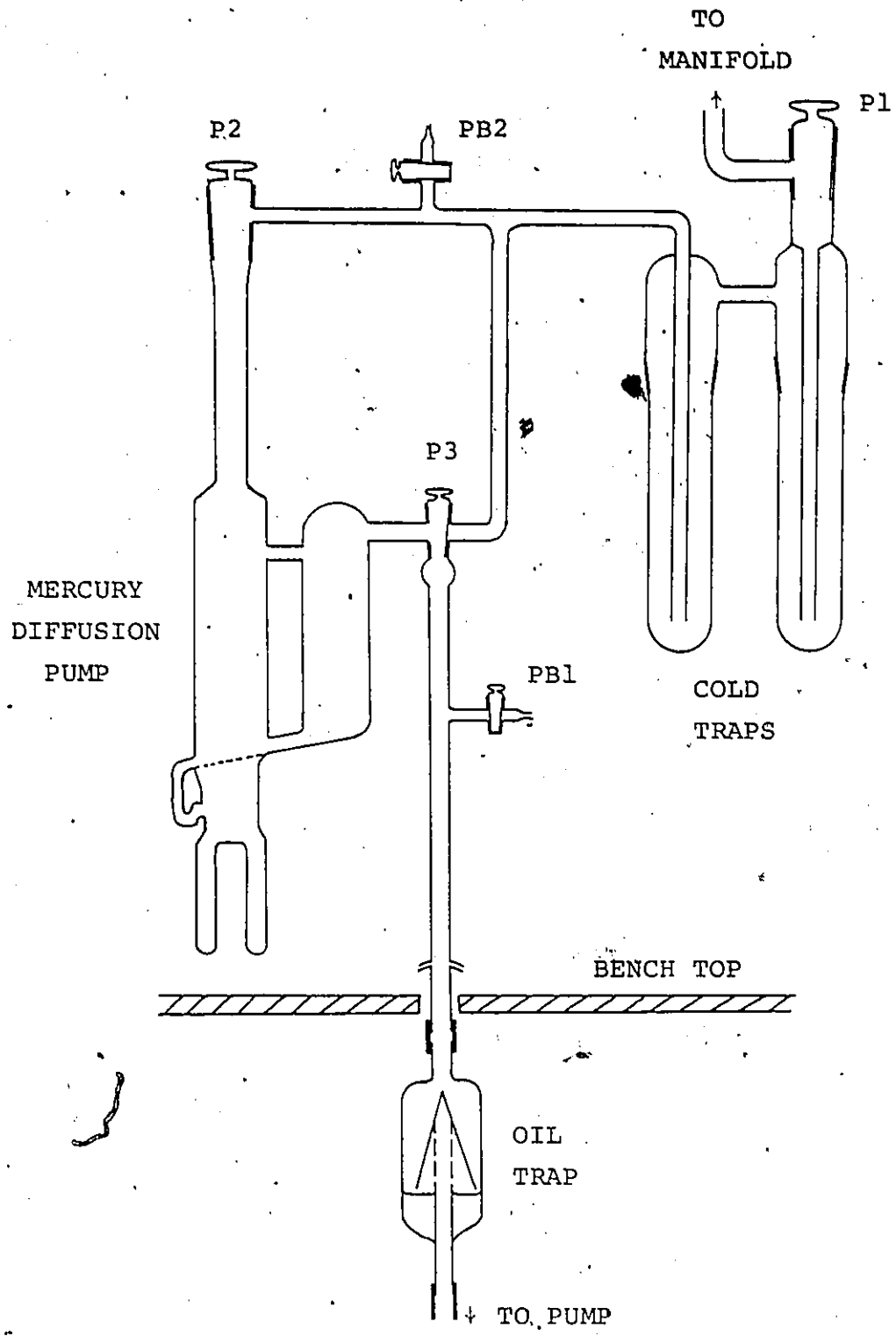
Figure A.2   The pumping system

use of special traps (see Figure A.3F), as in the preparation of CH_3SiI_3, (chapter I.2).

The pumping system consisted of a mechanical rotary pump (Edwards High Vacuum, Crawley, U.K.) and a glass mercury diffusion pump, which by manipulation of stopcocks P2 and P3 could be used in series with the rotary pump or by-passed. Shut-down of the pump was effected by closing P3, and opening the air bleed stopcock PB1 before switching off, so that the pump would be full of air before stopping. This prevented seizure of the moving parts by the vacuum in the system (especially from a still-hot diffusion pump) sucking the oil out of the pump.

Removal of the cold traps was effected by first isolating them by closing P1, P2 and P3. The air bleed stopcock PB2 could then be connected to a nitrogen supply, and the traps filled with the gas. (From the nature of chemicals used in this work, it was inadvisable to fill with air). They could then be removed to a fume hood, where the frozen contents were allowed to warm up and dissipate. This was usually performed once a week.

A.I.1 Trap-to-trap Distillation

Separation of mixtures using low temperature slush baths (Table A.1) depends on many variables, such as quantity of sample, surface area of the trap, time spent by the sample passing through the trap and the contents of the mixture. For most separations, A6 or B6 would be closed and the distillation would take place in a closed system. If non-

Table A.1   Low temperature baths*

Material	Temp(°C)	Material	Temp(°C)
ice/water †	0	ethyl acetate	-84
ice/water/salt †	-12-0	toluene	-95
carbon tetrachloride	-23	bromobutane	-112
chlorobenzene	-45	methylcyclohexane	-126
chloroform	-63	iso-pentane	-160
dry ice/methanol †	-78	liquid nitrogen	-196

* all prepared as slushes with liquid nitrogen except
as marked †.

condensible gases or low volatility liquids were present,
the system could be opened to the pump. Generally, best
results are obtained when there is a large difference in
boiling points of the constituents (more than 70°C).

A.I.2   Capillary Tubes

These were hand drawn from fairly thick walled
(ca. 2 mm) Pyrex tubing, so that the length and wall thickness
could be varied to suit the quantity and volatility of the
sample, and fitted with a ball joint. After evacuation of
the tube on the manifold, the tip was immersed in liquid
nitrogen and the sample allowed to condense into the finger.
With some manipulation of the liquid nitrogen Dewar and with
local warming of the tube either with the fingers or an air
gun, the sample could be coaxed into the tip of the tube.
When the manometer indicated that there was no more sample
in the manifold the Dewar was adjusted so that all of the
sample was frozen and the tube and manifold were opened to
the pump. The tube was sealed using a small blue flame to

soften the glass at three or four points and allowing the
vacuum to draw the glass in to effect the seal. The capillary
was then immersed totally in the liquid nitrogen and event-
ually left to warm in a fume hood. Care had to be taken to
leave sufficient room for expansion of the frozen sample;
some compounds almost doubled their volume when they melted.

Returning a sample held in a capillary tube to the
vacuum line was accomplished by means of a tube-breaker
(Figure A.3J) with a solid glass barrel which was inserted
in the open position. The capillary was placed in the tube-
breaker so that it passed through the barrel and the appara-
tus attached to the vacuum line with a plug of glass wool
inserted just inside the joint. When evacuated, turning the
stopcock broke the tube, the glass wool preventing glass from
the broken tube entering the manifold stopcocks or the mani-
fold itself. If the sample was fairly volatile, it was
advantageous to cool the lower portion of the breaker with
liquid nitrogen, which immediately condensed some of the
sample on breaking, thus reducing the sudden increase in
pressure. For very volatile compounds (for example SiH_4 or
B_2H_6), the breaker was filled with dry nitrogen to provide
a heat conducting medium while the lower portion was cooled,
so that the sample itself could be frozen or at least
cooled prior to breaking.

CsI plates

o-rings
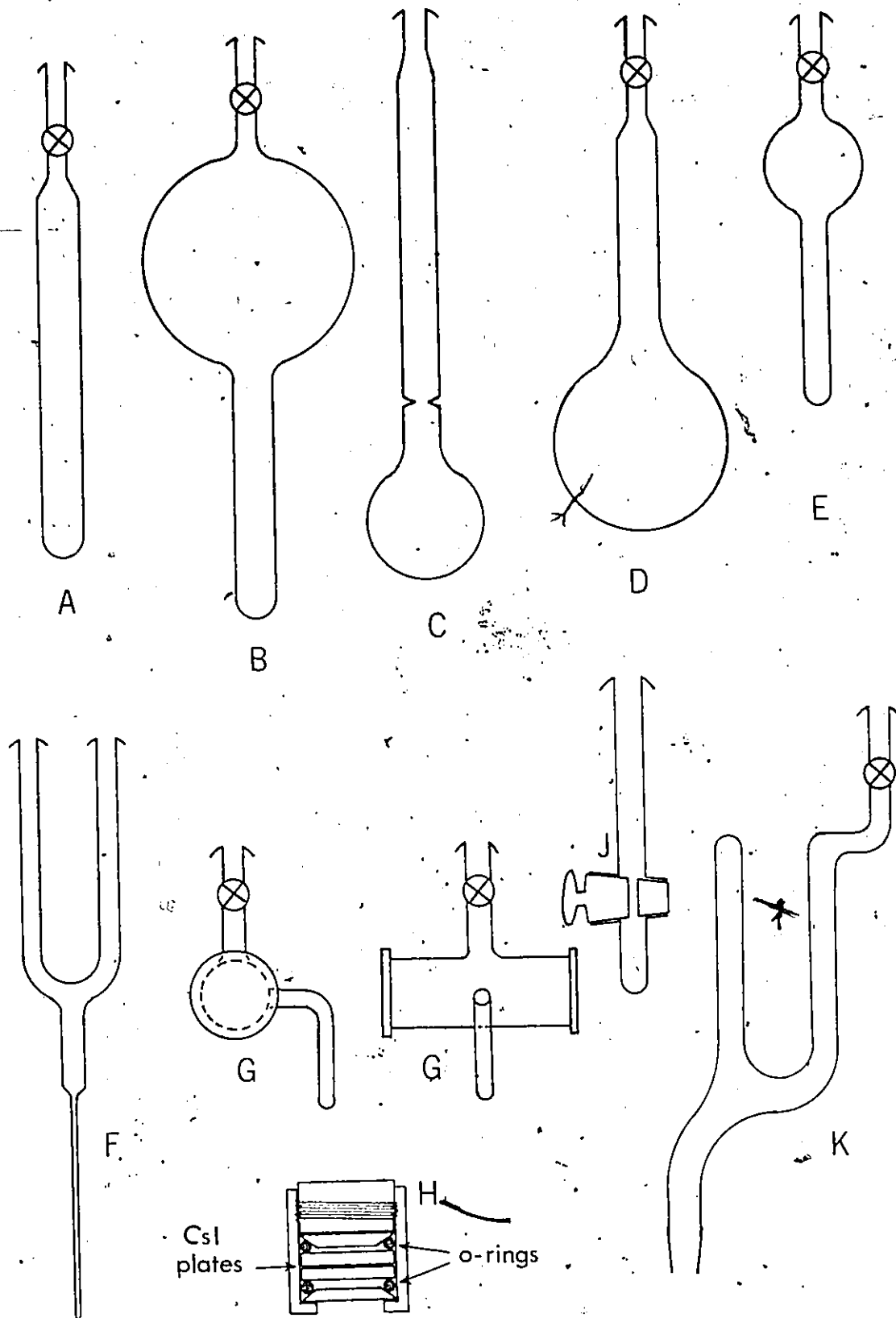
Figure A3   Reaction and Storage Vessels

APPENDIX II

STARTING MATERIALS

The compounds listed below were used as reagents for preparations described in this work, or as solvents or spectroscopic standards. They were either commercially available or had known preparative routes. Purity was checked by ^{1}H n.m.r., infrared (i.r.), Raman (Ra) spectroscopy and/or vapour pressure (v.p.) measurements. Commercial suppliers are listed at the end. For storage or reaction vessel type refer to Figure A.3. Compounds were stored at room temperature unless otherwise stated.

__Aluminium trihalides__: $AlCl_3$, $AlBr_3$, AlI_3[b,e]; sublimed and dried in vacuo.

__Antimony trifluoride__: SbF_3[j]; heated under vacuum, or pre-treated by passing BF_3 through the exchange column (type C) on the vacuum line.

__Boron tribromide__: BBr_3[b]; stored in an A-type vessel; degassed at -78°C prior to use. i.r., Ra.[3]

__Boron trichloride__: BCl_3[h]; stored in an A-type vessel; degassed at -112°C prior to use. i.r.[4]

__Boron trifluoride__: BF_3[h,n]; stored in a __dry__ B-type vessel with Teflon stopcock (avoiding all grease) at less than one atmosphere pressure. i.r., Ra[5,6]; v.p.[6]

__Butyl lithium__: $BuLi$[b]; in various solvents. Original container fitted with rubber septum, stored in refrigerator. Withdrawn

using syringe.

<u>Chlorodimethylsilane</u>: <u>Me$_2$SiHCl</u>[b,k]; stored in an A-type vessel; the portion passing from a trap at -45°C into one at -78°C was used. n.m.r.[7]

<u>Chlorotrimethylsilane</u>: <u>Me$_3$SiCl</u>[b,k]; stored in an A-type vessel; the portion passing from a trap at -45°C into one at -78°C was used. n.m.r.[7]; i.r.[8]; v.p.[9]

<u>Cyclohexane</u>: <u>C$_6$H$_{12}$</u>; n.m.r. grade solvent, stored in an A-type vessel. Used as received.

<u>Deuterium chloride</u>: <u>DCl</u>[i]; "99.8% D", used from lecture bottle without further treatment.

<u>Deuterium oxide</u>: <u>D$_2$O</u>[i,m]; "99.8% D", bottle fitted with rubber septum under nitrogen in a glove bag; removed by syringe as required.

<u>Di-n-butyl ether</u>: (<u>n-C$_4$H$_9$</u>)$_2$<u>O</u>[a]; stored in a D-type vessel over LiAlH$_4$; degassed at -78°C prior to use.

<u>Dichlorodimethylsilane</u>: <u>Me$_2$SiCl$_2$</u>[b,k,l]; stored in an A-type vessel; the portion passing through a -63°C trap into a trap at -78°C was used. n.m.r.[10]; v.p.[9]

<u>Dichloromethylsilane</u>: <u>MeSiHCl$_2$</u>[b,k,l]; stored in an A-type vessel; the portion passing through a -63°C trap and condensing in a -78°C trap was used. n.m.r.[7]; v.p.[9]

<u>Hexamethylphosphoramide</u>: (<u>Me$_2$N</u>)$_3$<u>PO</u>[a,d]; stored in original bottle over 4Å molecular seive; degassed at 0°C before use.

<u>Hydrogen bromide</u>: <u>HBr</u>[h]; stored in a B-type container; degassed at -196°C before use. i.r.[11]

<u>Hydrogen chloride</u>: <u>HCl</u>[h]; as above.

Hydrogen iodide: HI; prepared, by the dropwise addition of
hydroiodic acid on P_2O_5. Passed through a $-78^\circ C$ trap to
remove water vapour. Stored in an A-type vessel; kept cool
when possible; degassed at $-78^\circ C$ prior to use. i.r.[11]

Hydroiodic acid: HI[b]; 48% aqueous solution. Used as supplied.

Iodomethane -d$_3$: CD_3I[i]; stored in light-protected (matt black)
A-type vessel. Used as supplied.

Lithium tetrahydroaluminate: $LiAlH_4$[b]; stored in tightly sealed
plastic bag in metal container. Transferred to tipping tube
or solvent vessel in glove bag.

Lithium tetrahydroaluminate-d$_4$: $LiAlD_4$[b]; stored in 1 gm vials
as received; see above.

Mercury(II) chloride: $HgCl_2$[g]; dried in column type C under
vacuum.

Phosphorus pentoxide: P_2O_5[f]; stored and used as received.

Potassium metal: K[c]; stored under mineral oil as received.
Cut under oil, and washed in 30°-60° petroleum ether and
dried in dry nitrogen immediately before use.

Silane: SiH_4[h]; supplied in gas cylinder, transferred to and
stored in B-type vessel; passed through $-126^\circ C$ trap prior
to use. n.m.r.[12]; i.r.[13]

Silane-d$_4$: SiD_4; prepared by the $LiAlD_4$ reduction of $SiCl_4$
in di-n-butyl ether, stored in a B-type vessel. Passed
through a trap at $-126^\circ C$ prior to use. i.r.[13]

Silver bromide: AgBr[d]; dried in column C prior to use.

Sodium dimethylarsonate: $Me_2As(O)ONa.3H_2O$[e,f]; stored and
used as supplied.

Tetrachlorosilane: $\underline{SiCl_4}$[b]; stored in an A-type vessel; passed through a trap at $-45°C$ into one at $-78°C$ prior to use. i.r.[14]; v.p.[9]

Tetramethyldisilazane: $\underline{(Me_2SiH)_2NH}$[k]; stored in an A-type vessel as supplied.

Tetramethylsilane (TMS): $\underline{Me_4Si}$[b]; n.m.r. grade solvent; stored in an A-type vessel.

Trichloromethylsilane: $\underline{MeSiCl_3}$[b,k,l]; stored in an A-type vessel; purified as for Me_2SiCl_2. n.m.r.[10]; i.r.[8]; v.p.[9]

Trimethylsilyldimethylarsine: $\underline{Me_3SiAsMe_2}$; prepared[15], by the reaction between Me_3SiCl and Me_2AsLi (from a reaction between BuLi and Me_2AsH). n.m.r.[15]

A.II.1 Commercial Suppliers

a) Aldrich Chemical Co., Milwaukee, Wisc.

b) Alfa Divsion, Ventron Corp., Beverley, Mass.

c) Anachemia Chemicals Ltd., Toronto, Ont.

d) J.T. Baker Chemical Co., Phillipsburg, N.J.

e) British Drug Houses Ltd., Poole, Dorset, U.K.

f) Fisher Scientific Co., Fair Lawn, N.J.

g) Mallinkrodt, St. Louis, Mo.

h) Matheson Gas Products, East Rutherford, N.J.

i) Merck, Sharpe and Dohme Ltd., Montreal, P.Q.

j) Ozark-Mahoning, Tulsa, Okla.

k) Petrarch Systems, Levittown, Penn.

l) Research Organic/Inorganic Chemical Corp., Hillside, N.J.

m) Stohler Isotope Chemicals, Montreal, P.Q.

n) Union Carbide Corp., Specialty Gas Products, Linde Division, New York, N.Y.

APPENDIX III

INSTRUMENTAL TECHNIQUES

All measurements of vibrational spectra were made using both infrared and Raman methods. Most of the infrared spectra were run in the gas phase, while the remainder and all of the Raman spectra were recorded on neat, liquid samples. Purity checks were made mostly by n.m.r. spectroscopy, but also using Raman and, a few times, mass spectrometry. The following is a description of the instrumentation and techniques used in this study.

A.III.1 N.m.r. Spectroscopy

Two different instruments were used for ^{1}H n.m.r. measurements, depending on the accuracy required. Most purity checks and all chemical shift measurements were made on a JEOL model C60-HL spectrometer operating at 60 MHz. For quick, routine checks, a Varian EM-360 permanent magnet instrument was also used, also operating at 60 MHz. Although possessing lower resolution than the JEOL, it was found to be quite satisfactory for the purposes of identification. The ^{19}F n.m.r. spectra were recorded on the JEOL instrument, operating for fluorine nuclei at 56.4 MHz. The ^{13}C spectra were recorded on a Bruker CPX 100 multinuclear pulsed Fourier transform spectrometer operating at 22.64 MHz, all spectra being recorded under ^{1}H noise-decoupling conditions.

The probes in all three instruments accepted standard 5 mm o.d. sample tubes. Samples were sealed directly

from the vacuum line, usually into hand-drawn capillary tubes, or occasionally into 5 mm glass tubing acceptable to the probes. The capillaries were placed in standard n.m.r. tubes, which for ^1H and ^{19}F n.m.r. measurements were then partially filled with carbon tetrachloride to damp the motion of the capillary during spinning of the n.m.r. tube. For chemical shift measurements an internal standard (usually TMS, sometimes cyclohexane) was distilled into the capillary along with the sample. Integration of the signals gave a measurement of the concentration of the various components in the sample. For ^{13}C spectra deuterochloroform, $CDCl_3$, was used instead of carbon tetrachloride; as well as damping the spinning of the capillary it was used as a deuterium lock signal and external standard. The Bruker's data processing system converted all shifts to a TMS scale. Although integration signals were recorded by the instrument they could not be used as a measure of concentration due to the large difference in relaxation times of ^{13}C nuclei compared to protons.

A.III.2 Infrared Spectroscopy

Although two different instruments were used, almost all infrared spectra (and all those which are reported in this thesis) were recorded on a Beckman IR-12 spectrometer operating from 200 to 4000 cm^{-1}. This is a high resolution instrument with expansion facilities in both wavenumber and absorption scales. Some quick, routine scans were made on a Beckman IR-20 instrument when convenient, recording from

400-4000 cm^{-1}. Wavenumber reproducibility was checked period-
ically against polystyrene film, and was generally ±1 cm^{-1}.

During the course of this work several infrared cells
were used. Gas cells were custom made, either 60 or 90 mm
long and 50 mm (for KBr windows) or 25 mm (for CsI) in
diameter. A typical gas cell is shown in Figure A.3G.
Nearly all spectra were recorded using KBr windows, and
although the transparent range is less than for CsI, very
few bands were missed because of their use. The windows
were ground first on fine (320 grade) Wet-or-Dry paper with
methanol and then on silk stretched over a sheet of glass
using cesium oxide powder and methanol as the polishing
compound. When the windows were clear and gave a flat,
transparent response on the spectrometer, they were attached
to the body of the gas cell. The ends of the gas cell were
covered with a thin (ca. 0.5 mm), even layer of Apiezon A40
wax and attached to the vacuum line. The wax was softened
with a hot air gun, and the windows pulled into place by
opening the stopcock to the evacuated manifold. The stop-
cock was either ground glass or (later) Teflon-in-glass with
Viton O-rings. The cold finger was used to condense material
into the cell when the compound was of low volatility, or
when there was too little sample to generate sufficient
vapour pressure in the system. Typically, several spectra
were run at gas pressures ranging from just under 10 mm Hg
to over 100 mm Hg, so that almost all absorption bands would
appear approximately full scale on at least one scan. Where

the signal was weak due to low volatility or quantity of sample available, the scale expansion facility was used. Each band was scanned at fourfold wavenumber scale expansion (12.5 cm^{-1} per inch) at slow scan rates (8 cm^{-1} min^{-1}), the wavenumbers being recorded directly onto the chart. It was from these scans that the frequencies reported in this work were taken.

Where sample pressure was a problem for low volatility compounds, spectra were sometimes recorded in the liquid phase. For this purpose a liquid cell as shown in Figure A.3H was used. The sample was introduced between the two CsI plates in a glove bag or dry box and the top screwed down. This arrangement was relatively air-tight over a short period, but a band could be seen to grow at ca. 1030 cm^{-1} due to the strong asymmetric Si-O-Si stretch of the hydrolysis product. The first spectrum was run with as much liquid as possible between the plates, and the film thickness subsequently reduced by screwing the top of the holder down. In some experiments, the cell was opened in the air after the spectra had been recorded, and another scan made so that as many absorptions due to hydrolysis product(s) could be identified in the original spectra.

A.III.3 Raman Spectroscopy

A Spectra-Physics 700 instrument equipped with an argon ion laser and model 265 exciter was used for recording Raman spectra. The strongest exciting line at 488.0 nm ($20,492$ cm^{-1}) was used in conjunction with a cooled photo-

multiplier with S20 characteristics. Since all the samples were essentially colourless, no absorption or fluorescence problems were encountered with the blue-green line, even at fairly high laser power. This was available up to just over 1 W, with spectra routinely run at 300-600 mW. The spectral slit width could be varied from 8 cm^{-1} for routine scans, to 4 or 2 cm^{-1} for higher resolution work. However, the 2 cm^{-1} slit was only used for fairly strong bands, as the compensating increase in either laser power or photomultiplier sensitivity increased the background noise, and although this could be reduced by an increase in the period (response of the pen), a point was reached where it was counterproductive to use a very small slit width. Wavenumber checks were performed periodically using liquid carbon tetrachloride and benzene. The largest deviation found was ± 1.5 cm^{-1}.

The samples, as neat liquids and usually in the same capillaries used for recording n.m.r. spectra, were at first aligned by eye in the sample compartment. A strong peak was then found and the recorder stopped at the maximum. The signal was then optimised by use of the fine controls that adjust the sample holder in essentially all three directions as well as moving the collimator of the photomultiplier tube. After the base line and background compensation were set, the spectrum was run, first with the polariser-analyser (positioned in front of the collimator) in the parallel position (for the "normal" or "depolarised" spectrum) and then on the same chart, without adjustment of laser power or sensitivity, in

the perpendicular position (for the "polarised" scan).
Again, as with the measurement of band position in the infra-
red, each peak was recorded at almost maximum intensity, and
if necessary with an expanded wavenumber scale to better
determine the peak maximum or "centre of gravity" if this was
unclear.

The compounds studied in this work were all found to be
stable under the conditions used, even after several hours
in the laser beam. For some fluoro- derivatives, however
(notably trifluoromethylsilane), even relatively low powers
(ca. 300 mW) produced vapour bubbles in the samples, which
of course disrupted the spectra. Unfortunately it is
precisely for these compounds that higher laser power is
desirable to make up for the relatively low intensity of
their Raman bands.

A.III.4 Mass Spectrometry

The instrument used was a Varian GMAT CH5 spectro-
meter, operating in the electron impact mode at 70 eV. A
Pyrex inlet system terminated 2 mm from the electron source,
and was fitted by means of Viton O-rings and a short length
of flexible vacuum tubing to a portable vacuum manifold, with
three takeoff points and a Pirani vacuum gauge. Two cold
traps and a two stage rotary pump completed the pumping
system. A cold finger between the manifold and the inlet
system could be isolated by greaseless stopcocks each side
of it. A capillary tube containing the sample was broken
open, allowed to expand into the manifold and was condensed

into the cold finger, which was then isolated from the manifold. The stopcock between the finger and inlet system was opened as the sample melted, and adjusted to maintain a steady vapour pressure, monitored by the instrument, into the electron source. Several spectra were recorded and the most consistently reproducible spectra retained for final measurements or for a computer print-out of the data.

APPENDIX IV

COMPUTER PROGRAMMES

The two computer programs used in this work were SOTONVIB[16] and LARMOL[17]. Although both are basically variations on Schachtschneider's original programs[18] they differ in several respects, mainly in format. The following is a description of the input and output of each program.

A.IV.1   Input

The basic input for both programs is the spatial arrangement of the atoms. In SOTONVIB this is in Cartesian co-ordinates and mass for each atom, followed by the internal co-ordinates which describe which atoms are bonded to each other, and thus defines the bond lengths and angles. For large molecules where calculation of the Cartesian co-ordinates by simple trigonometry is tedious, any number of internal co-ordinates can be ascribed the desired bond lengths and angles and a preliminary set of Cartesians can be refined to these values. This is not necessary for LARMOL, where instead of using Cartesian co-ordinates, the atoms and their connections to the other atoms are defined in a framework of dummy atoms in a manner described by Hilderbrandt[19]. Once the spatial relationships are described, the bond lengths and angles are defined to complete the "structure" and the Cartesian co-ordinates calculated. This approach has an advantage over SOTONVIB where a series of related molecules is being studied, as is the case for most of this

work, where the "spatial relationships" of the atoms are the same. Thus each member of the series is defined in the same way and the dimensions merely changed. It also permits changing the values of the bond lengths and angles, or rotation of part of a molecule with respect to the rest without having to calculate a new set of Cartesian co-ordinates every time. As in SOTONVIB, the internal co-ordinates are introduced at this stage. This is followed in both by the remaining information which consists of the observed frequencies, the Z matrix, or force constant definitions in terms of the internal co-ordinates, and the values and constraints for the force constants to be used in the calculation. The order of input differs slightly for the two programs, as they do in other details. For example, all calculated frequencies are listed in decreasing magnitude, as are the input observed frequencies, but should they not correspond (for example should and e and an a_1 mode be interchanged in order in the calculated frequencies) then SOTONVIB allows for the reordering of the observed frequencies, instead of having to retype the card containing the observed frequencies in the desired order. On the other hand, a number must be entered for every fundamental in SOTONVIB. Should there be an unobserved or inactive fundamental however, then an estimated frequency must be inserted, and if this is inaccurate then its inclusion in the least squares refinement will restrict the usefulness of any resultant convergence. By contrast, LARMOL allows for such a fundamental to be left out of the refine-

ment without disturbing the order of the observed frequencies.

Up to this point both programs are quite similar in approach, but it is in the treatment of isotopic molecules that a significant difference exists. Here LARMOL uses data from all frequency sets in the force constant refinement, whereas SOTONVIB refines the force constants to the data for one isotopic molecule, then uses an "overlay" technique, calculating the frequencies for the other isotopic species from this refined force constant set. This difference is quite noticeable in molecules where there are large anharmonicity effects, as LARMOL will produce a set of force constants which averages the effect, whereas SOTONVIB will refine to one frequency set as closely as possible, which leaves the molecule in the "overlay" calculation with a much poorer fit. For example, in the study on the variously deuterated methylsilanes[20] (chapter I.1) the CH_3 and CD_3 stretches were approximately the same for both pairs of CH_3- and CD_3 derivatives, at 2975 and 2918 cm^{-1}, and 2230 and 2130 cm^{-1}, for the asymmetric and symmetric stretches, respectively. For these pure modes, LARMOL calculated values of 2982 and 2939 cm^{-1}, and 2225 and 2114 cm^{-1} respectively; the former pair too high and the latter pair too low, but in proportionate amounts. If SOTONVIB had been used with the overlay calculation, one of the pairs would have been reproduced almost exactly, with a much larger error for the other. While this would not be very significant in this region (there is nothing else the frequencies could be attributed to) it could produce results in the hydrogen bending and

skeletal stretching region (ca. 350-1000 cm^{-1}) which would
limit the usefulness of this application. However the main
advantage of the simultaneous calculation of protonated and
deuterated molecules has already been pointed out, in that
it introduces more observables, ideally approaching a point
where a unique set of force constants can be obtained.

A.IV.2 Output

The Cartesian co-ordinates are the first output
for both programs, calculated in LARMOL (along with the
interatomic distances) and input in SOTONVIB. If the Car-
tesians are being calculated in SOTONVIB, there follows a
comparison of the observed and calculated values for the
internal co-ordinates (bond lengths and angles) and the trial
Cartesian co-ordinates for each refinement until the struc-
tural data is matched as closely as possible. Otherwise,
the input internal co-ordinates are followed by the "B matrix",
relating the Cartesian to the internal co-ordinates and a
calculation of the moments of inertia (from which infrared
band contours can be predicted). Both now follow with the
input force constant values, those which will be allowed to
vary and the "Z matrix", with SOTONVIB adding the reordering
information. LARMOL now prints out two matrices, the "D
matrix", corresponding to SOTONVIB's B matrix, and the "Y
matrix", describing the relative motion of each atom in terms
of the Cartesian co-ordinates for each calculated vibrational
frequency in the preliminary set. (These are useful for
determining whether the calculated frequency is symmetric or

asymmetric). They are called the "LX vectors" in SOTONVIB, but are calculated in this program from the _final_ set of calculated frequencies, and so appear at the end of the program. Both sets of observed and calculated frequencies are now output in both programs, SOTONVIB including a difference column, but LARMOL calculating the potential energy distribution for each refinement, which can be very useful. The corrections to the force constants and hence the new set of values follow, with a correlation matrix in LARMOL which indicates the degree to which each force constant can be refined independently of the others. After the preset number of iterations LARMOL is finished, but SOTONVIB prints out the "LX vectors" (described above), the "LR vectors", which are similar, except express the calculated frequencies in terms of the internal co-ordinates, and the "JZ matrix". (See equation 1.8). This is a most useful set of information as it describes the effect that a change in a force constant will have on each frequency even if the force constant has no value. Thus it can help reduce the number of interaction terms by allowing for only those which will have a critical effect on the frequencies to be selected. Finally, the p.e.d. for the final set of calculated frequencies is listed.

APPENDIX V

This appendix contains the full data for the NCA calculations on the fluoromethylgermane series, from which the pertinent data has been drawn and appears in Chapter 1.5.

Table A2. Description and class of fundamentals for CH₃GeF₃

Description	a_1	a_2	e
CH_3 str.(asym)			ν_7
CH_3 str.(sym)	ν_1		
CH_3 def.(asym)			ν_8
CH_3 def.(sym)	ν_2		
CH_3 rock			ν_9
GeC stretch	ν_3		
GeF_3 str.(asym)			ν_{10}
GeF_3 str.(sym)	ν_4		
GeF_3 rock			ν_{11}
GeF_3 def.(asym)			ν_{12}
GeF_3 def.(sym)	ν_5		
torsion		ν_6	

Table A3. Observed and calculated frequencies (cm^{-1}), and potential energy destribution for CH₃GeF₃

Mode	obs.[a]	calc.	p.e.d.[b]
ν_1	2949	2952.6	98(1)
ν_2	1269	1268.6	51(4)+48(5)+10(2)-4(13,14)
ν_3	630	629.9	67(2)+24(3)+4(4,5)
ν_4	730	729.9	68(3)+22(2)+5(12)
ν_5	254	253.3	65(9)+33(8)
ν_6	–	–	not calculated
ν_7	3035	3034.8	100(1)
ν_8	1410	1413.1	92(4)+4(5,13)
ν_9	837	837.2	88(5)+4(3,4,14)
ν_{10}	744[*]	743.9	98(3)+4(5)-4(12)
ν_{11}	194	193.9	99(8)
ν_{12}	292	292.4	99(9)

a) ref. 21; liquid Raman frequencies, except [*] gas i.r.

b) contributions greater than 2%

Table A4. Description and class of fundamentals for $(CH_3)_2GeF_2$

Description	a_1	a_2	b_1	b_2
CH_3 str. (asym)	ν_1	ν_{10}	ν_{15}	ν_{21}
CH_3 str. (sym)	ν_2			ν_{22}
CH_3 def. (asym)	ν_3	ν_{11}	ν_{16}	ν_{23}
CH_3 def. (sym)	ν_4			ν_{24}
CH_3 rock	ν_5	ν_{12}	ν_{17}	ν_{25}
GeC_2 str.	ν_6			ν_{26}
GeF_2 str.	ν_7		ν_{18}	
GeC_2 bend	ν_8			
GeF_2 bend	$\nu_9(sc)$	$\nu_{13}(tw)$	$\nu_{19}(r)$	$\nu_{27}(wag)$
CH_3 torsion		ν_{14}	ν_{20}	

Table A5. Description and class of fundamentals for $(CH_3)_3GeF$

Description	a_1	a_2	e	
CH_3 str. (asym)	ν_1	ν_9	ν_{13}	ν_{14}
CH_3 str. (sym)	ν_2		ν_{15}	
CH_3 def. (asym)	ν_3	ν_{10}	ν_{16}	ν_{17}
CH_3 def. (sym)	ν_4		ν_{18}	
CH_3 rock	ν_5	ν_{11}	ν_{19}	ν_{20}
GeC_3 stretch	ν_6		ν_{21}	
GeF stretch	ν_7			
GeC_3 def.	ν_8			
GeC_3 rock			ν_{22}	
CH_3 torsion			ν_{23}	
		ν_{12}	ν_{24}	

Table A6. Observed and calculated frequencies (cm^{-1}) and potential energy distribution for $(CH_3)_2GeF_2$

Mode	obs.[a]	calc.	p.e.d.[b]
ν_1	3015	3016.8	100(1)
ν_2	2935	2934.7	98(1)
ν_3	1417	1426.5	90(4)+6(13)
ν_4	1259	1249.9	52(4)+30(5)+16(6)+9(2)-6(13)
ν_5	836*	835.0	58(6)+29(5)+5(15)
ν_6	599	599.2	67(2)+24(3)+4(4)
ν_7	685*	688.3	72(3)+22(2)
ν_8	219	218.6	82(7)+15(8)
ν_9	259	259.2	87(9)+8(8)+4(7)
ν_{10}	3015	3016.1	100(1)
ν_{11}	1417	1424.0	91(4)+6(13)
ν_{12}	765*	761.4	101(5)-5(14)
ν_{13}	192	194.5	99(8)
ν_{14}	n.o.	–	
ν_{15}	3015	3016.1	100(1)
ν_{16}	1417	1421.9	91(4)+6(13)
ν_{17}	765*	774.6	91(5)+10(3)-4(14)
ν_{18}	698*	697.4	91(3)+11(5)
ν_{19}	185	185.0	98(8)
ν_{20}	n.o.	–	
ν_{21}	3015	3015.9	100(1)
ν_{22}	2935	2934.9	98(1)
ν_{23}	1417	1424.0	90(4)+6(13)
ν_{24}	1259	1252.4	52(4)+30(5)+15(6)+10(2)-6(13)
ν_{25}	826*	826.6	63(6)+26(5)+5(15)+4(4)
ν_{26}	663	661.7	88(2)+6(4)+5(5)
ν_{27}	199	198.1	99(8)

a) see footnote to Table A3.

b) contributions greater than 4%

Table A7. Observed and calculated frequencies (cm^{-1}) and
potential energy distribution for $(CH_3)_3GeF$

Mode	obs.[a]	calc.	p.e.d.[b]
ν_1	2990	2989.9	100(1)
ν_2	2917	2913.5	98(1)
ν_3	1416	1419.6	93(4)+4(13)
ν_4	1255	1255.8	51(4)+33(5)+13(6)+8(2)
ν_5	836*	833.4	62(6)+21(5)+7(15)+4(4)
ν_6	578	577.6	79(2)+10(3)+4(4)
ν_7	662*	662.7	88(3)+11(2)
ν_8	195	198.4	62(7)+36(8)
ν_9	i.a.[c]	2989.9	101(1)
ν_{10}	i.a.	1420.6	92(4)+4(13)
ν_{11}	i.a.	765.8	107(5)−10(14)
ν_{12}	i.a.	−	−
ν_{13}	2990	2989.9	101(1)
ν_{14}	2990	2989.9	101(1)
ν_{15}	2917	2913.5	98(1)
ν_{16}	1416	1419.6	92(4)+4(13)
ν_{17}	1416	1419.6	93(4)+4(13)
ν_{18}	1255	1255.8	51(4)+33(5)+13(6)+8(2)
ν_{19}	836*	833.4	61(6)+24(5)+8(15)+4(4)
ν_{20}	760*	765.8	103(5)−10(14)
ν_{21}	629	629.4	90(2)+5(4)+4(5)
ν_{22}	230	228.3	97(7)
ν_{23}	185	185.1	99(8)
ν_{24}	n.o.	−	−

a) see footnote to Table A3.

b) contributions greater than 3%

c) inactive   * infrared frequencies

Table A8. Force constant values for the series MeGeX$_3$

Force Constant	X=	F*			Cl*			Br	I
		(a)	(b)	(c)	(d)	(e)	(f)		
1	f CH	493.8	493.8	493.8	486.4	486.5	486.5	483.3	482.6
2	f GeC	332.9	333.3	332.9	303.5	303.5	305.3	292.6	275.1
3	f GeX	477.4	477.4	478.1	246.4	245.5	246.1	190.1	136.1
4	f HCH	49.6	51.9	50.5	49.0	48.8	48.8	46.5	45.9
5	f HCGe	46.2	43.9	45.1	45.0	45.3	45.3	47.4	46.4
6	f CGeX	59.5	45.2	95.8	60.7	36.0	34.0	60.6	64.8
7	f XGeX	79.9	94.2	45.8	71.7	106.5	85.2	68.2	75.6
8	f CH/CH	3.6	3.6	3.6	3.9	3.9	4.0	3.7	3.4
9	f GeX/GeX	17.8	19.2	17.5	22.6	23.1	23.7	25.0	20.9
10	f HCH/HCH	-2.0	0.3	-1.1	-2.1	-2.3	-2.3	-4.4	-5.3
11	f HCGe/HCGe	-1.7	-4.0	-2.4	-2.3	-2.2	-2.2	-3.4	1.2
12	f CGeX/CGeX	14.4	0+	17.9	6.2	0.7	-1.3	3.8	0.9
13	f XGeX/XGeX	9.1	0+	4.5	8.9	9.4	-12.0	4.4	3.6

* see text for explanation of assignments.

+ fixed; initial values less than 0.1

Table A9.   Calculated frequencies (cm^{-1}) and p.e.d.'s[+] for $MeGeF_3$[*]

	Mode		(a) calc.	(a) p.e.d.	(b) calc.	(b) p.e.d.	(c) calc.	(c) p.e.d.
e	CH_3 str.	ν_7	3035	100(1)	3035	100(1)	3035	100(1)
a_1	CH_3 str.	ν_1	2949	98(1)	2949	98(1)	2949	98(1)
e	CH_3 def.	ν_8	1410	92(4)+4(5,10)	1410	94(4)+4(5)	1410	96(4)+4(5)
a_1	CH_3 def.	ν_2	1269	51(4)+47(5)+10(2)	1269	51(4)+46(5)+10(2)-5(11)	1269	53(4)+45(5)+10(2)-5(11)
e	CH_3 rock	ν_9	833	88(5)+4(3)	833	85(5)+5(3,11)	833	84(5)+8(11)+4(4)
a_1	GeC str.	ν_3	630	68(2)+22(3)+4(4,5)	630	68(2)+22(3)+4(4,5)	630	70(2)+21(3)+4(4,5)
e	GeF_3 str.	ν_{10}	744	98(3)-4(9)+4(5)	744	98(3)+5(5)+4(9)	744	98(3)-4(9)+4(5)
a_1	GeF_3 str.	ν_4	730	70(3)+20(2)+5(9)	730	70(3)+20(2)+5(9)	730	71(3)+19(3)+6(9)
e	GeF_3 rock	ν_{11}	194	130(6)-32(12)	254	120(6)-22(12)	194	99(6)
a_1	GeF_3 def.	ν_5	292	42(7)+31(6)+15(12)+9(13)	292	50(6)+24(7)+19(12)+5(13)	253	66(7)+32(6)
e	GeF_3 def.	ν_{12}	254	112(7)-13(13)	194	110(7)-11(13)	292	99(7)
a_2	torsion	ν_6						

+   contributions greater than 3%

*   for explanation of assignments, see Chapter 1.4.

Table A10. Calculated frequencies (cm^{-1}) and p.e.d.'s[+] for $MeGeCl_3$.[*]

Mode			(d) calc.	(d) p.e.d.	(e) calc.	(e) p.e.d.	(f) calc.	(f) p.e.d.
e	CH_3 str.	ν_7	3011	100(1)	3011	100(1)	3011	100(1)
a_1	CH_3 str.	ν_1	2929	98(1)	2929	98(1)	2929	98(1)
e	CH_3 def.	ν_8	1403	92(4)+4(5,10)	1403	92(4)	1403	92(4)+4(5,10)
a_1	CH_3 def.	ν_2	1242	52(4)+48(5)+9(2)-4(10,11)	1242	52(4)+48(5)+9(2)-5(10,11)	1242	52(5)+48(5)+9(2)-5(10,11)
e	CH_3 rock	ν_9	825	90(5)+5(11)+4(4)	825	91(5)+4(4,11)	825	91(5)+4(4,11)
a_1	GeC str.	ν_3	630	87(2)+5(4,5)	630	87(2)+5(4,5)	630	88(2)+5(4,5)
e	$GeCl_3$ str.	ν_{10}	428	105(3)-10(9)	428	104(3)-10(9)+5(7)	428	104(3)-10(9)+4(7)
a_1	$GeCl_3$ str.	ν_4	397	80(3)+15(9)	397	80(3)+15(9)	397	81(3)+16(9)
e	$GeCl_3$ rock	ν_{11}	144	106(6)-11(12)	179	99(6)	179	94(6)+4(12)
a_1	$GeCl_3$ def.	ν_5	179	43(7)+37(6)+11(13)+7(12)	179	64(7)+21(6)+11(13)+5(3)	136	91(7)+36(6)-25(13)
e	$GeCl_3$ def.	ν_{12}	179	110(7)-14(13)	144	103(7)-9(13)	144	83(7)+12(13)+5(3)
a_2	torsion	ν_6						

[+] contributions greater than 3%

[*] for explanation of assignments, see Chapter 1.4.

Tables A11 and A12. Calculated frequencies(cm^{-1}) and
p.e.d.'s for MeGeBr$_3$ and MeGeI$_3$

Mode			calc.	p.e.d.[a]
MeGeBr$_3$				
e	CH$_3$ str.	ν_7	3002.0	100(1)
a$_1$	CH$_3$ str.	ν_1	2918.0	98(1)
e	CH$_3$ def.	ν_8	1401.0	88(4)+8(10)+4(5)
a$_1$	CH$_3$ def.	ν_2	1245.0	50(4)+51(5)−9(10)+8(2)
e	CH$_3$ rock	ν_9	822.0	96(5)
a$_1$	GeC str.	ν_3	617.0	90(2)+4(4,5)
e	GeBr$_3$str.	ν_{10}	312.0	98(3)−13(9)+10(6)
a$_1$	GeBr$_3$str.	ν_4	264.0	72(3)+19(9)
e	GeBr$_3$rock	ν_{11}	162.0	96(6)+11(3)−6(12)
a$_1$	GeBr$_3$def.	ν_5	125.0	43(7)+38(6)+6(3,13)+5(12)
e	GeBr$_3$def.	ν_{12}	94.0	101(7)−7(13)+6(3)
a$_2$	torsion	ν_6		
MeGeI$_3$				
e	CH$_3$ str.	ν_7	3001.0	100(1)
a$_1$	CH$_3$ str.	ν_1	2914.0	98(1)
e	CH$_3$ def.	ν_8	1404.0	86(4)+10(10)+4(5)
a$_1$	CH$_3$ def.	ν_2	1229.0	50(4)+51(5)−12(10)+8(12)
e	CH$_3$ rock	ν_9	806.0	98(5)
a$_1$	GeC str.	ν_3	598.0	91(2)+4(4,5)
e	GeI$_3$str.	ν_{10}	258.0	79(3)+24(6)−12(9)
a$_1$	GeI$_3$str.	ν_4	200.0	63(3)+19(9)+8(7)+7(6)
e	GeI$_3$rock	ν_{11}	156.0	76(6)+27(3)−4(9)
a$_1$	GeI$_3$def.	ν_5	98.0	42(7)+36(6)+13(3)+4(9,13)
e	GeI$_3$def.	ν_{12}	72.0	95(7)+11(3)−5(13)
a$_2$	torsion	ν_6		

a) contributions greater than 3%

APPENDIX REFERENCES

1. D.F. Shriver, "The Manipulation of Air-Sensitive Compounds," McGraw-Hill, New York, N.Y., 1969.

2. W.L. Jolly, "The Synthesis and Characterization of Inorganic Compounds," Prentice-Hall, Englewood Cliffs, N.J., 1970.

3. T. Wentink and V.H. Tiensuu, J. Chem. Phys. 28, 826, (1958)

4. R.E. Scruby, J.R. Lacher and J.D. Park, J. Chem. Phys. 19, 386 (1951)

5. R.G. Steinhardt, G.E.S. Fetsch and M.W. Jordan, J. Chem. Phys. 43, 4528 (1965)

6. R.C. Lord and E. Nielsen, J. Chem. Phys. 19, 1 (1951)

7. E.A.V. Ebsworth and S.G. Frankiss, Trans. Faraday Soc. 63, 1574 (1967)

8. A.L. Smith, Spectrochim. Acta 19, 849 (1963)

9. A.C. Jenkins and G.F. Chambers, Ind. Eng. Chem. 46, 2367 (1954)

10. H. Vahrenkamp and H. Nöth, J. Organomet. Chem. 12, 281 (1968)

11. R.H. Pierson, A.N. Fletcher and E.S.C. Gantz, Anal. Chem. 28, 1218 (1956)

12. E.A.V. Ebsworth and J.J. Turner, J. Chem. Phys. 36, 2628 (1962); J. Phys. Chem. 67, 805 (1963)

13. D.F. Ball and D.C. McKean, Spectrochim. Acta 18, 1019; 1029 (1962); I.W. Levin and W.T. King, J. Chem. Phys. 37, 1375 (1962)

14. T.E. Thomas and W.J. Orville-Thomas, J. Inorg. Nucl. Chem. 34, 839 (1972)

15. E.W. Abel, R. Honigschmidt-Grossich and S.M. Illingworth, J. Chem. Soc. A1968, 2623

16. I.R. Beattie, N. Cheetham, M. Gardner and D.E. Rogers, J. Chem. Soc. A1971, 2240

17. J.L. Hencher, Ph.D. thesis, McMaster University, 1964.

18. J.H. Schachtschneider, Tech. Rep. No. 57-65, Shell Development Co., Emeryville, Califormia, 1964.

19. R.L. Hilderbrandt, J. Chem. Phys. 51,1654 (1969)

20. A.J.F. Clark and J.E. Drake, Can. J. Spectry. 22,79 (1977)

21. J.W. Anderson, G.K. Barker, A.J.F. Clark, J.E. Drake and R.T. Hemmings, Spectrochim. Acta 30A,1081 (1974)

22. D.F. Van de Vondel, G.P. Van der Kelen and G. Van Hooydonk, J. Organomet. Chem. 23,431 (1970)

23. J.W. Anderson, G.K. Barker, J.E. Drake and R.T. Hemmings, Can. J. Chem. 49,2931 (1971); J.R. Durig, C.F. Jumper and J.N. Willis Jr., J. Mol. Spectry. 37,260 (1971)

VITA AUCTORIS

<u>Name</u>	Allan Jörgen Frederik Clark
<u>Born</u>	18 September 1947, in Skive, Denmark son of Ian Scott and Bitten Clark
<u>Citizenship</u>	British; Canadian Landed Immigrant
<u>Marital Status</u>	Single

<u>Education</u>

Brighton, Hove and Sussex Grammar School,
   : Hove, Sussex, U.K.   1959-67

University of Kent at Canterbury · 1967-70
    Canterbury, Kent, U.K.
    B.Sc.(Chemical Physics)

University of Windsor   1970-79
    Windsor, Ontario

<u>Positions Held</u>

Teaching Assistant (Physics)	1970-71
Teaching Assistant (Chemistry)	1971-75
Laboratory Coordinator (Chemistry)	1975-76
Demonstrator (Chemistry)	1976-78

<u>Society</u>

Chemical Institute of Canada
   (Student Member)